REGULATORY MECHANISMS OF IRON METABOLISM AND THEIR BIOLOGICAL IMPACT

by

Cole Parker Anderson

A dissertation submitted to the faculty of
The University of Utah
in partial fulfillment of the requirements for the degree of

Doctor of Philosophy

Department of Oncological Sciences

The University of Utah

December 2016

The University of Utah Graduate School

STATEMENT OF DISSERTATION APPROVAL

The dissertation of **Cole Parker Anderson**

has been approved by the following supervisory committee members:

Elizabeth A. Leibold	, Chair	**08.19.2016** Date Approved
Jody Rosenblatt	, Member	**08.23.2016** Date Approved
Donald E. Ayer	, Member	**08.17.2016** Date Approved
Jared P. Rutter	, Member	**08.23.2016** Date Approved
Carl Sennrich Thummel	, Member	**08.17.2016** Date Approved

and by **Bradley Cairns** , Chair/Dean of

the Department/College/School of **Oncological Sciences**

and by David B. Kieda, Dean of The Graduate School.

ABSTRACT

Iron is a critical micronutrient required for nearly all organisms to live. It is an important cofactor in proteins involved in DNA replication, cellular energy production, and oxygen transport. Nonphysiological levels of iron have pathological consequences ranging from iron deficiency that affects billions worldwide, to the iron overload disorder Hereditary Hemochromatosis that causes debilitating organ failure. Considering the dual nature of iron in healthy and diseased states, organisms have evolved elegant mechanisms to regulate iron homeostasis. This thesis examines the cellular mechanisms involved in controlling cellular iron uptake and storage, and highlights the importance of iron in the innate immune response and endocrine function of the mammalian pancreas.

Using *C. elegans* as a model to study iron metabolism, we show that the nuclear receptor, NHR-14, is a potent repressor of intestinal iron uptake through the iron importer SMF-3. In addition to iron import, NHR-14 regulates a transcriptional response to bacterial infection that is dependent upon the insulin/IGF-1-like signaling (IIS) pathway transcription factor PQM-1.

In mammals, cellular iron is maintained by the Iron Regulatory Proteins (IRPs). Mice lacking Iron Regulatory Protein 2 (IRP2) were shown to develop fasting hyperglycemia as a result of defective insulin biosynthesis that likely stems from mitochondrial dysfunction and Endoplasmic Reticulum (ER) stress.

I wish to dedicate this thesis to my parents, Dennis and Pamela, and sister, Paige. Through all their unconditional love and encouragement, none of this would have been possible.

TABLE OF CONTENTS

LIST OF TABLES

Tables

LIST OF FIGURES

Figures

ACKNOWLEDGEMENTS

I want to thank family and friends for all the support they have given me over the course of my graduate studies. They endured years of complaints and worry, for that I am truly grateful. To my parents, Dennis and Pam, and sister, Paige, without the constant love and encouragement, I wouldn't be the person I am today. Moving away from my birthplace and entire family was difficult, but I can honestly say that these past few years in Utah have been the most memorable in my life. I thank my family for their willingness to let me explore.

As a student in the Leibold lab with two very disparate projects, I had the wonderful opportunity to tinker with many different techniques and model systems. I owe a great deal of gratitude and respect to Josh Romney, who has helped me think critically about science and everyday aspects of life. I want to thank Betty. The tenacity and intellectual curiosity that is instilled by her fostered an environment that promoted creative thinking and scientific independence.

I would also like to acknowledge the various extramural programs that I have been associated with while at the University which helped broaden my skills and interests. The educational outreach program with the Salt Lake Center for Science Education was a wonderful alternative to a traditional teaching assistantship. I have also had the opportunity to work with the University Technology and Venture CommercializationOffice and the Lassonde New Venture Development Program, both of

which provided exposure to the business side of science and technology. Lastly, it was a pleasure volunteering with the Department of Parks, Recreation, and Tourism Urban Ranger program. Promoting environmental stewardship and trail etiquette on the Bonnieville Shoreline Trail were key objectives for the program, and I'm proud to have been involved.

Utah is a wonderful place to live, and the friendships I've made here are held dear to my heart. Backcountry skiing and mountain biking are very important to my wellbeing, and I'm happy to have shared those experiences with my best friends and fellow Utah transpants, Matt and Brian. Lastly, to my love Ava, your unconditional support and companionship have brightened my life. I look forward to our future together and the experiences life has in store for us.

CHAPTER 1

AN INTRODUCTION INTO IRON HOMEOSTASIS

The first law of thermodynamics states that energy cannot be created nor destroyed; energy can only be transferred or changed from one form to another. Similarly, for our purposes here on Earth, iron is neither created or destroyed but transitions from one oxidation state to another. Elemental iron on Earth was created billions of years ago by large and extremely hot stars through the silicone burning process. Through these celestial processes, iron became the 4th most abundant element on Earth and an absolute requirement for life. Hence, iron is incorporated in hemoproteins, Fe-S cluster proteins, and enzyme catalytic sites that are essential for many biological processes, including DNA replication, mitochondrial energy production, and oxygen transport.

The biological dependency on iron has not come without evolutionary challenges for its regulation. Iron bioavailability is restricted due to rapid oxidation and hydrolysis in the environment, and limited solubility causes problems for acquisition and transport. Defects in iron homeostasis can have severe pathological consequences, ranging from iron deficient anemia that affects a third of the world's population to iron overload disorders that can cause significant organ failure (Clark, 2008; Papanikolaou and Pantopoulos, 2005). Thus, the dual nature of iron has resulted in the evolution of unique mechanisms to acquire, transport, and store iron. The following is an overview of the mechanisms that regulate iron metabolism in both *C. elegans* and mammals with roles that extend into host-pathogen interactions and glucose homeostasis. Specifically, I highlight the conservation of iron metabolism between *C. elegans* and mammals. Readers are directed to Chapters 1 and 3 for detailed reviews on mechanisms of iron metabolism in *C. elegans* and mammals, respectively (Anderson and Leibold, 2014;

Anderson et al., 2012). Several topics that I consider relevant background for Chapters 2 and 4 will also be discussed in this introduction. For Chapter 2, this includes nuclear receptor signaling, innate immune mechanisms, and the insulin/insulin-like growth factor pathway in *C. elegans*. Lastly, models of IRP2 deficiency, iron in diabetes, and mitochondrial and ER perturbations that lead to impaired glucose metabolism will be reviewed as background for Chapter 4.

In human adults, approximately 3-4 mg of dietary iron is absorbed at the apical membrane of duodenal enterocytes by divalent-metal transporter 1 (DMT1) after being reduced by ferrireductases such as duodenal cytochrome B (DCTYB). Within the cell, ferrous iron comprises the labile iron pool where it is utilized as a cofactor in proteins for key cellular processes, stored into the iron storage protein ferritin, or transported across the basolateral membrane into circulation by ferroportin. Circulating iron is quickly bound by transferrin (Tf) and delivered to cells expressing transferrin receptor 1 (TfR1), such as maturing red blood cells. Tf-Fe-TfR1 complexes are internalized by receptor-mediated endocytosis. Acidification of the endosome releases Fe^{3+} from these complexes where it is reduced and exported across the endosomal membrane into the cytoplasm by STEAP3 and DMT1, respectively.

Since a regulated process of iron excretion has yet to be discovered, sloughing of intestinal enterocytes every 3 days is the only mechanism of iron efflux from the body. Therefore, precise control of intestinal iron uptake and storage is needed to maintain iron homeostasis throughout the body. It is not surprising due to the importance of iron that many genes involved in iron homeostasis are conserved across metazoa. Indeed, there is a high degree of conservation between iron metabolic genes in *C. elegans* and mammals

(Anderson and Leibold, 2014). The intestine is one of the major organs of *C. elegans*, roughly comprising one third of the entire somatic mass of the worm (Kormish et al., 2010). Similar to vertebrates, iron absorption in *C. elegans* occurs at the basal brush boarder of intestinal enterocytes by SMF-3, the principal ferric iron transporter (Bandyopadhyay et al., 2009). The worm also expresses two DMT1-like transporters, SMF-1 and SMF-3 that share 55-58% amino acid identity with DMT1. Their role in iron uptake is limited compared to SMF-3, however, they appear to act as key regulators of manganese transport and the response to pathogenic bacteria (Au et al., 2009). The transport across the apical membrane to the interstitial space and other organs is not well understood. Worms do however express three ferroportin orthologs (FPN-1.1-1.3) that likely transport iron in a similar fashion as mammalian ferroportin.

The ferritin orthologs FTN-1 and FTN-2 are responsible for storing ferric iron in *C. elegans*, a form that is unable to generate free radicals. Interestingly FTN-1 and FTN-2 both exhibit ferroxidase activity that is a specific feature of the heavy subunit (FTH) of mammalian ferritin. The light subunit (FTL) on the other hand is responsible for iron nucleation that results in a core or shell that can store up to 4500 Fe^{3+} atoms. Ferritin is ubiquitously expressed, and in *C. elegans* FTN-1 is highly enriched in the intestine while FTN-2 is expressed in many tissues that include the pharynx, hypodermis, body-wall muscle, and intestine. Essential for maintaining proper iron balance, uptake, and storage are tightly regulated processes and are carried out by very distinct mechanisms in *C. elegans* and mammals.

In *C. elegans*, iron homeostasis is predominantly regulated transcriptionally by the basic helix-loop-helix (bHLH) transcription factor hypoxia inducible factor 1 (HIF-1).

The lability of hypoxia inducible factors (HIF-1α and HIF-2α in mammals, HIF-1 in *C. elegans*) in response to oxygen tension is well known, however their sensitivity to iron is often overlooked. During iron deficiency, HIFs are stabilized due to reduced activity of the oxygen and iron dependent prolyl hydroxylase (PHD) (Peyssonnaux et al., 2007). Our lab has shown that stabilized HIF-1 during iron deficiency transcriptionally activates SMF-3 while simultaneously repressing FTN-1 and to a lesser degree FTN-2 to increase iron uptake and reduce storage (Romney et al., 2008, 2011a). A similar mechanism occurs in mammals, where HIF-2α activates the transcription of DMT1, FPN1, and DCYTB in the intestine to increase iron absorption (Mastrogiannaki et al., 2009).

In mammals, cellular iron metabolism in maintained by Iron Regulatory Proteins 1 and 2 (IRP1 and IRP2) (Anderson et al., 2012). The IRPs are RNA binding proteins that bind with high affinity to specific stem-loop structures called Iron Response Elements (IREs) present in the 5' and 3' untranslated regions (UTRs) of target mRNAs that mediate their translational efficiency or stability. IRPs bind to IREs in the mRNAs involved in iron uptake (TfR1), sequestration (FtH and FtL) and export (FPN). During iron deficiency the IRPs bind to 5' IREs in ferritin and ferroportin to repress their translation, and to 3' IREs in TfR1 to stabilize its mRNA. During normal iron conditions the IRPs bind to cognate IREs at a low affinity, which enables enhanced translation of ferritin and ferroportin, and mediating TfR1 mRNA instability and degradation. In essence, IRPs are responsible for increasing iron uptake and reducing storage during iron deficiency, and vice versa when iron levels are high. In addition to mRNAs involved in iron metabolism, the IRPs regulate expression of mRNAs involved in diverse biological processes, all of which rely on proper iron levels. These IRE containing mRNAs include;

aconitase (TCA cycle), erythroid aminolevulinate synthase (heme biosynthesis), HIF-2α (hypoxia), MRCKα (cytoskeletal dynamics), and CDC14a (mitosis) (Sanchez et al., 2011). IRPs themselves are also iron regulated, but in two distinct ways. IRP1 contains a 4Fe-4S cluster that enables it to perform as a bifunctional protein. Iron promotes assembly of the 4Fe-4S cluster that results in its conversion from an RNA-binding protein to a cytosolic aconitase. IRP2 on the other hand is targeted by a iron-regulated ubiquitin ligase (FBXL5) for proteasomal degradation (Salahudeen et al., 2009; Vashisht et al., 2009).

In Chapter 2, I discuss the identification and characterization of the nuclear hormone receptor 14 (NHR-14) as a novel regulator of iron metabolism and innate immunity. Nuclear receptors (NRs) are a hallmark of metazoan evolution that comprises a highly specialized family of ligand gated transcription factors. Family members can bind ligands such as vitamins, fatty acids, and steroids; and are tasked with the coordination of critical processes that range from xenobiotic metabolism to growth and development (Antebi, 2015). DNA binding domains of NRs consist of two zinc-fingers at the N-terminus that facilitate contact with DNA. At the C-terminus the ligand binding domain coordinates ligand binding and interaction with transcriptional coactivators and corepressor that dictate NR activity. There are two classes of NRs: class 1 members are activated when bound by their ligand, while class 2 receptors are also ligand activated but they also function as transcriptional repressors in the absence of ligand. Nuclear receptors with unidentified ligands are considered to be orphan receptors

The *C. elegans* genome contains 284 NRs, which is remarkable considering only 48 have been identified in humans (Antebi, 2015). Out of the 284, 269 are considered to

be an expansion by gene duplication of the HNF4 family, while the remainder shares a high degree of conservation with mammalian NRs. To date, less than 10% of NRs have been genetically characterized in *C. elegans*. Previous to our findings NHR-14 remained a relatively uncharacterized NR. One study demonstrated that NHR-14 was responsible for the estrogen dependent activation of vitellogenin-2 (*vit-2*) (Mimoto et al., 2007). The group went further to show that NHR-14 binds estrogen by surface plasma resonance. However a later study showed that *nhr-14* RNAi had no affect on vitellogenin expression, hence, the role of NHR-14 in estrogen signaling remains to be determined (Fischer et al., 2012). I discuss in Chapter 2 that NHR-14 represses iron transport through SMF-3, and this mechanism has key implications for C. elegans' innate immune response. NHR-14 is the first identified NR in *C. elegans* to regulate iron metabolism and the innate immune response. Notably these two processes are not mutually exclusive. Rather, the regulation of iron availability is a core component of the immune response.

Nutritional immunity relies on host mechanisms that limit the acquisition of micronutrients such as iron, manganese, and zinc by pathogens (Hood and Skaar, 2012). The importance of iron during infections is underscored by enhanced susceptibility with iron supplementation and in individuals with the iron overload disease hemochromatosis (Khan et al., 2007). Thus, a combination of systemic and cellular mechanisms has evolved to sequester micronutrients away from pathogens. During an infection in mammals, the iron hormone hepcidin is upregulated and secreted by the liver. Hepcidin binds to ferroportin expressed in duodenal enterocytes and macrophages to prevent the export of iron into circulation (Nemeth et al., 2004). As an acute phase reactant, ferritin expression also increases in response to infection and is an important factor in

intracellular iron withholding. Overall, these mechanisms lead to hypoferremia and anemia of inflammation that comprise an important host defense strategy for limiting iron to pathogens.

At the other end the spectrum, pathogens acquire host iron through the production of small high affinity iron chelating compounds called siderophores. Siderophores bind ferric iron with affinities that exceed host transferrin and lactoferrin, effectively stealing iron from the host (Miethke and Marahiel, 2007). Millions of years of coevolution have enabled mammals to develop mechanisms that inhibit siderophore-mediated iron acquisition by bacteria. Lipocalin-2 (also known as, siderocalin, neutrophil gelatinase-associated lipocalin, or 24p3) is the most abundant antimicrobial secreted by epithelial cells and neutrophils in response to intestinal and respiratory infections. Specifically, lipocalin-2 is able to bind and sequester siderophores thus limiting iron bioavailability (Flo et al., 2004). Due to the intense molecular arms race between hosts and pathogens, it is not surprising that pathogens have evolved ways to evade lipocalin-2. Certain pathogens including *Salmonella enterica* and uropathogenic *E. coli* synthesize siderophore derivatives that cannot be bound by lipocalin-2, which enables their iron uptake (Muller et al., 2009).

The vast majority of data regarding nutritional immunity has come from mammalian studies with very little contribution from *C. elegans*. However, regulating micronutrient availability is an important factor for potential hosts, and *C. elegans* is no exception. Worms grown in high iron conditions are more susceptible to *Salmonella* infection (Kortman et al., 2015), and *smf-3* mutants with disrupted iron and manganese homeostasis have decreased survival compared to wild-type when infected with

Staphylococcus aureus (Bandyopadhyay et al., 2009). These studies introduce important aspects of *C. elegans* that make them useful models for studying host-pathogen interactions and the innate immune response. Most importantly, human pathogens such as *P. aeruginosa*, *S. enterica*, and *S. aureus* have been shown to infect and elicit a highly specific immune response in *C. elegans* that rely on conserved signaling pathways including, FOXO transcription factors, β-catenin, and p38 mitogen-activated protein kinase (MAPK) (Miyata et al., 2008; Roberts et al., 2010; Troemel, 2006). These signaling pathways function in parallel to induce overlapping expression of antimicrobial effectors, including c-type lectins, ShK toxins, lysozymes, saposins, and genes involved in iron metabolism (Cohen and Troemel, 2015). In Chapter 2, we identify a transcriptional profile in *nhr-14* mutants that significantly overlaps with transcriptional responses seen during infection with *Pseudomonas*, *Salmonella*, and other various pathogens. This signature also correlates with DAF-16/FOXO dependent transcription, which is the primary transcription factor in the insulin/insulin-like growth factor signaling pathway in *C. elegans*.

Coordination of nutrient availability with development, metabolism, and the stress response is a conserved process among vertebrates and *C. elegans* that is mediated by insulin/insulin-like (IIS) growth factor signaling. The insulin pathway is activated by insulin and insulin-like growth factors that bind to tyrosine kinase receptors (DAF-2/IGFR-1), leading to the phosphorylation of the Forkhead Box, Class O transcription factor (DAF-16/FOXO) (Lin et al., 2001). Phosphorylated DAF-16/FOXO is retained in the cytoplasm, thus preventing activation of its transcriptional targets. Conversely during nutrient starvation or stress, DAF-2/IGFR-1 is not activated and DAF-16 does not

become phosphorylated, which allows for nuclear translocation and activation of genes involved in metabolism, stress response, and innate immunity.

Mutants lacking *daf-2* were shown to have constitutively active DAF-16/FOXO and an upregulation of DAF-16/FOXO target genes, designated Class 1 genes that are important in the stress response. The gene subset downregulated in these mutants are designated as Class 2 genes, and are considered to be important for growth and development. It was shown that Class 1 gene promoters contain a DAF-16 binding element (DBE) important for DAF-16/FOXO binding and activation, while Class 2 promoters contain a DAF-16 associated element (DAE) (Murphy et al., 2003). A recent study discovered that the transcription factor PQM-1 activated Class 2 genes through their DAE (Tepper et al., 2013). The study also demonstrated that nuclear localization of DAF-16 and PQM-1 was mutually antagonistic. For instance, when DAF-16 is nuclear localized, PQM-1 remains in the cytoplasm and vice versa. PQM-1 was originally discovered to be upregulated in response to paraquat-induced oxidative stress, and is considered to be a stress response transcription factor (Tawe et al., 1998). This is inconsistent however with its role in activating Class 2 genes that are thought be important for growth and development. In fact, Class 2 genes have a higher correlation with genes involved in the innate immune response, and *pqm-1* RNAi is shown to enhance susceptibility to bacterial infection (Kawli and Tan, 2008). Further research is needed to better understand the dynamics between DAF-16/FOXO and PQM-1, and how they balance stress responses with growth and development signals.

In Chapter 4, I discuss defects in glucose homeostasis resulting from a loss of IRP2. To date there have been several global and tissue specific deletions of IRP2, which

are discussed in the next section. In mice, whole body deletion of IRP2 results in microcytic anemia, erythropoietic protoporphyria, altered body iron distribution, and neurological defects (Galy et al., 2005a; LaVaute et al., 2001; Zumbrennen-Bullough et al., 2014). Iron content is elevated in intestine and liver and is associated with increased ferritin expression and decreased TfR1 expression, while iron is reduced in splenic macrophages and is associated with decreased ferritin expression. In comparison, IRP1 deficient mice have no overt phenotype while deletion of both IRP1 and IRP2 results in embryonic lethality. IRP2 has been conditionally ablated in several cell types that include splenic and bone marrow macrophages, hepatocytes, and duodenal enterocytes (Ferring-Appel et al., 2009; Galy et al., 2005b, 2008). One of the most severe phenotypes was observed in mice with intestinal-specific deletion of both IRP1 and IRP2, where 80% of the animals died shortly after weaning (Galy et al., 2008). IRP deficient enterocytes from these mice displayed less structured duodenal crypts and villi, and intestinal enterocytes exhibited mitochondriopathy along with increased apoptosis. Ferritin and ferroportin levels were profoundly increased, and TfR1 and DMT1-IRE isoform mRNAs and protein were decreased.

It is well established that elevated iron levels pose as a major risk factor for developing Type 2 diabetes (T2D). Readers are directed to an in depth review by Simcox and McClain that covers iron and diabetes risk (Simcox and McClain, 2016). Risk association was first identified in patients suffering from iron overload disorders including hereditary hemochromatosis (HH), beta-thalassemia, and transfusional iron overload (Fernández-Real et al., 2002). Insulin deficiency is commonly observed in these pathological states; interestingly however, HH individuals have increased insulin

sensitivity rather than insulin resistance seen with tranfusional iron overload. Similarly, mouse models of HH exhibit reduced insulin secretion stemming from elevated oxidative stress, reduced glucose sensitivity, and increased beta cell apoptosis (Huang et al., 2011). Further evidence linking iron with diabetes comes from observations that showed improvements in insulin secretion capacity with phlebotomy and chelation therapy. Elevated iron stores measured by serum ferritin is also positively correlated with T2D risk, and high ferritin enhances risk for metabolic syndrome and cardiovascular disease.

At the other end of the spectrum, there is a high prevalence of iron deficiency in obese individuals, where obesity is a major predisposing factor for T2D (Hotamisligil, 2006). Evidence suggests that low iron in these individuals is caused by anemia of inflammation rather than iron-poor diets. Chronic inflammation is associated with increased hepcidin and ferritin expression, and is a hallmark of obesity. Studies show that inflammatory markers such as serum ferritin and C Reactive Protein are better predictors of iron deficiency in obese individuals than dietary iron levels (Jehn et al., 2004). In Chapter 4, I discuss iron deficiency as a major consequence of IRP2 deficiency. Unlike the examples discussed above, these animals do not suffer from chronic inflammation and obesity. Instead these mice are leaner than wild-type littermates and have normal insulin sensitivity. Our observations indicate that hyperglycemia stems from insulin deficiency that is caused by defects in insulin processing. Despite data associating iron with diabetes, very little is known about the role of iron in insulin processing. Discussed below is the process of producing mature insulin, and potential iron-dependent mechanisms that perturb this process. The production and secretion of mature insulin is a highly complex process that involves the

tight coordination of transcriptional, ER, and vesicular trafficking machinery. Transcription of the *ins1* and *ins2* genes in mice results in the insulin precursor, preproinsulin, that is cleaved and folded into proinsulin in the ER. Proinsulin transits to Golgi vesicles where it is further cleaved by the prohormone convertases PC1/3, PC2, and Carboxypeptidase E to form mature insulin. Within Golgi vesicles, mature insulin utilizes Zn^{2+} to crystalize into dense core granules that are ready to be secreted in response to glucose. Defects in ER maintenance (Zhang et al., 2006), proinsulin processing enzymes (Zhu et al., 2002), and proinsulin structure itself can ultimately lead to reduced insulin production and often times an accumulation of proinsulin that wreaks havoc on the ER and Golgi. In fact, elevated serum proinsulin has become a marker of prediabetes and an early indicator of β-cell dysfunction (Pfützner et al., 2004).

The relationship between oxidative protein folding in the ER and mitochondrial metabolism is becoming more appreciated (Simmen et al., 2010). The exchange of calcium, ATP, and metabolites such as flavin adenine dinucleotide (FAD) has shown to be important for chaperone function and protein disulfide isomerase (PDI) activity that is responsible for disulfide bridge formation and proper folding of nascent polypeptides (Inaba et al., 2010).

Besides ATP production, mitochondria are best known for Fe-S cluster biogenesis, and defects in this process can have dramatic pathological consequences. Defects in Fe-S cluster machinery, for example, results in Friedrich's Ataxia (FA), Sideroblastic anemia, and myopathy; all of which exhibit reduced activity of Fe-S cluster containing proteins and increased mitochondrial iron deposition (Rouault, 2015). The link between Fe-S cluster metabolism and diabetes is not well understood. Incidence of

diabetes in individuals with FA is high, and β-cell specific deletion of Frataxin causes glucose intolerance and reduced β-cell mass in mice (Ristow et al., 2003). CISD2 and CDKAL1 are Fe-S cluster containing proteins that have also been implicated in diabetes. Mutations in CISD2 cause Wolfram Syndrome, a neurodegenerative disorder characterized by optic atrophy, deafness, and diabetes (Chen et al., 2009). Cdkal1 is consistently associated with T2D risk across heterogeneous populations, and mutations have been associated with reduced insulin secretion (Dehwah et al., 2010). More recently, Cdkal1 was shown to be responsible for the methylthiolation of $tRNA^{Lys}(UUU)$ that is important for accurate translation of AAA and AAG codons in proinsulin (Wei et al., 2011). β-cells lacking Cdkal1 have a reduction in insulin secretion and are glucose intolerant, defects resulting from improper proinsulin synthesis.

In summary, like diabetes itself, the etiology of iron in diabetes is multifaceted. Levels outside the normal physiological range have severe consequences at the cellular and organismal level, thus additional research is needed to better understand these consequences in disease contexts. Improved understanding of iron's role in the processes mentioned in this chapter will undoubtledly lead to better treatment and management of diabetes.

References

Aballay, A., Yorgey, P., and Ausubel, F.M. (2000). *Salmonella typhimurium* proliferates and establishes a persistent infection in the intestine of *Caenorhabditis elegans*. Curr. Biol. *10*, 1539–1542.

Ackerman, D., and Gems, D. (2012). Insulin/IGF-1 and hypoxia signaling act in concert to regulate iron homeostasis in *Caenorhabditis elegans*. PLoS Genet. *8*, e1002498.

Ahn, S.-H., Shah, Y.M., Inoue, J., Morimura, K., Kim, I., Yim, S., Lambert, G., Kurotani, R., Nagashima, K., Gonzalez, F.J., et al. (2008). Hepatocyte nuclear factor 4alpha in the intestinal epithelial cells protects against inflammatory bowel disease. Inflamm. Bowel Dis. *14*, 908–920.

Alper, S., McBride, S.J., Lackford, B., Freedman, J.H., and Schwartz, D.A. (2007). Specificity and complexity of the *Caenorhabditis elegans* innate immune response. Mol. Cell. Biol. *27*, 5544-5553.

Anderson, G.J. (2013). Encyclopedia of Metalloproteins. R.H. Kretsinger, V.N. Uversky, and E.A. Permyakov, eds. (New York, NY: Springer New York), pp. 985–995.

Anderson, C.P., and Leibold, E.A. (2014). Mechanisms of iron metabolism in *Caenorhabditis elegans*. Front. Pharmacol. *5*.

Anderson, C.P., Shen, M., Eisenstein, R.S., and Leibold, E. a (2012). Mammalian iron metabolism and its control by iron regulatory proteins. Biochim. Biophys. Acta *1823*, 1468–1483.

Antebi, A. (2015). Nuclear receptor signal transduction in *C. elegans*. WormBook 1–49.

Au, C., Benedetto, A., Anderson, J., Labrousse, A., Erikson, K., Ewbank, J.J., and Aschner, M. (2009). SMF-1, SMF-2 and SMF-3 DMT1 orthologues regulate and are regulated differentially by manganese levels in *C. elegans*. PLoS One *4*, e7792.

Babeu, J.-P., and Boudreau, F. (2014). Hepatocyte nuclear factor 4-alpha involvement in liver and intestinal inflammatory networks. World J. Gastroenterol. *20*, 22–30.

Bandyopadhyay, J., Song, H.-O., Park, B.-J., Singaravelu, G., Sun, J.L., Ahnn, J., and Cho, J.H. (2009). Functional assessment of Nramp-like metal transporters and manganese in *Caenorhabditis elegans*. Biochem. Biophys. Res. Commun. *390*, 136–141.

Beard, J.L. (2001). Iron biology in immune function, muscle metabolism, and neuronal functioning. J. Nutr. *131*, 568-579.

Brenner, S. (1974). The genetics of *Caenorhabditis elegans*. Genetics *77,* 71-94.

Canonne-Hergaux, F., Gruenheid, S., Ponka, P., and Gros, P. (1999). Cellular and subcellular localization of the Nramp2 iron transporter in the intestinal brush border and regulation by dietary iron. Blood *93*, 4406–4417.

Chen, Y.-F., Kao, C.-H., Chen, Y.-T., Wang, C.-H., Wu, C.-Y., Tsai, C.-Y., Liu, F.-C., Yang, C.-W., Wei, Y.-H., Hsu, M.-T., et al. (2009). Cisd2 deficiency drives premature aging and causes mitochondria-mediated defects in mice. Genes Dev. *23* , 1183–1194.

Clark, S.F. (2008). Iron deficiency anemia. Nutr. Clin. Pract. *23*, 128–141.

Cohen, L.B., and Troemel, E.R. (2015). Microbial pathogenesis and host defense in the nematode *C. elegans*. Curr. Opin. Microbiol. *23*, 94–101.

Dehwah, M.A.S., Wang, M., and Huang, Q.-Y. (2010). CDKAL1 and type 2 diabetes: a global meta-analysis. Genet. Mol. Res. *9*, 1109–1120.

Doitsidou, M., Poole, R.J., Sarin, S., Bigelow, H., and Hobert, O. (2010). *C. elegans* Mutant identification with a one-step whole-genome-sequencing and SNP mapping strategy. PLoS One *5*, e15435.

Eden, E., Navon, R., Steinfeld, I., Lipson, D., and Yakhini, Z. (2009). GOrilla: a tool for discovery and visualization of enriched GO terms in ranked gene lists. BMC Bioinformatics *10*, 48.

Fernández-Real, J.M., López-Bermejo, A., and Ricart, W. (2002). Cross-talk between iron metabolism and diabetes. Diabetes *51*, 2348–2354.

Ferring-Appel, D., Hentze, M.W., and Galy, B. (2009). Cell-autonomous and systemic context-dependent functions of iron regulatory protein 2 in mammalian iron metabolism. Blood *113*, 679–687.

Fischer, M., Regitz, C., Kahl, M., Werthebach, M., Boll, M., and Wenzel, U. (2012). Phytoestrogens genistein and daidzein affect immunity in the nematode *Caenorhabditis elegans* via alterations of vitellogenin expression. Mol. Nutr. Food Res. *56*, 957–965.

Fleming, R.E., and Ponka, P. (2012). Iron Overload in Human Disease. N. Engl. J. Med. *366*, 348–359.

Flo, T.H., Smith, K.D., Sato, S., Rodriguez, D.J., Holmes, M.A., Strong, R.K., Akira, S., and Aderem, A. (2004). Lipocalin 2 mediates an innate immune response to bacterial infection by sequestrating iron. Nature *432*, 917–921.

Galy, B., Ferring, D., Minana, B., Bell, O., Janser, H.G., Muckenthaler, M., Schümann, K., and Hentze, M.W. (2005a). Altered body iron distribution and microcytosis in mice deficient in iron regulatory protein 2 (IRP2). Blood *106*, 2580–2589.

Galy, B., Ferring, D., and Hentze, M.W. (2005b). Generation of conditional alleles of the murine Iron Regulatory Protein (IRP)-1 and -2 genes. Genesis *43*, 181–188.

Galy, B., Ferring-Appel, D., Kaden, S., Gröne, H.-J., and Hentze, M.W. (2008). Iron regulatory proteins are essential for intestinal function and control key iron absorption molecules in the duodenum. Cell Metab. *7*, 79–85.

Ganz, T., and Nemeth, E. (2011). Hepcidin and disorders of iron metabolism. Annu. Rev. Med. *62*, 347–360.

Garsin, D.A., Sifri, C.D., Mylonakis, E., Qin, X., Singh, K. V, Murray, B.E., Calderwood, S.B., and Ausubel, F.M. (2001). A simple model host for identifying Gram-positive virulence factors. Proc. Natl. Acad. Sci. U. S. A. *98*, 10892–10897.

Van Gilst, M.R., Hadjivassiliou, H., Jolly, A., and Yamamoto, K.R. (2005). Nuclear hormone receptor NHR-49 controls fat consumption and fatty acid composition in C. elegans. PLoS Biol. *3*.

Gonzalez, F.J. (2008). Regulation of hepatocyte nuclear factor 4 alpha-mediated transcription. Drug Metab. Pharmacokinet. *23*, 2–7.

Govoni, G., Gauthier, S., Billia, F., Iscove, N.N., and Gros, P. (1997). Cell-specific and inducible Nramp1 gene expression in mouse macrophages in vitro and in vivo. J. Leukoc. Biol. *62*, 277–286.

Hoeckendorf, A., and Leippe, M. (2012). SPP-3, a saposin-like protein of *Caenorhabditis elegans*, displays antimicrobial and pore-forming activity and is located in the intestine and in one head neuron. Dev. Comp. Immunol. *38*, 181–186.

Hood, M.I., and Skaar, E.P. (2012). Nutritional immunity: transition metals at the pathogen-host interface. Nat. Rev. Microbiol. *10*, 525–537.

Hotamisligil, G.S. (2006). Inflammation and metabolic disorders. Nature *444*, 860–867.

Huang, D.W., Sherman, B.T., and Lempicki, R. a (2009). Systematic and integrative analysis of large gene lists using DAVID bioinformatics resources. Nat. Protoc. *4*, 44–57.

Huang, J., Jones, D., Luo, B., Sanderson, M., Soto, J., Abel, E.D., Cooksey, R.C., and McClain, D. a (2011). Iron overload and diabetes risk: a shift from glucose to Fatty Acid oxidation and increased hepatic glucose production in a mouse model of hereditary hemochromatosis. Diabetes *60*, 80–87.

Hwang, A.B., Ryu, E.-A., Artan, M., Chang, H.-W., Kabir, M.H., Nam, H.-J., Lee, D., Yang, J.-S., Kim, S., Mair, W.B., et al. (2014). Feedback regulation via AMPK and HIF-1 mediates ROS-dependent longevity in *Caenorhabditis elegans*. Proc. Natl. Acad. Sci. U. S. A. *111*, E4458–E4467.

Inaba, K., Masui, S., Iida, H., Vavassori, S., Sitia, R., and Suzuki, M. (2010). Crystal structures of human Ero1alpha reveal the mechanisms of regulated and targeted oxidation of PDI. EMBO J. *29*, 3330–3343.

Irazoqui, J.E., Urbach, J.M., and Ausubel, F.M. (2010). Evolution of host innate defence: insights from *Caenorhabditis elegans* and primitive invertebrates. Nat. Rev. Immunol. *10*, 47–58.

Jehn, M., Clark, J.M., and Guallar, E. (2004). Serum ferritin and risk of the metabolic syndrome in U.S. adults. Diabetes Care *27*, 2422–2428.

Jones, L.M., Rayson, S.J., Flemming, A.J., and Urwin, P.E. (2013). Adaptive and specialised transcriptional responses to xenobiotic stress in *Caenorhabditis elegans* are regulated by nuclear hormone receptors. PLoS One *8*, e69956.

Kawli, T., and Tan, M.-W. (2008). Neuroendocrine signals modulate the innate immunity of *Caenorhabditis elegans* through insulin signaling. Nat. Immunol. *9*, 1415–1424.

Khan, F.A., Fisher, M.A., and Khakoo, R.A. (2007). Association of hemochromatosis with infectious diseases: expanding spectrum. Int. J. Infect. Dis. *11*, 482–487.

Kirienko, N. V, Kirienko, D.R., Larkins-Ford, J., Wählby, C., Ruvkun, G., and Ausubel, F.M. (2013). Pseudomonas aeruginosa disrupts *Caenorhabditis elegans* iron homeostasis, causing a hypoxic response and death. Cell Host Microbe *13*, 406–416.

Kormish, J.D., Gaudet, J., and McGhee, J.D. (2010). Development of the *C. elegans* digestive tract. Curr. Opin. Genet. Dev. *20*, 346–354.

Kortman, G.A.M., Mulder, M.L.M., Richters, T.J.W., Shanmugam, N.K.N., Trebicka, E., Boekhorst, J., Timmerman, H.M., Roelofs, R., Wiegerinck, E.T., Laarakkers, C.M., et al. (2015). Low dietary iron intake restrains the intestinal inflammatory response and pathology of enteric infection by food-borne bacterial pathogens. Eur. J. Immunol. *45*, 2553–2567.

LaVaute, T., Smith, S., Cooperman, S., Iwai, K., Land, W., Meyron-Holtz, E., Drake, S.K., Miller, G., Abu-Asab, M., Tsokos, M., et al. (2001). Targeted deletion of the gene encoding iron regulatory protein-2 causes misregulation of iron metabolism and neurodegenerative disease in mice. Nat. Genet. *27*, 209–214.

Lee, S.-H., Wong, R.-R., Chin, C.-Y., Lim, T.-Y., Eng, S.-A., Kong, C., Ijap, N.A., Lau, M.-S., Lim, M.-P., Gan, Y.-H., et al. (2013). *Burkholderia pseudomallei* suppresses *Caenorhabditis elegans* immunity by specific degradation of a GATA transcription factor. Proc. Natl. Acad. Sci. *110* , 15067–15072.

Lee, S.-J., Murphy, C.T., and Kenyon, C. (2009). glucose shortens the life span of *C. elegans* by downregulating DAF-16/FOXO activity and aquaporin gene expression. Cell

Metab. *10*, 379–391.

Lee, S.S., Kennedy, S., Tolonen, A.C., and Ruvkun, G. (2003). DAF-16 target genes that control *C. elegans* life-span and metabolism. Science. *300*, 644–647.

Lill, R., and Muhlenhoff, U. (2008). Maturation of iron-sulfur proteins in eukaryotes: mechanisms, connected processes, and diseases. Annu. Rev. Biochem. *77*, 669–700.

Lin, K., Hsin, H., Libina, N., and Kenyon, C. (2001). Regulation of the *Caenorhabditis elegans* longevity protein DAF-16 by insulin/IGF-1 and germline signaling. Nat. Genet. *28*, 139–145.

Mallo, G. V, Kurz, C.L., Couillault, C., Pujol, N., Granjeaud, S., Kohara, Y., and Ewbank, J.J. (2002). Inducible antibacterial defense system in *C. elegans*. Curr. Biol. *12*, 1209-1214.

Mann, F.G., Van Nostrand, E.L., Friedland, A.E., Liu, X., and Kim, S.K. (2016). Deactivation of the gata transcription factor ELT-2 is a major driver of normal aging in *C. elegans*. PLoS Genet. *12*, e1005956.

Mastrogiannaki, M., Matak, P., Keith, B., Simon, M.C., Vaulont, S., and Peyssonnaux, C. (2009). HIF-2α, but not HIF-1α, promotes iron absorption in mice. J. Clin. Invest. *119*, 1159–1166.

Matsuo, S., Ogawa, M., Muckenthaler, M.U., Mizui, Y., Sasaki, S., Fujimura, T., Takizawa, M., Ariga, N., Ozaki, H., Sakaguchi, M., et al. (2015). Hepatocyte Nuclear Factor 4α Controls Iron Metabolism and Regulates Transferrin Receptor 2 in Mouse Liver. J. Biol. Chem. *290*, 30855-30865.

McElwee, J.J., Schuster, E., Blanc, E., Thomas, J.H., and Gems, D. (2004). Shared transcriptional signature in *Caenorhabditis elegans* dauer larvae and long-lived daf-2 mutants implicates detoxification system in longevity assurance. J. Biol. Chem. *279*, 44533–44543.

McGhee, J.D., Sleumer, M.C., Bilenky, M., Wong, K., McKay, S.J., Goszczynski, B., Tian, H., Krich, N.D., Khattra, J., Holt, R.A., et al. (2007). The ELT-2 GATA-factor and the global regulation of transcription in the *C. elegans* intestine. Dev. Biol. *302*, 627–645.

Miethke, M., and Marahiel, M.A. (2007). Siderophore-based iron acquisition and pathogen control. Microbiol. Mol. Biol. Rev. *71*, 413–451.

Mimoto, A., Fujii, M., Usami, M., Shimamura, M., Hirabayashi, N., Kaneko, T., Sasagawa, N., and Ishiura, S. (2007). Identification of an estrogenic hormone receptor in *Caenorhabditis elegans*. Biochem. Biophys. Res. Commun. *364*, 883–888.

Minevich, G., Park, D.S., Blankenberg, D., Poole, R.J., and Hobert, O. (2012).

CloudMap: A cloud-based pipeline for analysis of mutant genome sequences. Genetics *192*, 1249–1269.

Miyata, S., Begun, J., Troemel, E.R., and Ausubel, F.M. (2008). DAF-16-dependent suppression of immunity during reproduction in *Caenorhabditis elegans*. Genetics *178*, 903–918.

Muller, S.I., Valdebenito, M., and Hantke, K. (2009). Salmochelin, the long-overlooked catecholate siderophore of Salmonella. Biometals *22*, 691–695.

Murphy, C.T. (2003). Genes that act downstream of DAF-16 to influence the lifespan of *Caenorhabditis elegans*. Nature *424*, 277–283.

Murphy, C.T., McCarroll, S. a, Bargmann, C.I., Fraser, A., Kamath, R.S., Ahringer, J., Li, H., and Kenyon, C. (2003). Genes that act downstream of DAF-16 to influence the lifespan of *Caenorhabditis elegans*. Nature *424*, 277–283.

Murphy, C.T., Lee, S.-J., and Kenyon, C. (2007). Tissue entrainment by feedback regulation of insulin gene expression in the endoderm of *Caenorhabditis elegans*. Proc. Natl. Acad. Sci. U. S. A. *104*, 19046–19050.

Nemeth, E., Tuttle, M.S., Powelson, J., Vaughn, M.B., Donovan, A., Ward, D.M., Ganz, T., and Kaplan, J. (2004). Hepcidin regulates cellular iron efflux by binding to ferroportin and inducing its internalization. Science *306*, 2090–2093.

Nevo, Y., and Nelson, N. (2006). The NRAMP family of metal-ion transporters. Biochim. Biophys. Acta *1763*, 609–620.

Niu, W., Lu, Z.J., Zhong, M., Sarov, M., Murray, J.I., Brdlik, C.M., Janette, J., Chen, C., Alves, P., Preston, E., et al. (2011). Diverse transcription factor binding features revealed by genome-wide ChIP-seq in *C. elegans*. Genome Res. *21*, 245–254.

Nix, D.A., Courdy, S.J., and Boucher, K.M. (2008). Empirical methods for controlling false positives and estimating confidence in ChIP-Seq peaks. BMC Bioinformatics *9*, 1–9.

Papanikolaou, G., and Pantopoulos, K. (2005). Iron metabolism and toxicity. Toxicol. Appl. Pharmacol. *202*, 199–211.

Pathare, P.P., Lin, A., Bornfeldt, K.E., Taubert, S., and Van Gilst, M.R. (2012). Coordinate regulation of lipid metabolism by novel nuclear receptor partnerships. PLoS Genet. *8*, e1002645.

Peyssonnaux, C., Zinkernagel, A.S., Schuepbach, R.A., Rankin, E., Vaulont, S., Haase, V.H., Nizet, V., and Johnson, R.S. (2007). Regulation of iron homeostasis by the hypoxia-inducible transcription factors (HIFs). J. Clin. Invest. *117*, 1926–1932.

Pfützner, A., Kunt, T., Hohberg, C., Mondok, A., Pahler, S., Konrad, T., Lübben, G., and Forst, T. (2004). Fasting intact proinsulin is a highly specific predictor of insulin resistance in type 2 diabetes. Diabetes Care *27*, 682–687.

Pocock Oliver, R. (2008). Oxygen levels affect axon guidance and neuronal migration in Caenorhabditis elegans. Nat. Neurosci. *11*, 894–900.

Reboul, J., Vaglio, P., Tzellas, N., Thierry-Mieg, N., Moore, T., Jackson, C., Shin-i, T., Kohara, Y., Thierry-Mieg, D., Thierry-Mieg, J., et al. (2001). Open-reading-frame sequence tags (OSTs) support the existence of at least 17,300 genes in *C. elegans*. Nat. Genet. *27*, 332–336.

Ristow, M., Mulder, H., Pomplun, D., Schulz, T.J., Müller-schmehl, K., Krause, A., Fex, M., Puccio, H., Müller, J., Isken, F., et al. (2003). Frataxin deficiency in pancreatic islets causes diabetes due to loss of β cell mass. J. Clin. Invest. *112*, 527–534.

Roberts, A.F., Gumienny, T.L., Gleason, R.J., Wang, H., and Padgett, R.W. (2010). Regulation of genes affecting body size and innate immunity by the DBL-1/BMP-like pathway in *Caenorhabditis elegans*. BMC Dev. Biol. *10*, 1–10.

Romney, S.J., Thacker, C., and Leibold, E.A. (2008). An Iron Enhancer Element in the FTN-1 Gene Directs Iron-dependent Expression in *Caenorhabditis elegans* Intestine. J. Biol. Chem. *283* , 716–725.

Romney, S.J., Newman, B.S., Thacker, C., and Leibold, E. a (2011). HIF-1 regulates iron homeostasis in *Caenorhabditis elegans* by activation and inhibition of genes involved in iron uptake and storage. PLoS Genet. *7*, e1002394.

Rouault, T.A. (2015). Mammalian iron-sulphur proteins: novel insights into biogenesis and function. Nat. Rev. Mol. Cell. Biol. *16*, 45–55.

Salahudeen, A. a, Thompson, J.W., Ruiz, J.C., Ma, H.-W., Kinch, L.N., Li, Q., Grishin, N. V, and Bruick, R.K. (2009). An E3 ligase possessing an iron-responsive hemerythrin domain is a regulator of iron homeostasis. Science *326*, 722–726.

Sanchez, M., Galy, B., Schwanhaeusser, B., Blake, J., Bähr-Ivacevic, T., Benes, V., Selbach, M., Muckenthaler, M.U., and Hentze, M.W. (2011). Iron regulatory protein-1 and -2: transcriptome-wide definition of binding mRNAs and shaping of the cellular proteome by iron regulatory proteins. Blood *118*, e168–e179.

Sarov, M., Murray, J.I., Schanze, K., Pozniakovski, A., Niu, W., Angermann, K., Hasse, S., Rupprecht, M., Vinis, E., Tinney, M., et al. (2012). A genome-scale resource for in vivo tag-based protein function exploration in *C. elegans*. Cell *150*, 855–866.

Schulenburg, H., Hoeppner, M.P., Weiner, J., and Bornberg-Bauer, E. (2008). Specificity of the innate immune system and diversity of C-type lectin domain (CTLD) proteins in

the nematode Caenorhabditis elegans. Immunobiology *213*, 237–250.

Shapira, M., Hamlin, B.J., Rong, J., Chen, K., Ronen, M., and Tan, M.-W. (2006). A conserved role for a GATA transcription factor in regulating epithelial innate immune responses. Proc. Natl. Acad. Sci. U. S. A. *103*, 14086–14091.

Simcox, J.A., and McClain, D.A. (2016). Iron and diabetes risk. Cell Metab. *17*, 329–341.

Simmen, T., Lynes, E.M., Gesson, K., and Thomas, G. (2010). Oxidative Protein Folding in the Endoplasmic Reticulum: Tight Links to the Mitochondria-Associated Membrane (MAM). Biochim. Biophys. Acta *1798*, 1465–1473.

Simonsen, K.T., Møller-Jensen, J., Kristensen, A.R., Andersen, J.S., Riddle, D.L., and Kallipolitis, B.H. (2011). Quantitative proteomics identifies ferritin in the innate immune response of *C. elegans*. Virulence *2*, 120–130.

Simonsen, K.T., Gallego, S.F., Færgeman, N.J., and Kallipolitis, B.H. (2012). Strength in numbers: "Omics" studies of *C. elegans* innate immunity. Virulence *3*, 477–484.

Tan, M.W., Mahajan-Miklos, S., and Ausubel, F.M. (1999). Killing of *Caenorhabditis elegans* by *Pseudomonas aeruginosa* used to model mammalian bacterial pathogenesis. Proc. Natl Acad. Sci. USA *96*, 715–720.

Taubert, S., Ward, J.D., and Yamamoto, K.R. (2011). Nuclear hormone receptors in nematodes: evolution and function. Mol. Cell. Endocrinol. *334*, 49–55.

Tawe, W.N., Eschbach, M.L., Walter, R.D., and Henkle-Duhrsen, K. (1998). Identification of stress-responsive genes in *Caenorhabditis elegans* using RT-PCR differential display. Nucleic Acids Res. *26*, 1621–1627.

Tepper, R.G., Ashraf, J., Kaletsky, R., Kleemann, G., Murphy, C.T., and Bussemaker, H.J. (2013). PQM-1 complements DAF-16 as a key transcriptional regulator of DAF-2-mediated development and longevity. Cell *154*, 676–690.

Torti, F.M., and Torti, S. V (2002). Regulation of ferritin genes and protein. Blood *99*, 3505–3516.

Troemel, E.R. (2006). p38 MAPK regulates expression of immune response genes and contributes to longevity in *C. elegans*. PLoS Genet. *2*, e183.

Truksa, J., Lee, P., and Beutler, E. (2009). Two BMP responsive elements, STAT, and bZIP/HNF4/COUP motifs of the hepcidin promoter are critical for BMP, SMAD1, and HJV responsiveness. Blood *113*, 688–695.

Vashisht, A. a, Zumbrennen, K.B., Huang, X., Powers, D.N., Durazo, A., Sun, D.,

Bhaskaran, N., Persson, A., Uhlen, M., Sangfelt, O., et al. (2009). Control of iron homeostasis by an iron-regulated ubiquitin ligase. Science *326*, 718–721.

Visvikis, O., Ihuegbu, N., Labed, S.A., Luhachack, L.G., Alves, A.-M.F., Wollenberg, A.C., Stuart, L.M., Stormo, G.D., and Irazoqui, J.E. (2014). Innate host defense requires TFEB-mediated transcription of cytoprotective and antimicrobial genes. Immunity *40*, 896–909.

Ward, R.J., Zucca, F.A., Duyn, J.H., Crichton, R.R., and Zecca, L. (2014). The role of iron in brain ageing and neurodegenerative disorders. Lancet. Neurol. *13*, 1045–1060.

Wei, F.-Y., Suzuki, T., Watanabe, S., Kimura, S., Kaitsuka, T., Fujimura, A., Matsui, H., Atta, M., Michiue, H., Fontecave, M., et al. (2011). Deficit of tRNA(Lys) modification by Cdkal1 causes the development of type 2 diabetes in mice. J. Clin. Invest. *121*, 3598–3608.

Wessling-Resnick, M. (2010). Iron homeostasis and the inflammatory response. Annu. Rev. Nutr. *30*, 105–122.

Wiesenfahrt, T., Berg, J.Y., Osborne Nishimura, E., Robinson, A.G., Goszczynski, B., Lieb, J.D., and McGhee, J.D. (2016). The function and regulation of the GATA factor ELT-2 in the *C. elegans* endoderm. Development *143*, 483–491.

Wong, D., Bazopoulou, D., Pujol, N., Tavernarakis, N., and Ewbank, J.J. (2007). Genome-wide investigation reveals pathogen-specific and shared signatures in the response of *Caenorhabditis elegans* to infection. Genome Biol. *8*, R194.

Yuan, X., Ta, T.C., Lin, M., Evans, J.R., Dong, Y., Bolotin, E., Sherman, M.A., Forman, B.M., and Sladek, F.M. (2009). Identification of an endogenous ligand bound to a native orphan nuclear receptor. PLoS One *4*, e5609.

Zhang, P., Judy, M., Lee, S.-J., and Kenyon, C. (2013). Direct and indirect gene regulation by a life-extending FOXO protein in *C. elegans*: roles for GATA factors and lipid gene regulators. Cell Metab. *17*, 85–100.

Zhang, W., Feng, D., Li, Y., Iida, K., McGrath, B., and Cavener, D.R. (2006). PERK EIF2AK3 control of pancreatic beta cell differentiation and proliferation is required for postnatal glucose homeostasis. Cell Metab. *4*, 491–497.

Zhu, X., Orci, L., Carroll, R., Norrbom, C., Ravazzola, M., and Steiner, D.F. (2002). Severe block in processing of proinsulin to insulin accompanied by elevation of des-64,65 proinsulin intermediates in islets of mice lacking prohormone convertase 1/3. Proc. Natl. Acad. Sci. U. S. A. *99*, 10299–10304.

Zumbrennen-Bullough, K.B., Becker, L., Garrett, L., Holter, S.M., Calzada-Wack, J., Mossbrugger, I., Quintanilla-Fend, L., Racz, I., Rathkolb, B., Klopstock, T., et al. (2014).

Abnormal brain iron metabolism in Irp2 deficient mice is associated with mild neurological and behavioral impairments. PLoS One *9*, e98072.

CHAPTER 2

MECHANISMS OF IRON METABOLISM IN *CAERNORHABDITIS ELEGANS*

frontiers in
PHARMACOLOGY

REVIEW ARTICLE
published: 21 May 2014
doi: 10.3389/fphar.2014.00113

Mechanisms of iron metabolism in *Caenorhabditis elegans*

Cole P. Anderson and Elizabeth A. Leibold*

Department of Medicine, Division of Hematology and Hematologic Malignancies and Department of Oncological Sciences, University of Utah, Salt Lake City, UT, USA

Edited by:
Paolo Arosio, University of Brescia, Italy

Reviewed by:
Deliang Zhang, National Institute of Child Health and Human Development – National Institute of Health, USA
Deborah Chiabrando, University of Torino, Italy

***Correspondence:**
Elizabeth A. Leibold, Department of Medicine, Division of Hematology and Hematologic Malignancies and Department of Oncological Sciences, University of Utah, 15 N 203 E, Room 3240, Salt Lake City, UT 84112, USA
e-mail: betty.leibold@genetics.utah.edu

Iron is involved in many biological processes essential for sustaining life. In excess, iron is toxic due to its ability to catalyze the formation of free radicals that damage macromolecules. Organisms have developed specialized mechanisms to tightly regulate iron uptake, storage and efflux. Over the past decades, vertebrate model organisms have led to the identification of key genes and pathways that regulate systemic and cellular iron metabolism. This review provides an overview of iron metabolism in the roundworm *Caenorhabditis elegans* and highlights recent studies on the role of hypoxia and insulin signaling in the regulation of iron metabolism. Given that iron, hypoxia and insulin signaling pathways are evolutionarily conserved, *C. elegans* provides a genetic model organism that promises to provide new insights into mechanisms regulating mammalian iron metabolism.

Keywords: ferritin, DMT1, SMF-3, iron deficiency, hypoxia, hypoxia-inducible factor, insulin signaling, *C. elegans*

INTRODUCTION

Iron is essential due to its presence in proteins involved in key metabolic processes such as DNA synthesis, mitochondrial respiration, and oxygen transport. Regulation of cellular iron content is crucial as excess iron catalyzes the generation of reactive oxygen species that damage DNA and proteins, while cellular iron deficiency causes cell cycle arrest and cell death. Disruption of iron metabolism, by iron excess or iron deficiency, leads to common hematological, neurodegenerative, and metabolic diseases (Fleming and Ponka, 2012). As a consequence, organisms have developed strategies to sense, transport and store this metal.

Our understanding of the mechanisms that regulate iron metabolism has advanced through the use of model organisms. Physiological and genetic studies in transgenic mice have revealed the mechanism regulating systemic iron metabolism by the ferroportin–hepcidin axis. *Saccharomyces cerevisiae* have been used to unravel the complex pathways involved in Fe-S cluster synthesis (Lill and Muhlenhoff, 2008), while zebrafish have been critical in the identification of genes involved in hematopoiesis (Shafizadeh and Paw, 2004). More recently, the soil nematode *Caenorhabditis elegans* has emerged as a model of iron metabolism. The advantages of *C. elegans* include a short generation time and life span, the feasibility of genetic screens and the opportunity to study physiological processes in a whole organism context. *C. elegans* orthologs have been identified for many human genes (Shaye and Greenwald, 2011) and many of the key genes and pathways regulating mammalian iron metabolism are conserved in *C. elegans*. The genetic tractability of *C. elegans* can provide a complementary approach to mammalian systems to identify novel genes and unravel complex pathways involved in iron metabolism. This review provides an overview of our current understanding of iron metabolism in *C. elegans*, how iron metabolism integrates with oxygen and insulin signaling, and how this genetic model can provide insights in mammalian iron metabolism.

CONSERVATION OF IRON METABOLISM IN *C. ELEGANS*

All organisms must maintain cellular iron content within a narrow range to avoid the adverse consequences of iron depletion or excess. This is accomplished in vertebrates by precise mechanisms that regulate iron uptake, storage and efflux (Andrews and Schmidt, 2007; Zhang and Enns, 2009; **Figure 1**). Mammals acquire iron solely from the diet. Dietary non-heme iron is reduced by membrane bound ferrireductases (e.g. DCYTB, also known as CYBRD) and transported across the apical membrane of intestinal enterocytes by divalent-metal transporter 1 (DMT1, also known as NRAMP2, SLC11A2 and DCT1; Mackenzie and Garrick, 2005; Shawki et al., 2012). Iron is released into a cellular labile iron pool thought to consist of low molecular weight iron complexes. This pool is kept small due to the ability of iron to catalyze the production of reactive oxygen species. Iron is utilized by the mitochondria for Fe-S cluster and heme biosynthesis, and by iron-containing proteins in the cytosol and nucleus. Iron is exported across the basolateral membrane into the circulation by ferroportin (FPN1, also known as SLC40A1, IREG1 and MTP1) in concert with its oxidation by the multicopper oxidase hephaestin (HEPH). Iron enters the circulation where it binds with high affinity to transferrin for delivery to cells expressing transferrin receptor 1 (TfR1, also known as TFRC). TfR1-transferrin-Fe(III) complexes are internalized by receptor mediated endocytosis. Iron is released from transferrin, reduced to Fe(II) by the ferrireductase STEAP3 and transported across the endosomal membrane to the cytoplasm by DMT1. Thus, DMT1 is essential in intestinal non-heme iron absorption as well as transport of endosomal iron released by transferrin into the cytoplasm. Although most cell types express TfR1, erythroid

precursors are dependent on Tf-TfR1-DMT1 for iron uptake as disruption of *Tfrc* gene in mice (Levy et al., 1999) or mice with reduced transferrin (Trenor et al., 2000) developed severe anemia. DMT1 mutations in humans (Shawki et al., 2012), the *mk* mouse (Fleming et al., 1997), and the Belgrade rat (Fleming et al., 1998) also cause a severe microcytic hypochromic anemia, underscoring the importance of DMT1 in intestinal and erythroid iron acquisition.

Mammals can also acquire iron by the intestinal absorption of heme iron that comes primarily from animal sources. Although several heme importers have been identified (Yuan et al., 2013), the mechanism regulating intestinal heme import is not well understood. It is likely that heme oxygenase 1 releases iron from dietary heme, which is then exported by ferroportin into the circulation.

When body iron stores are high, cytosolic iron is not exported, and is instead sequestered in ferritin in an inert form unable to catalyze free radical formation (Harrison and Arosio, 1996; Torti and Torti, 2002; Theil, 2011). After 3 days, iron in ferritin is lost by enterocyte sloughing into the intestinal lumen. The regulation of intestinal ferritin is crucial as it serves as a cellular iron "sink" to limit efflux of iron into the circulation (Vanoaica et al., 2010; Galy et al., 2013). Because there is no regulated mechanism for iron excretion, precise regulation of intestinal iron uptake and storage is required. Given the fundamental nature of iron metabolism, it is not surprising that many proteins involved in intestinal iron uptake, storage and export are highly conserved between *C. elegans* and mammals. *C. elegans* express orthologs for DMT1 (SMF-3), ferritin (FTN-1, FTN-2), and ferroportin (FPN-1.1, FPN-1.2, FPN-1.3; **Figure 1**). The *C. elegans* genome also encodes potential orthologs for DCYTB ferrireductase and hephaestin multicopper oxidase. The intestinal anatomy in *C. elegans* is similar to vertebrates in that they contain an apical brush border facing the lumen and a basolateral membrane facing the interstitial space (circulation in mammals) (McGhee, 2013) (**Figure 1**). The intestine serves as the major site for absorption of dietary nutrients and a defense against xenobiotics and pathogens. *C. elegans* lack adipose tissue, liver, and pancreas and the intestine fulfills these functions by serving as a major site of lipid and glucose metabolism. Unlike mammals, *C. elegans* are heme auxotrophs and are dependent on acquiring heme from the environment (Rao et al., 2005; Hamza and Dailey, 2012; Yuan et al., 2013).

SMF-3 is the principal intestinal Fe(II) transporter in *C. elegans*. Consistent with its role in intestinal iron transport, SMF-3 is highly expressed at the apical membrane of intestinal epithelium (Au et al., 2009; Bandyopadhyay et al., 2009), transcriptionally activated during iron deficiency (Romney et al., 2011) and loss of SMF-3 expression leads to reduced iron content in *smf-3(ok1035)* null mutants (Romney et al., 2011). SMF-3 also transports Mn(II) as demonstrated by reduced Mn content in *smf-3(ok1035)* mutants (Romney et al., 2011), increased tolerance of *smf-3(ok1035)* mutants to Mn overload (Au et al., 2009) and Mn-mediated reduction in *smf-3* mRNA and SMF-3 protein in intestine (Au et al., 2009; Settivari et al., 2009). Like SMF-3, DMT1 transports Mn(II), which competes with Fe(II) uptake (Gunshin et al., 1997; Illing et al., 2012). The DMT1-deficient Belgrade rat displays impaired Mn uptake in intestine and erythroid precursors consistent with a physiological role for DMT1 in Mn uptake in mammals (Chua and Morgan, 1997). In excess, manganese is toxic, and in humans chronic occupational nasopulmonary exposure to Mn causes a neurological disease known as manganism (Roth and Garrick, 2003). Because Mn(II) and Fe(II) compete for DMT1 transport, this suggests that iron deficiency may be an important factor in the predisposition to Mn toxicity. Consistent with this are

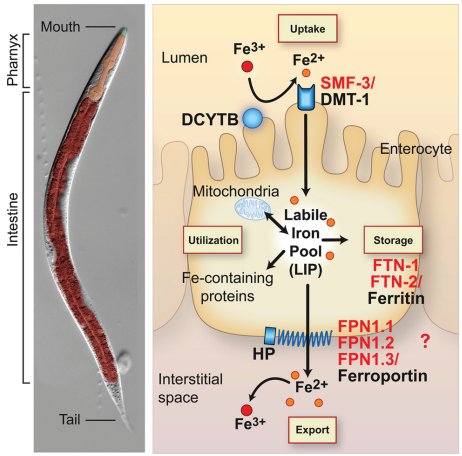

FIGURE 1 | Conservation of intestinal iron metabolism in mammals and *Caenorhabditis elegans*. *C. elegans* anatomy is shown in the *left panel*. The body plan of *C. elegans* is made up of two concentric tubes separated by the interstitial space (pseudocoelum). The inner tube consists of the intestine and the outer tube consists of cuticle, hypodermis, muscle and nervous tissue. The digestive tract is an epithelial tube containing the mouth, pharynx (foregut) and intestine (midgut). *Right panel*, an intestinal epithelial cell is shown with an apical brush border membrane facing the lumen and a basolateral membrane facing the interstitial space or blood in mammals. Mammalian proteins (black) and *C. elegans* orthologs (red) are indicated. Dietary non-heme iron is reduced by ferrireductases (e.g. DCYTB1) and transported across the apical intestinal membrane by SMF-3/DMT1. Cytosolic iron is incorporated in iron-containing proteins and transported to mitochondria for Fe-S cluster biosynthesis and heme biosynthesis in mammals. *C. elegans* are heme auxotrophs and are dependent on acquiring heme from the environment (Rao et al., 2005). Iron is also exported across the basolateral membrane into the interstitial space (blood in mammals) by FPN-1.1, FPN-1.2, FPN-1.3/ferroportin. Ferroportin is the sole iron exporter in mammals, whereas *C. elegans* express three orthologs whose specific functions in iron export are not well understood. Iron export by ferroportin is coupled to the oxidation of iron by the multicopper oxidase hephaestin (HEPH). The *C. elegans* genome harbors putative *DCYTB* and *HEPH* homologs. Iron not utilized or exported is stored in FTN-1, FTN-2/ferritin. Iron deficiency stabilizes *C. elegans* HIF-1 and mammalian HIF-2α, leading to the transcriptional activation of *smf-3/DMT1* to increase iron absorption. Mammalian DCYTB and ferroportin are also activated by HIF-2α during iron deficiency. HIF-1 regulation of *C. elegans* DCYTB and FPN-1-1, FPN1.2, and FPN-1.3 orthologs remains to be determined. Iron deficiency reduces ferritin abundance in *C. elegans* and mammals by different mechanisms: *C. elegans* lack the IRP-IRE network and ferritin is transcriptionally repressed by HIF-1, whereas mammalian ferritin is translationally repressed by IRPs.

studies showing that iron deficiency is associated with increased Mn content in the brain of rats (Chua and Morgan, 1996; Erikson et al., 2002), in the olfactory epithelium of the DMT1-deficient Belgrade rat (Thompson et al., 2007) and in serum of humans with anemia or an iron deficient diet (Davis et al., 1992; Rahman et al., 2013).

Caenorhabditis elegans also express DMT1-like proteins SMF-1 and SMF-2 that share about 55–58% amino acid identity with DMT1 (Settivari et al., 2009). SMF-1 is widely expressed, but showed high expression in the apical intestinal membrane (Au et al., 2009; Bandyopadhyay et al., 2009), whereas SMF-2 is mainly cytoplasmic with high expression in pharyngeal epithelium (Au et al., 2009). *smf-3* and *smf-1* are transcriptionally induced upon exposure to pathogenic *Staphylococcus aureus,* and *smf-3(ok1035)*, and *smf-1(ok1748)* mutants showed hypersensitivity to this pathogen, indicating a role for these proteins in innate immunity (Bandyopadhyay et al., 2009). Like *smf-3*, exposure to high Mn reduces *smf-1* and *smf-2* mRNA levels, suggesting that reduced expression of these transporters may be a mechanism to reduce Mn toxicity (Settivari et al., 2009). This is consistent with a study showing that SMF-1 expression in dopamine neurons contributes to Mn^{2+}-mediated neuronal death (Settivari et al., 2009). The roles of SMF-1 and SMF-2 in iron metabolism are not well understood; however, unlike *smf-3* mutant worms, iron and manganese content were not significantly reduced in *smf-1* and *smf-2* mutants compared to wildtype worms consistent with a prominent role of SMF-3 in iron and manganese transport (Romney et al., 2011).

The mechanism regulating basolateral transfer of iron to the interstitial space and to tissues in *C. elegans* is not known. In mammals, ferroportin is the sole exporter of iron to the circulation. *C. elegans* express three ferroportin orthologs, FPN1.1, FPN-1.2, and FPN-1.3, but their specific roles in iron export remains to be determined.

Caenorhabditis elegans express genes orthologous to human ferritin heavy subunit (*FTH*) and ferritin light subunit (*FTL*) genes. Ferritin is a ubiquitously expressed protein that stores iron in a form that is unable to generate free radicals. Mammalian ferritin is composed of a mixture of 24 FTL and FTH subunits that form a shell containing up to 4500 iron atoms (Theil, 2013). FTH exhibits ferroxidase activity that facilitates oxidation of iron, while FTL participates with FTH in the nucleation of iron (Bou-Abdallah, 2010; Liu and Theil, 2005). *C. elegans* FTN-1 and FTN-2 are more similar to human FTH than to FTL and both FTN-1 and FTN-2 contain ferroxidase active-site residues (Gourley et al., 2003). *ftn-1* is highly expressed in intestine whereas *ftn-2* is expressed in many tissues such as pharynx, body-wall muscle, hypodermis and intestine (Gourley et al., 2003; Kim et al., 2004). *ftn-1,* and to a lesser extent *ftn-2*, are induced by high iron exposure (Gourley et al., 2003; Kim et al., 2004). Only *ftn-1* mutants are iron sensitive and have reduced lifespans when exposed to high iron (Kim et al., 2004; Valentini et al., 2012).

Iron induces ferritin expression in mammals and in *C. elegans*, but the mechanism regulating ferritin differs in these organisms. In mammals, ferritin is primarily regulated at the translational level by iron-regulatory proteins 1 and 2 (IRP1 and IRP2) (Hentze et al., 2010; Anderson et al., 2012). During iron deficiency, IRPs bind to an RNA stem-loop known as the iron-responsive element (IRE) in the 5′ untranslated regions of *FTH* and *FTL* mRNAs to repress ferritin synthesis. When cellular iron increases, IRP1 is converted to its Fe-S cluster aconitase form concomitant with loss of RNA-binding activity, while IRP2 is targeted for ubiquitination and proteasomal degradation causing ferritin synthesis to increase (Salahudeen et al., 2009; Vashisht et al., 2009). *C. elegans* lack the IRP-IRE system, but express a cytosolic aconitase (ACO-1; Gourley et al., 2003; Kim et al., 2004). ACO-1 is homologous to mammalian IRP1 and its aconitase activity is regulated by iron, but unlike IRP1, it lacks RNA-binding ability. Despite lacking IRP-IRE regulation, *C. elegans* have evolved unique mechanisms to regulate iron storage.

HIF-1 REGULATES IRON UPTAKE AND STORAGE DURING IRON DEFICIENCY

In *C. elegans*, hypoxia signaling is the predominant mechanism for regulating iron metabolism (Romney et al., 2011; Ackerman and Gems, 2012). Hypoxia signaling is a highly conserved process that conditions organisms to low oxygen and iron environments by regulating diverse biologic processes, including glucose metabolism, angiogenesis and iron metabolism (Semenza, 2007; Kaelin and Ratcliffe, 2008). During iron deficiency in mammals, hypoxia-inducible factor 2α (HIF-2α, also known as EPAS1) activates the transcription of *DMT1*, *FPN1* and *DCYTB* genes in the intestine to increase iron absorption (Taylor et al., 2011; Mastrogiannaki et al., 2009; Shah et al., 2009). Hypoxia-inducible factors (HIF-1 and HIF-2) are basic helix-loop-helix (bHLH) transcription factors that consist of oxygen-regulated α subunits (HIF-1α and HIF-2α) and a constitutively expressed β subunit (HIF-1β, also known as aryl hydrocarbon nuclear translocator or ARNT) (Semenza, 2007; Kaelin and Ratcliffe, 2008; Kaluz et al., 2008). Under normal conditions, in the presence of oxygen and iron, HIF-α subunits are hydroxylated by prolyl hydroxylase (PHD2, also known as EGLN1) whose activity is dependent upon oxygen and iron. Hydroxylated HIF-α is targeted for proteasomal degradation by the E3 ubiquitin ligase von Hippel Lindau tumor suppressor protein (VHL) (Ivan et al., 2001). During hypoxia or iron deficiency, PHDs are inactive, thus allowing HIF-α subunits to translocate to the nucleus, dimerize with HIF-1β and recruit coactivators to activate target gene expression in pathways such as erythropoiesis, iron metabolism, glucose metabolism and angiogenesis (Semenza, 2007; Kaelin and Ratcliffe, 2008; Kaluz et al., 2008). HIF-1α and HIF-2α regulate overlapping, but distinct sets of target genes (Kaluz et al., 2008). For example, only HIF-2α is responsible for the coordinate upregulation of *DMT1*, *DCYTB* and *FPN1* in intestine during iron deficiency (Mastrogiannaki et al., 2009; Shah et al., 2009; Taylor et al., 2011). HIF-2α regulation of intestinal iron metabolism during iron deficiency ensures that sufficient iron is absorbed and delivered to the bone marrow for production of red blood cells (Shah and Xie, 2014).

The HIF signaling pathway is conserved in *C. elegans. C. elegans* express HIF-1, AHA-1, VHL-1, and EGL-9, which are orthologs of HIF-1α/HIF-2α, HIF-1β, VHL and PHD, respectively, in vertebrates (Epstein et al., 2001; Jiang et al., 2001). Unlike mammals, *C. elegans* express a single *hif-1* gene that shares homology to *HIF1α*

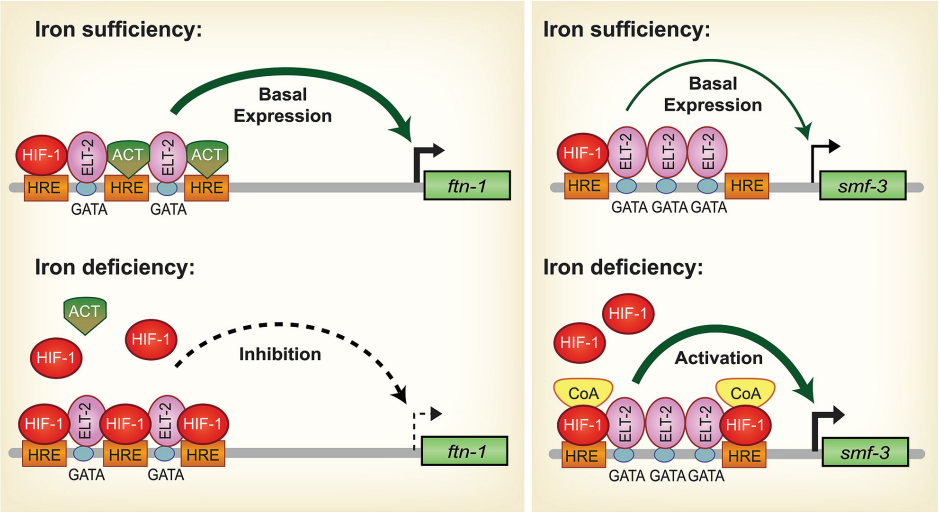

FIGURE 2 | Model for HIF-1 iron-dependent activation and inhibition of intestinal iron uptake and storage in *C. elegans*. *Iron sufficiency*: ELT-2 binds to GATA binding sites located in the *ftn-1* and *ftn-2* IDEs. We propose that ELT-2 cooperates with an unidentified transcriptional activator (ACT) that binds to the hypoxia-response elements (HREs) to regulate transcription. As HREs resemble E-box elements, which are binding sites for bHLH transcription factors, it is possible that a bHLH transcription factor serves this role. *smf-3* is transcribed at basal levels during iron sufficiency to limit iron absorption. HIF-1 is expressed during normal growth conditions, but at low levels. *Iron deficiency*: HIF-1 accumulates and dimerizes with AHA-1. HIF-1/AHA-1 (denoted by HIF-1) displaces the transcriptional activator ACT binding to the *ftn-1* and *ftn-2* HREs and inhibits transcription. Another possible mechanism for HIF-1 mediated *ftn-1* repression is the displacement of ELT-2 by HIF-1. HIF-1/AHA-1 binds to the *smf-3* HREs, recruits coactivators (CoA) and cooperates with ELT-2 to activate *smf-3* transcription. Whether ELT-2 is bound to the *ftn-1* GATA sites during iron deficiency and to the *smf-3* GATA sites during iron sufficiency has not been determined. (Adapted from Romney et al., 2011).

and *HIF2α* (Jiang et al., 2001). HIF-1 functions in a variety of biological processes ranging from stress response, innate immunity, neuronal development, ageing and iron metabolism as discussed below (Shen et al., 2005; Chang and Bargmann, 2008; Pocock and Hobert, 2008; Luhachack et al., 2012; Jones et al., 2013).

During iron deficiency, *ftn-1* and *ftn-2* transcription is repressed and is dependent upon a *cis*-regulatory element termed the iron-dependent enhancer (IDE) located in the *ftn-1* and *ftn-2* promoters (Kim et al., 2004; Romney et al., 2008) (**Figure 2**). Basal expression of *ftn-1* and *ftn-2* is mediated by the intestinal GATA transcription factor ELT-2 that binds GATA sites located in ferritin IDEs (Romney et al., 2008). Further studies revealed that HIF-1 binds to hypoxia response elements (HREs) located in the IDEs of *ftn-1* and *ftn-2* to repress transcription during iron deficiency (Romney et al., 2011; Ackerman and Gems, 2012). Intestinal iron uptake through SMF-3 is also regulated by HIF-1 during iron deficiency. Similar to *ftn-1* and *ftn-2* IDEs, *smf-3* contains an IDE in its promoter that contains HRE binding sites that confer HIF-1 dependent activation during iron deficiency (Romney et al., 2011) (**Figure 2**). Romney et al. (2011) also showed that *hif-1 (ia04)* mutants have reduced iron and manganese content and are developmentally delayed when grown in iron deficient conditions. Notably, development of *hif-1(ia04)* mutants was restored when the cellular iron pool was increased by RNAi depletion of *ftn-1* and *ftn-2*. It is not known whether the ferroportin homologs *fpn-1.1*, *fpn-1.2* and *fpn-1.3* and *DCYTB* homologs are regulated by hypoxia. These studies show that regulation of iron uptake and storage by HIF-1 is crucial for ensuring proper growth and development during iron deficiency.

HIF-1 is well known as a transcriptional activator but less is known about its role as a transcriptional repressor. The question arises regarding the mechanism of HIF-1 transcriptional repression of *ftn-1* and *ftn-2*. Chromatin immunoprecipitation analysis and electrophoretic mobility gel assays showed direct HIF-1 binding to the *ftn-1* IDE (Romney et al., 2011; Ackerman and Gems, 2012). Another study showed that mutations of all three HREs in the *ftn-1* IDE abolished expression of a *pftn-1::gfp* transcriptional reporter, suggesting that an activator may bind the HREs during normal conditions (Romney et al., 2011; **Figure 2**). HREs resemble E-box elements and it is possible that this activator may be a member of the basic helix loop helix (bHLH) transcription factor family that can bind to non-canonical E-boxes (Kewley et al., 2004). A MAD-like transcription factor MDL-1 was identified in an RNAi screen as a

transcriptional activator of *ftn-1* expression (Ackerman and Gems, 2012). *mdl-1* encodes a bHLH transcription factor that bind E-box sequences as a dimer with MXL-1 to regulate target genes(Yuan et al., 1998). MDL-1 transcriptional regulation of *ftn-1* was shown to be iron independent (Ackerman and Gems, 2012), suggesting the possibility that MDL-1 may bind to the *ftn*-1 and *ftn-2* HREs when iron is sufficient, but is displaced by HIF-1 when iron is low. Alternatively, it is possible that during iron deficiency the displacement of ELT-2 from its GATA binding sites by HIF-1 results in decreased *ftn-1* and *ftn-2* transcription. Further work is required to define this mechanism. In mammals, ferritin has not been reported to be regulated by HIF-2α; however, hypoxia regulates ferritin expression by altering IRP1 RNA binding activity and IRP2 protein abundance (Schneider and Leibold, 2003; Meyron-Holtz et al., 2004; Salahudeen et al., 2009; Vashisht et al., 2009).

FERRITIN REGULATION BY THE INSULIN/INSULIN-LIKE GROWTH FACTOR SIGNALING PATHWAY

Ferritin is regulated by the insulin/insulin-like (IIS) growth factor signaling pathway in *C. elegans.* The IIS pathway is a conserved pathway in vertebrates and *C. elegans* that coordinates nutrient availability with development, metabolism and stress responses (Accili and Arden, 2004; **Figure 3**). When nutrients are available, insulin and insulin-like growth (IGF) factors activate tyrosine kinase receptors DAF-2/IGFR1, triggering a kinase cascade that leads to the phosphorylation of the Forkhead box, Class O (FOXO) transcription factor DAF-16/FOXO and its cytoplasmic retention and inhibition. When IIS is reduced during nutrient deprivation, DAF-16/FOXO phosphorylation is reduced, promoting DAF-16/FOXO translocation to the nucleus where it regulates the expression of target genes involved in stress resistance, metabolism, and innate immunity (Murphy and Hu, 2013). A recent study showed that *ftn-1* expression was elevated in *daf-2* mutants compared to *daf-16;daf-2* mutants, indicating that DAF-16 activated *ftn-1* expression (Ackerman and Gems, 2012). Further genetic studies showed that *hif-1* and *daf-16* act in parallel pathways to regulate *ftn-1* and that DAF-16 regulation of *ftn-1* was not iron dependent (Ackerman and Gems, 2012). Less is known about the role of IIS in *smf-3* regulation. One study showed that glucose treatment induced the *smf-3* expression, suggesting a potential role for IIS and DAF-16 in *smf-3* downregulation (Lee et al., 2009). Reduced IIS leads to DAF-16 dependent upregulation and downregulation of a diverse set of genes, which are designated as class 1 and class II genes, respectively (Lee et al., 2003; McElwee et al., 2003; Oh et al., 2006). More recently, the transcription factor PQM-1 was discovered to regulate class II genes by binding to the DAF-16 associated element (DAE) located in the promoter of these genes, whereas DAF-16 regulates class 1 genes by binding to the DAF-16 binding element (DBE; Tepper et al., 2013). The *smf-3* promoter contains both DBE and DAE binding sites, but whether DAF-16 or PQM-1 regulates *smf-3* awaits future studies. Taken together, these studies suggest that DAF-16 activation of *ftn-1* during reduced IIS provides *C. elegans* with a mechanism to increase iron storage, thereby limiting iron toxicity during stress conditions (**Figure 3**). When IIS is stimulated, DAF-16 is inhibited and *ftn-1* transcription is reduced,

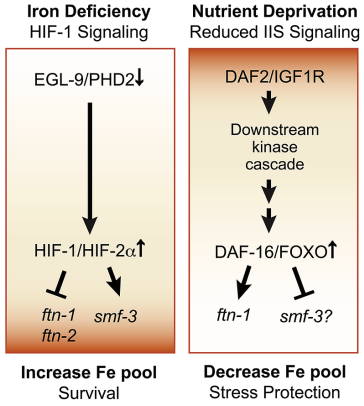

FIGURE 3 | Pathways regulating cellular iron metabolism in *C. elegans*. *Iron deficiency-HIF-1 pathway*: this pathway is activated in response to iron deficiency or hypoxia and results in HIF-1 dependent repression of *ftn-1* and *ftn-2* and activation of *smf-3*. This leads to reduced iron storage and increased iron uptake, ultimately increasing the cellular iron pool and promoting survival during iron limitation. *Insulin/insulin growth factor-1 (IGF-1) signaling (IIS) pathway:* the IIS pathway is a conserved pathway in worms, flies and in vertebrates that regulates the transcription factor DAF-16/FOXO. DAF-16/FOXO regulates genes in essential processes, such as metabolism, stress resistance, pathogen defense and lifespan extension. Activated IIS initiates a phosphorylation cascade that leads to the cytoplasmic retention of DAF-16/FOXO and inhibits its function. Nutrient deprivation reduces IIS leading to the nuclear localization of DAF-16 to activate *ftn-1*. Glucose upregulates *smf-3* expression, but whether DAF-16 directly regulates *smf-3* remains to be determined. This pathway provides a mechanism to increase cellular iron by reducing *ftn-1* when nutrients are abundant to promote growth and to reduce cellular iron during stress by increasing *ftn-1* to limit iron-catalyzed oxidative stress.

increasing the availability of iron required for development and growth

Insulin signaling and FOXO regulation of mammalian ferritin has not been reported. However, mammalian ferritin is transcriptionally activated by oxidative stress (Thimmulappa et al., 2002; Pietsch et al., 2003a,b; Hintze and Theil, 2005) and repressed by oncogenes, providing a mechanism to sequester iron during stress and to increase iron availability during cell proliferation (Tsuji et al., 1993, 1995; Wu et al., 1999). Similarly, several studies have shown that ferritin depletion stimulates cell proliferation by increasing available iron, whereas sequestration of iron by ferritin overexpression slows cell proliferation (Cozzi et al., 2000; Kakhlon et al., 2001; Cozzi et al., 2004; Baldi et al., 2005). Like *C. elegans*, changes in ferritin expression in response to environmental stimuli are essential for survival during stress and growth during normal conditions.

OTHER REGULATORS OF FERRITIN EXPRESSION

ftn-1 transcription has also been shown to be repressed by the REF-1-like protein HLH-29 (Quach et al., 2013) and UNC-62 a member of the TALE family of homeobox transcription factors (Catoire

et al., 2011; Ackerman and Gems, 2012). HLH-29 is homologous to the HairyVEnhancer of Split (HES) transcription factors that regulate embryonic development through Notch-dependent and independent pathway (Fischer and Gessler, 2007). HLH-29 was recently shown to bind promoter sequences upstream of the *ftn-1* IDE and repress its transcriptional expression independent of the iron responsive HIF pathway (Quach et al., 2013). Additionally, *hlh-29* mutants have elevated levels of *ftn-1* and are resistant to peroxide stress. Further studies are needed to define the mechanism and significance of this regulation.

unc-62 encodes the mammalian ortholog of MEIS1 that has a crucial role in normal development and in leukemia (Azcoitia et al., 2005; Argiropoulos et al., 2007). MEIS1 has also been identified as a Restless Leg Syndrome (RLS) predisposing gene (Winkelmann et al., 2007; Xiong et al., 2009; Spieler et al., 2014). RLS is a sensorimotor disorder that is associated with iron insufficiency in brain, but the role of iron in RLS is not well understood (Clardy et al., 2006; Allen and Earley, 2007; Catoire et al., 2011). It is of interest that *ftn-1* expression is significantly decreased in *C. elegans* treated with *unc-62* RNAi (Ackerman and Gems, 2012), suggesting that dysregulation of MEIS-1/MEIS can lead to altered iron metabolism.

Ferritin regulation spans beyond iron and nutrient stress. For instance, *ftn-2*, but not *ftn-1*, was shown to be necessary for proper innate immune response to pathogenic *S. aureus* (Simonsen et al., 2011). During infection, *ftn-2* was also transcriptionally upregulated along with several DAF-16 targets. It is likely that DAF-16 activates *ftn-2* to protect *C. elegans* from bacterial infection by limiting iron availability.

CONCLUDING REMARKS

We have highlighted recent studies showing the potential of *C. elegans* as a useful genetic platform to explore mechanisms integrating iron and oxygen metabolism. Future genomic studies are needed to identify additional target genes of HIF-1 that are specific to hypoxia or iron deficiency and the unique HIF-1 partner proteins that coordinate these responses. A better understanding of how iron and insulin signaling are coordinated in *C. elegans* could provide new knowledge about the role of iron in glucose metabolism and in the pathogenesis of diabetes in humans. Finally, these studies have set a foundation for the development of genetic screens to identify novel regulators that are involved in iron sensing, uptake, storage and utilization. *C. elegans* holds promise as a system to decipher complex pathways regulating iron metabolism that can be followed up in mammals.

ACKNOWLEDGMENTS

This work was supported by the National Institute of Health grants R01GM45201 and R01DK068602 to Elizabeth A. Leibold. Cole P. Anderson was supported by National Institute of Health Research Training in Hematology grant T32DK007115. We thank Dr. Paul Rindler for critical comments on the manuscript and Ms. Diana Lim for help with illustrations.

REFERENCES

Accili, D., and Arden, K. C. (2004). FoxOs at the crossroads of cellular metabolism, differentiation, and transformation. *Cell* 117, 421–426. doi: 10.1016/S0092-8674(04)00452-0

Ackerman, D., and Gems, D. (2012). Insulin/IGF-1 and hypoxia signaling act in concert to regulate iron homeostasis in *Caenorhabditis elegans*. *PLoS Genet.* 8:e1002498. doi: 10.1371/journal.pgen.1002498

Allen, R. P., and Earley, C. J. (2007). The role of iron in restless legs syndrome. *Movem. Disord.* 22(Suppl. 18), S440–S448. doi: 10.1002/mds.21607

Anderson, C. P., Shen, M., Eisenstein, R. S., and Leibold, E. A. (2012). Mammalian iron metabolism and its control by iron regulatory proteins. *Biochim. Biophys. Acta* 1823, 1468–1483. doi: 10.1016/j.bbamcr.2012.05.010

Andrews, N. C., and Schmidt, P. J. (2007). Iron homeostasis. *Annu. Rev. Physiol.* 69, 69–85. doi: 10.1146/annurev.physiol.69.031905.164337

Argiropoulos, B., Yung, E., and Humphries, R. K. (2007). Unraveling the crucial roles of Meis1 in leukemogenesis and normal hematopoiesis. *Genes Dev.* 21, 2845–2849. doi: 10.1101/gad.1619407

Au, C., Benedetto, A., Anderson, J., Labrousse, A., Erikson, K., Ewbank, J. J., et al. (2009). SMF-1, SMF-2 and SMF-3 DMT1 orthologues regulate and are regulated differentially by manganese levels in *C. elegans*. *PLoS ONE* 4:e7792. doi: 10.1371/journal.pone.0007792

Azcoitia, V., Aracil, M., Martinez, A. C., and Torres, M. (2005). The homeodomain protein Meis1 is essential for definitive hematopoiesis and vascular patterning in the mouse embryo. *Dev. Biol.* 280, 307–320. doi: 10.1016/j.ydbio.2005.01.004

Baldi, A., Lombardi, D., Russo, P., Palescandolo, E., De Luca, A., Santini, D., et al. (2005). Ferritin contributes to melanoma progression by modulating cell growth and sensitivity to oxidative stress. *Clin. Cancer Res.* 11, 3175–3183. doi: 10.1158/1078-0432.CCR-04-0631

Bandyopadhyay, J., Song, H. O., Park, B. J., Singaravelu, G., Sun, J. L., Ahnn, J., et al. (2009). Functional assessment of Nramp-like metal transporters and manganese in *Caenorhabditis elegans*. *Biochem. Biophys. Res. Commun.* 390, 136–141. doi: 10.1016/j.bbrc.2009.09.082

Bou-Abdallah, F. (2010). The iron redox and hydrolysis chemistry of the ferritins. *Biochim. Biophys. Acta* 1800, 719–731. doi: 10.1016/j.bbagen.2010.03.021

Catoire, H., Dion, P. A., Xiong, L., Amari, M., Gaudet, R., Girard, S. L., et al. (2011). Restless legs syndrome-associated MEIS1 risk variant influences iron homeostasis. *Ann. Neurol.* 70, 170–175. doi: 10.1002/ana.22435

Chang, A. J., and Bargmann, C. I. (2008). Hypoxia and the HIF-1 transcriptional pathway reorganize a neuronal circuit for oxygen-dependent behavior in *Caenorhabditis elegans*. *Proc. Natl. Acad. Sci. U.S.A.* 105, 7321–7326. doi: 10.1073/pnas.0802164105

Chua, A. C., and Morgan, E. H. (1996). Effects of iron deficiency and iron overload on manganese uptake and deposition in the brain and other organs of the rat. *Biol. Trace Elem. Res.* 55, 39–54. doi: 10.1007/BF02784167

Chua, A. C., and Morgan, E. H. (1997). Manganese metabolism is impaired in the Belgrade laboratory rat. *J. Comp. Physiol. B* 167, 361–369. doi: 10.1007/s003600050085

Clardy, S. L., Earley, C. J., Allen, R. P., Beard, J. L., and Connor, J. R. (2006). Ferritin subunits in CSF are decreased in restless legs syndrome. *J. Lab. Clin. Med.* 147, 67–73. doi: 10.1016/j.lab.2005.06.011

Cozzi, A., Corsi, B., Levi, S., Santambrogio, P., Albertini, A., and Arosio, P. (2000). Overexpression of wild type and mutated human ferritin H-chain in HeLa cells: in vivo role of ferritin ferroxidase activity. *J. Biol. Chem.* 275, 25122–25129. doi: 10.1074/jbc.M003797200

Cozzi, A., Corsi, B., Levi, S., Santambrogio, P., Biasiotto, G., and Arosio, P. (2004). Analysis of the biologic functions of H- and L-ferritins in HeLa cells by transfection with siRNAs and cDNAs: evidence for a proliferative role of L-ferritin. *Blood* 103, 2377–2383. doi: 10.1182/blood-2003-06-1842

Davis, C. D., Malecki, E. A., and Greger, J. L. (1992). Interactions among dietary manganese, heme iron, and nonheme iron in women. *Am. J. Clin. Nutr.* 56, 926–932.

Epstein, A. C., Gleadle, J. M., McNeill, L. A., Hewitson, K. S., O'Rourke, J., Mole, D. R., et al. (2001). *C. elegans EGL-9* and mammalian homologs define a family of dioxygenases that regulate HIF by prolyl hydroxylation. *Cell* 107, 43–54. doi: 10.1016/S0092-8674(01)00507-4

Erikson, K. M., Shihabi, Z. K., Aschner, J. L., and Aschner, M. (2002). Manganese accumulates in iron-deficient rat brain regions in a heterogeneous fashion and is associated with neurochemical alterations. *Biol. Trace Elem. Res.* 87, 143–156. doi: 10.1385/BTER:87:1-3:143

Fischer, A., and Gessler, M. (2007). Delta-Notch – and then? Protein interactions and proposed modes of repression by Hes and Hey bHLH factors. *Nucleic Acids Res.* 35, 4583–4596. doi: 10.1093/nar/gkm477

Fleming, M. D., Romano, M. A., Su, M. A., Garrick, L. M., Garrick, M. D., and Andrews, N. C. (1998). Nramp2 is mutated in the anemic Belgrade (b) rat: evidence of a role for Nramp2 in endosomal iron transport. *Proc. Natl. Acad. Sci. U.S.A.* 95, 1148–1153. doi: 10.1073/pnas.95.3.1148

Fleming, M. D., Trenor, C. C. III, Su, M. A., Foernzler, D., Beier, D. R., Dietrich, W. F., et al. (1997). Microcytic anaemia mice have a mutation in Nramp2, a candidate iron transporter gene. *Nat. Genet.* 16, 383–386. doi: 10.1038/ng0897-383

Fleming, R. E., and Ponka, P. (2012). Iron overload in human disease. *N. Engl. J. Med.* 366, 348–359. doi: 10.1056/NEJMra1004967

Galy, B., Ferring-Appel, D., Becker, C., Gretz, N., Grone, H. J., Schumann, K., et al. (2013). Iron regulatory proteins control a mucosal block to intestinal iron absorption. *Cell Rep.* 3, 844–857. doi: 10.1016/j.celrep.2013.02.026

Gourley, B. L., Parker, S. B., Jones, B. J., Zumbrennen, K. B., and Leibold, E. A. (2003). Cytosolic aconitase and ferritin are regulated by iron in *Caenorhabditis elegans*. *J. Biol. Chem.* 278, 3227–3234. doi: 10.1074/jbc.M210333200

Gunshin, H., Mackenzie, B., Berger, U., Gunshin, Y., Romero, M. F., Boron, W. F., et al. (1997). Cloning and characterization of a mammalian proton-coupled metal-ion transporter. *Nature* 388, 482–488. doi: 10.1038/41343

Hamza, I., and Dailey, H. A. (2012). One ring to rule them all: trafficking of heme and heme synthesis intermediates in the metazoans. *Biochim. Biophys. Acta* 1823, 1617–1632. doi: 10.1016/j.bbamcr.2012.04.009

Harrison, P. M., and Arosio, P. (1996). The ferritins: molecular properties, iron storage function and cellular regulation. *Biochim. Biophys. Acta* 1275, 161–203. doi: 10.1016/0005-2728(96)00022-9

Hentze, M. W., Muckenthaler, M. U., Galy, B., and Camaschella, C. (2010). Two to tango: regulation of Mammalian iron metabolism. *Cell* 142, 24–38. doi: 10.1016/j.cell.2010.06.028

Hintze, K. J., and Theil, E. C. (2005). DNA and mRNA elements with complementary responses to hemin, antioxidant inducers, and iron control ferritin-L expression. *Proc. Natl. Acad. Sci. U.S.A.* 102, 15048–15052. doi: 10.1073/pnas.0505148102

Illing, A. C., Shawki, A., Cunningham, C. L., and Mackenzie, B. (2012). Substrate profile and metal-ion selectivity of human divalent metal-ion transporter-1. *J. Biol. Chem.* 287, 30485–30496. doi: 10.1074/jbc.M112.364208

Ivan, M., Kondo, K., Yang, H., Kim, W., Valiando, J., Ohh, M., et al. (2001). HIFalpha targeted for VHL-mediated destruction by proline hydroxylation: implications for O2 sensing. *Science* 292, 464–468. doi: 10.1126/science.1059817

Jiang, H., Guo, R., and Powell-Coffman, J. A. (2001). The *Caenorhabditis elegans* hif-1 gene encodes a bHLH-PAS protein that is required for adaptation to hypoxia. *Proc. Natl. Acad. Sci. U.S.A.* 98, 7916–7921. doi: 10.1073/pnas.141234698

Jones, L. M., Rayson, S. J., Flemming, A. J., and Urwin, P. E. (2013). Adaptive and specialised transcriptional responses to xenobiotic stress in *Caenorhabditis elegans* are regulated by nuclear hormone receptors. *PLoS ONE* 8:e69956. doi: 10.1371/journal.pone.0069956

Kaelin, W. G. Jr., and Ratcliffe, P. J. (2008). Oxygen sensing by metazoans: the central role of the HIF hydroxylase pathway. *Mol. Cell.* 30, 393–402. doi: 10.1016/j.molcel.2008.04.009

Kakhlon, O., Gruenbaum, Y., and Cabantchik, Z. I. (2001). Repression of ferritin expression increases the labile iron pool, oxidative stress, and short-term growth of human erythroleukemia cells. *Blood* 97, 2863–2871. doi: 10.1182/blood.V97.9.2863

Kaluz, S., Kaluzova, M., and Stanbridge, E. J. (2008). Regulation of gene expression by hypoxia: integration of the HIF-transduced hypoxic signal at the hypoxia-responsive element. *Clin. Chim. Acta* 395, 6–13. doi: 10.1016/j.cca.2008.05.002

Kewley, R. J., Whitelaw, M. L., and Chapman-Smith, A. (2004). The mammalian basic helix-loop-helix/PAS family of transcriptional regulators. *Int. J. Biochem. Cell Biol.* 36, 189–204. doi: 10.1016/S1357-2725(03)00211-5

Kim, Y. I., Cho, J. H., Yoo, O. J., and Ahnn, J. (2004). Transcriptional regulation and life-span modulation of cytosolic aconitase and ferritin genes in *C. elegans*. *J. Mol. Biol.* 342, 421–433. doi: 10.1016/j.jmb.2004.07.036

Lee, S. J., Murphy, C. T., and Kenyon, C. (2009). Glucose shortens the life span of *C. elegans* by downregulating DAF-16/FOXO activity and aquaporin gene expression. *Cell Metab.* 10, 379–391. doi: 10.1016/j.cmet.2009.10.003

Lee, S. S., Kennedy, S., Tolonen, A. C., and Ruvkun, G. (2003). DAF-16 target genes that control *C. elegans* life-span and metabolism. *Science* 300, 644–647. doi: 10.1126/science.1083614

Levy, J. E., Jin, O., Fujiwara, Y., Kuo, F., and Andrews, N. C. (1999). Transferrin receptor is necessary for development of erythrocytes and the nervous system. *Nat. Genet.* 21, 396–399. doi: 10.1038/7727

Lill, R., and Muhlenhoff, U. (2008). Maturation of iron-sulfur proteins in eukaryotes: mechanisms, connected processes, and diseases. *Annu. Rev. Biochem.* 77, 669–700. doi: 10.1146/annurev.biochem.76.052705.162653

Liu, X., and Theil, E. C. (2005). Ferritins: dynamic management of biological iron and oxygen chemistry. *Acc. Chem. Res.* 38, 167–175. doi: 10.1021/ar0302336

Luhachack, L. G., Visvikis, O., Wollenberg, A. C., Lacy-Hulbert, A., Stuart, L. M., and Irazoqui, J. E. (2012). EGL-9 controls *C. elegans* host defense specificity through prolyl hydroxylation-dependent and -independent HIF-1 pathways. *PLoS Pathog.* 8:e1002798. doi: 10.1371/journal.ppat.1002798

Mackenzie, B., and Garrick, M. D. (2005). Iron Imports. II. Iron uptake at the apical membrane in the intestine. *Am. J. Physiol. Gastrointest. Liver Physiol.* 289, G981–G986. doi: 10.1152/ajpgi.00363.2005

Mastrogiannaki, M., Matak, P., Keith, B., Simon, M. C., Vaulont, S., and Peyssonnaux, C. (2009). HIF-2alpha, but not HIF-1alpha, promotes iron absorption in mice. *J. Clin. Invest.* 119, 1159–1166. doi: 10.1172/JCI38499

McElwee, J., Bubb, K., and Thomas, J. H. (2003). Transcriptional outputs of the *Caenorhabditis elegans* forkhead protein DAF-16. *Aging Cell* 2, 111–121. doi: 10.1046/j.1474-9728.2003.00043.x

McGhee, J. D. (2013). The *Caenorhabditis elegans* intestine. Wiley interdisciplinary reviews. *Dev. Biol.* 2, 347–367. doi: 10.1002/wdev.93

Meyron-Holtz, E. G., Ghosh, M. C., and Rouault, T. A. (2004). Mammalian tissue oxygen levels modulate iron-regulatory protein activities in vivo. *Science* 306, 2087–2090. doi: 10.1126/science.1103786

Murphy, C. T., and Hu, P. J. (2013). Insulin/insulin-like growth factor signaling in *C. elegans*. WormBook : the online review of *C. elegans. Biology* 1, 43.

Oh, S. W., Mukhopadhyay, A., Dixit, B. L., Raha, T., Green, M. R., and Tissenbaum, H. A. (2006). Identification of direct DAF-16 targets controlling longevity, metabolism and diapause by chromatin immunoprecipitation. *Nat. Genet.* 38, 251–257. doi: 10.1038/ng1723

Pietsch, E. C., Chan, J. Y., Torti, F. M., and Torti, S. V. (2003a). Nrf2 mediates the induction of ferritin H in response to xenobiotics and cancer chemopreventive dithiolethiones. *J. Biol. Chem.* 278, 2361–2369. doi: 10.1074/jbc.M210664200

Pietsch, E. C., Hurley, A. L., Scott, E. E., Duckworth, B. P., Welker, M. E., Leone-Kabler, S., et al. (2003b). Oxathiolene oxides: a novel family of compounds that induce ferritin, glutathione S-transferase, and other proteins of the phase II response. *Biochem. Pharmacol.* 65, 1261–1269. doi: 10.1016/S0006-2952(03)00081-9

Pocock, R., and Hobert, O. (2008). Oxygen levels affect axon guidance and neuronal migration in *Caenorhabditis elegans*. *Nat. Neurosci.* 11, 894–900. doi: 10.1038/nn.2152

Quach, T. K., Chou, H. T., Wang, K., Milledge, G. Z., and Johnson, C. M. (2013). Genome-wide microarrray analysis reveals roles for the REF-1 family member HLH-29 in ferritin synthesis and peroxide stress response. *PLoS ONE* 8:e59719. doi: 10.1371/journal.pone.0059719

Rahman, M. A., Rahman, B., and Ahmed, N. (2013). High blood manganese in iron-deficient children in Karachi. *Public Health Nutr.* 16, 1677–1683. doi: 10.1017/S1368980013000839

Rao, A. U., Carta, L. K., Lesuisse, E., and Hamza, I. (2005). Lack of heme synthesis in a free-living eukaryote. *Proc. Natl. Acad. Sci. U.S.A.* 102, 4270–4275. doi: 10.1073/pnas.0500877102

Romney, S. J., Newman, B. S., Thacker, C., and Leibold, E. A. (2011). HIF-1 regulates iron homeostasis in *Caenorhabditis elegans* by activation and inhibition of genes involved in iron uptake and storage. *PLoS Genet.* 7:e1002394. doi: 10.1371/journal.pgen.1002394

Romney, S. J., Thacker, C., and Leibold, E. A. (2008). An iron enhancer element in the FTN-1 gene directs iron-dependent expression in *Caenorhabditis elegans* intestine. *J. Biol. Chem.* 283, 716–725. doi: 10.1074/jbc.M707043200

Roth, J. A., and Garrick, M. D. (2003). Iron interactions and other biological reactions mediating the physiological and toxic actions of manganese. *Biochem. Pharmacol.* 66, 1–13. doi: 10.1016/S0006-2952(03)00145-X

Salahudeen, A. A., Thompson, J. W., Ruiz, J. C., Ma, H. W., Kinch, L. N., Li, Q., et al. (2009). An E3 ligase possessing an iron-responsive hemerythrin domain is a regulator of iron homeostasis. *Science* 326, 722–726. doi: 10.1126/science.1176326

Schneider, B. D., and Leibold, E. A. (2003). Effects of iron regulatory protein regulation on iron homeostasis during hypoxia. *Blood* 102, 3404–3411. doi: 10.1182/blood-2003-02-0433

Semenza, G. L. (2007). Life with oxygen. *Science* 318, 62–64. doi: 10.1126/science.1147949

Settivari, R., Levora, J., and Nass, R. (2009). The divalent metal transporter homologues SMF-1/2 mediate dopamine neuron sensitivity in *Caenorhabditis elegans* models of manganism and parkinson disease. *J. Biol. Chem.* 284, 35758–35768. doi: 10.1074/jbc.M109.051409

Shafizadeh, E., and Paw, B. H. (2004). Zebrafish as a model of human hematologic disorders. *Curr. Opin. Hematol.* 11, 255–261. doi: 10.1097/01.moh.0000138686.15806.71

Shah, Y. M., Matsubara, T., Ito, S., Yim, S. H., and Gonzalez, F. J. (2009). Intestinal hypoxia-inducible transcription factors are essential for iron absorption following iron deficiency. *Cell Metab.* 9, 152–164. doi: 10.1016/j.cmet.2008.12.012

Shah, Y. M., and Xie, L. (2014). Hypoxia-inducible factors link iron homeostasis and erythropoiesis. *Gastroenterology* 146, 630–642. doi: 10.1053/j.gastro.2013.12.031

Shawki, A., Knight, P. B., Maliken, B. D., Niespodzany, E. J., and Mackenzie, B. (2012). H(+)-coupled divalent metal-ion transporter-1: functional properties, physiological roles and therapeutics. *Curr. Top. Membr.* 70, 169–214. doi: 10.1016/B978-0-12-394316-3.00005-3

Shaye, D. D., and Greenwald, I. (2011). OrthoList: a compendium of *C. elegans* genes with human orthologs. *PLoS ONE* 6:e20085. doi: 10.1371/journal.pone.0020085

Shen, C., Nettleton, D., Jiang, M., Kim, S. K., and Powell-Coffman, J. A. (2005). Roles of the HIF-1 hypoxia-inducible factor during hypoxia response in *Caenorhabditis elegans*. *J. Biol. Chem.* 280, 20580–20588. doi: 10.1074/jbc.M501894200

Simonsen, K. T., Moller-Jensen, J., Kristensen, A. R., Andersen, J. S., Riddle, D. L., and Kallipolitis, B. H. (2011). Quantitative proteomics identifies ferritin in the innate immune response of *C. elegans*. *Virulence* 2, 120–130. doi: 10.4161/viru.2.2.15270

Spieler, D., Kaffe, M., Knauf, F., Bessa, J., Tena, J. J., Giesert, F., et al. (2014). Restless legs syndrome-associated intronic common variant in Meis1 alters enhancer function in the developing telencephalon. *Genome Res.* 24, 592–603. doi: 10.1101/gr.166751.113

Taylor, M., Qu, A., Anderson, E. R., Matsubara, T., Martin, A., Gonzalez, F. J., et al. (2011). Hypoxia-inducible factor-2alpha mediates the adaptive increase of intestinal ferroportin during iron deficiency in mice. *Gastroenterology* 140, 2044–2055. doi: 10.1053/j.gastro.2011.03.007

Tepper, R. G., Ashraf, J., Kaletsky, R., Kleemann, G., Murphy, C. T., and Bussemaker, H. J. (2013). PQM-1 complements DAF-16 as a key transcriptional regulator of DAF-2-mediated development and longevity. *Cell* 154, 676–690. doi: 10.1016/j.cell.2013.07.006

Theil, E. C. (2011). Ferritin protein nanocages use ion channels, catalytic sites, and nucleation channels to manage iron/oxygen chemistry. *Curr. Opin. Chem. Biol.* 15, 304–311. doi: 10.1016/j.cbpa.2011.01.004

Theil, E. C. (2013). Ferritin: the protein nanocage and iron biomineral in health and in disease. *Inorg. Chem.* 52, 12223–12233. doi: 10.1021/ic400484n

Thimmulappa, R. K., Mai, K. H., Srisuma, S., Kensler, T. W., Yamamoto, M., and Biswal, S. (2002). Identification of Nrf2-regulated genes induced by the chemopreventive agent sulforaphane by oligonucleotide microarray. *Cancer Res.* 62, 5196–5203.

Thompson, K., Molina, R. M., Donaghey, T., Schwob, J. E., Brain, J. D., and Wessling-Resnick, M. (2007). Olfactory uptake of manganese requires DMT1 and is enhanced by anemia. *FASEB J.* 21, 223–230. doi: 10.1096/fj.06-6710com

Torti, F. M., and Torti, S. V. (2002). Regulation of ferritin genes and protein. *Blood* 99, 3505–3516. doi: 10.1182/blood.V99.10.3505

Trenor, C. C. III, Campagna, D. R., Sellers, V. M., Andrews, N. C., and Fleming, M. D. (2000). The molecular defect in hypotransferrinemic mice. *Blood* 96, 1113–1118.

Tsuji, Y., Akebi, N., Lam, T. K., Nakabeppu, Y., Torti, S. V., and Torti, F. M. (1995). FER-1, an enhancer of the ferritin H gene and a target of E1A-mediated transcriptional repression. *Mol. Cell. Biol.* 15, 5152–5164.

Tsuji, Y., Ninomiya-Tsuji, J., Torti, S. V., and Torti, F. M. (1993). Augmentation by IL-1 alpha of tumor necrosis factor-alpha cytotoxicity in cells transfected with adenovirus E1A. *J. Immunol.* 150, 1897–1907.

Valentini, S., Cabreiro, F., Ackerman, D., Alam, M. M., Kunze, M. B., Kay, C. W., et al. (2012). Manipulation of in vivo iron levels can alter resistance to oxidative stress without affecting ageing in the nematode *C. elegans*. *Mech Ageing Dev.* 133, 282–290. doi: 10.1016/j.mad.2012.03.003

Vanoaica, L., Darshan, D., Richman, L., Schumann, K., and Kuhn, L. C. (2010). Intestinal ferritin H is required for an accurate control of iron absorption. *Cell Metab.* 12, 273–282. doi: 10.1016/j.cmet.2010.08.003

Vashisht, A. A., Zumbrennen, K. B., Huang, X., Powers, D. N., Durazo, A., Sun, D., et al. (2009). Control of iron homeostasis by an iron-regulated ubiquitin ligase. *Science* 326, 718–721. doi: 10.1126/science.1176333

Winkelmann, J., Schormair, B., Lichtner, P., Ripke, S., Xiong, L., Jalilzadeh, S., et al. (2007). Genome-wide association study of restless legs syndrome identifies common variants in three genomic regions. *Nat. Genet.* 39, 1000–1006. doi: 10.1038/ng2099

Wu, K. J., Polack, A., and Dalla-Favera, R. (1999). Coordinated regulation of iron-controlling genes, H-ferritin and IRP2, by c-MYC. *Science* 283, 676–679. doi: 10.1126/science.283.5402.676

Xiong, L., Catoire, H., Dion, P., Gaspar, C., Lafreniere, R. G., Girard, S. L., et al. (2009). MEIS1 intronic risk haplotype associated with restless legs syndrome affects its mRNA and protein expression levels. *Hum. Mol. Genet.* 18, 1065–1074. doi: 10.1093/hmg/ddn443

Yuan, J., Tirabassi, R. S., Bush, A. B., and Cole, M. D. (1998). The *C. elegans MDL*-1 and MXL-1 proteins can functionally substitute for vertebrate MAD and MAX. *Oncogene* 17, 1109–1118. doi: 10.1038/sj.onc.1202036

Yuan, X., Fleming, M. D., and Hamza, I. (2013). Heme transport and erythropoiesis. *Curr. Opin. Chem. Biol.* 17, 204–211. doi: 10.1016/j.cbpa.2013.01.010

Zhang, A. S., and Enns, C. A. (2009). Iron homeostasis: recently identified proteins provide insight into novel control mechanisms. *J. Biol. Chem.* 284, 711–715. doi: 10.1074/jbc.R800017200

Conflict of Interest Statement: The authors declare that the research was conducted in the absence of any commercial or financial relationships that could be construed as a potential conflict of interest.

Received: 18 March 2014; paper pending published: 05 April 2014; accepted: 28 April 2014; published online: 21 May 2014.

*Citation: Anderson CP and Leibold EA (2014) Mechanisms of iron metabolism in Caenorhabditis elegans. Front. Pharmacol. **5**:113. doi: 10.3389/fphar.2014.00113*

This article was submitted to Drug Metabolism and Transport, a section of the journal Frontiers in Pharmacology.

CHAPTER 3

THE NHR-14 NUCLEAR RECEPTOR COORDINATES IRON UPTAKE INNATE IMMUNITY IN *C. ELEGANS*

Abstract

Iron metabolism in *Caenorhabditis elegans* is maintained by the regulation of iron uptake and storage through a HIF-1-dependent transcriptional mechanism. We previously showed that defective iron uptake in *hif-1(ia4)* mutants grown in low iron conditions results in delayed larval development. In this study, we performed a genetic screen to identify novel genes involved in iron metabolism that would rescue the developmental delay of *hif-1(ia4)* mutants. This screen led to the isolation of nuclear hormone receptor-14 (NHR-14), a homolog of mammalian hepatocyte nuclear factor 4α (HNF4α). We found that NHR-14 regulates iron uptake and innate immunity through the transcription factor PQM-1, a components of the insulin/IGF-like (IIS) pathway that controls the response of *C. elegans* to *Pseudomonas aeruginosa* and *Salmonella enterica* infection. Importantly, we showed that regulation of iron uptake by NHR-14 in *C. elegans* is a conserved process, in that the mammalian iron importer DMT1 is repressed by HNF4α. These data underscore the interplay between iron metabolism and innate immunity during host-pathogen interactions, and provide insight into how *C. elegans* and potentially mammals utilize nuclear receptor and insulin/IGF-1-like (IIS) signaling to sense and respond to pathogenic stress.

Introduction

Iron is an essential micronutrient required by nearly all organisms for biological processes including DNA replication, mitochondrial respiration, and oxygen transport (Anderson, 2013). As a redox active element, iron also plays an important role in the production of reactive oxygen species (ROS) through the Fenton reaction, which can be

deleterious to cellular proteins, DNA and membranes. Iron deficiency impacts billions of individuals per year worldwide that results in a variety of health issues ranging from impaired neurological development in infants to anemia in adults (Functioning and Beard, 2001; Ward et al., 2014). Meanwhile, iron overload leads to cirrhosis, cardiomyopathy, and diabetes mellitus, and is associated with neurodegenerative diseases (Ganz and Nemeth, 2011; Huang et al., 2011). Given the dual nature of iron in healthy and diseased states, it is critical for organisms to maintain cellular iron concentration in a tight physiological range.

C. elegans is a useful model for studying iron metabolism (McElwee et al., 2004; Pocock Oliver, 2008; Romney et al., 2008). In addition to its genetic tractability and ease of maintenance, key proteins involved in mammalian iron uptake, storage and efflux are conserved in *C. elegans*. *C. elegans* express genes orthologous to the intestinal iron transporter divalent-metal transporter 1 or DMT1 (SMF-3), the iron-storage protein ferritin (FTN-1 and FTN-2) and the iron export protein ferroportin (FPN-1.1-3). In *C. elegans*, iron is transported across the apical enterocyte membrane by SMF-3. Iron is used for the metallation of iron-containing proteins and by mitochondria for the biosynthesis of Fe-S clusters and heme (Lill and Muhlenhoff, 2008). Iron not utilized is stored in FTN-1 and FTN-2 within the enterocyte or exported across the basolateral enterocyte membrane by FPN-1.1-3 into the interstitial space. Like mammals, intestinal iron absorption is upregulated during iron deficiency by hypoxia-inducible factor (HIF) transcriptional activation of *smf-3*/*DMT1* (*C. elegans,* HIF-1; mammals, HIF-2α) (Ackerman and Gems, 2012; Anderson et al., 2012; Romney et al., 2011a). One difference between iron homeostasis in *C. elegans* and mammals is that during iron

deficiency, HIF-1 represses *ftn-1* and *ftn-2*, whereas in mammals, ferritin is translationally repressed by iron-regulatory proteins (IRPs) (Anderson et al., 2012). In addition to iron, *ftn-1* is upregulated by DAF-16/FOXO transcription factor during stress (Ackerman and Gems, 2012) and *ftn-2* is upregulated in *C. elegans* exposed to *Staphylococcus aureus* (Simonsen et al., 2011). The regulation of *smf-3* and *ftn-1* and *ftn-2* by HIF-1 provides a mechanism to elevate the intracellular iron pool by increasing iron uptake and reducing iron storage. This is consistent with our study showing that *hif-1(ia4)* mutants are developmentally delayed when grown under low iron conditions (Romney et al., 2011).

Iron is critical in the establishment of bacterial infections as pathogens synthesize and release siderophores that are responsible for acquiring iron from the host. As a consequence, mammalian enterocytes have evolved specialized mechanisms to limit iron availability that include the secretion of iron chelators such as lipocalins and increasing iron storage by ferritin induction (Hood and Skaar, 2012; Miethke and Marahiel, 2007; Torti, 2002; Wessling-Resnick, 2010). *C. elegans* do not have an adaptive immune system and rely exclusively on innate immune mechanisms for sensing and resolving bacterial infections (Cohen and Troemel, 2015; Irazoqui et al., 2010). Human pathogens, such as *S. enterica* and *P. aeruginosa,* cause lethal intestinal infections in *C. elegans*. In *C. elegans*, *smf-3* mutants are susceptible to *S. aureus* infections (Bandyopadhyay et al., 2009), and loss of HIF-1 has been reported to enhance susceptibility to *P. aeruginosa* through an iron-dependent hypoxic death mechanism (Kirienko et al., 2013). Accordingly, *C. elegans* has emerged as an important model for identifying virulence factors involved in pathogenesis and novel effectors of the host innate immune response

(Aballay et al., 2000; Tan et al., 1999).

The expansion of nuclear receptors (NRs) in *C. elegans* has widely diversified their biological function, spanning from sex determination and molting to xenobiotic response and metabolic control (Jones et al., 2013; Taubert et al., 2011). The *C. elegans* genome contains 284 NRs, of which 269 are related to mammalian hepatic nuclear factor 4 (HNF4) (Antebi, 2015). The majority of *C. elegans* NRs have not been analyzed, and those that have are related to conserved homologs in higher eukaryotes. For instance, *nhr-49* is a homolog of mammalian Hepatic Nuclear Factor 4 (HNF4) family of NRs and is controls fatty acid metabolism and longevity (Van Gilst et al., 2005; Pathare et al., 2012). As a class of transcription factors, NRs contain a conserved N-terminal zinc finger DNA-binding domain and a more divergent C-terminal ligand-binding domain (LBD). Small lipophilic ligands are generally associated with regulating NR function (Yuan et al., 2009), but in *C. elegans* most NR ligands have not been identified. In addition to binding ligands, the LBD can coordinate binding of corepressor and coactivator complexes to regulate gene expression (Antebi, 2015).

Here, we identify NHR-14, a previously uncharacterized NR, as a novel regulator of iron uptake and the innate immune response. We found that NHR-14 represses iron uptake through *smf-3* in a manner dependent on the transcription factor PQM-1, a coregulator that cooperates with DAF-16/FOXO in the IIS pathway. Finally, the regulation of *smf-3* by NHR-14 is a conserved process in part wherein HNF4α, a mammalian homolog of NHR-14, transcriptionally represses the iron importer DMT1 in intestinal enterocytes.

Materials and methods

Worms were grown on nematode growth medium (NGM) agar plates seeded with *Escherichia coli* OP50 at 20 °C unless otherwise noted. For iron experiments, worms synchronized by hypochlorite treatment at the L4 to young adult stage were grown overnight on NGM plates and then transferred to NGM plates supplemented with 6.6 mg/ml ferric ammonium citrate (FAC) or 0.1 mM 2,2'-dipyridyl (BP, iron chelator) and grown overnight.

The expression pattern of NHR-14 was determined using transgenic animals expressing a fosmid (40 kb) encoding a NHR-14::FLAG::GFP transgene (TransgeneOme) (Sarov et al., 2012). This fosmid contains the entire *nhr-14* locus as well as large amounts of flanking DNA that are critical for endogenous *nhr-14* expression. The fosmid was injected into *ttTi5606;unc-119* worms and three independent lines were established.

Human HT29 colorectal cells (ATC HT-38) were maintained in McCoy's 5a medium (Life Technologies) supplemented with 10% fetal bovine serum and 1% penicillin-streptomycin at 37 ^{o}C with 5% CO_2. For HNF4α shRNA knockdown, the hairpin targeting sequence was cloned into the pLL3.7 (Addgene) vector that was co-transfected into EBNA 293 T-cells with pVSVG and pGag-Pol for viral production. Lentivirus containing empty vector (EV) shRNA or *HNF4α* shRNA was used to transduce HT29 cells, where puromycin was used for selecting clones. HT29 cells (70% confluency) were treated with 50 uM deferoxamine (DFO, iron chelator) or 50 ug/ul FAC for 18 h. Mouse duodenum, jejunum, ileum and colon isolated from intestinal epithelial cell-specific HNF4α mice (*Hnf4*$\alpha^{\triangle IEpC}$) and control floxed mice (*Hnf4*$\alpha^{F/F}$) were

generously provided by Dr. Frank Gonzalez (NCI) (Ahn et al., 2008).

Ethyl methanesulfonate (EMS) mutagenesis was performed as previously described (Brenner, 1974). Briefly, L4 stage *hif-1(ia4)* worms were treated with 50 mM EMS in M9 buffer (22 mM KH_2PO_4, 42 mM Na_2HPO_4, 86 mM NaCl), for 4 h. Mutagenized worms were then washed five times to remove excess EMS and then plated on NGM plates and grown till gravid. Gravid F1s were then bleached, and F2 eggs plated on NGM plates. Gravid F2 worms were transferred to 25 uM BP plates and removed after laying F3 eggs. F3 progeny that rescued the low iron phenotype of *hif-1(ia4*) mutants (determined by body length measurements in ImageJ) were scored as suppressors and collected for whole genome sequencing (WGS). SNP mapping to identify the causative mutation was performed as previously described (Doitsidou et al., 2010). Our Bristol *hif-1* mutant strain was outcrossed to the polymorphic Hawaiian strain CB4856 six times. Suppressor mutants were crossed with *hif-1(ia4)* mutant Hawaiian strain worms and F1 progeny were moved to fresh NGM plates. Gravid F1 adults were allowed to lay eggs overnight on NGM plates containing 25 uM BP. Adults were removed the next day and ~50 F2 recombinants that reached adulthood within five days were isolated and DNA from their F3 and F4 progeny was purified using the PureLink Genomic DNA Mini kit (Invitrogen). WGS was performed using an Illumina HiSeq sequencer. Hawaiian SNP positions were mapped on the genomes of suppressor mutants E17 and V2B using the single-step SNP-mapping pipeline CloudMap (Minevich et al., 2012).

Five gravid adults from each strain were picked to either NGM or NGM containing 25 uM BP plates and allowed to lay eggs overnight. Adults were removed the

following day and progeny were incubated for five days at 20 °C after which images were collected using a Leica M205 FA microscope and Leica DFC 310 FX camera (Leica Microsystems). Progeny were scored based on length using Image J.

For indicated conditions and time-points, worms were washed off the plate with M9 buffer washed three times to remove external bacteria, and rocked for 2 h in M9 buffer to clear bacteria from the gut. RNA was extracted using TRIzol Reagent (Invitrogen) according to manufacturer's protocol. cDNA synthesis was performed using SuperScript III First-Strand Synthesis SuperMix (Invitrogen). After reverse transcription, qPCR was performed using TaqMan Gene Expression Assays (Applied Biosystems) and analyzed using an Applied Biosystems 7900 HT thermocycler. Similar methods were used for qRT-PCR analysis of *Hnf4*$\alpha^{\triangle \text{IEpC}}$ and *Hnf4*$\alpha^{F/F}$ intestinal tissue except that Power SYBR Green detection (Invitrogen) was used. For HT29 cells, qRT-PCR was performed using TaqMan Gene Expression Assays and primers..

The *smf-3(-1500)::GFP-his* reporter line (Romney et al., 2011) was synchronized by hypochlorite treatment and arrested L1 larvae were grown on 10 cm NGM plates containing *nhr-14* RNAi or EV RNAi for 48 h. Worms were washed in M9 buffer and transferred to *nhr-14* RNAi or EV RNAi plates supplemented with either 100 μM BP or 6.6 mg/mL FAC and grown overnight. Worms were collected by centrifugation and washed several times in M9 buffer to remove bacteria and debris. Worms were analyzed using COPAS Biosort where L4 to young adult worms were gated based on extinction and time of flight parameters (TOF). Extinction and TOF parameters were held constant for subsequent GFP fluorescence acquisition throughout all conditions. GFP fluorescence for 1000 worms was analyzed using FlowJo.

RNAi clones *nhr-14* (T01B10) and *pqm-1* (F40F8.7) were obtained from the ORFeome-based RNAi library (Reboul et al., 2001) and empty vector (L4440) was used as a control. RNAi clones were verified by sequencing. Five *hif-1(ia4)* gravid adults were allowed to lay eggs overnight on NGM or NGM-BP plates (supplemented with 1 mM isopropyl β-D-1-thiogalactopyranoside (IPTG**)** and 100 μg/ml ampicillin) seeded with bacteria expressing dsRNA corresponding to *nhr-14* or L4440. The following day adults were removed and progeny scored for rescue against BP as described above.

Eggs were obtained by treating gravid adults from each strain with alkaline hypochlorite. Eggs were allowed to hatch overnight in Egg Buffer (118 mM NaCl, 48 mM KCl, 2 mM $CaCl_2$, 2 mM $MgCl_2$, and 25 mM HEPES) and arrest in the L1 stage. Synchronized L1 worms were grown on NGM plates seeded with OP50 until reaching the L4 stage. Worm were washed extensively with M9 buffer and incubated in M9 buffer at room temperature for 2 h to allow for purging of the gut followed by three rinses with ddH_2O. Worms were pelleted and dried, and metal content determined by ICP-OES (Children's Hospital Oakland Research Institute (CHORI) Elemental Analysis Facility). Empty tubes were run in parallel to serve as controls. Iron and manganese content was normalized to sulfur content.

Images of NHR-14::GFP expression were captured using an Olympus FV1000 confocal microscope and camera using Olympus FV10-ASW 3.1 confocal imaging software. Images of *smf-3(-1500)::GFP-his* and PQM-1::GFP were captured using a Leica DM6000B. Following acquisition, images were rotated, cropped and sized using Adobe Photoshop.

At indicated time points, worms were washed off the plate with ddH_2O and

washed three times to remove bacteria. Worms were resuspended in lysis buffer (20 mM HEPES pH 7.5, 25 mM KCl, 0.5% NP-40) and disrupted by two 5-sec pulses using an Ultrasonic Processor (Sonics) at 50% amplitude. Protein concentrations were determined using Coomassie Plus Protein Assay Reagent (Thermo Scientific). Protein samples were incubated for 10 min at 95 °C in NuPage LDS Sample Buffer (Invitrogen) containing 10 mM DTT then subjected to electrophoresis using NuPage 4-12% Bis-Tris gels (Invitrogen) and transferred to Amersham Hybond ECL nitrocellulose (GE Healthcare). Antibody treatments were carried out in 1x TBS (0.01% Tween-20) containing 5% nonfat dry milk. Horseradish peroxidase-conjugated secondary antibodies (Jackson Laboratories) were visualized using Western Lighting Plus-ECL Chemiluminescence Substrate (Perkin Elmer). HT29 cells were lysed in Triton Buffer (20 mM HEPES pH 7.5, 25 mM KCl, and 0.01% Triton X-100) and protein was analyzed by NuPage 4-12% Bis-Tris gels as described above. Primary antibodies used in this study are: mouse monoclonal antiFLAG (Sigma, 1:2000); mouse antitubulin (MP Biomedical, 1:2000); rabbit antiHNF4α (Novex, 1:2000) and rabbit antiβ-actin (Ambion, 1:2000). Densitometry analysis was performed using Image J (National Institutes of Health).

N2 wild-type and *nhr-14(tm1473)* L1 worms were grown on NGM plates seeded with OP50 and harvested at L4 stage (48 h at 22 ^{o}C). Worms were collected by centrifugation and washed with M9 buffer to remove bacteria and RNA was extracted using a modified TRIzol procedure. Briefly, the aqueous phase was mixed with an equal volume of 70% EtOH and added to RNeasy spin columns (Qiagen). RNA concentration and quality were determined using a NanoDrop spectrophotometer followed by further quality control with the Bioanalyzer RNA 9000 Nano Chip. Library construction was

performed using the Illumina TruSeq RNA Sample Preparation Kit v2 (RS-122-2001 and RS-122-2002) and was sequenced with the Illumina HiSeq (50 cycle, single-end). Sequenced reads were aligned to the Ce10 (WormBase Build 220) transcriptome index using Novoalign, and differential expression was determined using Useq 8.7.4 (Nix et al., 2008). Transcripts with a log2 ratio of 1 or higher at a false discovery rate (FDR) ≤ 0.05 were considered differentially expressed. Gene enrichment analysis was performed using GOrilla (Eden et al., 2009), which determines enriched GO terms at the top of a ranked list of genes. The overlap of upregulated genes in *nhr-14(tm1473)* mutants with those in previously reported pathogen infection studies was determined as previously described and significance was calculated using exact hypergeometric probability (Hwang et al., 2014). BioProspector was used for de novo motif finding with the width parameter set to 16. Consistent motifs were identified using 1000 bp upstream of up- and downregulated genes.

Bacterial lethality studies were performed as previously described (Tan et al., 1999). Briefly, 20-30 gravid adult worms were transferred to slow-killing (SK) plates containing lawns of *S. enterica* or *P. aeriguinosa* (PA14). Worms that failed to respond to light prodding were scored as dead and removed. Live worms were transferred to fresh plates to prevent interference from progeny.

Worms were grown on NGM or pathogen formulated plates supplemented with 75 μM 5-Fluoro-2'-deoxyuridine (FUDR) to prevent egg hatching. Approximately 30 of L4 synchronized N2 wild-type, *nhr-14(tm1473)* and *smf-3(ok1035)* worms were placed on the plates and incubated for 24 h at 22 ^{o}C. Life span analysis began at the L4 larval stage (t = 0). Worms were scored as dead if they did move, pump, or respond to

prodding. Worms that died of a bursting vulva (gonad extruding through the vulva) or had crawled off the plate were censored from analysis. Experiments were performed at least three times.

Colony forming assay was performed as previously described (Garsin et al., 2001). Briefly, L4 staged N2 wild-type and *nhr-14(tm1473)* worms were transferred to SK plates containing lawns of *S. enterica* and allowed to feed for 8, 24, and 48 h. At the indicated time points, five worms were transferred to NGM agar plates containing 100 ug/ml gentamicin and washed two times in 4 µl drops of M9 buffer containing 25 mM levamisole. Washed worms were transferred to tubes containing 20 µl of M9 lysis buffer (1% Triton in M9 buffer) and disrupted with a pestle. Lysate volume was brought up to 50 µl with M9 lysis buffer, serially diluted, and plated on MacConkey agar plates for *S. enterica* selection or LB agar plates for *P. aeuroginosa* selection.

Results are displayed as the mean ± SE, and comparisons between two groups were performed using a Student's t-test. For each variable, at least three independents experiments were carried out. Survival comparisons were made using the Mantel-Cox log-rank test. All data were evaluated at the significance level $p \leq 0.05$ and analyzed using Prism 6 (Graphpad).

Results

We previously showed that *hif-1(ia4)* mutant worms are developmentally delayed when grown under iron limiting conditions using the iron chelator, 2,2-dipyridyl (BP) (Romney et al., 2011). To discover novel genes involved in iron homeostasis, a suppressor screen was performed to identify mutations that rescued the low iron

phenotype observed in *hif-1(ia4)* animals. This screen led to the isolation of six suppressor mutants, two of which (E17 and V2B) were identified as strong suppressors of the *hif-1(ia4)* low iron phenotype (Figure 3.1A). The causative mutation within these lines was determined using whole genome sequencing and Hawaiian strain SNP mapping (see Materials and Methods). Both E17 and V2B displayed a similar ~1 Mb region of the X chromosome that have a Hawaiian/Bristol reads ratio of close to zero (Figure 3.1B). Sequence analysis revealed that suppressors E17 and V2B possess distinct mutations within the nuclear hormone receptor gene *nhr-14* (T01B10.4). E17 contains a G>A substitution that changes Trp33 to a STOP codon and V2B contains a G>A substitution that changes Gly49 to Arg. Double mutant *hif-1(ia4)*;*nhr-14(tm1473)* worms develop normally under iron limited conditions (Figure 3.1C), confirming that mutations within *nhr-14* are responsible for the rescue observed in lines E17 and V2B.

Given that NHR-14 was identified in a screen for *hif-1* mutants that enabled normal development under low iron conditions, we questioned whether *nhr-14* was regulated by changes in iron status. N2 wild-type worms displayed no change in *nhr-14* transcript levels when grown under low or high iron conditions compared to NGM conditions (Figure 3.2A). To determine whether NHR-14 protein levels are affected by iron status, we generated a transgenic line carrying an *nhr-14* fosmid transgene that utilizes the endogenous *cis*-elements and promoter of *nhr-14* to drive the expression of NHR-14 tagged with 3xFLAG and GFP. We validated NHR-14::FLAG::GFP as a functional replacement for endogenous NHR-14 by injecting *nhr-14(tm1473)*;*hif-1(ia4)* double mutants with the *nhr-14* fosmid transgene and showing that these worms displayed the *hif-1(ia4)* delayed developmental phenotype when grown under low iron

conditions (Figure S3.1). NHR-14::FLAG levels did not change with low or high iron treatment compared to worms grown on NGM (Figure 3.2B). Furthermore, fluorescent imaging revealed that NHR-14::FLAG::GFP is predominately expressed within the nuclei of intestinal cells as well as cells in the head, and that this pattern was not affected by iron (Figure 3.2C).

To determine the mechanism by which *nhr-14(tm1473)* mutants rescued the low iron phenotype of *hif-1(ia4)* mutants, we compared the transcription profiles of L4 stage *nhr-14(tm1473)* mutants with N2 wild-type animals using RNAseq. We identified 676 differentially expressed genes, 458 of which were upregulated and 218 downregulated in *nhr-14(tm1473)* mutants that changed at least two-fold compared to N2 wild-type animals at a 5% false discovery rate (FDR) (Table 3.1). We also identified *smf-3*, which encodes the intestinal iron transporter, as one of the most highly upregulated genes in *nhr-14(tm1473)* mutants. This observation suggested increased iron uptake as a possible mechanism to explain rescue of *hif-1(ia4)* mutants.

We first confirmed upregulation of *smf-3* in *nhr-14(tm1473)* mutants and in *hif-1(ia4);nhr-14(tm1473)* double mutants compared to N2 wild-type animals and *hif-1(ia4)* mutants by qPCR (Figure 3.3A). Consistent with increased *smf-3* expression, content of iron (and manganese) was increased in *nhr-14(tm1473)* mutants compared to N2 wild-type animals (Figure 3.3B). We also found that *nhr-14(tm1473);hif-1(ia4);smf-3(ok1035)* triple mutants failed to grow on low iron, indicating that upregulation of *smf-3* in *nhr-14(tm1473)* mutants is required for the rescue of *hif-1(ia4)* mutants (Figure 3.3C). Taken together, these data revealed that NHR-14 negatively regulates *smf-3* expression and that loss of NHR-14 rescues the *hif-1(ia4)* low iron phenotype through *smf-3*-

dependent iron uptake.

We next questioned whether NHR-14 directly regulates *smf-3* expression using transgenic worms expressing a GFP-his transcriptional reporter containing the 123-bp IDE located in the *smf-3* promoter. This element contains hypoxia response motifs (HREs) critical for HIF-1 binding, and are required for *smf-3* activation in the intestine during iron deficiency (Romney et al., 2011). The IDE also contains three DAE motifs that are associated for PQM-1 occupancy (modENCODE) (Figure 3.4A).

Transgenic worms expressing *smf-3(1500)::GFP-his* were fed control RNAi or *nhr-14* RNAi and grown under normal, low iron (BP) or high iron (FAC) treatments. Consistent with our previous study (Romney et al., 2011), GFP expression increased with BP and decreased with FAC treatment in worms fed control RNAi, reflecting HIF-1 regulation (Figure 3.4B). In *nhr-14* RNAi fed worms, GFP expression was further increased under normal, BP and FAC treatments, suggesting that NHR-14 acts in parallel to the HIF-1 pathway (Figure 3.4B). These data showed that the *smf-3* 123-bp IDE is important for NHR-14 regulation; however, we did not observe a direct interaction between NHR-14 and the IDE by electrophoretic mobility gel shift assays or ChIP assays (data not shown), suggesting that NHR-14 indirectly regulates *smf-3*.

Given the presence of DAE motifs in the *smf-3* IDE and the modENCODE PQM-1 ChIP-seq data, we tested the hypothesis that PQM-1 directly regulates *smf-3*. We found that GFP expression in *smf-3(-1500)::GFP-his* transgenic worms fed *pqm-1* RNAi was reduced compared to control RNAi (Figure 3.4C). Strikingly, mutating the DAE 1, 2, or 3 motifs from T**G**ATAAG to T**C**ATAAG abolished GFP expression in untreated and BP-treated worms compared to control *smf-3(-1500)::GFP-his* worms (Figure 3.4D).

Consistent with *smf-3* transgenic reporter studies, endogenous *smf-3* expression in *pqm-1(ok485)* mutants was reduced by 50% compared to N2 wild-type worms (Figure 3.4E). PQM-1 as an activator of *smf-3* was also evidenced by a low iron developmental delay seen in *pqm-1(ok485)* mutants (Figure 3.5F). Importantly, the ability of *nhr-14(tm1473)* mutants to rescue the low iron developmental defect in *hif-1(ia4)* mutants was reduced as a result of diminished *smf-3* expression when *nhr-14(tm1473)* mutants were grown on *pqm-1* RNAi (Figure 3.4G and 3.4H). Since *pqm-1* expression is not altered in *nhr-14(tm1473)* mutants, we wanted to determine whether PQM-1 nuclear localization is affected. L3 worms expressing a PQM-1::GFP fosmid that were fed *nhr-14* RNAi had significantly more nuclear GFP staining compared to worms fed control RNAi (Figure 3.4I). Collectively, these data provide strong evidence that PQM-1 activates *smf-3* expression by binding to DAE motifs in the *smf-3* promoter and that NHR-14 acts upstream of PQM-1 to inhibit its nuclear translocation and transcriptional activity.

In addition to intestinal iron uptake, *nhr-14* regulates innate immune and antimicrobial genes. Of the 458 upregulated genes in *nhr-14(tm1473)* mutants versus N2 wild-type, 38 genes are involved in the innate immune response (Figure 3.5A). Gene-set enrichment analysis using DAVID (Huang et al., 2009) showed that over-represented functional categories within this dataset included C-type lectin (carbohydrate binding proteins), CUB-domain proteins (extracellular and membrane proteins), peptidases, glutathione S-transferases (xenobiotic metabolism), lysozymes, metridin-like Shk toxin, and collagens, all of which are part of a core immune response program in *C. elegans* (Simonsen et al., 2012) (Figure 3.5B). Genes that are upregulated in *nhr-14(tm1473)* mutants include classical immune response genes such as; lysozymes (*lys-7*, *2*, and *1)*

(Alper et al., 2007), downstream of *daf-16* (*dod-24, 19, 22,* and *17)* (Murphy et al., 2003), C-type lectins (*clec-86*, *41*, *62*, and *66*) (Schulenburg et al., 2008), antimicrobial peptides (*spp-18* and *3*) (Hoeckendorf and Leippe, 2012), and glutathione S-transferase (*gst-38* and *22)* (Figure 3.4C). Ferritin (*ftn-2*), a known innate immune gene (Simonsen et al., 2011), was also induced *nhr-14(tm1473)* mutants (Figure 3.5C). We verified *nhr-14*-dependent upregulation of eight genes within the immune response group by qPCR (Figure 3.5D). Among the downregulated genes, there was enrichment in genes involving cellular organization and body morphogenesis including; *dpy-3*, *noah-1*, *ptr-4*, and *mlt-8*.

Given that the transcriptional profile of *nhr-14(tm1473)* mutants is enriched for immune response genes, we examined the overlap between *nhr-14* upregulated genes and previously published genes that are induced by infection to various pathogenic bacteria. We found significant overlap between genes upregulated in *nhr-14(tm1473)* mutants and genes upregulated in response to *P. aeruginosa* (Shapira et al., 2006; Troemel, 2006), *Pseudomonas luminescens* (Wong et al., 2007), *Enterococcus faecalis* (Wong et al., 2007) and *Staphylococcus aureus* (Visvikis et al., 2014) (Table 3.2). These genes include lysozymes, c-type lectins, and antimicrobial peptides that were identified in *nhr-14(tm1473)* mutants. Interestingly, we did not observe an overlap between *nhr-14* upregulated genes with *Serratia marscens* (Wong et al., 2007). This is likely due to the considerable variation with transcriptome profiling between infection studies (Mallo et al., 2002; Simonsen et al., 2012; Wong et al., 2007).

The pathogen response in *C. elegans* is controlled through three distinct signaling pathways that converge on inducing a highly specific innate immune transcriptional program (Cohen and Troemel, 2015; Irazoqui et al., 2010). We compared our *nhr-14*

RNAseq dataset with p38-MAPK (Troemel, 2006), TGF-β (Roberts et al., 2010) and DAF-2/DAF-16 (Murphy et al., 2003) innate immune pathway datasets, and found significant gene expression overlap. There was significant overlap (R.F.= 6.4, *p*-value=4.1e-12) with *pmk-1*-dependent genes (p38-MAPK); however, an increase in phosphorylated PMK-1 (p38), which is an indicator of activation, was not observed in *nhr-14(tm1473)* mutants (Figure S3.2). This does not rule out the possibility that the terminal transcription factors in the p38-MAPK cascade, AFT-7 and SKN-1, are transcriptionally active independent of PMK-1 phosphorylation. The highest degree of overlap (R.F.= 6.5, *p*-value =2.4e-22) occurred with the DAF-2/DAF-16 Class 2 subset of genes that include the downstream-of-daf-16 (dod) gene group (Murphy, 2003) and classic antimicrobial genes such as *lys-7*, *spp-1* and *spp-12* (Figure S3.2B). Similarly, PMK-1 dependent genes also show considerable overlap with Class 2 genes and essentially no overlap with Class 1 genes, which are activated by DAF-16/FOXO (Troemel, 2006). These genes are characterized as being repressed by DAF-16/FOXO and contain a GATA-like DAF-16-associated element (DAE), T/CTTATCA or TGATAAG/A, which is targeted by the transcriptional activator PQM-1 (Tepper et al., 2013). Troemel's group had also shown *pqm-1* to be induced by approximately 4-fold in response to *P. aeruginosa* infection. This led us to question whether genes upregulated in *nhr-14(tm1473)* mutants contain DAEs, and are potential targets of PQM-1. Among the upregulated genes in *nhr-14(tm1473)* mutants, the DAE was present in 288 of 457 promoters tested (*p*-value = 5.4e-45), including three tandem TGATAAG/A motifs in the *smf-3* promoter. Analysis of chromatin-immunoprecipitation-seq (ChIP-seq) data from modENCODE (Niu et al., 2011) revealed significant PQM-1 binding within 16 out of the

top 25 upregulated genes in *nhr-14(tm1473)* mutants, while only 4 out of 25 for the downregulated subset One of the most prominent PQM-1 signals was observed in the *smf-3* IDE (IV: 2618542..2619063; qValue $1.7e^{-32}$), suggesting PQM-1 might be involved in the activation of *smf-3* in *nhr-14(tm1473)* mutants.

Considering PQM-1's role in pathogen resistance (Kawli and Tan, 2008; Lee et al., 2013) and the induction of innate immune genes in *nhr-14(tm1473)* mutants, we questioned whether *nhr-14(tm1473)* mutants were more resistant to pathogenic infection. To test this, we infected N2 wild-type and *nhr-14(tm1473)* mutant worms with *P. aeruginosa* PA14 and *S. enterica*, and measured survivability over time. Compared to N2 wild-type worms, *nhr-14(tm1473)* mutants were more resistant to both PA14 and *S. enterica* infection (Figure 3.6A and F). In addition to increased resistance, PA14 and *S. enterica* colonization is significantly reduced in *nhr-14(tm1473)* mutants after 24 h or 12 h, respectively, of infection (Figure 3.6B and F). Analysis of *nhr-14* expression after PA14 infection (24 h) or *S. enterica* infection (72 h) revealed reduced *nhr-14* mRNA with a corresponding increase in *smf-3* mRNA levels (Figure 3.6C and G and H). This was also observed for NHR-14 protein content over the same time period in transgenic worms expressing NHR-14::GFP::FLAG that were infected with PA15 or *S. enterica* (Figure 3.6D and H). Since iron is an important factor in bacterial infections where both host and pathogen have evolved unique mechanisms to control its availability (Hood and Skaar, 2012), it appears that reduced NHR-14 expression during infection could be a mechanism to limit iron in the intestinal lumen by increasing cellular import through SMF-3. Along these lines, a previous study showed that *smf-3(1035)* mutants are sensitive to *S. aureus* infection (Bandyopadhyay et al., 2009). We questioned whether

the resistance of *nhr-14(tm1473)* mutants to PA14 was partly dependent on the increased expression of *smf-3*. We found that *smf-3(ok1035)* mutants are more susceptible to PA14 infection compared to N2 wild-type worms and *nhr-14(tm1473)* mutants (Figure 3.5I). A role for *smf-3* was further evidenced by the observation that *nhr-14(tm1473);smf-3(ok1035)* mutants were more susceptible to infection compared to *nhr-14(tm1473)* mutants (Figure 3.5I). Survival of *nhr-14(tm1473)* mutants infected with PA14 was reduced when slow killing plates were supplemented with 6.6 mg/mL FAC (Figure 3.5J).

By implicating a role for *nhr-14* in regulating iron uptake through *smf-3*, we questioned whether a similar mechanism was conserved in mammals. Amino acid sequence alignment between NHR-14 and mammalian HNF4α revealed a 65% identity within the N-terminal Zn finger DNA-binding domain and a 29% identity within the C-terminal ligand-binding domain (Figure 3.7A). Recent studies have shown that HNF4α regulates several iron-related genes in hepatocytes, including hepcidin (*Hamp*) and transferrin receptor 2 (*Tfr2*) (Matsuo et al., 2015; Truksa et al., 2009). In mammals, dietary iron is absorbed by intestinal enterocytes through apically localized DMT1 (Canonne-Hergaux et al., 1999), which is the SMF-3 ortholog. Due to the sequence similarities between NHR-14 and HNF4α and the role of HNF4α in iron metabolism, we wondered whether HNF4α regulates DMT1 expression. HT29 human colorectal cells were stably transduced with an shRNA targeting HNF4α (shHNF4α) to deplete HNF4α or empty vector (EV) (Figure 3.7B). Cells were then treated with the iron chelator desferrioxamine (DFO) or FAC, and HNF4α protein and *DMT1* mRNA levels were assessed. In EV cells treated with DFO, HNF4α levels were unexpectedly reduced

compared to untreated cells, and were further reduced in shHNF4α cells (Figure 3.7B). *DMT1* mRNA expression was unchanged in untreated shHNF4α cells, but increased ~2-fold in shHNF4α cells treated with DFO compared to EV cells (Figure 3.7C). These data suggested that loss of HNF4α correlates with reduced DMT1 expression in colorectal cells, and that unlike NHR-14, HNF4α expression is regulated by iron.

To further examine the regulation of HNF4α on DMT1 expression in intestine, we assessed DMT1 protein and mRNA in the small and large intestine of intestinal-epithelial cell specific *Hnf4α* null mice (*Hnf4*$\alpha^{\triangle IEpC}$) and control floxed mice (*Hnf4*$\alpha^{F/F}$) (Ahn et al., 2008). *Dmt1* mRNA was significantly increased in the duodenum, jejunum, and colon of *Hnf4*$\alpha^{\triangle IEpC}$ mice compared to *Hnf4*$\alpha^{F/F}$ mice (Figure 3.7D). DMT1 protein levels were only modestly increased in colonic lysates from *Hnf4*$\alpha^{\triangle IEpC}$ compared to *Hnf4*$\alpha^{F/F}$ mice (Figure 3.7E). Together these data suggest a role for HNF4α in the regulation of DMT1 in the mammalian intestine.

Discussion

Using a genetic suppressor screen to rescue the low iron developmental delay phenotype of *hif-1(ia4)* mutants, we found that the HNF4α homolog, NHR-14, is a repressor of iron uptake through *smf-3* in *C. elegans*. In determining a mechanism for *smf-3* regulation we showed that the IIS transcription factor PQM-1 is necessary for the upregulation of *smf-3* in *nhr-14(tm1473)* mutants. While uncovering a role for *nhr-14* in iron metabolism, we also unexpectedly identified *nhr-14* to be a regulator of the innate immune response. Genome wide expression profiling in *nhr-14(tm1473)* mutants revealed an induction of immune response genes that are likely to be responsible for the

resistance of *nhr-14(tm1473)* mutants to *P. aeruginosa* and *S. enterica* infection. Out of the 284 NRs in *C. elegans*, our study has identified NHR-14 as the first NR to be involved in iron metabolism and immunity.

Only about 7% of NRs have been characterized in *C. elegans* and this is likely a consequence of no observable phenotype for the vast majority of NRs. Known functions of NRs include sex determination, xenobiotic metabolism, fatty acid metabolism, and neural differentiation. NHR-14 adds to this list due its involvement in iron metabolism and the immune response. Hallmarks of NR structure are a conserved N-terminal DNA binding domain and a C-terminal ligand-binding domain, so it was surprising NHR-14 would regulate *smf-3* transcription indirectly through PQM-1. Originally discovered to be induced in response to paraquat-mediated stress, PQM-1 has recently been shown to be responsible for the activation of the Class 2 subset of IIS genes. It has been known for some time that reduced IIS leads to the upregulation of Class 1 (stress) and down-regulation of Class 2 (development) genes. DAF-16/FOXO directly activates Class 1 genes through the DAF-16 binding element (DBE), however the mechanism activating Class 2 genes containing the DAF-16 associated element (DAE) remained unknown (Murphy, 2003). Tepper et al. (2013) showed that PQM-1 activates Class 2 genes through the DAE, and antagonizes DAF-16/FOXO nuclear localization when the DAF-2 insulin receptor is active (Tepper et al., 2013). Many of the upregulated genes in *nhr-14(tm1473)* mutants contain the T/CTTATCA DAE and are potential targets of PQM-1. Of those, *smf-3*, was an obvious candidate for PQM-1 activation in *nhr-14(tm1473)* mutants. As a Class 2 gene, *smf-3* was reported to rank relatively weak, but our results suggest otherwise. The observation that *smf-3* is highly induced in worms treated with

glucose, which activates the DAF-2 insulin receptor, provides further evidence that *smf-3* is a strong Class 2 gene (Lee et al., 2009). The question of how NHR-14 regulates PQM-1 is thought provoking. Since PQM-1 targets are upregulated and its nuclear localization enhanced in *nhr-14(tm1473)* mutants, its reasonable to suggest that NHR-14 inhibits PQM-1. The phosphorylation of DAF-16/FOXO by DAF-2 signaling causes DAF-16/FOXO to be retained in the cytoplasm, thus allowing nuclear translocation of PQM-1.

The mechanism by which DAF-16/FOXO antagonizes PQM-1 is unknown, as is the signal(s) that retains PQM-1 in the cytoplasm. It is possible that NHR-14 prevents PQM-1 nuclear localization directly through a protein-protein interaction or indirectly through an unknown pathway. Another interesting observation is the upregulation of *ins-7* in *nhr-14(tm1473)* mutants. INS-7 is one of the 40 insulin-like peptides in *C. elegans* and has been shown to be a strong DAF-2 agonist (Murphy et al., 2007). It is entertaining to speculate a feed-forward mechanism by which the de-repression of PQM-1 in *nhr-14(tm1473)* mutants is amplified by INS-7 autocrine signaling, where INS-7 would activate the DAF-2 insulin receptor causing a cytoplasmic to nuclear shift in PQM-1 localization. Another issue that remains unanswered deals with the reverse complement of the DAE motif, TGATAAG/A, which is important for binding of the intestinal specific GATA transcription factor ELT-2 (McGhee et al., 2007). ELT-2 is considered to be the predominant transcription factor in the intestine that is responsible for differentiation and function of enterocytes (Kormish et al., 2010; McGhee et al., 2007). The functional diversity of ELT-2 also includes the response to environmental toxins, pathogenic infection, and regulating the downstream signals of the IIS pathway. ELT-2 is thought to be constitutively localized to the nucleus, which is consistent with its

role in regulating basal expression of intestinal genes throughout larval development. ELT-2 has been shown to bind the DAE element of *dod-8* (Zhang et al., 2013), and a recent ChIP-seq study showed ELT-2 occupancy of the *smf-3* promoter (Mann et al., 2016). However, another ELT-2 ChIP-seq study failed to show interaction with *smf-3* (Wiesenfahrt et al., 2016). Importantly, *smf-3* expression was not affected by *elt-2* RNAi in L1 or L4 larva (Mann et al., 2016), but this could be a consequence of redundancy with ELT-7. The data suggest a model where ELT-2 is important for basal levels of intestinal expression, where PQM-1 adds an inducible switch that is controlled by NHR-14, in response to bacterial infection for example. We cannot ignore the possibility that the regulatory network between NHR-14 and PQM-1 includes a role for ELT-2.

The upregulation of Class 2 genes in *nhr-14(tm1473)* mutants was also complemented with an enrichment of genes involved in the innate immune response. This was unexpected as Class 2 genes are regarded as important in growth and development, whereas Class 1 genes are though to be involved in the stress response (Lee et al., 2003; Murphy, 2003). Additionally, the increased activity of DAF-16/FOXO in *daf-2* mutants is thought to confer resistance to infection (Miyata et al., 2008). How this occurs is still debatable, because DAF-16/FOXO has never been shown to be nuclear localized during infection, and PQM-1 RNAi enhances susceptibility to *P. aeruginosa* (Kawli and Tan, 2008). This is also confounded by the observations that show virtually no overlap between targets of DAF-16/FOXO and p38/MAPK, the primary immune response pathway in *C. elegans*. In fact, p38/MAPK targets have more overlap with Class 2 genes (Troemel, 2006). Having a primed immune response, we hypothesized that *nhr-14(tm1473)* had a resistance phenotype when grown on pathogenic bacteria. As

expected, we saw increased survival of *nhr-14(tm1473)* mutants infected with *P. aeruginosa* and *S. enterica*. However, the loss of NHR-14 and the induction of *smf-3* during infection were unexpected. The degradation of NHR-14 in response to infection gives us clues into potential ligands for NHR-14. Since iron didn't seem to affect NHR-14, at in least protein levels or nuclear localization, pathogen associated molecular patterns (PAMPs) and other bacterial metabolites are interesting ligand possibilities that may modulate NHR-14 activity.

It is well established, that iron is an essential nutrient for pathogens, and is the basis for the evolution of mechanisms to acquire and sequester iron from the host and pathogen, respectively. In line with this, the iron chelator ciclopirox olamine (CPX) was recently identified to inhibit PA14 pathogenesis in a *C. elegans* liquid killing assay and that PA14 virulence was dependent upon the siderophore, pyoverdin, where loss of HIF-1 exacerbated pathogenesis (Kirienko et al., 2013). Since HIF-1 is important for the activation of *smf*-3, one could predict that *smf-3* induction would be important during PA14 infection. To date however, a change in *smf-3* has not been observed in expression profiling studies involving *C. elegans*' response to pathogenic bacteria. However, it has been shown that *smf-3(ok1035)* mutants are susceptible to *S. aureus* (Bandyopadhyay et al., 2009), which is consistent with our findings that *smf-3* is important for the increased survival of *nhr-14(tm1473)* mutants infected with *P. aeruginosa*. Together these data suggest that the regulation of *smf-3* by NHR-14 is part of the innate immune response to potentially regulate iron availability during infection. Since the death rate between wild-type and *nhr-14* mutants appears to be the same when infected with *Salmonella* and *Pseudomonas,* it appears that increased survival of *nhr-14* mutants is due to a delay in

initial pathogen colonization of the gut lumen. This is likely a result of having a primed immune response that is composed of an increased production of antimicrobial effectors and minimal iron bioavailability in the gut. The very nature of an innate immune response in *C. elegans* is broad and nonspecific; therefore, it is unlikely that a single gene attributes to the resistance seen in *nhr-14* mutants and rather the result of an immune response gene repertoire that protects the organism from initial infection.

Of the 284 NRs in *C. elegans*, only 17 (6%) are conserved in humans; and among these 17, NHR-14 is considered to be a homolog of HNF4α. Tissue distribution of HNF4α includes the liver, kidney, intestine, and the colon; and activates expression of genes involved in glucose, fatty acid, and xenobiotic metabolism (Gonzalez, 2008). Various studies have also shown that HNF4α plays a role in controlling iron metabolism, specifically through the activation and repression of transferrin and hepcidin gene expression (Truksa et al., 2009). More recently HNF4α was shown to be important for the hepatic expression of transferrin receptor 2 (*Tfr2*), and mice lacking HNF4α in the liver developed hypoferremia (Matsuo et al., 2015). Genome wide association studies have also implicated HNF4α in inflammatory bowel disease and ulcerative colitis, and mice with an intestinal deletion of HNF4α overexpress inflammatory cytokines including IL-1β, TNFα, IFNγ, and CCR2 (Babeu and Boudreau, 2014). In mice with an intestinal deletion of *Hnf4α* (*Hnf4*$\alpha^{\triangle IEpC}$), we found that the mammalian ortholog of *smf*-3, *Dmt1*, was significantly up regulated and this was most notable in the colon. Highest DMT-1 expression is found in the duodenum, which is the primary site of dietary iron absorption, and this is in contrast to the colon where *Dmt1* expression is minimal. Given that HNF4α regulates DMT-1 to a greater extent in the colon, combined with our data showing a role

for *nhr-14* in innate immunity, it is possible that the suppression of *Dmt1* by HNF4α is a way to control iron in an innate immune context similar to what we observed in *C. elegans*. Mutations in the DMT-1 family member, natural resistance associated macrophage protein-1 (NRAMP-1) were found to confer susceptibility to several different pathogens in mice (Nevo and Nelson, 2006). It is also known that NRAMP-1 is induced by cytokines and is important in the nitric oxide and proinflammatory response in macrophages. Similarly, iron uptake by DMT-1 in monocytes is stimulated by cytokines (Govoni et al., 1997). Whether *Hnf4*$\alpha^{\triangle IEpC}$ mice are more resistant to gastrointestinal pathogens is an area for future investigation. Additional experiments are also needed to identify how HNF4α regulates DMT-1. Is it a direct mechanism, or indirect similar to what occurs with NHR-14 in *C. elegans*?

In summary, *nhr-14* adds a new layer of regulation in a manner dependent on IIS that integrates iron metabolism with the innate immune response. This study also highlights the conserved nature of NRs between *C. elegans* and mammals, with NHR-14 and HNF4α being prime examples. Importantly, our data underscores the power of *C. elegans* as a model organism with respect to understanding host-pathogen interactions and identifying novel regulators of metabolic pathways mammals.

References

Abad P. 2008. Genome sequence of the metazoan plant-parasitic nematode *Meloidogyne incognita*. Nat. Biotechnol. *26*, 909–915.

Ackerman D, Gems D. 2012. Insulin/IGF-1 and hypoxia signaling act in concert to regulate iron homeostasis in *Caenorhabditis elegans*. PLoS Genet *8*, e1002498.

Anderson CP, Leibold EA. 2014. Mechanisms of iron metabolism in *Caenorhabditis elegans*. Front Pharmacol. *5*.

Anderson CP, Shen M, Eisenstein RS, Leibold E a. 2012. Mammalian iron metabolism and its control by iron regulatory proteins. Biochim. Biophys. Acta. *1823*, 1468–83..

Anderson GJ. 2013. Encyclopedia of Metalloproteins. In (eds. R.H. Kretsinger, V.N. Uversky, and E.A. Permyakov), pp. 985–995, Springer New York, New York, NY.

Au C, Benedetto A, Anderson J, Labrousse A, Erikson K, Ewbank JJ, Aschner M. 2009. SMF-1, SMF-2 and SMF-3 DMT1 orthologues regulate and are regulated differentially by manganese levels in *C. elegans*. PLoS One *4*, e7792.

Bandyopadhyay J, Song H-O, Park B-J, Singaravelu G, Sun JL, Ahnn J, Cho JH. 2009. Functional assessment of Nramp-like metal transporters and manganese in *Caenorhabditis elegans*. Biochem. Biophys. Res. Commun. *390*, 136–141.

Brenner S. 1974. The genetics of *Caenorhabditis elegans*. Genetics *77*, 71-94.

Cohen LB, Troemel ER. 2015. Microbial pathogenesis and host defense in the nematode C. elegans. Curr. Opin. Microbiol. *23*, 94–101.

Doitsidou M, Poole RJ, Sarin S, Bigelow H, Hobert O. 2010. *C. elegans* mutant identification with a one-step whole-genome-sequencing and snp mapping strategy. PLoS One *5*, e15435.

Dowen RH, Breen PC, Tullius T, Conery AL, Ruvkun G. 2016. A microRNA program in the *C. elegans* hypodermis couples to intestinal mTORC2/PQM-1 signaling to modulate fat transport. Genes Dev. *30*, 1515–1528.

Eden E, Navon R, Steinfeld I, Lipson D, Yakhini Z. 2009. GOrilla, a tool for discovery and visualization of enriched GO terms in ranked gene lists. BMC Bioinformatics 10, 48.

Fang B, Mane-Padros D, Bolotin E, Jiang T, Sladek FM. 2012. Identification of a binding motif specific to HNF4 by comparative analysis of multiple nuclear receptors. Nucleic Acids Res. *40*, 5343–5356.

Fleming RE, Ponka P. 2012. Iron overload in human disease. N. Engl. J. Med. *366*, 348–

359.

Ganz T, Nemeth E. 2011. Hepcidin and disorders of iron metabolism. Annu. Rev. Med. *62*, 347–60.

Garsin DA, Sifri CD, Mylonakis E, Qin X, Singh K V, Murray BE, Calderwood SB, Ausubel FM. 2001. A simple model host for identifying Gram-positive virulence factors. Proc. Natl. Acad. Sci. U. S. A. *98*, 10892–10897.

Ghedin E, Wang S, Spiro D, Caler E, Zhao Q, Crabtree J, Allen JE, Delcher AL, Guiliano DB, Miranda-Saavedra D, et al. 2007. Draft genome of the filarial nematode parasite *Brugia malayi*. Science *317*, 1756–1760.

Gonzalez FJ. 2008. Regulation of hepatocyte nuclear factor 4 alpha-mediated transcription. Drug Metab. Pharmacokinet. *23*, 2–7.

Gourley BL, Parker SB, Jones BJ, Zumbrennen KB, Leibold EA. 2003. Cytosolic aconitase and ferritin are regulated by iron in *Caenorhabditis elegans*. J. Biol. Chem. *278*, 3227–3234.

Hentze MW, Muckenthaler MU, Galy B, Camaschella C. 2010. Two to tango, regulation of mammalian iron metabolism. Cell *142*, 24–38.

Hood MI, Skaar EP. 2012. Nutritional immunity, transition metals at the pathogen-host interface. Nat. Rev. Microbiol. *10*, 525–537.

Huang DW, Sherman BT, Lempicki R a. 2009. Systematic and integrative analysis of large gene lists using DAVID bioinformatics resources. Nat. Protoc. *4*, 44–57.

Hwang AB, Ryu E-A, Artan M, Chang H-W, Kabir MH, Nam H-J, Lee D, Yang J-S, Kim S, Mair WB, et al. 2014. Feedback regulation via AMPK and HIF-1 mediates ROS-dependent longevity in *Caenorhabditis elegans*. Proc. Natl. Acad. Sci. U. S. A. *111*, E4458-67.

Irazoqui JE, Urbach JM, Ausubel FM. 2010. Evolution of host innate defence, insights from *Caenorhabditis elegans* and primitive invertebrates. Nat. Rev. Immunol. *10*, 47–58.

Kawli T, Tan M-W. 2008. Neuroendocrine signals modulate the innate immunity of *Caenorhabditis elegans* through insulin signaling. Nat. Immunol. *9*, 1415–1424.

Kim Y-I, Cho JH, Yoo OJ, Ahnn J. 2004. Transcriptional regulation and life-span modulation of cytosolic aconitase and ferritin genes in *C. elegans*. J. Mol. Biol. *342*, 421–433.

Kirienko N V, Kirienko DR, Larkins-Ford J, Wählby C, Ruvkun G, Ausubel FM. 2013. *Pseudomonas aeruginosa* disrupts *Caenorhabditis elegans* iron homeostasis, causing a

hypoxic response and death. Cell Host Microbe *13*, 406–16.

Kormish JD, Gaudet J, McGhee JD. 2010. Development of the *C. elegans* digestive tract. Curr. Opin. Genet. Dev. *20*, 346–54.

Kortman GAM, Mulder MLM, Richters TJW, Shanmugam NKN, Trebicka E, Boekhorst J, Timmerman HM, Roelofs R, Wiegerinck ET, Laarakkers CM, et al. 2015. Low dietary iron intake restrains the intestinal inflammatory response and pathology of enteric infection by food-borne bacterial pathogens. Eur. J. Immunol. *45*, 2553–2567.

Laftah AH, Sharma N, Brookes MJ, McKie AT, Simpson RJ, Iqbal TH, Tselepis C. 2006. Tumour necrosis factor α causes hypoferraemia and reduced intestinal iron absorption in mice. Biochem. J. *397*, 61–67.

Lee S-H, Wong R-R, Chin C-Y, Lim T-Y, Eng S-A, Kong C, Ijap NA, Lau M-S, Lim M-P, Gan Y-H, et al. 2013. *Burkholderia pseudomallei* suppresses *Caenorhabditis elegans* immunity by specific degradation of a GATA transcription factor. Proc. Natl. Acad. Sci. U.S.A. *110*, 15067–15072.

Lee S-J, Murphy CT, Kenyon C. 2009. Glucose shortens the life span of *c. elegans* by downregulating DAF-16/FOXO activity and aquaporin gene expression. Cell Metab. *10*, 379–391.

Liu X, Brutlag DL, Liu JS. 2001. BioProspector, discovering conserved DNA motifs in upstream regulatory regions of co-expressed genes. Pac. Symp. Biocomput. 127–138.

Mann FG, Van Nostrand EL, Friedland AE, Liu X, Kim SK. 2016. Deactivation of the GATA transcription factor ELT-2 is a major driver of normal aging in *C. elegans*. PLoS Genet. *12*, e1005956.

Mastrogiannaki M, Matak P, Keith B, Simon MC, Vaulont S, Peyssonnaux C. 2009. HIF-2α, but not HIF-1α, promotes iron absorption in mice. J. Clin. Invest. *119*, 1159–1166.

Matsuo S, Ogawa M, Muckenthaler MU, Mizui Y, Sasaki S, Fujimura T, Takizawa M, Ariga N, Ozaki H, Sakaguchi M, et al. 2015. Hepatocyte nuclear factor 4α controls iron metabolism and regulates transferrin receptor 2 in mouse liver. J. Biol. Chem. *290*, 30855-30865.

McGhee JD, Sleumer MC, Bilenky M, Wong K, McKay SJ, Goszczynski B, Tian H, Krich ND, Khattra J, Holt RA, et al. 2007. The ELT-2 GATA-factor and the global regulation of transcription in the *C. elegans* intestine. Dev. Biol. *302*, 627–45.

Minevich G, Park DS, Blankenberg D, Poole RJ, Hobert O. 2012. CloudMap, A cloud-based pipeline for analysis of mutant genome sequences. Genetics *192*, 1249–1269.

Murphy CT. 2003. Genes that act downstream of DAF-16 to influence the lifespan of

Caenorhabditis elegans. Nature *424*, 277–283.

Murphy CT, Lee S-J, Kenyon C. 2007. Tissue entrainment by feedback regulation of insulin gene expression in the endoderm of *Caenorhabditis elegans*. Proc. Natl. Acad. Sci. U. S. A. *104*, 19046–19050.

Murphy CT, McCarroll S a, Bargmann CI, Fraser A, Kamath RS, Ahringer J, Li H, Kenyon C. 2003. Genes that act downstream of DAF-16 to influence the lifespan of *Caenorhabditis elegans*. Nature *424*, 277–283.

Niu W, Lu ZJ, Zhong M, Sarov M, Murray JI, Brdlik CM, Janette J, Chen C, Alves P, Preston E, et al. 2011. Diverse transcription factor binding features revealed by genome-wide ChIP-seq in *C. elegans*. Genome Res *21*, 245–254.

Nix DA, Courdy SJ, Boucher KM. 2008. Empirical methods for controlling false positives and estimating confidence in ChIP-Seq peaks. BMC Bioinformatics *9*, 1–9.

Quach TK, Chou HT, Wang K, Milledge GZ, Johnson CM. 2013. Genome-wide microarrray analysis reveals roles for the REF-1 family member HLH-29 in ferritin synthesis and peroxide stress response. PLoS One *8*, e59719.

Reboul J, Vaglio P, Tzellas N, Thierry-Mieg N, Moore T, Jackson C, Shin-i T, Kohara Y, Thierry-Mieg D, Thierry-Mieg J, et al. 2001. Open-reading-frame sequence tags (OSTs) support the existence of at least 17,300 genes in *C. elegans*. Nat. Genet. *27*, 332–336.

Roberts AF, Gumienny TL, Gleason RJ, Wang H, Padgett RW. 2010. Regulation of genes affecting body size and innate immunity by the DBL-1/BMP-like pathway in *Caenorhabditis elegans*. BMC Dev. Biol. *10*, 1–10.

Robinson-Rechavi M, Maina C, Gissendanner C, Laudet V, Sluder A. 2005. Explosive lineage-specific expansion of the orphan nuclear receptor hnf4 in nematodes. J. Mol. Evol. *60*, 577–586.

Romney SJ, Newman BS, Thacker C, Leibold EA. 2011. HIF-1 regulates iron homeostasis in *Caenorhabditis elegans* by activation and inhibition of genes involved in iron uptake and storage. PLoS Genet. *7*, e1002394.

Romney SJ, Thacker C, Leibold EA. 2008. An iron enhancer element in the *ftn-1* gene directs iron-dependent expression in *Caenorhabditis elegans* intestine. J. Biol. Chem. *283*, 716–725.

Rouault TA. 2015. Mammalian iron-sulphur proteins, novel insights into biogenesis and function. Nat. Rev. Mol. Cell. Biol. *16*, 45–55.

Sarov M, Murray JI, Schanze K, Pozniakovski A, Niu W, Angermann K, Hasse S, Rupprecht M, Vinis E, Tinney M, et al. 2012. A genome-scale resource for in vivo tag-

based protein function exploration in *C. elegans*. Cell *150*, 855–866.

Settivari R, Levora J, Nass R. 2009. The divalent metal transporter homologues SMF-1/2 mediate dopamine neuron sensitivity in *Caenorhabditis elegans* models of manganism and parkinson disease. J. Biol. Chem. *284*, 35758–35768.

Shah YM, Matsubara T, Ito S, Yim S-H, Gonzalez FJ. 2009. Intestinal hypoxia-inducible transcription factors are essential for iron absorption following iron deficiency. Cell Metab. *9*, 152–164.

Shapira M, Hamlin BJ, Rong J, Chen K, Ronen M, Tan M-W. 2006. A conserved role for a GATA transcription factor in regulating epithelial innate immune responses. Proc. Natl. Acad. Sci. U. S. A. *103*, 14086–91.

Siggs OM, Beutler B. 2012. The BTB-ZF transcription factors. Cell Cycle *11*, 3358–3369.

Simcox JA, McClain DA. 2016. Iron and diabetes risk. Cell Metab *17*, 329–341.

Simonsen KT, Gallego SF, Færgeman NJ, Kallipolitis BH. 2012. Strength in numbers, "Omics" studies of *C. elegans* innate immunity. Virulence *3*, 477–484.

Simonsen KT, Møller-Jensen J, Kristensen AR, Andersen JS, Riddle DL, Kallipolitis BH. 2011. Quantitative proteomics identifies ferritin in the innate immune response of *C. elegans*. Virulence *2*, 120–130.

Stehling O, Lill R. 2013. The role of mitochondria in cellular iron–sulfur protein biogenesis, mechanisms, connected processes, and diseases. Cold Spring Harb Perspect Biol *5*, a011312.

Stuart LM, Paquette N, Boyer L. 2013. Effector-triggered versus pattern-triggered immunity, how animals sense virulent pathogens. Nat. Rev. Immunol. *13*, 199–206.

Tan MW, Mahajan-Miklos S, Ausubel FM. 1999. Killing of *Caenorhabditis elegans* by *Pseudomonas aeruginosa* used to model mammalian bacterial pathogenesis. Proc. Natl. Acad. Sci. U.S.A. *96*, 715–720.

Taubert S, Ward JD, Yamamoto KR. 2011. Nuclear hormone receptors in nematodes, evolution and function. *Mol. Cell Endocrinol. 334*, 49–55.

Tawe WN, Eschbach ML, Walter RD, Henkle-Duhrsen K. 1998. Identification of stress-responsive genes in *Caenorhabditis elegans* using RT-PCR differential display. Nucleic Acids Res. *26*, 1621–1627.

Tepper RG, Ashraf J, Kaletsky R, Kleemann G, Murphy CT, Bussemaker HJ. 2013. PQM-1 complements DAF-16 as a key transcriptional regulator of DAF-2-mediated

development and longevity. Cell *154*, 676–690.

Troemel ER. 2006. p38 MAPK regulates expression of immune response genes and contributes to longevity in *C. elegans*. PLoS Genet. *2*, e183.

Truksa J, Lee P, Beutler E. 2009. Two BMP responsive elements, STAT, and bZIP/HNF4/COUP motifs of the hepcidin promoter are critical for BMP, SMAD1, and HJV responsiveness. Blood *113*, 688–695.

Visvikis O, Ihuegbu N, Labed SA, Luhachack LG, Alves A-MF, Wollenberg AC, Stuart LM, Stormo GD, Irazoqui JE. 2014. Innate host defense requires TFEB-mediated transcription of cytoprotective and antimicrobial genes. Immunity *40*, 896–909.

Wang X, Garrick MD, Yang F, Dailey LA, Piantadosi CA, Ghio AJ. 2005. TNF, IFN-gamma, and endotoxin increase expression of DMT1 in bronchial epithelial cells. Am. J. Physiol. Lung Cell Mol. Physiol. *289*, L24-33.

Ward D, Kaplan J. 2012. Ferroportin-mediated iron transport, expression and regulation. Biochim. Biophys. Acta. *1823*, 1426–1433.

Wessling-Resnick M. 2010. Iron Homeostasis and the Inflammatory Response. Annu Rev Nutr. *30*, 105–122.

Wessling-Resnick M. 2015. Nramp1 and Other Transporters Involved in Metal Withholding during Infection. J. Biol. Chem. *290*, 18984–18990.

Wiesenfahrt T, Berg JY, Osborne Nishimura E, Robinson AG, Goszczynski B, Lieb JD, McGhee JD. 2016. The function and regulation of the GATA factor ELT-2 in the *C. elegans* endoderm. Development *143*, 483–491.

Wong D, Bazopoulou D, Pujol N, Tavernarakis N, Ewbank JJ. 2007. Genome-wide investigation reveals pathogen-specific and shared signatures in the response of *Caenorhabditis elegans* to infection. Genome Biol. *8*, R194.

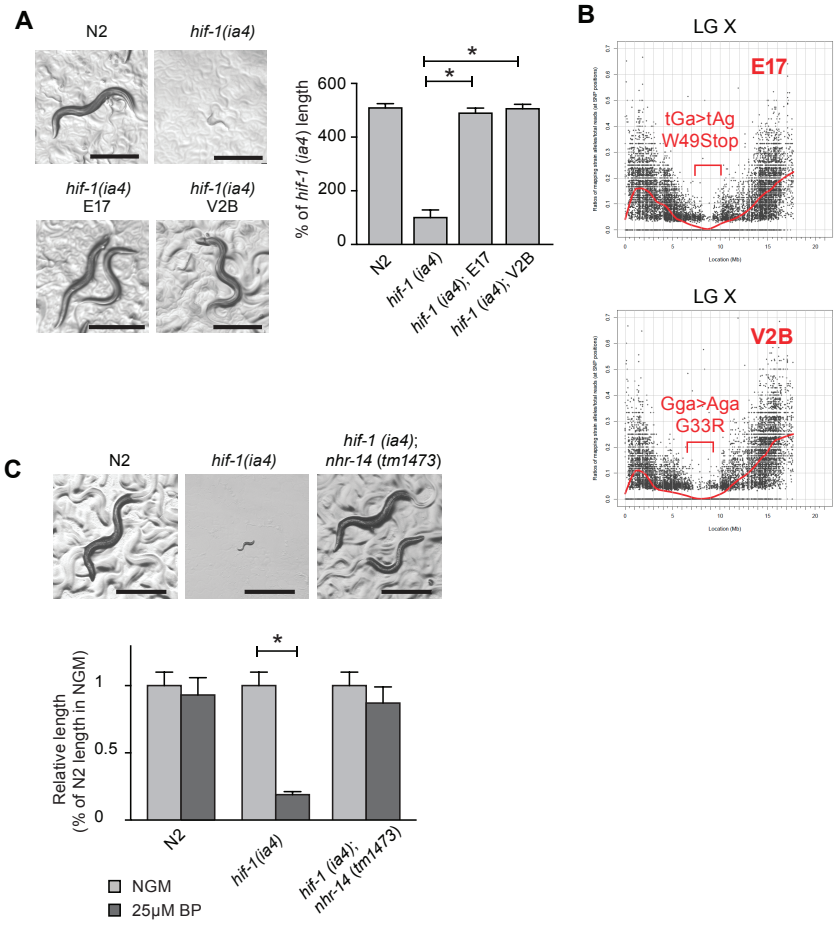

Figure 3.1. Mutations in nhr-14 rescue the low iron developmental delay in *hif-1(ia4)* mutants. A) Representative images of N2 wild-type worms and *hif-1(ia4)* mutants grown on NGM plates containing 20 uM BP (iron chelator) after 5 days. Quantification of worm length from panel A as a percentage of *hif-1(ia4)* length (n = 50). B) CloudMap SNP Mapping are shown as XY-scatter plots where the ratio of Hawaiian SNPs to Bristol SNPs is represented for the E17 and V2B mutants. C) Representative images of N2 wild-type and *hif-1(ia4)* mutants, and *hif-1(ia4);nhr-14(tm1473)* double mutants grown in NGM 25 uM BP after 5 days. Quantification of worm length from panel D after 5 days growth in NGM or NGM-25 uM BP (n = 15) and calculated as a percentage of N2 wild-type worms grown in NGM. Values are the mean ± SEM; *$p < 0.05$.

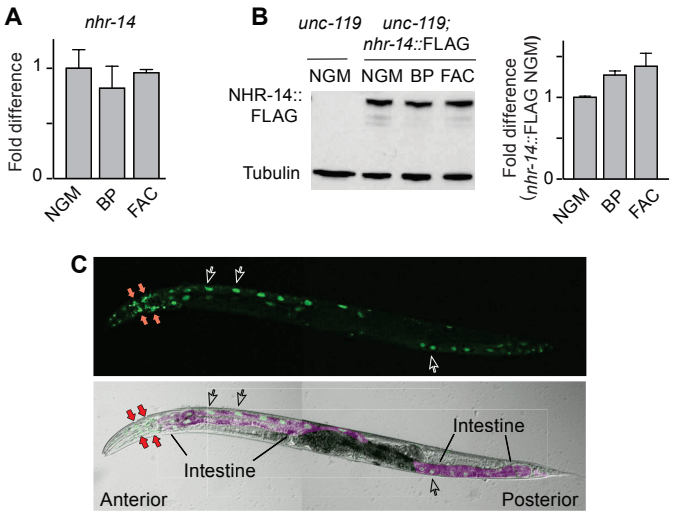

Figure 3.2. NHR-14 is expressed within the nucleus of intestinal cells and is unaltered by changes in iron availability. A) *nhr-14* expression measured by qRT-PCR in N2 adults grown in NGM, NGM-BP, and NGM-FAC and normalized to N2 worms on NGM (n = 3). B) Representative western blot of NHR-14::GFP::FLAG protein in noninjected worms (unc-119) versus injected transgenic worms grown in NGM, NGM-BP or NGM-FAC. C) Subcellular localization of NHR-14::GFP::FLAG by confocal microscopy in young adult transgenic worms. Values are the mean ± SEM.

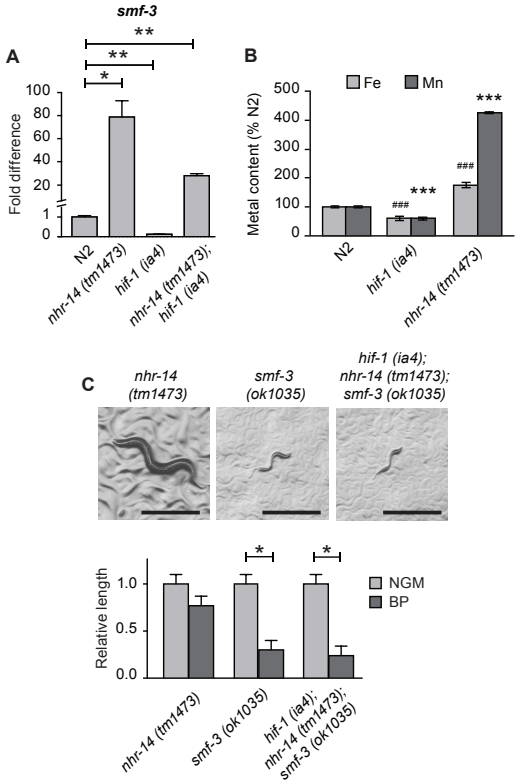

Figure 3.3. NHR-14 is a repressor of the intestinal iron importer smf-3. A) smf-3 expression measured by qRT-PCR in N2 wild-type, *hif-1(ia4)*, *nhr-14(tm1473)*, and *hif-1(ia4);nhr-14(tm1473)* double mutants grown in NGM (n = 3). B) Total iron and manganese content of N2 wild-type worms, and *nhr-14(tm1473)* and *hif-1(ia4)* mutants grown in NGM (n = 3) quantified by ICP-OES. C) Representative images of *nhr-14(tm1473), smf-3(ok1035)*, and *nhr-14(tm1473);hif-1(ia4);smf-3(ok1035)* mutants grown in NGM-25 uM BP for 5 days. Worm length was quantified after 5 days growth in NGM or NGM-25 uM BP (n = 15) and calculated as a percentage of worms grown in NGM. Values are the mean ± SEM; *p < 0.05, **p < 0.01, and ***p < 0.001.

Figure 3.4. PQM-1 is downstream of NHR-14 and is an activator of smf-3. A) Illustration of the *smf-3(-1500bp)::GFP-his* transcriptional reporter containing 1500 bp of 5' regulatory sequences of *smf-3* (-105 to -228 bp relative to the putative ATG initiator encompassing the 123-bp IDE containing putative DAE sites. B) GFP intensity in *smf-3(-1500bp)::GFP-his* worms fed control RNAi (grey bars) or *nhr-14* RNAi (red bars) in NGM, NGM-BP or NGM-FAC plates (n = 1000 worms per treatment) was quantified using the COPAS Biosorter. C) Representative images of *smf-3(-1500)::GFP-his* transgenic worms grown on either control (empty vector) or *pqm-1* RNAi. D) GFP intensity in smf-3(-1500)::GFP-his transgenic worms with a single nucleotide mutation in each of the DAE motifs grown on NGM or 100 μM BP-NGM. E) Endogenous smf-3 gene expression in N2 wild-type versus pqm-1(ok485) mutants grown on NGM. F) Length of N2, *hif-1(ia4)*, and *pqm-1(ok485)* mutants grown on NGM or BP treated plates. G) *smf-3* expression in N2 wild-type and *nhr-14(tm1473)* mutants grown on EV or *pqm-1* RNAi. H) Length of N2, *hif-1(ia4)*, and *nhr-14(tm1473);hif-1(ia4)* mutants grown on 25 μM BP and treated with EV or *pqm-1* RNAi. I) Representative images of L3 PQM-1::GFP worms fed control or *nhr-14* RNAi along with quantification of the percentage of worms with nuclear GFP localization. Values are the mean ± SEM; *$p < 0.05$, **$p < 0.01$ and ***$p < 0.001$.

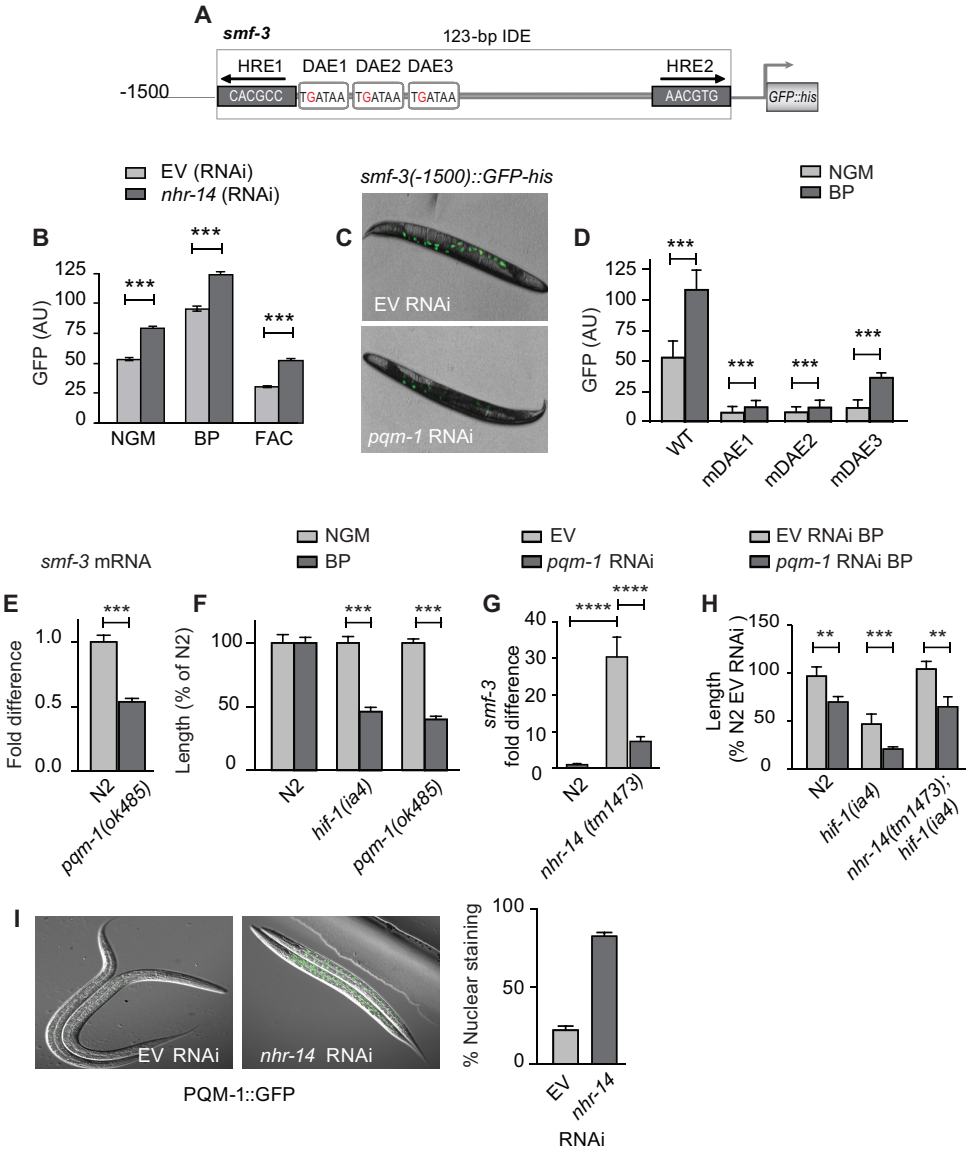
A
smf-3
123-bp IDE
HRE1
DAE1 DAE2 DAE3
HRE2
-1500
CACGCC
TGATAA TGATAA TGATAA
AACGTG
GFP::his
B
EV (RNAi)
nhr-14 (RNAi)
GFP (AU)
NGM
BP
FAC
C
smf-3(-1500)::GFP-his
EV RNAi
pqm-1 RNAi
D
NGM
BP
GFP (AU)
WT
mDAE1
mDAE2
mDAE3
E
smf-3 mRNA
Fold difference
N2
pqm-1(ok485)
F
NGM
BP
Length (% of N2)
N2
hif-1(ia4)
pqm-1(ok485)
G
EV
pqm-1 RNAi
smf-3 fold difference
N2
nhr-14 (tm1473)
H
EV RNAi BP
pqm-1 RNAi BP
Length (% N2 EV RNAi)
N2
hif-1(ia4)
nhr-14(tm1473); hif-1(ia4)
I
EV RNAi
nhr-14 RNAi
PQM-1::GFP
% Nuclear staining
EV
nhr-14
RNAi

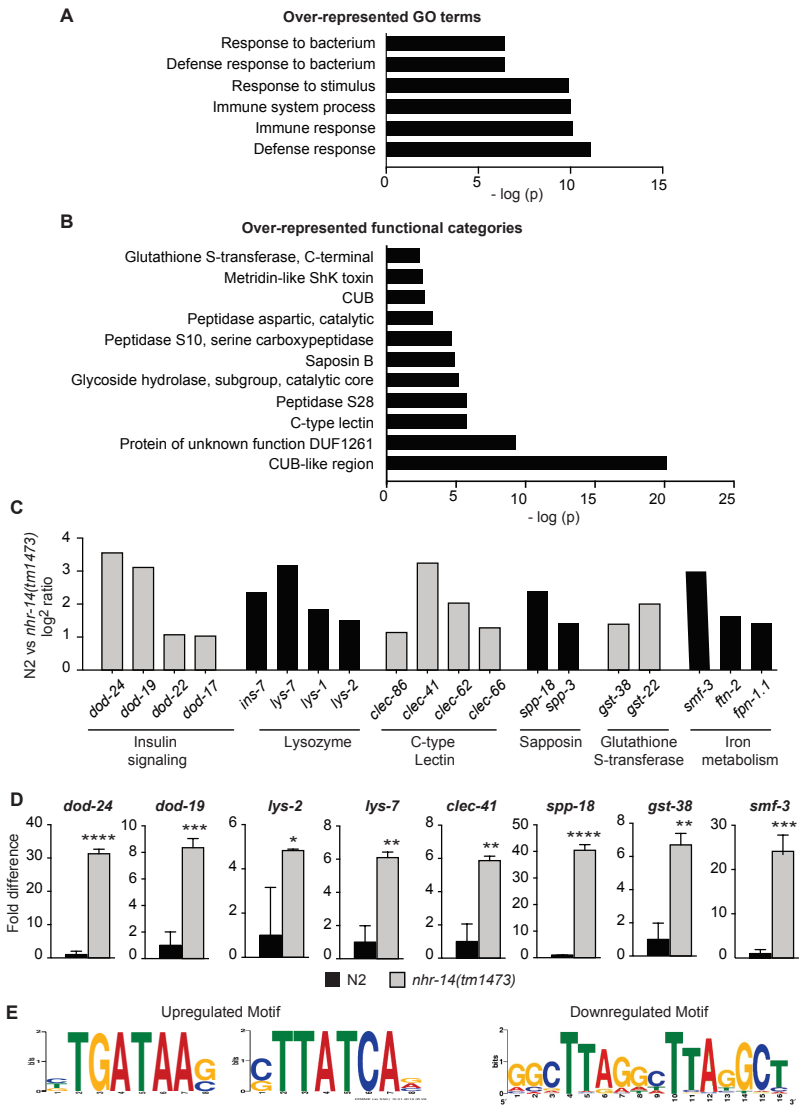

Figure 3.5. NHR-14 regulates an innate immune transcriptional program. A) Gene ontology analysis of genes that were upregulated in *nhr-14(tm1473)* mutants compared to N2 wild-type worms. B) DAVID functional category analysis of upregulated genes in *nhr-14(tm1473)* mutants compared to N2 wild-type worms. C) Selection of innate immune genes that are upregulated in *nhr-14(tm1473)* mutants. D) qRT-PCR confirmation of select innate immune genes that are upregulated in *nhr-14(tm1473)* mutants (n = 3). E) Motif enrichment analysis for upregulated and downregulated genes in *nhr-14(tm1473)* mutants. Values are the mean fold-difference compared to N2 wild-type worms ± SEM.; *p < 0.05, **p < 0.01, and ***p < 0.001.

Figure 3.6. NHR-14 is downregulated in response to *P. aeruginosa* PA14, and loss of NHR-14 confers resistance to PA14 infection. A) Survival curves of N2 wild-type and *nhr-14(tm1473)* mutants infected with P. aeruginosa on standard SK medium. Data represent three independent experiments. Values are the mean ± SEM; *p < 0.05 and ***p < 0.001 relative to N2 (Log-rank Mantel-Cox test). B) *P. aeruginosa* PA14 colonization of N2 wild-type and *nhr-14(tm1473)* worms after 24 h of infection. C) *smf-3* and *nhr-14* mRNA expression after 24 h on E. coli OP50 or *P. aeruginosa* PA14 measured by qRT-PCR (n = 3). D) NHR-14::GFP::FLAG immunoblots after 24 h on *E. coli* OP50 or *P. aeruginosa* PA14 (n = 3). Tubulin is a loading control. Values in B and C are the mean ± SEM; *p < 0.05, **p < 0.01 and ***p < 0.001. E) Survival curve of N2 wild-type and nhr-14(tm1473) worms infected with S. enterica. Values are presented as the mean ± SEM; ***p < 0.001 (Log-rank Mantel-Cox test). F) *S. enterica* colonization of N2 wild-type and *nhr-14(tm1473)* worms after 72 h of infection. G) *smf-3* and *nhr-14* expression after 72 h on *E. coli* OP50 or *S. enterica* measured by qRT-PCR (n = 3). H) NHR-14::GFP::FLAG immunoblot after 72 h on E. coli OP50 or S. enterica (n = 3). I) Survival curve of *nhr-14(tm1473), smf-3(ok1035)*, *and nhr-14(tm1473);smf-3(ok1035)* worms infected with *P. aeruginosa* PA14 on standard SK medium, and J) Survival curves of *nhr-14(tm1473)* mutants infected with P. aeruginosa on standard SK medium or FAC-supplemented SK medium. Data represent 3 independent experiments. Values are presented as the mean ± SEM; *p < 0.05 and ***p < 0.001 relative to N2 NGM, (Log-rank (Mantel-Cox) test). Values for F-H are the mean ± SEM; *p <0.05 (Student's t-test).

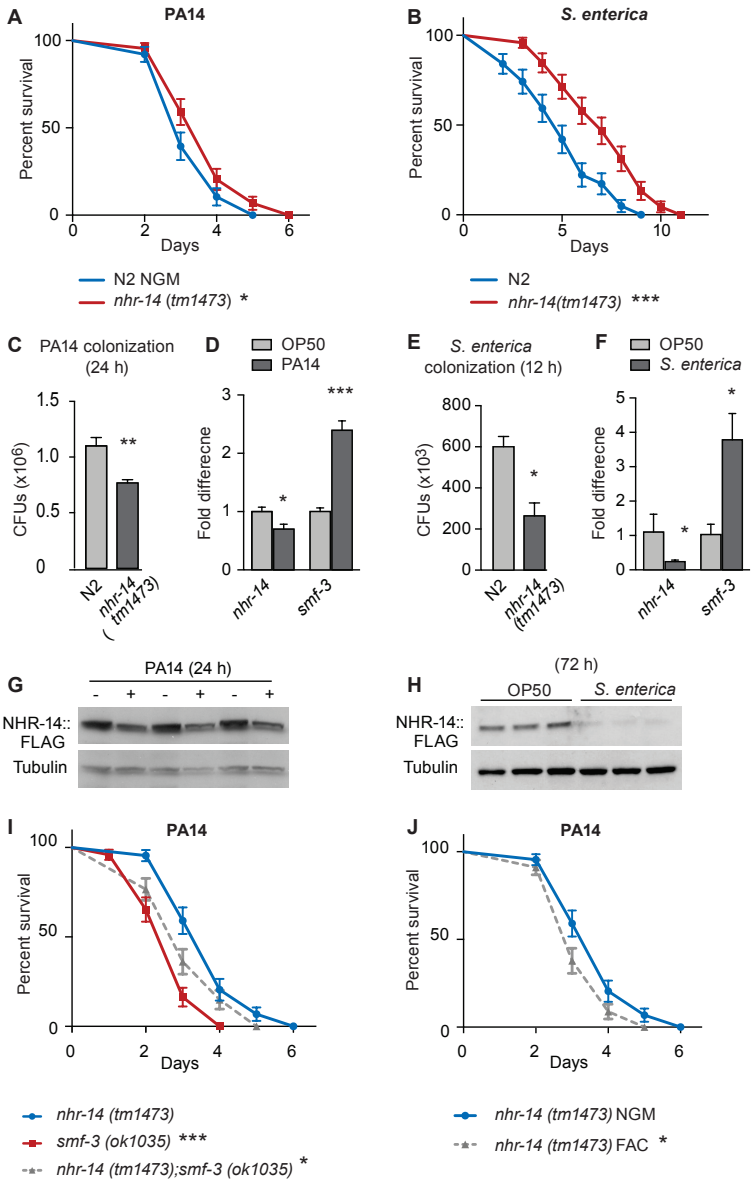
A
PA14
Percent survival
Days
N2 NGM
nhr-14 (tm1473) *
B
S. enterica
Percent survival
Days
N2
nhr-14(tm1473) ***
C
PA14 colonization (24 h)
CFUs (x10^6)
N2
nhr-14 (tm1473)
**
D
OP50
PA14
Fold differecne
nhr-14
smf-3
***
*
E
S. enterica colonization (12 h)
CFUs (x10^3)
N2
nhr-14 (tm1473)
*
F
OP50
S. enterica
Fold differecne
nhr-14
smf-3
*
G
PA14 (24 h)
- + - + - +
NHR-14:: FLAG
Tubulin
H
(72 h)
OP50
S. enterica
NHR-14:: FLAG
Tubulin
I
PA14
Percent survival
Days
nhr-14 (tm1473)
smf-3 (ok1035) ***
nhr-14 (tm1473);smf-3 (ok1035) *
J
PA14
Percent survival
Days
nhr-14 (tm1473) NGM
nhr-14 (tm1473) FAC *

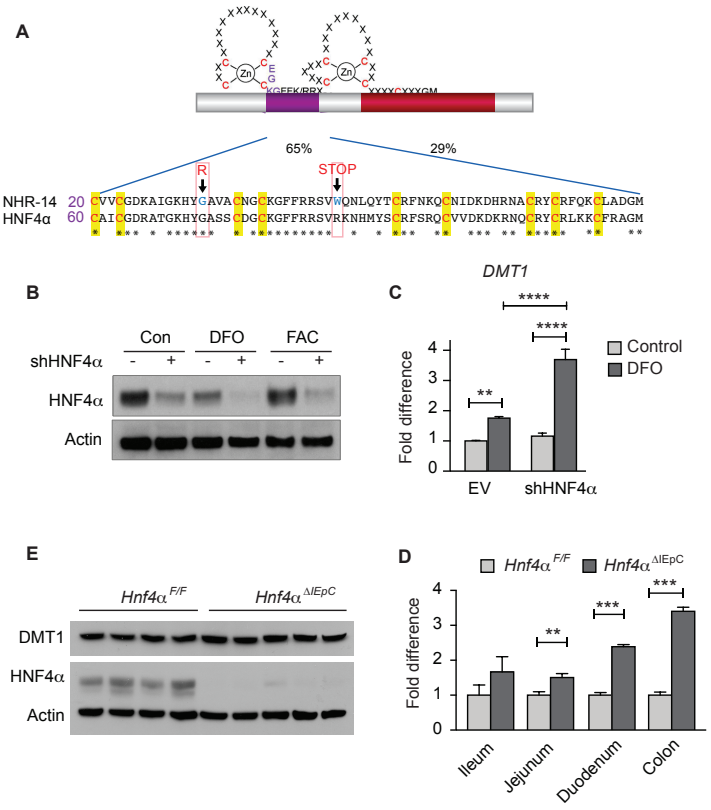

Figure 3.7. HNF4α, the mammalian ortholog of NHR-14, regulates DMT-1 expression in the intestinal epithelia. A) Protein alignment of the DNA binding domains for HNF4α and NHR-14 with locations of the E17 and V2B mutations. B) HNF4α immunoblot indicating shRNA knockdown in HT29 colorectal cells treated overnight with DFO or FAC. C) Expression of DMT-1 in EV shRNA or shHNF4α transformed HT29 cells grown under normal iron conditions or DFO chelation. D) DMT-1 immunoblot of WT and HNF4αVillin/Cre lysates from colonic epithelial scrapings. E) Expression of DMT-1 in intestinal tissues of WT and HNF4αVillin/Cre mice. Values are presented as the mean ± SEM; *$p < 0.05$, **$p < 0.01$, and ***$p < 0.0001$.

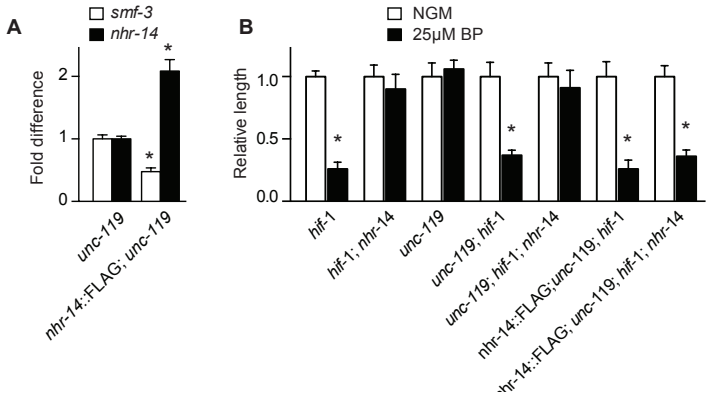

Figure S3.1. NHR-14::GFP::FLAG functions similarly to endogenous NHR-14. The functionality of NHR-14::GFP::FLAG was tested by its ability to downregulate *smf-3* transcript levels, as well as replace endogenous NHR-14. A) To test transcriptional regulation of smf-3, smf-3 and nhr-14 mRNAs were measured by qRT-PCR in noninjected worms (unc-119) versus NHR-14::GFP::FLAG; ttTi5606; unc-119 transgenic worms (n = 3). *nhr-14* mRNA levels increased and smf-3 mRNA levels decreased in NHR-14::GFP::FLAG transgenic worms compared to noninjected ttTi5606;unc-119 worms. B) To test for functional replacement of NHR-14, mutations in hif-1 and nhr-14 genes were introduced into the unc-119 double mutant and then injected with the NHR-14::GFP::FLAG expressing fosmid. Relative worm length of strains grown under normal (white bars) or low iron (black bars) conditions was determined (n = 15). Note that *unc-119; hif-1; nhr-14* triple mutants expressing NHR-14::GFP::FLAG displayed the hif-1-dependent developmental delay as compared to *hif-1(ia4); nhr-14(tm1473)* mutants, indicating that NHR-14::GFP::FLAG is functional. C) Lifespan was determined for N2 wild-type and *nhr-14(tm1473)* mutants grown in NGM or NGM-25 uM BP; *$p < 0.05$ (log-rank Mantel-Cox test). Values are presented as the mean ± S.D.; *$p < 0.01$ indicates a significant difference between strains or iron conditions.

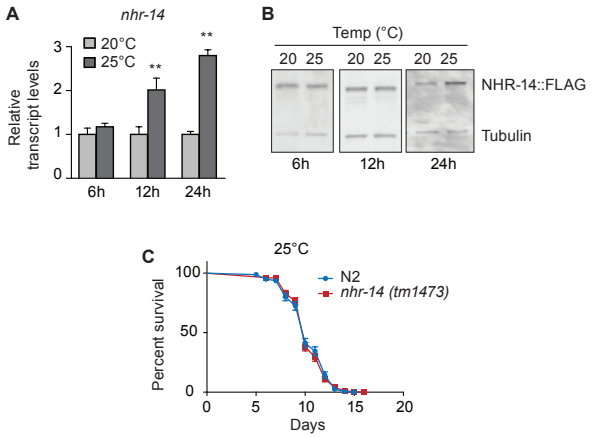

Figure S3.2. NHR-14 is induced during heat stress. A) *nhr-14* expression in N2 wild-type worms grown at 20 oC or 25 oC for 6, 12, and 24 h. B) NHR-14::GFP::FLAG expression in transgenic worms grown at 20 oC or 25 oC for 6, 12, and 24 h. C) Percent survival of N2 wild-type and nhr-14(tm1473) mutants grown at 25 oC. Values are the mean ± SEM, *p < 0.05 (Student's t-test). Log-rank (Mantel-Cox) test was used to compare survival curves, **p < 0.01.

A

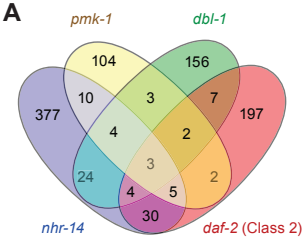

B **Table S3.** Expression profile comparisons between *nhr-14tm1473* mutants and published innate immune pathway models

Microarray data used in previous publications (reference)	Upregulated genes	Overlapping genes	Representation factor	P-value
pmk-1/p388 MAPK (47)	133	22	6.4	4.1e-12
dbl-1/TGFβ (52)	203	28	5.3	5.0e-13
daf-2 Class 2 (43)	250	42	6.5	2.4e-22

C

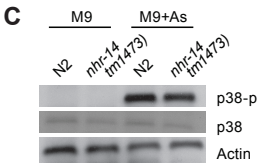

Figure S3.3. Analysis of transcriptional overlap between innate immune pathways and *nhr-14(tm1473)* mutants. A) Venn diagram of gene expression overlap between up-regulated genes in *nhr-14(tm1473)* mutants and genes activated in the p38-MAPK (*pmk-1*), TGFβ (*dbl-1*), and DAF-2/DAF-16 (*daf-2*) pathways. B) Hypergeometric probabilities for the gene expression overlap in A. C) Immunoblot for p38 (PMK-1) phosphorylation in N2 wild-type and *nhr-14(tm1473)* mutants treated with M9 or M9 plus 5 mM sodium arsenite to induce stress.

Table 3.1 Differentially expressed genes in *nhr-14(tm1473)* mutants

A. Top 25 up-regulated genes

Gene Name	log2	Description
B0024.4	5.69	Unknown
F26A1.8	5.55	Unknown
dod-21	4.25	Epoxide Hydrolase
T19C9.8	3.91	Epoxide Hydrolase
asp-17	3.77	Aspartic Peptidase
dod-24	3.56	Epoxide Hydrolase
C32H11.9	3.48	Epoxide Hydrolase
col-129	3.31	Surfactant Protein
Y47H10A.5	3.27	Exoribonuclease
clec-41	3.25	C-type Lectin
lys-7	3.19	Lysozyme
tsp-2	3.16	Tetraspanin
dod-23	3.12	Unknown
dod-19	3.12	Unknown
col-139	3.03	Cuticle
smf-3	3.00	Divalent Metal Ion Transporter
col-81	2.98	Cuticle
tsp-1	2.82	Tetraspanin
Y37H2A.14	2.82	Unknown
ZK6.11	2.81	Unknown
T27D12.6	2.78	Unknown
oac-14	2.78	Acyl Transferase
C14C6.5	2.73	Metridin-like ShK Toxin
C49C3.9	2.67	Epoxide Hydrolase
oac-20	2.64	Acyl Transferase

B. Top 25 down-regulated genes

Gene Name	log2	Description
R09D1.12	-4.51	Kinase
cpt-6	-4.28	Carnitine Palmitoyltransferase
H20E11.2	-3.80	Unknown
str-25	-3.69	Transmembrane Receptor
H34I24.3	-3.65	TRP Channel Like
fmi-1	-3.59	Cadherin
smg-5	-3.50	Nonsense Mediated Decay
C06B8.3	-3.35	Hydroxysteroid Dehydrogenase
F33H12.8	-3.27	Unknown
C28G1.6	-3.21	Ret Finger Protein
tag-244	-3.19	Unknown
Y46D2A.8	-3.16	Unknown
Y47H10A.6	-3.10	Unknown
cyp-35D2	-3.09	Cytochrome P450
ZK484.6	-3.04	Unknown
Y54G2A.10	-2.96	Unknown
clec-187	-2.94	C-type Lectin
R10D12.10	-2.92	Tau Tubulin Kinase
spp-4	-2.89	Saposin
C51E3.11	-2.84	Unknown
mys-4	-2.82	Histone Acetyltransferase
C14C6.3	-2.76	Fucosyltransferase
acr-12	-2.67	Acetylcholine Receptor
acd-1	-2.66	Sodium Channel
fbxa-159	-2.59	F-box A Protein

Table 3.2 Overlap between the 457 upregulated genes in *nhr-14 (tm1473)* mutants and genes induced upon infection with various pathogens.

Microarray data used in previous publications (reference)	No. of up-regulated genes	No. of overlapping genes	Representation factor	P-value
***P. aeruginosa* (Shapira et al. 2007)**	**196**	**73**	**10.59**	**P < 0.0001**
***P. aeruginosa* (Troemel et al. 2006)**	**303**	**96**	**9.01**	**P <0 .0001**
***P. luminescens* (Wong et al. 2007)**	**659**	**63**	**2.71**	**P < 0.0001**
***S. aureus* (Visvikis et al. 2014)**	**803**	**56**	**2.59**	**P<0.001**
***E. faecalis* (Wong et al. 2007)**	**639**	**44**	**1.95**	**P < 0.01**
***Serratia marscens* (Wong et al. 2007)**	**599**	**5**	**0.23**	**P = 0.999**

CHAPTER 4

MAMMALIAN IRON METABOLISM AND ITS CONTROL BY IRON REGULATORY PROTEINS

From Cole P. Anderson, Macy Shen, Richard S. Eisenstein and Elizabeth A. Leibold. Biochim Biophys Acta. 2012;1823(9):1468-83.

Biochimica et Biophysica Acta 1823 (2012) 1468–1483

Contents lists available at SciVerse ScienceDirect

Biochimica et Biophysica Acta

journal homepage: www.elsevier.com/locate/bbamcr

Review

Mammalian iron metabolism and its control by iron regulatory proteins ☆

Cole P. Anderson [a], Macy Shen [b], Richard S. Eisenstein [b], Elizabeth A. Leibold [a,c,*]

[a] Department of Oncological Sciences, University of Utah, 15 N. 2030 E., Salt Lake City, UT 84112, USA
[b] Department of Nutritional Sciences, University of Wisconsin, 1415 Linden Drive, Madison, WI 53706, USA
[c] Department of Medicine, University of Utah, 15 N. 2030 E., Salt Lake City, UT 84112, USA

ARTICLE INFO

Article history:
Received 19 March 2012
Received in revised form 7 May 2012
Accepted 11 May 2012
Available online 17 May 2012

Keywords:
Iron
IRP
Iron-responsive element
RNA-binding protein
Iron–sulfur protein
Post-transcriptional regulation

ABSTRACT

Cellular iron homeostasis is maintained by iron regulatory proteins 1 and 2 (IRP1 and IRP2). IRPs bind to iron-responsive elements (IREs) located in the untranslated regions of mRNAs encoding protein involved in iron uptake, storage, utilization and export. Over the past decade, significant progress has been made in understanding how IRPs are regulated by iron-dependent and iron-independent mechanisms and the pathological consequences of IRP2 deficiency in mice. The identification of novel IREs involved in diverse cellular pathways has revealed that the IRP–IRE network extends to processes other than iron homeostasis. A mechanistic understanding of IRP regulation will likely yield important insights into the basis of disorders of iron metabolism. This article is part of a Special Issue entitled: Cell Biology of Metals.

1. Introduction

Iron is required by most organisms as it serves as a prosthetic group for proteins involved in central cellular processes, including respiration, DNA synthesis and oxygen transport. In excess, cellular iron catalyzes the generation of free radicals that damage protein, DNA and lipids, whereas cellular iron deficiency impairs cellular proliferation. In humans, with the inherited diseases hemochromatosis, excess cellular iron can result in cirrhosis, cardiomyopathy and diabetes mellitus (reviewed in [1]). Excess iron content in the brain is associated with several inherited neurodegenerative diseases, including neurodegeneration with brain iron accumulation (NBIA) and Friedreich's ataxia (FA), as well as common neurodegenerative disorders such as Parkinson's and Alzheimer's diseases (reviewed in [1–3]). On the other hand, iron deficiency affects billions of people worldwide, and results in cognitive defects in children and anemia in adults. Cellular iron content must therefore be maintained within a narrow range to avoid the adverse consequences of iron deficiency or excess. Maintenance of cellular iron homeostasis is accomplished by the coordinated regulation of iron uptake, storage and export by iron-regulatory proteins 1 and 2 (IRP1 and IRP2, also known as ACO1 and IREB2). This review focuses on advances in IRP regulation of iron metabolism focusing on the past 6 years. We direct readers to several excellent reviews on IRPs [4–7] and to chapters in this volume on systematic iron homeostasis, iron–sulfur (Fe–S) cluster biogenesis, iron trafficking, and SKP1–CUL1–FBXL5 structure and function.

2. Overview of systemic and cellular iron metabolism

2.1. Systemic iron metabolism

Approximately, 1–3 mg of iron is absorbed by humans each day, in order to replace iron losses in the urine, sweat and from desquamated enterocytes. As mammals lack a regulated physiological mechanism for iron excretion, intestinal iron absorption is a highly regulated process. Dietary non-heme ferric iron is absorbed by enterocytes by divalent metal transporter 1 (SLC11A2, also known as DMT1 and NRAMP2) after reduction by membrane bound ferrireductases (such as duodenal cytochrome *b* (CYBRD1, also known as DCYTB)) (Fig. 1). Heme iron is also taken up by enterocytes by an undefined mechanism. Cellular iron is translocated through the enterocyte and is exported into the circulation by the basolateral exporter ferroportin (SLC40A1). Iron export is dependent on the oxidation of iron by the membrane bound multicopper oxidase hephaestin enabling it to bind to plasma transferrin (Tf). Diferric Tf (Tf-Fe(III) is the major form of iron for most cells with erythroid precursors being the major user as iron is required for heme synthesis. Tf-Fe(III) binds to cell surface transferrin receptor 1 (TFRC, also known as TfR1) followed by internalization of the Tf-Fe(III)–TfR1 complex by clathrin-mediated endocytosis. On acidification of the endosome, ferric iron is released from Tf and reduced by STEAP3, and exported into

☆ This article is part of a Special Issue entitled: Cell Biology of Metals.

* Corresponding author at: Department of Oncological Sciences, University of Utah, 15 N. 2030 E., Salt Lake City, UT 84112, USA. Tel.: +1 801 585 5002; fax: +1 801 585 3501.
E-mail address: betty.leibold@genetics.utah.edu (E.A. Leibold).

0167-4889/$ – see front matter © 2012 Elsevier B.V. All rights reserved.
doi:10.1016/j.bbamcr.2012.05.010

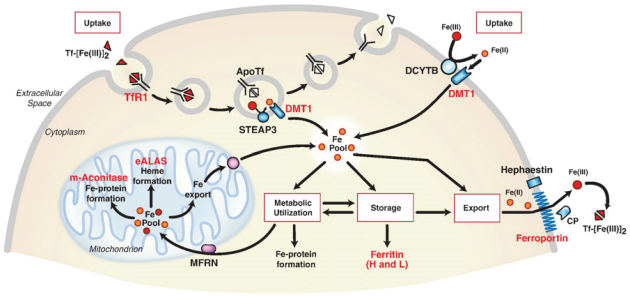

Fig. 1. Control of mammalian cellular iron homeostasis by the IRE–IRP regulatory network. A generic mammalian cell depicting roles of proteins encoded by IRE-containing mRNAs (*red lettering*). Transferrin bound to two iron atoms (Tf-[Fe(III)$_2$) binds to TfR1 on the cell surface where the Tf-[Fe(III)$_2$–TfR1 complex is endocytosed. Acidification of the endosome causes the release of Fe(III) (*red balls*) from Tf where it is reduced to Fe(II) (*orange balls*) by the STEAP3 oxidoreductase before export by DMT1 (divalent metal transporter 1). ApoTf/TfR1 complex is returned to the cell surface where it dissociates and initiates another round of iron uptake. Tf-bound iron is taken up by most cells, but it is especially important in erythroid precursors where it is the primary source of iron for heme synthesis. DMT1 is also localized on the apical membrane of duodenal enterocytes where it transports Fe(II) after reduction by membrane reductases, such as DCYTB. Iron taken up by either TfR1 or DMT1 enters a cytosolic free labile iron pool thought to consist of Fe(II) bound to small molecular weight molecules. IRPs sense iron in this pool and regulate the translation of 5′ IRE-containing mRNAs (H-ferritin and L-ferritin, eALAS (erythroid aminolevulinate synthase), mitochondrial (m)-aconitase and ferroportin) or the stability of 3′ IRE-containing mRNAs (TfR1 and DMT1). eALAS serves as the rate-limiting enzyme in heme synthesis in erythroid precursors. Mitochondrial aconitase is an enzyme in the TCA cycle that requires a [4Fe–4S] cluster for activity. Iron that is not utilized or stored in ferritin is exported by ferroportin. Export of iron from cells is coupled to the oxidation of iron by membrane-bound hephaestin or serum multicopper oxidase ceruloplasmin (CP). Modified from Wallander et al. [4].

the cytosol by DMT1. Cytosolic iron is used for the formation of iron-containing proteins and by the mitochondria for biosynthesis of Fe–S clusters and heme. When body iron stores and erythropoiesis are adequate, iron export from enterocytes is reduced by hepcidin-mediated internalization and degradation of ferroportin, and instead iron is stored in ferritin. Iron in ferritin is lost after 3 days by desquamation of intestinal cells.

The small amount of iron (1–3 mg) absorbed by humans each day represents only a fraction of the total body iron, and most of the circulating iron comes from the recycling of heme from senescent erythrocytes by reticuloendothelial macrophages. The iron released from heme is exported into the circulation by ferroportin where it binds to apoTf for delivery to bone marrow for hemoglobin synthesis. Elevated hepatic iron stores and inflammation increase hepcidin production, which mediates ferroportin degradation in intestinal cells and in reticuloendothelial macrophages, leading to reduced plasma iron levels.

2.2. IRPs are the principal cellular iron regulators in vertebrates

Maintaining cellular iron content requires precise mechanisms for regulating its uptake, storage and export. IRP1 and IRP2 are the principal regulators of cellular iron homeostasis in vertebrates. IRPs are cytosolic proteins that bind to iron-responsive elements (IREs) in the 5′ or 3′ untranslated regions of mRNAs encoding proteins involved in iron uptake (TfR1, DMT1), sequestration (H-ferritin subunit (FTH1) and L-ferritin subunit (FTL)) and export (ferroportin) (Fig. 2). When cells are iron deficient, IRPs bind to 5′ IREs in ferritin and ferroportin mRNAs with high affinity to repress translation, and to 3′ IREs in TfR1 mRNA to block its degradation. When iron is in excess, IRPs do not bind to IREs, increasing synthesis of ferritin and ferroportin, while promoting the degradation of TfR1 mRNA. The coordinated regulation of iron uptake, storage and export by the IRPs ensures that cells acquire adequate iron for their needs without reaching toxic levels.

IRPs also regulate other mRNAs that contain 5′ IREs, including mitochondrial aconitase (ACO2, also known as m-acon, tricarboxylic acid cycle (TCA)), erythroid aminolevulinate synthase (ALAS2, also known as eALAS, heme biosynthesis), hypoxia-inducible transcription factor-2α (EPAS1 also known as HIF-2α, hypoxia adaptation) and amyloid beta precursor protein (APP, Alzheimer's disease), and 3′ IREs, including DMT1 (metal transport), CDC14A (mitotic phosphatase), CDC42-binding protein kinase α (also known as MRCKα, cytoskeletal dynamics) and hydroxyacid oxidase 1 (HAO1, peroxisomal enzyme) [8–17]. More recently, a transcriptome-wide approach was utilized to identify 35 novel putative IRE-containing mRNAs, some of which have exclusivity for IRP1 or IRP2 [18]. While these mRNAs each contain an IRE, the roles of many of these IREs *in vivo* remain to be determined. The presence of IREs in a variety of mRNAs indicates that IRP regulation extends to processes other than iron homeostasis.

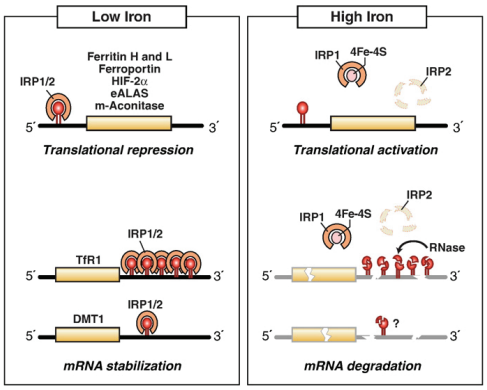

Fig. 2. IRPs regulate translation and stability of IRE-containing mRNAs. IRPs bind to IREs located in either the 5′ or 3′ untranslated regions of specific mRNAs. When iron is limited, IRPs bind with high affinity to 5′ IRE mRNAs and repress translation, and to the five 3′ IREs in TfR1 mRNA and to the single IRE in DMT1 mRNA and stabilize these mRNAs. When iron is abundant, IRPs do not bind IREs, resulting in the translation of 5′ IRE-containing mRNAs and degradation of TfR1 mRNA. Iron mediates the conversion of the IRP1 RNA binding form into the [4Fe–4S] cluster c-aconitase form and the ubiquitination and targeted proteasomal degradation IRP2 by FBXL5 E3 ligase. IRE-containing mRNAs indicated are those that have been shown to be functional *in vivo*.
Modified from Wallander et al. [4].

3. Recent advances in IRP1 regulation

Although IRP1 and IRP2 share approximately 64% identity, bind RNA and are regulated by iron, they differ in several ways. First, IRP1 is a bifunctional protein serving either as a high affinity IRE binding protein in its apoprotein form or the cytosolic isoform of the iron–sulfur (Fe–S) enzyme aconitase (c-acon) (Fig. 3). Formation and loss of the [4Fe–4S] cluster regulates RNA binding and provides unique links between IRP1 and cellular Fe–S cluster biogenesis. Second, IRP1 has distinctive roles in the adaptive response to oxygen availability as well as in sensing reactive oxygen species (ROS) or reactive nitrogen species (RNS). Third, IRP1 is controlled by multiple iron-dependent mechanisms, including targeted protein degradation to limit accumulation of the RNA binding form of IRP1 [19]. Fourth, phosphorylation of IRP1 at serine 138 dictates the mechanism of its regulation by iron. Unlike IRP1, IRP2 lacks a [4Fe–4S] cluster and aconitase activity, and functions as an RNA binding protein. IRP2 is primarily regulated by iron-mediated degradation. Thus, IRP1 responds to iron-dependent and iron-independent signals that control its function through multiple mechanisms in order to maintain IRE-binding activity within a range that permits the optimal maintenance of cellular iron homeostasis.

3.1. Regulation of IRP1 RNA binding activity by the 4Fe–4S cluster

The key role of the [4Fe–4S] cluster in IRP1 in controlling RNA binding activity provides a means for linking cellular pathways involved in formation of these cofactors to cellular iron status. In recent years, many studies have focused on unraveling the mechanism and pathways of Fe–S biogenesis in model organisms and their dysfunction in human disease [20–23] [see also Lill et al. in this volume]. In brief, the evidence indicates that the major pathway for biogenesis of Fe–S clusters and their insertion into cytosolic proteins, such as IRP1, first involves targeting of iron to the mitochondria where it is imported through the action of mitoferrin [24] [see also Paw et al. in this volume]. A transient Fe–S cluster is formed on the scaffold protein ISCU through the action of iron, the iron binding protein frataxin and sulfide derived from cysteine via the cysteine desulfurase NFS1 and its partner ISD11 [25–30]. The Fe–S cluster on ISCU, or in some cases other scaffold proteins [31], is donated to apoprotein targets with the assistance of protein chaperones (e.g. HSCB in humans) and electron donors (e.g. FDX, ferredoxin) [21]. Activities of the mitochondrial Fe–S cluster biogenesis machinery along with the export machinery components (e.g. ABCB7) are required for activation of the cytosolic Fe–S cluster assembly (CIA) pathway. Genetic approaches using IRP1 expressed in yeast led to discovery of the first CIA factor, Cfd1 [32]. Additional elegant studies primarily in yeast led to identification of Nbp35 that together with Cfd1 forms the initial Fe–S scaffold for cytosolic cluster formation with the assistance of DRE2 and TAH18 [30,32–36]. Transfer of the labile cluster from Cfd1/Nbp35 to some apoprotein targets requires the Nar1/Cia1 heteromer while for others Nbp35 suffices (reviewed in [22]). Interestingly, recent studies have begun to identify "specificity factors" that target specific apoFe–S proteins (e.g. complex 1) [37,38]. Whether or not separate pathways for Fe–S cluster biogenesis exist for sensory and regulatory roles of Fe–S proteins in mammalian cells, such as IRP1, remains to be determined.

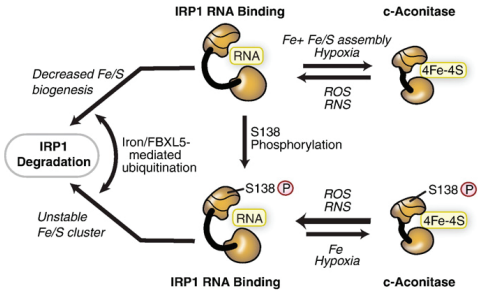

Fig. 3. Iron-dependent and iron-independent mechanisms for regulating IRP1. IRP1 can be regulated through mechanisms dependent or independent of the [4Fe–4S] cluster. In the cluster-dependent pathway, IRP1 has dual roles either as a high affinity IRE-binding protein when devoid of the [4Fe–4S] cluster or as a c-aconitase when the [4Fe–4S] cluster is assembled. The c-aconitase form does not bind RNA. The [4Fe–4S] cluster is accessible to low molecular cluster perturbants, including reactive oxygen species (ROS), such as $O_2^{\bullet -}$, H_2O_2 or reactive nitrogen species (RNS), such as NO• or $ONOO^-$. Hypoxia stabilizes the c-aconitase form by reducing the level of oxygen or ROS. IRP1 can be phosphorylated at S138. IRP1 phosphomimetic mutants indicate that the Fe–S cluster can be assembled and the protein exhibits aconitase activity; however, the Fe–S cluster is more sensitive to disruption by oxygen and hydrogen peroxide. Iron stimulates the FBXL5-mediated degradation of IRP1 S138 phosphomimetic mutants and non-phosphorylated IRP1 when Fe–S cluster biogenesis is impaired.
Modified from Wallander et al. [4].

Primarily through the use of RNAi-based knockdown approaches, the activity of the Fe–S biogenesis pathways have been shown to influence cellular iron sensing and distribution in mammalian cells. Disruption of components of the mitochondrial Fe–S biogenesis pathway, including the cysteine desulfurase NFS1 and its partner ISD11 [25,39], the Fe–S scaffolds ISCU [40] and ISCA [41], the iron binding protein frataxin [27,42], glutaredoxin 5 [43], protein chaperone HSC20 [44,45] and electron donors ferredoxins 1 and 2 [39,46], impairs the activity of both mitochondrial, cytosolic, and presumably nuclear Fe–S proteins in mammalian cells. The ensuing reduction in c-acon activity is reflected in IRP1 activation that is associated with an increase in TfR1 and reduction in ferritin expression. That IRP2 is stabilized suggests a general cytosolic iron deficiency [39,43,44,47,48]. While the increase in TfR1 and repression of ferritin induced by IRP activation may reflect a compensatory mechanism to combat cytosolic iron deficiency, failure to prevent further inappropriate iron accumulation in the face of excess iron reflects an inability to downregulate IRP activity that could be cytotoxic [40]. There is also evidence of cellular iron maldistribution with abnormal cellular iron deposits and mitochondrial overload coupled with cytosolic iron deficiency when mitochondrial Fe–S biogenesis is impaired [40,43,47]. Similar changes have been observed in yeast [49–53]. While these studies confirm the concept that cytosolic Fe–S cluster biogenesis is dependent on active mitochondrial cluster formation in mammalian cells, they also demonstrate that the impact of impaired mitochondrial Fe–S biogenesis may in part involve indirect effects on IRPs or IRP targets. Future studies should address questions concerning what pathways of Fe–S cluster biogenesis are sensed by IRP and whether trafficking of iron through mitochondria is an obligate process through which IRP senses iron.

The impact of impaired cytosolic Fe–S cluster biogenesis on IRP1 has also been examined [54–58]. Reduction of NUBP1 and NAR1 specifically impairs cytosolic Fe–S proteins, including c-acon and others [56–58]. Concomitant with this is the activation of IRP1 along with an increase in TfR1 and a reduction in ferritin expression. Interestingly, IRP2 is not affected suggesting that the response of IRP2 observed when mitochondrial Fe–S biogenesis is impaired is a secondary response to the maldistribution of cellular iron. Thus, as is the case when the cytosolic Fe–S cluster biogenesis system is inhibited in yeast, inhibition of the cognate proteins in mammalian cells has a selective impact on cytosolic Fe–S proteins. The finding that IRP2 is stabilized in ABCB7-deficient mammalian cells may reflect a feedback effect on mitochondrial Fe–S cluster formation or iron metabolism [55]. Deletion of the yeast homolog of ABCB7, Atm1p, also leads to an abnormal distribution of iron [51]. Taken together, these studies suggest that unlike IRP1, IRP2 does not sense the flux of iron through the cytosolic Fe–S biogenesis pathway.

Investigations of the etiology of FA provide the most clearly understood example linking a human disease of Fe–S cluster biogenesis and alterations in IRP function (reviewed in [59–61]). FA is the most common inherited ataxia in humans. It is primarily caused by formation

of triplet expansion repeats in the frataxin gene leading to reduced expression of this small acidic mitochondrial protein although missense mutations of frataxin are also a cause. Frataxin binds to a complex containing the Fe–S scaffold protein ISCU and the cysteine desulfurase NFS1 and its partner ISD11, and in this process is believed to function as an iron chaperone [27–29,62]. One study reported that a small portion of frataxin also functions in the cytosol where it interacts with IRP1 and facilitates conversion to c-acon [42]. At the cellular level, FA is characterized by a loss of activities of mitochondrial, cytosolic, and presumably nuclear Fe–S proteins. Similar to what has been observed with the knockdown of other participants in mitochondrial Fe–S cluster biogenesis pathway, FA is associated with mitochondrial iron overload and signs of cytosolic iron deficiency [27,63,64]. Both IRPs are activated, and this is associated with a reduction in ferritin and increase in TfR1 expression. Furthermore, expression of the iron exporter ferroportin is reduced further contributing to the abnormal iron distribution, and presumably to oxidative stress observed in FA [64]. Interestingly, frataxin deficiency is associated with a reduction of other components of the mitochondrial Fe–S cluster machinery, including ISCU and NFS1, along with defects in heme synthetic enzymes [64]. The fact that frataxin expression is itself reduced in iron deficiency suggests that the induction of cytosolic iron deficiency due to impaired mitochondrial Fe–S cluster biogenesis could be amplified by a downstream impact of reduced frataxin expression [27]. An interesting area for further investigation concerns the extent to which enhanced accumulation of IRE RNA binding activity, especially that provided by the large latent pool of IRP1 RNA binding activity in the form of c-acon, coupled with impaired ability to down-regulate IRP due to inhibition of the iron-dependent SKP1–CUL1–FBXL5 (S-phase kinase-associated protein 1-Cullin 1-F-box-leucine rich repeat protein 5) E3 ubiquitin ligase further exacerbates disease etiology. This issue likely has relevance to numerous diseases of Fe–S cluster biogenesis (reviewed in [46,59]).

3.2. Fe–S cluster disassembly in c-acon facilitates sensing reactive oxygen and nitrogen species

The discovery that IRP1 RNA binding activity could be generated from c-acon raised a key issue of how, and under what conditions, could the Fe–S cluster be removed. Iron deficiency per se was not believed to be sufficient to promote loss of the cluster on its own. However, aconitases have long been known to sense ROS and RNS because their [4Fe–4S] cluster is solvent accessible and these reactive species can initiate cluster loss (reviewed in [65]). In fact, for one isoform of aconitase in *Escherichia coli*, the ease with which it was inactivated by superoxide anion appears to function as a feedback mechanism to modulate an overactive electron transport chain [66]. This only requires conversion to the [3Fe–4S] cluster species that, in the case of c-acon, is not sufficient to generate RNA binding activity. A further important fact is that aconitases differ in their sensitivity to ROS and RNS, where c-acon is more resistant [67–69]. Thus, although the Fe–S switch mechanism was accepted as a bonafide means for iron regulation of IRP1, the mechanistic basis through which it occurred was not clear.

Insight into this problem came from early studies showing that tumor cell aconitase was a target of NO generated by activated macrophages (reviewed in [70]). On this basis, a large number of studies were initiated demonstrating that NO and its reactive product $ONOO^-$ can facilitate conversion of c-acon to IRP1 (reviewed in [71]). NO also influenced IRP2, but the mechanism for this regulation and the impact on iron metabolism was unclear [72,73]. Recent studies using mice lacking IRP1 or IRP2 have assessed the role of each IRP in the NO-dependent regulation of macrophage iron metabolism. These studies demonstrated that IRP1 was solely responsible for alterations in macrophage iron metabolism in response to NO [74]. Furthermore, NO-dependent activation of IRP1 could ameliorate abnormal iron storage in *Irp2*$^{-/-}$ bone marrow macrophages *ex vivo* by repressing ferritin expression. Similarly, activation of IRP1 by the pharmacological nitroxide Tempol prevented the neurodegenerative symptoms in *Irp2*$^{-/-}$ mice [75]. Tempol is best known as a free radical scavenger; however, in *Irp2*$^{-/-}$ mice Tempol appeared to promote cluster loss from c-acon through the direct action of RNS.

While the ability of NO to activate IRP1 may be necessary for macrophage activation or action, the physiological role of ROS is less clear. Loss of the Fe–S cluster from aconitases can be initiated by superoxide leading to the generation of the [3Fe–4S] non-RNA binding form and H_2O_2 generates IRP1 from c-acon although the mechanism through which this occurs is not clear (reviewed in [76,77]). Increased conversion of c-acon to IRP1 by H_2O_2 may enhance iron uptake while impairing storage and export, leading to iron overload. However a recent report suggests a mechanism to partially evade IRP action under these conditions [78]. Perhaps the physiological role of ROS involves the constant conversion of a small fraction of c-acon into IRP1. Depending on the cellular iron status, IRP1 could then be converted back to c-acon or remain in the RNA binding form to regulate IRE-containing mRNAs. In other words, physiological generation of ROS may be necessary for iron sensing by IRP1.

An additional, but not necessarily alternative view is that the sensitivity of c-acon to ROS and RNS can be regulated allowing for the existence of pools of protein with a stable versus unstable Fe–S cluster. Previous studies demonstrated that two protein kinase C phosphorylation sites exist in IRP1, S138 and S711. S138 phosphomimetic mutants of c-acon are much more oxygen labile compared to the wildtype protein and are also at least 10-fold more sensitive to NO in terms of cluster disassembly [79,80]. Furthermore, these phosphomutants undergo spontaneous disassembly of the Fe–S cluster even in the absence of a perturbant [80]. Another study showed that IRP1 activation by H_2O_2 requires a signaling pathway possibly involving phosphorylation [81]. Taken together, these studies show that rapid recruitment of IRE-binding activity can be achieved by cluster perturbants or phosphorylation induced alterations in Fe–S cluster stability.

3.3. Iron regulation of IRP1 protein degradation

Early studies on the mechanism of IRP1 regulation by iron suggested that protein degradation was the primary mechanism for inactivation of RNA binding [82]. With the demonstration that IRP1 is the cytosolic isoform of aconitase, and that insertion and loss of the [4Fe–4S] cluster regulated RNA binding, the “Fe–S switch” mechanism was widely accepted as the dominant mechanism for controlling IRP1 RNA binding activity [83]. This view was further advanced by the observation that total levels of IRP1/c-acon protein did not change as a function of iron status. In many cases, however, the c-acon pool is in vast excess relative to IRP1 [84,85]. Thus, the much larger and more stable c-acon pool would mask iron-dependent changes in abundance of IRP1. Liver provides a case in point as c-acon exceeds IRP1 by more than 100-fold. Severe dietary iron deficiency results in an increase of IRP1 RNA binding activity of no more than 4-fold, indicating that a small portion of the c-acon pool was recruited [84]. Hence, iron-mediated degradation of IRP1 would not be routinely observed using immunoblots. Some evidence indicated that IRP1 could be regulated through protein degradation during iron overload or through phosphorylation [86,87]. The role of protein degradation in controlling IRP1 was examined anew using models where the Fe–S switch was disrupted either by mutation of cluster-ligating cysteines or through genetic manipulation of Fe–S cluster assembly or disassembly [54,88]. In this manner, regulation of IRP1 can be examined without c-acon. Under these conditions, IRP1 stability was clearly iron-regulated, and led to the view that iron-mediated IRP1 degradation was a compensatory mechanism to prevent excess RNA binding activity when the Fe–S cluster switch mechanism is not active, which can be lethal [19,54]. The relevance of this mechanism to IRP1 function was further substantiated with the finding that the FBXL5 E3 ligase that targets IRP2 for degradation also acts on IRP1 [89–91].

Given these findings, it is of interest that studies where Fe–S cluster biogenesis is impaired, IRP1 protein levels dropped significantly [25,41,44,47,48,54–58,92]. Under these conditions, IRP1 protein can be stabilized by iron chelation, suggesting that the loss of IRP1 is not merely due to instability of an apoprotein but instead is part of a second iron dependent mechanism to control accumulation of IRP1 RNA binding activity [54]. Impaired mitochondrial Fe–S biogenesis leads to cytosolic iron deficiency, presumably reducing FBXL5 activity as evidenced by increased IRP2 protein levels [23,27,39,44,47,48,55]. The mechanism by which IRP1 is degraded while IRP2 is stabilized under these conditions remains undetermined. Relative to normal cells, a reduction in FBXL5 activity in response to impaired mitochondrial Fe–S biogenesis could lead to increased IRP2 accumulation but still be sufficient to degrade excess IRP1 arising from an inability to accumulate c-acon. FBXL5 independent mechanisms may also account for this paradox, but further studies are required to determine FBXL5 function in response to impaired mitochondrial Fe–S cluster biogenesis. Regardless of the mechanism, the extent to which IRP1 and IRP2 RNA binding activity rises to pathological levels when Fe–S cluster formation is impaired is likely to be influenced by the abundance of c-acon and the extent to which FBXL5 is inactivated. These factors will likely be strong predictors of the extent to which IRP1 and IRP2 RNA binding activity rise to unacceptable levels in pathological states involving impaired Fe–S cluster formation or accelerated cluster disassembly.

3.4. S138 phosphorylation and the mechanism of IRP1 regulation by iron

The Fe–S switch and protein degradation mechanisms for controlling IRP1 function could each have unique uses in modulating iron metabolism in order to meet cellular needs. Hence, issues such as sensitivity to Fe–S biogenesis activity or the level of ROS or RNS may meet the distinctive iron requirements of specific cell types or physiological scenarios. A mechanism that could serve these needs involves S138 phosphorylation of IRP1 by protein kinase C because it leads to accumulation of the RNA binding form [93]. The finding that S138 phosphomimetic mutants of IRP1 could be converted to a form of c-acon with a highly unstable Fe–S cluster suggested an altered set-point for iron regulation [79]. Surprisingly, the S138E phosphomutant was still subjected to iron regulation but as a consequence of iron-stimulated protein degradation reminiscent of IRP2 regulation [87]. In order to determine if enhanced oxidative damage of IRP1 as a consequence of increased Fe–S cluster cycling in $IRP1^{S138E}$ promoted its degradation, the cluster-ligating cysteine residues were mutated to serine, blocking cluster insertion in S138E and wildtype IRP1 ($IRP1^{S138E/3C>3S}$ and $IRP1^{3C>3S}$). While this failed to block iron-dependent degradation of $IRP1^{S138E}$, the more surprising result was that the protein level of $IRP1^{3C>3S}$ and another cluster mutant were iron-regulated [54,88]. These observations were confirmed by the subsequent demonstration that IRP1 is a substrate for the FBXL5 E3 ligase [89,90]. Recent studies indicate that $IRP1^{S138E}$ can be regulated either by protein degradation or Fe–S cluster insertion depending on the level of ROS or RNS [80]. These studies suggest that S138 phosphorylation of IRP1 is a mechanism to rapidly increase IRP1 RNA binding activity and to facilitate formation of a pool of c-acon that is sensitive to cluster perturbants and cellular iron levels. Coupled with the iron-mediated degradation of IRP1 by FBXL5, inducible phosphorylation broadens the physiological scenarios of IRP1 action.

3.5. IRPs and oxygen sensing

The discovery of a functional IRE in the 5′ UTR of the mRNA encoding HIF-2α suggested new roles for IRPs in the adaptive response to hypoxia and iron deficiency [10]. A recent study reported that HIF-2α mRNA is translationally repressed in liver from iron-deficient rats, and is associated with increased IRP1 and IRP2 activity [94]. Other studies have provided evidence that the HIF-2α IRE is preferentially targeted by IRP1 [11,95]. HIF-2α is primarily regulated by protein stabilization in response to hypoxia and iron deficiency (reviewed in [96,97]). Under these conditions, HIF-2α stimulates erythropoiesis through activation of erythropoietin (EPO) and intestinal iron absorption through the activation of DMT1 and ferroportin [98–101], providing a mechanism to coordinate iron uptake with red cell production. IRP-dependent translational regulation of HIF-2α mRNA has been proposed as a mechanism to reduce EPO production during hypoxia resulting from impaired erythropoiesis in iron deficient anemia, thereby ensuring that microcytic hypochromic red blood cells are not produced [10]. Given the preferential regulation of HIF-2α mRNA by IRP1, this suggests that under hypoxic iron sufficient conditions IRP1 would exist in its c-acon form, and unable to bind RNA, ensuring that HIF-2α mRNA is translated and EPO is produced. The significance of the preferential regulation of the HIF-2α IRE by IRP1 requires further investigation.

3.6. Hierarchical regulation of IRE-containing mRNA

Vertebrate mRNAs containing consensus IREs encode proteins of widely varying function, from those with a direct role in iron metabolism to proteins involved in the regulation of citrate metabolism (m-acon), cell proliferation, cytoskeletal dynamics (MRCKα), cell cycle (CDC14A), and in the adaptive responses to hypoxia (HIF-2α). The broad functional spectrum of proteins encoded by IRE-containing mRNAs suggests that they are not identically regulated by IRPs. A comparison of the binding affinity of 5′ IRE-containing mRNAs to IRP1 provides a basis for determining the extent to which IRPs may act hierarchically in mammals.

One example of differential regulation of IRP target mRNAs is expression of ferritin and eALAS during erythroid differentiation. Erythroid precursors have a high iron requirement given the large quantity of heme and hemoglobin they produce. Thus, in erythroid precursors producing hemoglobin, iron would be diverted to mitochondria for heme formation and away from storage in ferritin. With regard to IRPs, the evidence indicates that eALAS mRNA is more weakly regulated than ferritin mRNA [9]. In primary murine erythroid progenitors upon differentiation, ferritin mRNA translation is tightly repressed with less than 5% of the mRNA polysome bound, whereas translation of eALAS mRNA is more efficiently translated with 40% of this mRNA associated with polysomes [102]. This 8-fold relative difference in translatability of these mRNAs occurred under conditions when IRPs are activated and TfR1 mRNA levels are enhanced. The higher affinity of the ferritin IRE for IRPs may in part explain its selective repression under these conditions [103]. It remains to be determined if the polysome bound eALAS mRNA present during normal erythroid differentiation has escaped IRP action due to its low-affinity IRE or because variants of the eALAS mRNA exist that lack the IRE. Regarding this point it is of interest that at least two studies indicate that both IRPs are critical for red cell heme formation. First, in $Irp2^{-/-}$ mice, eALAS biosynthesis is increased in erythroid bone marrow precursor cells, leading to inappropriate synthesis of protoporphyrin IX and anemia [104]. These mice also display reduced TfR1 and increased ferritin expression, indicating erythroid precursors are iron deficient. Although $Irp1^{-/-}$ mice do not develop microcytic anemia, the anemia is more severe in $Irp2^{-/-}$ $Irp1^{+/-}$ mice, indicating that IRP1 has a role in erythroid function [105]. Second, in zebrafish and humans, defects in glutaredoxin 5 lead to impairment of mitochondrial Fe–S biogenesis and cytosolic iron depletion that activates IRP1, and reduces eALAS expression [19,43]. Taken together, these studies suggest that differential targeting of 5′ IRE-containing mRNAs by IRPs is essential for optimal coordination of heme formation and iron storage during erythropoiesis.

Another example of differential regulation of IRP target mRNAs is the expression of ferritin and m-acon [84,106]. Dietary iron deficiency leads to a reduction of liver ferritin to undetectable levels. The decline of m-acon protein levels under these conditions is significant, but

reflects only about a 50% decrease. Thus, in response to the same signal, proteins encoded by 5′ IRE-containing mRNAs, are selectively regulated. These differences in expression can be attributed to the selective regulation of these proteins at the translational level, as observed in cultured cells and in cell-free protein synthesis systems programmed with IRP1 or IRP2 [84,106,107] and the finding that IRP1 binds less well to the m-acon versus L-ferritin IRE [108,109]. Consistent with these findings, genetic ablation of both IRP1 and IRP2 in mice leads to a substantial enhancement not only of ferritin, but also ferroportin expression in intestine, while there was a smaller fold increase in m-acon expression [110]. These studies support the view that m-acon mRNA is less efficiently repressed in tissues compared with other 5′ IRE-containing mRNAs.

A third example of differential regulation of 5′ IRE-containing mRNAs in mammals comes from a comparison of HIF-2α and L-ferritin mRNA translation in liver [94]. In iron-replete rat liver, about 3-fold more HIF-2α mRNA was found associated with polysomes compared with L-ferritin mRNA. Iron deficiency leads to increased IRP RNA binding activity and a further translational repression of both mRNAs, yet HIF-2α mRNA remained more highly polysome associated. Finally, the comparison of succinate dehydrogenase iron protein subunit and ferritin expression in *Drosophila* further indicates that IRP hierarchically regulate mRNA translation *in vivo* [111]. Thus, differential translational control of 5′ IRE-containing mRNA by IRPs is essential for adaptive changes in iron metabolism and in other metabolic processes.

What dictates the differential translational control of 5′ IRE-containing mRNAs? To determine how mRNAs containing functional 5′ IREs are differentially regulated, the affinity of IRP1 for six 5′ IRE-containing mRNAs was determined [108]. These IREs bound to IRP1 in a hierarchical manner that related to the function of the encoded protein, such that ferritin IREs had the highest affinity while m-acon had the lowest. IRP1 bound to 5′ IREs over a 9-fold range: L-ferritin, H-ferritin, ferroportin, HIF-2α, eALAS and m-acon (Fig. 4A). Similar results were reported for IRP1 binding affinities for ferritin and m-acon IRE using an alternative binding assay [109]. Given the high affinity of IRP1 for binding the IRE (pM affinity), a valid concern is whether the 9-fold difference in affinity is sufficient to alter regulation. To address this, the affinity of IRP1 with a L-ferritin mutant IRE observed in a case of hereditary hyperferritinemia–cataract syndrome (HHCS) was examined. The affinity of the mutant L-ferritin IRE differed from the wildtype by only 1.9 fold yet this was sufficient to produce L-ferritin dysregulation *in vivo* [108,112]. A more striking evaluation of this is seen when the affinities of a large number of HHCS IRE mutants were compared to the rise in serum ferritin due to mRNA derepression [113] (Fig. 4B). The plot of serum ferritin as a function of K_{rel} (relative binding affinity) revealed that the steepest slope occurred over the first 10-fold loss of affinity. Similar results were obtained for IRP2 [113]. This is essentially the same range of affinity differences observed for the binding of natural 5′ IREs to IRP1 (Fig. 4A). These findings indicate that small changes in IRP1 or IRP2 binding affinity lead to physiological and pathologically significant changes in the synthesis of proteins encoded by 5′ IRE-containing mRNAs.

How are these changes in affinity of interaction between IRP1 and IRE established? Binding affinity is dependent on the number and strength of bonds between receptor and ligand, and biologically significant differences in affinity are usually assumed to involve a loss or gain of multiple bonds. In the case of IRP1, however, it can be inferred that the 9-fold difference in binding affinity would arise due to small differences in binding energy equivalent to a single H-bond [108]. Consequently, Goforth, et al. proposed that the difference in bond strength and/or in an induced fit mechanism, but not bond number, may give rise to the regulatory binding hierarchy [108]. Indeed, the recent report of the crystal structure of IRP1 bound to the TfR1 B IRE indicated that overall the number of bonds in this complex was essentially the same as observed in the complex of IRP1 and the H-ferritin IRE [114]. Thus, subtle differences in binding of IREs to IRP

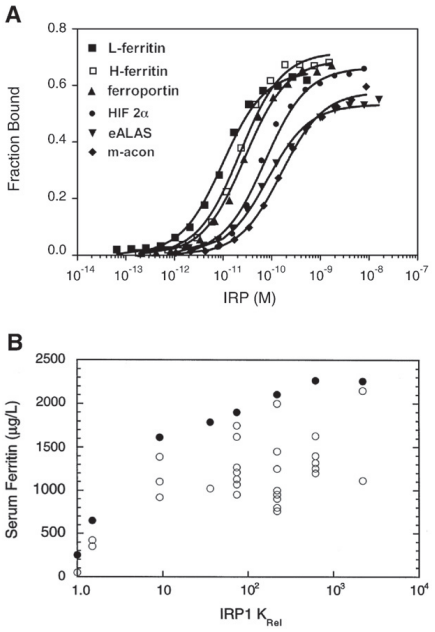

Fig. 4. Altered affinity of IRP1 for mutant and natural IREs. A) The affinity of interaction of IRP1 for six vertebrate 5′ IREs as determined by electrophoretic mobility shift assays (EMSA) [108]. The K_D for these IREs varied over a 9-fold range. B) Mutations in the human L-ferritin IRE were identified in seven patients with hereditary hyperferritinemia–cataract syndrome. The affinity of interaction of IRP1 with mutant human L-ferritin IREs was determined by EMSA and related to serum ferritin values reported for each patient on different occasions (*open circles*) [113]. Maximal serum ferritin for each patient (*closed circles*). Results on the x-axis are expressed as K_{rel} which is $K_{D,mutant}/K_{D\text{-wildtype}}$ and higher values for K_{rel} indicate lower binding affinity of the mutant IRE with IRP1. Note the steeper slope of the relationship between serum ferritin and K_{rel} over the range 1 to 10 for K_{rel}. A similar observation was made for IRP2 [113].

or in the pathway of binding are likely to be an important contributor to the hierarchical regulation of IRE-containing mRNA. A recent study reported that the ferritin IRE, but not the m-acon IRE directly binds ferrous iron, leading to a weakened interaction of IRP1 [109], suggesting an additional mechanism that contributes to the hierarchical regulation of IRE-containing mRNAs. There are also mechanisms to evade IRE action, such as mRNA isoforms that lack the IRE or those that contain internal ribosome entry sites [78,115].

3.7. What constitutes an IRE?

A key factor in the discovery of the IRE was the strong sequence identity of a short ~28–30 nt sequence in the 5′ UTR of both H- and L-ferritin mRNAs. Importantly, the sequence identity between these IREs (~90%) was substantially greater than that of the coding region (~50%) amongst vertebrate H- and L-ferritin mRNAs [116]. Of further significance were the accompanying "functional" discoveries of IRPs and that the IRE conferred iron regulation of translation when transferred to the 5′ UTR of a heterologous mRNA [117–119]. Shortly thereafter, multiple IREs were identified in the 3′ UTR of TfR1 mRNA where they served to control RNA stability yet could modulate translation if transferred to a 5′ UTR [120]. The conserved secondary structure of IREs established the concept that the canonical IRE was an RNA stem loop with a terminal hexanucleotide CAGUG(N) loop and

an unpaired C (C8) in the stem, 5′ of the loop [121] (Fig. 5). Structural and biochemical studies indicated that formation of the AGU pseudotriloop, as a consequence of base pairing of the first and fifth nucleotides of the CAGUGN sequence, occurs in solution and is critical for the binding of IRP1 [122–127]. Molecular and *in silico* studies identified IREs with the same canonical loop sequence and overall secondary structure in multiple metazoan mRNAs, and demonstrated key roles of the terminal loop and unpaired C stem in IRP binding [108,128,129].

The high resolution crystal structures of IRP1 bound to the ferritin IRE and the TfR1 B IRE provide key insights into the nature of this unusually high affinity RNA:protein interaction [114,130] (reviewed in [128]) (Fig. 6). IRP1 binds to the IRE through two sets of interactions separated over about 30 Å. IRP1 makes the majority of its bonds with the IRE in a sequence specific manner and involves canonical features of known functional IREs. Thus, the exposed nucleotides, including AGU of the terminal pseudotriloop and the unpaired C8 residue in the IRE stem, make 15 of 22 contacts with IRP1. The additional seven bonds are largely with sites in the phosphodiester backbone of the IRE stem. The two-site binding mode of IRP1, which bears strong similarities with the recognition of tRNA by tRNA synthetases, allows for enhanced specificity of RNA recognition, and likely contributes to the unusual high affinity of interaction [130]. When bound to IRP1, the ferritin IRE exhibits significant additional bending and twisting of the RNA helix as a consequence of the larger inter-helical junction around C8 and due to the presence of the unpaired U6 in ferritin IRE compared with the TfR1 B IRE. This causes a significant difference in the degree to which the lower stem of the IRE approaches the so-called stem-binding domain (domain 4) of IRP1 [114] (Fig. 6). Deviations in structure of the lower stem of IREs have been proposed to make key contributions to regulation [131].

Significant large scale structural changes occur in c-acon, particularly in domains 3 and 4, in order to accommodate the IRE [130] (Fig. 6). In comparing this structure to that of c-acon [132], Walden et al. provide unique insight into how structural plasticity of one polypeptide can support two widely different functions [130]. They proposed that residues within IRP1/c-acon that influence the ability to interconvert between these activities may dictate the ability of why some aconitases bind RNA but others do not. Importantly, this study establishes a structural framework from which to evaluate how the different canonical IREs as well as proposed IRE-like elements may make use of subtle differences in bonding or require major differences, possibly including additional binding partners, in order to allow for their unique regulation by IRPs.

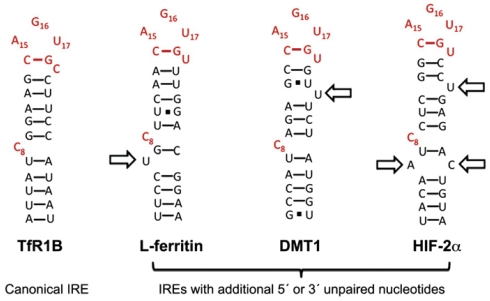

Fig. 5. Comparison of the proposed secondary structure of IREs. The key structural elements required for recognition of the IRE by IRP1 include the unpaired C (C_8) in the IRE stem and the $A_{16}G_{17}U_{18}$ nucleotides of the pseudotriloop. The canonical IRE secondary structure is represented by one of the five TfR1 IREs (TfR1 B), where the RNA helix is interrupted by only the unpaired C8. The L-ferritin IRE secondary structure showing the conserved unpaired U at position 6 (*arrow*). This additional unpaired nucleotide has been observed in the NMR of the ferritin IRE and the crystal structure of IRP1 bound to the ferritin IRE [124,130,133]. Proposed secondary structures of DMT1 and HIF-2α IREs. Note the additional unpaired nucleotides (*arrows*). IRE residue numbering is according to Walden et al. [130].

The first indication of structural differences amongst the known IREs that suggested altered ability to regulate mRNA fate came from studies of the ferritin IRE [122]. Initial computer predictions had suggested that the highly conserved unpaired C8 formed a single nucleotide bulge and gave rise to the canonical view of IRE secondary structure (Fig. 5). However, secondary structure mapping with small chemical probes confirmed other *in silico* predictions of a more complex stem structure compared to the canonical IREs [103,122,124]. Vertebrate ferritin IREs contain an unpaired U two base pairs 5′ of C8 (Fig. 5) as confirmed in both NMR and X-ray crystallography [124,130,133]. This contrasts with all other known functional IREs and even with ferritin IREs in lower organisms that appear to only have the single C8 bulge [134]. Interestingly, deletion of U6 from the ferritin IRE substantially diminishes the affinity of interaction with IRPs, particularly IRP2 [103,108,109,133,135]. Chemical probing studies suggested that this "double bulge" feature of vertebrate ferritin IREs is dynamic and may interconvert with a larger UGC/C internal loop perhaps facilitating direct binding of ferrous iron [103,109]. These additional features likely facilitate structural alterations that may underlie the stronger regulatory role of the IRE in ferritin relative to other mRNAs. Indeed, the recent structural studies comparing a single C-bulge IRE from TfR1 with the H-ferritin IRE bound to IRP1 revealed a substantial difference in the bend-angle and helical twist of the IRE stem and the degree to which the lower stem approaches IRP1 [114]. Since these two IREs bind IRP1 with similar affinities [114], it appears that significant plasticity of the RNA and protein allows for the accommodation of IREs with different structures. It will be of interest to determine if alternative structural alterations provide a mechanistic basis for the substantially weaker binding of the m-acon IRE, and to determine the impact of unpaired nucleotide(s) in the upper stem, such as observed for DMT1 and HIF-2α IREs (Fig. 5) [18].

Given the observations that U6 enhances the interaction of both IRPs with the ferritin IRE, one question is what is the role for bulge nucleotides in other IREs? While structures of IREs other than H-ferritin and TfR1 B have not been determined, secondary structure predictions suggest that several IREs possess additional unpaired nucleotides in the stem, especially on the 3′ side (Fig. 5). The HIF-2α and DMT1 each contain a single IRE with an additional 3′ unpaired nucleotide for which protein expression and RNA binding data are available (Fig. 5). In the case of both IREs, there is evidence suggesting that they are preferentially regulated by IRP1 [10,11,136]. Given the critical role of hypoxia in regulating intestinal absorption and erythropoiesis, the possibility that IRP1 may preferentially regulate these mRNAs is intriguing. A second issue of interest concerns whether unpaired nucleotides in different IREs program specific changes in regulation. Deletion of U6 lowers the affinity of IRP1 for the ferritin IRE and may have an even stronger effect on IRP2 binding [108,109,133]. In the case of HIF-2α and DMT1 IREs, the impact of the 3′ unpaired nucleotides may bias binding toward IRP1 not IRP2. In addition, the presence of this feature in the HIF-2α and DMT1 IREs may be critical for limiting the strength of IRP1 binding in order to fine tune regulation. Finally, a recent transcriptome-wide examination of mRNAs that interact with IRPs *in vitro* identified novel mRNAs containing canonical IREs, and demonstrated that IRPs may bind RNAs with differences in the location of unpaired nucleotides or in upper stem base pairing capacity [18]. Similarly, a recent *in silico* study has pointed to additional potential IREs in previously unidentified mRNAs [129]. Thus, the reach of the IRP–IRE network may extend into new areas of cellular function.

3.8. Roles for non-canonical IREs in IRP action

Test-tube RNA evolution experiments (SELEX) provided the first indication of the sequence and structure requirements for IRP recognition of IRE elements [125,126,137,138]. In this regard, one of the

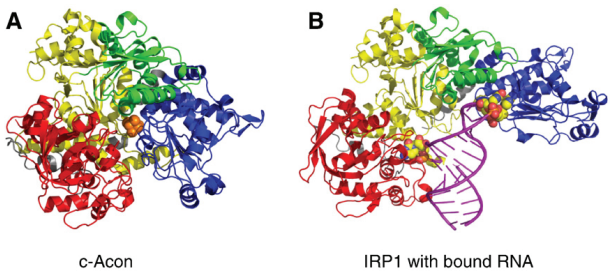

Fig. 6. Crystal structure of c-aconitase and the IRP1:IRE complex. The crystal structures of c-aconitase [132] and the IRP1:IRE complex [121,130] are shown. A) Cytosolic aconitase structure showing domain 1 (*yellow*), domain 2 (*green*), domain 3 (*blue*) and domain 4 (*red*) with the [4Fe–4S] cluster in the center (*orange* balls). B) IRP1:IRE complex structure shown with domains 1 to 4 as in (A). The ferritin IRE helix (*purple*) is shown with the two major contact sites of C8 (*left*) and the $A_{16}G_{17}U_{18}$ bases of the pseudotriloop shown (*right*) as enlarged balls.

more intriguing results came from studies where the entire IRE sequence was randomized and IRP1 was used to select high affinity RNA ligands. Intriguingly, an IRE-like RNA was identified that possessed a larger terminal loop (CAGUGUCA) along with a somewhat more complex pattern of unpaired nucleotides in the C8 region of the stem [138]. On this basis, studies on amyloid precursor protein (APP) and α-hemoglobin stabilizing protein (AHSPα) mRNAs, and the recent transcriptome-wide study potentially identifying a wide array of new IRP targets are of clear interest [18,139,140]. The evidence strongly suggests that both APP and AHSPα mRNAs are targets of IRP action. However, the proposed IRE-like element in these mRNA differs substantially from the canonical IRE, raising questions regarding the structural basis of their binding to IRP1. It is of interest in this regard that for the novel RNAs identified by SELEX that bind tightly to IRP1, this IRE contains the CAGUGU consensus sequence in a larger eight nucleotide terminal loop. This IRE is also proposed to have an unpaired pyrimidine on the 5′ side of the stem with the correct spacing from the critical AGU binding site in the terminal loop. In contrast, the APP and AHSPα IRE-like elements do not have these structural elements. Thus, while the evidence is strong that IRP1 associates with APP and AHSPα mRNAs in cells, the question as to whether IRP1 binds these elements indirectly or whether they require the assistance of protein partners remains to be determined. The recent transcriptome-wide analysis [18] suggested that IRPs may bind many non-canonical IRE RNAs, suggesting the presence of an expanded IRP-dependent post-transcriptional regulon.

4. Recent advances in IRP2 regulation

The last decade has seen major advances in IRP2 regulation. The identity of FBXL5 as the E3 ligase responsible for the iron-mediated degradation of IRP2 was discovered. New insights into the role of IRP2 in cell proliferation have been defined, and mouse models of IRP2 deficiency have provided mechanistic insight into its role in regulating cellular iron homeostasis.

4.1. Iron-mediated regulation of IRP2 stability

IRP2 is primarily regulated by protein stability: iron depletion and hypoxia stabilize IRP2, whereas iron promotes IRP2 ubiquitination and proteasomal degradation [141–144]. One early study reported that a cysteine rich 73-amino acid domain was required for iron-mediated degradation of IRP2 [144]. Several models were proposed whereby iron or heme oxidized specific cysteine residue(s) within the 73-amino acid domain, triggering the ubiquitination and degradation of IRP2 [145,146]. A protein designated heme-oxidized IRP2 Ub ligase (HOIL-1) was identified and shown to bind to heme-oxidized residues within the 73-amino acid domain [147,148]. Subsequent studies from several groups showed that mutation of cysteine residues within the 73-amino acid domain or deletion of the entire 73-amino acid domain did not affect iron-mediated degradation of IRP2 [149–151]. Furthermore, HOIL-1 silencing or overexpression in cultured cells had no effect on the degradation of IRP2 by iron [152]. These studies prompted investigation into other mechanisms to account for IRP2 degradation by iron.

Recently, a novel E3 ligase complex, SKP1–CUL1–FBXL5, was identified as the E3 ligase responsible for iron-mediated IRP2 degradation [89,90] (Fig. 7). FBXL5 was independently identified by two groups using different approaches. Vashisht et al. [90] used multidimensional protein identification technology (MUDPIT) to identify proteins that interact with epitope-tagged FBXL5. Salahudeen et al. [89] used a small interfering RNA (siRNA) screen to identify proteins that altered IRP2 degradation. FBXL5 is a member of the F-box family of adaptor proteins that confer substrate specificity to SCF E3 Ub ligases (reviewed in [153,154]). FBXL5 is conserved in vertebrates, and contains an N-terminal hemerythin domain, a F-box domain that mediates its association with SKP1 and four leucine-rich repeats that likely function in IRP2 binding. Hemerythrins are oxygen carrier proteins in marine organisms that bind to oxygen through a diiron L center [155]. Hemerythrin-like domains have been identified in bacterial proteins where they are thought to function as oxygen sensors [156,157]. FBXL5 represents the first eukaryotic protein to contain this domain.

Several experiments showed that FBXL5 regulates IRP2 stability [89,90,158]. First, FBXL5 forms a SCF complex that interacts with IRP2 *in vitro*. The region of IRP2 that binds FBXL5 is not yet known, but the 73-amino acid domain is not involved. A study showed that sequences in the C-terminal region of IRP2 are necessary, but not sufficient for IRP2 degradation [159]. Because IRP1 is a FBXL5 substrate, it is likely that IRP1 and IRP2 share a similar degron. Second, FBXL5 silencing stabilized IRP2, whereas FBXL5 overexpression promoted IRP2 degradation. Third, FBXL5 is stabilized in iron-replete cells, and destabilized by iron depletion and hypoxia. The hemerythrin domain is required for FBXL5 stability as mutations in specific histidine and glutamate residues within this domain reduced FBXL5 abundance and iron-dependent stability. Finally, reduced stability of FBXL5 during iron depletion or hypoxia provides an explanation for IRP2 accumulation during hypoxia [150,160,161]. Similarly, the enhanced degradation of IRP2 by antioxidants and stabilization of IRP2 by oxidants is also likely explained by changes in FBXL5 stability [88,161]. It should be noted that oxidative stress can also inactivate IRP2 RNA binding independent of changes in IRP2 protein levels [162–164], and in one study this was shown to be due to oxidation of cysteines that are predicted to lie in the RNA-binding cleft [164].

5. Pathological consequences of IRP and FBXL5 deficiencies in mice

Over the past decade, the generation of global and conditional mouse models of IRP2 and IRP2/IRP1 deficiency has demonstrated their importance in cellular iron metabolism. These studies have also underscored their critical role in mitochondrial iron metabolism.

5.1. Total body ablation of IRP1 and IRP2

Genetic inactivation of both *Irp1* and *Irp2* in mice leads to embryonic lethality at the blastocyst stage indicating a critical role for the IRP–IRE network during early development [110,179,180]. *Irp1*$^{-/-}$ mice lack an overt phenotype, despite mild ferritin dysregulation in kidneys and in brown fat [179]. The lack of an overt phenotype is surprising as c-acon is a highly conserved protein found in many diverse organisms and that c-aconitase is the principal form present in tissues of the body [160]. The function of c-acon is still not well understood, but apparently it is not required for normal physiology.

Two distinct strains of *Irp2*$^{-/-}$ mice have been generated. One strain was generated by the insertion of a PGK-neomycin gene into exon 3/4 of the *Irp2* gene [181] and the other strain was generated by Cre–Lox technology [182]. Both *Irp2*$^{-/-}$ mouse strains develop mild microcytic anemia and altered body iron distribution [104,183]. Iron content is elevated in intestine and liver and is associated with increased ferritin expression and decreased TfR1 expression, and is reduced in splenic macrophages and is associated with decreased ferritin expression.

Microcytic anemia in *Irp2*$^{-/-}$ mice is associated with normal transferrin saturation and serum iron parameters, and is thought to be due to cellular iron deficiency in erythroid precursors as a consequence of reduced TfR1 levels and increased ferritin levels [104,183]. Because erythroid precursors are dependent on transferrin-bound iron for heme synthesis, increased iron sequestration in ferritin and reduced iron uptake would lead to a reduction in the cellular labile iron pool, impairing heme synthesis. Mice lacking IRP2 in enterocytes, hepatocytes or macrophages do not develop microcytic anemia suggesting that microcytic anemia in *Irp2*$^{-/-}$ mice is an intrinsic defect of iron homeostasis in erythroid precursors [184]. *Irp2*$^{-/-}$ mice also develop erythropoietic protoporphyria characterized by increased protoporphryin IX in bone marrow, serum and liver [104]. Erythroid ALAS synthesis is upregulated in *Irp2*$^{-/-}$ erythroid precursors likely due to loss of IRP2 translational repression. The heme precursor protoporphyrin IX accumulates in erythroid precursors due to reduced iron availability required to complete heme synthesis.

The *Irp2*$^{-/-}$ strain generated by LaVaute et al. [181] develop a late onset neurodegenerative disorder characterized by abnormal gait, hind-limb weakness and tremors, and by reduced grooming and neuromuscular performance assayed by the hanging wire test. The cerebellum, substantia nigra, hippocampus and caudate putamen among other brains areas displayed elevated levels of ferric iron and ferritin that correlated with axonopathy and neuronal loss [105]. The onset and severity of neurodegeneration is exacerbated in *Irp2*$^{-/-}$ *Irp1*$^{+/-}$ mice, demonstrating a gene dosage effect with the IRPs [75,105]. Neurodegenerative symptoms in both *Irp2*$^{-/-}$ and *Irp2*$^{-/-}$ *Irp1*$^{+/-}$ mice were alleviated by Tempol, a membrane-permeable radical scavenger, where it reduced ferritin levels and lower iron content in cerebellar white matter tracts [75]. Tempol was shown to convert the c-acon form of IRP1 to the RNA binding form that stabilized TfR1 mRNA and repressed ferritin synthesis, and thus restored iron homeostasis. More recently, *Irp2*$^{-/-}$ mice were reported to have lower motor neuronal degeneration and spinal cord axonopathy that was more severe in *Irp2*$^{-/-}$*Irp1*$^{+/-}$ [185]. Lumbar spinal sections in *Irp2*$^{-/-}$ mice showed the accumulation of myelin dense bodies, which are hallmarks of neurodegeneration, in the ventral and lateral white matter. Mitochondria in the lumbar spinal cord were swollen, and displayed disrupted and vacuolized cristae. Ferritin and TfR1 levels were increased and decreased, respectively, in motor neurons, and total iron content was reduced in the spinal cord, consistent with cellular iron deficiency in motor neurons of *Irp2*$^{-/-}$ mice. Respiratory complexes I and II activities were reduced in lumbar spine mitochondria in *Irp2*$^{-/-}$ mice. As complexes I and II contain Fe–S clusters and heme prosthetic groups essential for activity, this suggested that cellular iron deficiency in motor neurons might impair mitochondrial function, leading to neuronal degeneration. This hypothesis was tested by treating *Irp2*$^{-/-}$ mice with Tempol and by crossing *Irp2*$^{-/-}$ or *Irp2*$^{-/-}$*Irp1*$^{+/-}$ mice into a *Fth*$^{-/+}$ background [186]. Motor neuron survival improved using both approaches consistent with the notion that cellular iron deficiency has a role in motor neuronal degeneration in *Irp2*$^{-/-}$ mice.

In contrast to *Irp2*$^{-/-}$ mice generated by LaVaute et al. [181], *Irp2*$^{-/-}$ mice generated by Galy et al. [187] did not display an abnormal gait, hind-limb weakness and tremors or neuropathological changes at 13–14 months of age. Perls' and TUNEL staining did not reveal signs of iron deposition or cellular degeneration in the brain, and electron microscopy showed no evidence of ultrastructural defects or mitochondriopathy. *Irp2*$^{-/-}$ mice also did not show impaired muscle strength when tested by the forepaw grip strength test (analogous to the hanging wire test used by LaVaute et al. [181]). In agreement with LaVaute et al. [181], the *Irp2*$^{-/-}$ strain generated by Galy et al. [187] displayed motor coordination and balance defects and reduced grooming activity when assayed by the rotarod and the modified-hole board tests. In addition, both strains displayed decreased TfR1 and increased ferritin expression in the brain [187]. Whether differences in severity of clinical and pathological signs of neurodegeneration between the two *Irp2*$^{-/-}$ strains are due to targeting strategies, genetic backgrounds or technical issues is not known.

5.2. Macrophage/monocyte ablation of IRPs

Splenic and bone marrow macrophages of *Irp2*$^{-/-}$ mice have reduced ferric iron stores with repressed levels of ferritin and ferroportin [104,183,184]. Interestingly, these mice have a slight increase in serum ferritin and normal hepcidin levels [104,183,184]. Ferritin secretion ensues when cellular ferritin synthesis occurs during iron depletion, and may explain reduced ferritin levels and splenic iron deposition seen in these animals [188]. A conditional deletion of IRP2 from macrophages/monocytes using *LysozymeM-Cre* did not recapitulate the splenic phenotype seen in *Irp2*$^{-/-}$ mice [184], suggesting that splenic iron mismanagement may be a result of IRP2 deficiency in another cell type or the combined effect of IRP2 deficiency in multiple tissues.

5.3. Intestinal ablation of IRPs

The function of IRPs in iron absorption was investigated by specific deletion of IRP2 alone or both IRP1 and IRP2 in intestinal epithelial cells [184]. Mice lacking IRP2 in the duodenum recapitulated the intestinal phenotype of duodenal iron loading and increased ferritin expression in *Irp2*$^{-/-}$ mice. Duodenal iron content and ferritin levels were not affected in mice lacking IRP2 in hepatocytes or in macrophages, suggesting that dysregulated iron homeostasis in IRP2 deficient duodenum is likely cell autonomous.

Mice lacking both IRP1 and IRP2 in intestinal epithelial cells were generated by breeding mice homozygous for floxed *Aco1* and *Ire2* alleles with mice expressing Cre-recombinase under control of the *Villin* promoter [110]. These mice displayed severe growth defects 7 days post-partum, and 80% of the animals died shortly after weaning likely due to dehydration, with the remaining 20% reaching adulthood due to incomplete IRP deletion. IRP deficient enterocytes from mice displayed less structured duodenal crypts and villi, and intestinal enterocytes exhibited mitochondriopathy along with increased apoptosis. Ferritin and ferroportin levels were profoundly increased, and TfR1 and DMT1-IRE isoform mRNAs and protein were decreased. The increase in ferroportin levels occurred without changes in mRNA levels and despite

increased hepcidin levels. Increased hepcidin levels could not be accounted by increased hepatic iron loading, and was postulated to be due to decreased erythropoiesis or inflammation. Surprisingly, blood parameters revealed no signs of systemic iron defects given the profound changes in cellular iron homeostasis in mice with IRP deficient enterocytes. It is possible that increased iron export by ferroportin equalizes reduced iron uptake and increased iron sequestration in ferritin. This study demonstrated that dysregulation of iron uptake, storage and export in IRP deficient enterocytes is consistent with cellular iron starvation as a possible cause for mitochondriopathy and impaired enterocyte function.

The importance of ferritin in iron absorption was demonstrated in mice with a specific deletion of H-ferritin subunit in intestinal epithelial cells [189]. These mice showed increased body iron stores and transferrin saturation, and as expected, increased hepatic hepcidin mRNA levels. Further analysis showed reduced levels of DMT1, DYCTB and TfR1 mRNAs, while ferroportin and L-ferritin subunit increased. IRP2 levels were reduced, suggesting an increase in the cellular labile iron pool, which would lead to the destabilization of DMT1 and TfR1 mRNAs and increased synthesis of ferroportin and L-ferritin subunit. DMT1 and DCYTB mRNAs are transcriptionally activated by HIF-2α in iron-deficient mice [98,99]. Whether reduced DMT1 and DCYTB mRNAs in H-ferritin deficient enterocytes are in part due to reduced HIF-2α accumulation is not known.

5.4. Hepatic ablation of IRPs

Conditional deletion of IRP2 in hepatocytes recapitulated the hepatic phenotype in *Irp2*$^{-/-}$ mice where iron loading was associated with ferritin derepression. In these mice, expression of TfR1 and DMT1 was unchanged, and the mechanism for increased hepatic iron loading is not clear. Mice lacking IRP2 in enterocytes or macrophages showed no evidence of iron loading in hepatocytes, showing that dysregulated iron homeostasis in hepatocytes in IRP2 deficient mice is intrinsic to hepatocytes.

The deletion of both IRP1 and IRP2 in hepatocytes has provided insight into IRP function *in vivo* [190]. Hepatocyte IRP deficiency causes mice to die between 8 and 12 days post-partum. Profound liver damage as characterized by internal bleeding, hepatic steatosis and increased apoptosis was apparent in these animals. Despite reduced hepcidin levels, there were no overt signs of systemic iron dysfunction. Analysis of IRP-target mRNAs showed that levels of ferritin and ferroportin were elevated, whereas levels of TfR1 and the DMT1-IRE mRNAs and protein are decreased. Zip14 (SLC39A14, iron transporter) and mitoferrin 2 (SLC25A28, mitochondrial iron transporter), which are not IRP regulated, were also downregulated. Total liver nonheme iron and mitochondrial nonheme iron were reduced 50% compared with control mice. The reduction in iron uptake coupled with increased iron sequestration in ferritin and increased iron export by ferroportin is consistent with severe cellular iron starvation in IRP deficient hepatocytes.

Mitochondrial dysfunction is a defining feature of many fatty liver diseases [191]. Consistent with this, mitochondriopathy is the major pathological consequence of hepatocyte IRP deficiency [190]. Mitochondria appear swollen, and contain hypodense matrices and abnormal cristae architecture, consistent with iron and copper deficiency in rodents [192]. Interestingly, the expression of the mitochondrial iron transporter mitoferrin 2 is reduced in IRP deficient hepatocytes and correlates with a reduction in mitochondrial nonheme iron. Mitochondria are responsible for the synthesis of Fe–S clusters and heme that are required by complexes I, II and III and by TCA cycle enzymes. IRP deficient hepatocytes display markedly reduced activities of complexes I, II and III and ferrochelatase, as well as the cytosolic Fe–S cluster containing protein xanthine dehydrogenase. It is likely that defects in the electron transport chain and TCA cycle are major contributing factors to the mitochondrial abnormalities seen in IRP deficient hepatocytes.

5.5. Mouse models of FBXL5 and FBXL5-IRP2 deficiencies

The importance of IRP2 in cellular iron metabolism was further highlighted by FBXL5 ablation in mice [91]. Total body ablation of FBXL5 in mice resulted in embryonic lethality at E8.5, and was associated with iron overload and oxidative stress in embryos. Embryonic lethality was prevented by simultaneous ablation of IRP2. *Fbxl5*$^{-/-}$*Irp2*$^{-/-}$ mice developed normally and were physically indistinguishable from littermate controls. Mice with hepatocyte specific ablation of FBXL5 were viable, but developed hepatic steatosis and mitochondriopathy in hepatocytes. Increased IRP levels were associated with increased TfR1 levels and ferrous iron in hepatocytes. Unexpectedly, L-ferritin protein and mRNA levels increased in FBXL5 deficient hepatocytes compared with control mice despite increased IRP expression. The most likely explanation for increased ferritin expression is transcriptional activation of the L-ferritin gene induced by oxidative stress in hepatocytes [193]. Mice lacking hepatocyte FBXL5 displayed reduced hepcidin mRNA expression as a consequence of reduced BMP signaling. These mice also showed reduced survival when fed a high iron diet. Taken together, this study showed that embryonic lethality in *Fbxl5*$^{-/-}$ mice is primarily due to dysregulation of IRP2 degradation, which leads to increased cellular iron and oxidative stress, and show that FBXL5 regulation of IRP2 is critical for regulation of cellular iron homeostasis.

5.6. IRP–IRE network in human disease

To date there are no reports of mutations in IRP1 or IRP2 that cause human disease, but mutations in IREs or in coding sequences of IRE-encoded genes have been linked to human disorders. Mutations in L-ferritin subunit mRNA cause autosomal dominant hereditary hyperferritinemia–cataract syndrome (HHCS) that is characterized by juvenile bilateral cataracts and high levels of serum ferritin without iron overload. These mutations reduce IRP binding to the 5′ IRE and lead to abnormal L-ferritin subunit accumulation in tissues and serum [194–196]. A point mutation in the 5′ IRE of H-ferritin subunit that increases its affinity for IRPs causes autosomal dominant iron overload disorder [197]. Coding region mutations in L-ferritin subunit cause hereditary ferritinopathy or neuroferritinopathy characterized by abnormal ferritin inclusion aggregates and iron in the globus pallidus [198]. These mutations alter the amino acid sequence at the C-terminus of L-ferritin subunit, reducing its stability and ability to incorporate iron [199,200]. The neurodegeneration and iron overload phenotype was replicated in mice expressing a mutant L-ferritin subunit form [201]. A missense mutation in the L-ferritin subunit coding sequence was identified that leads to high levels of serum ferritin without iron overload [202]. Kannengiesser and colleagues [188] postulated that this mutation may modify a signal sequence that increases secretion of L-ferritin subunits, and a subsequent study in cell culture shows that secretion of this mutant ferritin is increased as compared to wildtype ferritin [188]. Mutations have been reported in other IRE-encoded genes, such as eALAS (sideroblastic anemia) [203–205], ferroportin (hereditary hemochromatosis) [206,207] and DMT1 [208–210]. These studies show that abnormal expression of proteins encoded by IRE-containing mRNAs disrupts systematic and cellular iron metabolism and leads to iron overload and neurodegeneration.

A genome wide association study (GWAS) has associated various IRP2 polymorphisms with Alzheimer's disease (AD) [211]. A potentially functional single nucleotide polymorphism (SNP) in the IRP2 promoter region was located within a consensus binding site for the AP-1 and SP1 transcription factors, and could possibly explain altered IRP2 expression seen in AD patients. This is of interest as a study showed IRP2 co-localization with pathological features of AD, including

neurofibrillary tangles and senile plaques [212]. An additional link between IRP2 and neurodegenerative disease involves the regulation of amyloid precursor protein (APP). Studies have shown APP to be a functional ferroxidase that interacts with FPN in mediating iron export, and inhibition of ferroxidase activity leads to neuronal iron accumulation consistent with AD [213]. Similarly, neurons of Tau deficient mice retain iron and mislocalize APP, thus disrupting iron export by FPN [214]. More importantly, iron chelation with Clioquinol alleviated cognitive deficits seen in these Tau deficient mice. These observations highlight the importance of iron metabolism in maintaining proper neurological function, and provide therapeutic opportunities for treating neurodegenerative diseases such as Alzheimer's and Parkinson's. More recent GWAS have found strong associations between IRP2 and patients with chronic obstructive pulmonary disease (COPD) [215]. Three SNPs in IRP2 were found to correlate with reduced forced expiratory volume (FEV), a prominent feature of COPD [216]. It is known that IRP2 expression is altered in lung tissue from COPD patients, and iron deposition is increased in the lungs of smokers [215]. Further studies are needed to confirm a role for IRP2 in AD and COPD.

6. Outlook

Since their discovery over 20 years ago, IRPs still remain an active field of research. Iron-dependent and iron-independent mechanisms regulating IRP1 and IRP2 function have been identified and the physiological consequences of these mechanisms determined. The crystal structure of IRP1 bound to RNA has provided a basis to study the selectivity of IRE binding. Mouse models of IRP deficiency have shown the importance of IRPs in regulating cellular iron metabolism. The elusive E3 ligase mediating IRP2 degradation by iron has been identified, and the identification of novel IREs has broadened our vision of the IRP–IRE network.

At a mechanistic level, many questions regarding IRP function remain unanswered. One question regards the pathways of Fe–S cluster biogenesis that are directly sensed by IRPs and whether trafficking of iron through mitochondria is an obligate process through which IRPs sense iron. Additionally, the extent to which Fe–S cluster removal from c-acon versus *de novo* synthesis of IRP1 contribute to its role in homeostatic regulation of iron in animals needs attention. Another question is to determine how canonical and non-canonical IREs bind IRP1 to allow for their linkage to processes uniquely sensed by IRP1 (e.g. cytosolic Fe–S biogenesis). The discovery of novel IREs that preferentially bind to IRP1 or IRP2 is an opportunity to study links between iron homeostasis and other cellular or organismal processes. For example, what is the physiological significance of the preferential regulation of HIF-2α IRE by IRP1? The identification of FBXL5 E3 ligase raises the question whether other substrates are also targeted by FBXL5. The role of the IRP2 73-amino acid domain and Ser157 phosphorylation in cell proliferation requires further investigation. A better understanding of how iron contributes to neurodegeneration is needed with the goal of developing safer and effective therapies to treat these disorders.

Acknowledgements

This work was supported by grants from the NIH to EAL (GM45201 and DK068602), RSE (DK089212 and DK66600) and training grants to CPA (T32DK007115) and MS (T32DK007665). RSE also acknowledges support from the USDA Hatch Project WIS01324. We thank Josh Romney for critical reading of the review.

References

[1] R.E. Fleming, P. Ponka, Iron overload in human disease, N. Engl. J. Med. 366 (2012) 348–359.
[2] E. Madsen, J.D. Gitlin, Copper and iron disorders of the brain, Annu. Rev. Neurosci. 30 (2007) 317–337.
[3] D.A. Simmons, M. Casale, B. Alcon, N. Pham, N. Narayan, G. Lynch, Ferritin accumulation in dystrophic microglia is an early event in the development of Huntington's disease, Glia 55 (2007) 1074–1084.
[4] M.L. Wallander, E.A. Leibold, R.S. Eisenstein, Molecular control of vertebrate iron homeostasis by iron regulatory proteins, Biochim. Biophys. Acta 1763 (2006) 668–689.
[5] T.A. Rouault, The role of iron regulatory proteins in mammalian iron homeostasis and disease, Nat. Chem. Biol. 2 (2006) 406–414.
[6] M.U. Muckenthaler, B. Galy, M.W. Hentze, Systemic iron homeostasis and the iron-responsive element/iron-regulatory protein (IRE/IRP) regulatory network, Annu. Rev. Nutr. 28 (2008) 197–213.
[7] J. Wang, K. Pantopoulos, Regulation of cellular iron metabolism, Biochem. J. 434 (2011) 365–381.
[8] L. Zheng, M.C. Kennedy, G.A. Blondin, H. Beinert, H. Zalkin, Binding of cytosolic aconitase to the iron responsive element of porcine mitochondrial aconitase mRNA, Arch. Biochem. Biophys. 299 (1992) 356–360.
[9] T.C. Cox, M.J. Bawden, A. Martin, B.K. May, Human erythroid 5-aminolevulinate synthase: promoter analysis and identification of an iron-responsive element in the mRNA, EMBO J. 10 (1991) 1891–1902.
[10] M. Sanchez, B. Galy, M.U. Muckenthaler, M.W. Hentze, Iron-regulatory proteins limit hypoxia-inducible factor-2alpha expression in iron deficiency, Nat. Struct. Mol. Biol. 14 (2007) 420–426.
[11] M. Zimmer, B.L. Ebert, C. Neil, K. Brenner, I. Papaioannou, A. Melas, N. Tolliday, J. Lamb, K. Pantopoulos, T. Golub, O. Iliopoulos, Small-molecule inhibitors of HIF-2a translation link its 5′UTR iron-responsive element to oxygen sensing, Mol. Cell 32 (2008) 838–848.
[12] J.T. Rogers, A.I. Bush, H.H. Cho, D.H. Smith, A.M. Thomson, A.L. Friedlich, D.K. Lahiri, P.J. Leedman, X. Huang, C.M. Cahill, Iron and the translation of the amyloid precursor protein (APP) and ferritin mRNAs: riboregulation against neural oxidative damage in Alzheimer's disease, Biochem. Soc. Trans. 36 (2008) 1282–1287.
[13] H. Gunshin, B. Mackenzie, U. Berger, Y. Gunshin, M.F. Romero, W.F. Boron, S. Nussberger, J.L. Gollan, M.A. Hediger, Cloning and characterization of a mammalian proton-coupled metal-ion transporter, Nature 388 (1997) 482–488.
[14] M. Sanchez, B. Galy, T. Dandekar, P. Bengert, Y. Vainshtein, J. Stolte, M.U. Muckenthaler, M.W. Hentze, Iron regulation and the cell cycle: identification of an iron-responsive element in the 3′-untranslated region of human cell division cycle 14A mRNA by a refined microarray-based screening strategy, J. Biol. Chem. 281 (2006) 22865–22874.
[15] R. Cmejla, J. Petrak, J. Cmejlova, A novel iron responsive element in the 3′UTR of human MRCKalpha, Biochem. Biophys. Res. Commun. 341 (2006) 158–166.
[16] S.A. Kohler, E. Menotti, L.C. Kuhn, Molecular cloning of mouse glycolate oxidase. High evolutionary conservation and presence of an iron-responsive element-like sequence in the mRNA, J. Biol. Chem. 274 (1999) 2401–2407.
[17] S. Recalcati, L. Tacchini, A. Alberghini, D. Conte, G. Cairo, Oxidative stress-mediated down-regulation of rat hydroxyacid oxidase 1, a liver-specific peroxisomal enzyme, Hepatology 38 (2003) 1159–1166.
[18] M. Sanchez, B. Galy, B. Schwanhaeusser, J. Blake, T. Bahr-Ivacevic, V. Benes, M. Selbach, M.U. Muckenthaler, M.W. Hentze, Iron regulatory protein-1 and -2: transcriptome-wide definition of binding mRNAs and shaping of the cellular proteome by iron regulatory proteins, Blood 118 (2011) e168–e179.
[19] R.A. Wingert, J.L. Galloway, B. Barut, H. Foott, P. Fraenkel, J.L. Axe, G.J. Weber, K. Dooley, A.J. Davidson, B. Schmid, B.H. Paw, G.C. Shaw, P. Kingsley, J. Palis, H. Schubert, O. Chen, J. Kaplan, L.I. Zon, Deficiency of glutaredoxin 5 reveals Fe–S clusters are required for vertebrate haem synthesis, Nature 436 (2005) 1035–1039.
[20] D.C. Johnson, D.R. Dean, A.D. Smith, M.K. Johnson, Structure, function, and formation of biological iron–sulfur clusters, Annu. Rev. Biochem. 74 (2005) 247–281.
[21] R. Lill, Function and biogenesis of iron–sulphur proteins, Nature 460 (2009) 831–838.
[22] A.K. Sharma, L.J. Pallesen, R.J. Spang, W.E. Walden, Cytosolic iron–sulfur cluster assembly (CIA) system: factors, mechanism, and relevance to cellular iron regulation, J. Biol. Chem. 285 (2010) 26745–26751.
[23] H. Ye, T.A. Rouault, Human iron–sulfur cluster assembly, cellular iron homeostasis, and disease, Biochemistry 49 (2010) 4945–4956.
[24] I.J. Schultz, C. Chen, B.H. Paw, I. Hamza, Iron and porphyrin trafficking in heme biogenesis, J. Biol. Chem. 285 (2010) 26753–26759.
[25] C. Fosset, M.J. Chauveau, B. Guillon, F. Canal, J.C. Drapier, C. Bouton, RNA silencing of mitochondrial m-Nfs1 reduces Fe–S enzyme activity both in mitochondria and cytosol of mammalian cells, J. Biol. Chem. 281 (2006) 25398–25406.
[26] J. Gerber, U. Muhlenhoff, R. Lill, An interaction between frataxin and Isu1/Nfs1 that is crucial for Fe/S cluster synthesis on Isu1, EMBO Rep. 4 (2003) 906–911.
[27] K. Li, E.K. Besse, D. Ha, G. Kovtunovych, T.A. Rouault, Iron-dependent regulation of frataxin expression: implications for treatment of Friedreich ataxia, Hum. Mol. Genet. 17 (2008) 2265–2273.
[28] S. Schmucker, A. Martelli, F. Colin, A. Page, M. Wattenhofer-Donze, L. Reutenauer, H. Puccio, Mammalian frataxin: an essential function for cellular viability through an interaction with a preformed ISCU/NFS1/ISD11 iron–sulfur assembly complex, PLoS One 6 (2011) e16199.
[29] C.L. Tsai, D.P. Barondeau, Human frataxin is an allosteric switch that activates the Fe–S cluster biosynthetic complex, Biochemistry 49 (2010) 9132–9139.
[30] Y. Zhang, E.R. Lyver, E. Nakamaru-Ogiso, H. Yoon, B. Amutha, D.W. Lee, E. Bi, T. Ohnishi, F. Daldal, D. Pain, A. Dancis, Dre2, a conserved eukaryotic Fe/S cluster protein, functions in cytosolic Fe/S protein biogenesis, Mol. Cell. Biol. 28 (2008) 5569–5582.
[31] U. Muhlenhoff, N. Richter, O. Pines, A.J. Pierik, R. Lill, Specialized function of yeast Isa1 and Isa2 proteins in the maturation of mitochondrial [4Fe–4S] proteins, J. Biol. Chem. 286 (2011) 41205–41216.

[32] A. Roy, A. Solodovnikova, T. Nicholson, W. Antholine, W.E. Walden, A novel eukaryotic factor for cytosolic Fe–S assembly, EMBO J. 22 (2003) 2826–2835.
[33] J. Balk, D.J. Aguilar Netz, K. Tepper, A.J. Pierik, R. Lill, The essential WD40 protein Cia1 is involved in a late step of cytosolic and nuclear iron–sulfur protein assembly, Mol. Cell. Biol. 25 (2005) 10833–10841.
[34] J. Balk, A.J. Pierik, D.J. Netz, U. Muhlenhoff, R. Lill, The hydrogenase-like Nar1p is essential for maturation of cytosolic and nuclear iron–sulphur proteins, EMBO J. 23 (2004) 2105–2115.
[35] A. Hausmann, D.J. Aguilar Netz, J. Balk, A.J. Pierik, U. Muhlenhoff, R. Lill, The eukaryotic P loop NTPase Nbp35: an essential component of the cytosolic and nuclear iron–sulfur protein assembly machinery, Proc. Natl. Acad. Sci. U. S. A. 102 (2005) 3266–3271.
[36] D.J. Netz, M. Stumpfig, C. Dore, U. Muhlenhoff, A.J. Pierik, R. Lill, Tah18 transfers electrons to Dre2 in cytosolic iron–sulfur protein biogenesis, Nat. Chem. Biol. 6 (2010) 758–765.
[37] K. Bych, S. Kerscher, D.J. Netz, A.J. Pierik, K. Zwicker, M.A. Huynen, R. Lill, U. Brandt, J. Balk, The iron–sulphur protein Ind1 is required for effective complex I assembly, EMBO J. 27 (2008) 1736–1746.
[38] A.D. Sheftel, O. Stehling, A.J. Pierik, D.J. Netz, S. Kerscher, H.P. Elsasser, I. Wittig, J. Balk, U. Brandt, R. Lill, Human ind1, an iron–sulfur cluster assembly factor for respiratory complex I, Mol. Cell. Biol. 29 (2009) 6059–6073.
[39] Y. Shi, M. Ghosh, G. Kovtunovych, D.R. Crooks, T.A. Rouault, Both human ferredoxins 1 and 2 and ferredoxin reductase are important for iron–sulfur cluster biogenesis, Biochim. Biophys. Acta 1823 (2011) 484–492.
[40] W.H. Tong, T.A. Rouault, Functions of mitochondrial ISCU and cytosolic ISCU in mammalian iron–sulfur cluster biogenesis and iron homeostasis, Cell Metab. 3 (2006) 199–210.
[41] D. Song, Z. Tu, F.S. Lee, Human ISCA1 interacts with IOP1/NARFL and functions in both cytosolic and mitochondrial iron–sulfur protein biogenesis, J. Biol. Chem. 284 (2009) 35297–35307.
[42] I. Condo, F. Malisan, I. Guccini, D. Serio, A. Rufini, R. Testi, Molecular control of the cytosolic aconitase/IRP1 switch by extramitochondrial frataxin, Hum. Mol. Genet. 19 (2010) 1221–1229.
[43] H. Ye, S.Y. Jeong, M.C. Ghosh, G. Kovtunovych, L. Silvestri, D. Ortillo, N. Uchida, J. Tisdale, C. Camaschella, T.A. Rouault, Glutaredoxin 5 deficiency causes sideroblastic anemia by specifically impairing heme biosynthesis and depleting cytosolic iron in human erythroblasts, J. Clin. Invest. 120 (2010) 1749–1761.
[44] Y. Shan, G. Cortopassi, HSC20 interacts with frataxin and is involved in iron–sulfur cluster biogenesis and iron homeostasis, Hum. Mol. Genet. 21 (2012) 1457–1469.
[45] H. Uhrigshardt, A. Singh, G. Kovtunovych, M. Ghosh, T.A. Rouault, Characterization of the human HSC20, an unusual DnaJ type III protein, involved in iron–sulfur cluster biogenesis, Hum. Mol. Genet. 19 (2010) 3816–3834.
[46] A. Sheftel, O. Stehling, R. Lill, Iron–sulfur proteins in health and disease, Trends Endocrinol. Metab. 21 (2010) 302–314.
[47] Y. Shi, M.C. Ghosh, W.H. Tong, T.A. Rouault, Human ISD11 is essential for both iron–sulfur cluster assembly and maintenance of normal cellular iron homeostasis, Hum. Mol. Genet. 18 (2009) 3014–3025.
[48] A.D. Sheftel, O. Stehling, A.J. Pierik, H.P. Elsasser, U. Muhlenhoff, H. Webert, A. Hobler, F. Hannemann, R. Bernhardt, R. Lill, Humans possess two mitochondrial ferredoxins, Fdx1 and Fdx2, with distinct roles in steroidogenesis, heme, and Fe/S cluster biosynthesis, Proc. Natl. Acad. Sci. U. S. A. 107 (2010) 11775–11780.
[49] M. Babcock, D.d. Silva, R. Oaks, S. Davis-Kaplan, S. Jiralerspong, L. Montermini, M. Pandolfo, J. Kaplan, Regulation of mitochondrial iron accumulation by Yfh1p, a putative homolog of frataxin, Science 276 (1997) 1709–1712.
[50] J. Gerber, K. Neumann, C. Prohl, U. Muhlenhoff, R. Lill, The yeast scaffold proteins Isu1p and Isu2p are required inside mitochondria for maturation of cytosolic Fe/S proteins, Mol. Cell. Biol. 24 (2004) 4848–4857.
[51] G. Kispal, P. Csere, C. Prohl, R. Lill, The mitochondrial proteins Atm1p and Nfs1p are essential for biogenesis of cytosolic Fe/S proteins, EMBO J. 18 (1999) 3981–3989.
[52] J. Li, M. Kogan, S.A. Knight, D. Pain, A. Dancis, Yeast mitochondrial protein, Nfs1p, coordinately regulates iron–sulfur cluster proteins, cellular iron uptake, and iron distribution, J. Biol. Chem. 274 (1999) 33025–33034.
[53] B. Schilke, C. Voisine, H. Beinert, E. Craig, Evidence for a conserved system for iron metabolism in the mitochondria of *Saccharomyces cerevisiae*, Proc. Natl. Acad. Sci. U. S. A. 96 (1999) 10206–10211.
[54] S.L. Clarke, A. Vasanthakumar, S.A. Anderson, C. Pondarre, C.M. Koh, K.M. Deck, J.S. Pitula, C.J. Epstein, M.D. Fleming, R.S. Eisenstein, Iron-responsive degradation of iron-regulatory protein 1 does not require the Fe–S cluster, EMBO J. 25 (2006) 544–553.
[55] C. Pondarre, B.B. Antiochos, D.R. Campagna, S.L. Clarke, E.L. Greer, K.M. Deck, A. McDonald, A.P. Han, A. Medlock, J.L. Kutok, S.A. Anderson, R.S. Eisenstein, M.D. Fleming, The mitochondrial ATP-binding cassette transporter Abcb7 is essential in mice and participates in cytosolic iron–sulfur cluster biogenesis, Hum. Mol. Genet. 15 (2006) 953–964.
[56] D. Song, F.S. Lee, A role for IOP1 in mammalian cytosolic iron–sulfur protein biogenesis, J. Biol. Chem. 283 (2008) 9231–9238.
[57] D. Song, F.S. Lee, Mouse knock-out of IOP1 protein reveals its essential role in mammalian cytosolic iron–sulfur protein biogenesis, J. Biol. Chem. 286 (2011) 15797–15805.
[58] O. Stehling, D.J. Netz, B. Niggemeyer, R. Rosser, R.S. Eisenstein, H. Puccio, A.J. Pierik, R. Lill, Human Nbp35 is essential for both cytosolic iron–sulfur protein assembly and iron homeostasis, Mol. Cell. Biol. 28 (2008) 5517–5528.
[59] T.A. Rouault, W.H. Tong, Iron–sulfur cluster biogenesis and human disease, Trends Genet. 24 (2008) 398–407.
[60] S. Schmucker, H. Puccio, Understanding the molecular mechanisms of Friedreich's ataxia to develop therapeutic approaches, Hum. Mol. Genet. 19 (2010) R103–R110.
[61] T.L. Stemmler, E. Lesuisse, D. Pain, A. Dancis, Frataxin and mitochondrial FeS cluster biogenesis, J. Biol. Chem. 285 (2010) 26737–26743.
[62] Y. Zhang, E.R. Lyver, S.A. Knight, D. Pain, E. Lesuisse, A. Dancis, Mrs3p, Mrs4p, and frataxin provide iron for Fe–S cluster synthesis in mitochondria, J. Biol. Chem. 281 (2006) 22493–22502.
[63] N. Calmels, S. Schmucker, M. Wattenhofer-Donze, A. Martelli, N. Vaucamps, L. Reutenauer, N. Messaddeq, C. Bouton, M. Koenig, H. Puccio, The first cellular models based on frataxin missense mutations that reproduce spontaneously the defects associated with Friedreich ataxia, PLoS One 4 (2009) e6379.
[64] M.L. Huang, E.M. Becker, M. Whitnall, Y. Suryo Rahmanto, P. Ponka, D.R. Richardson, Elucidation of the mechanism of mitochondrial iron loading in Friedreich's ataxia by analysis of a mouse mutant, Proc. Natl. Acad. Sci. U. S. A. 106 (2009) 16381–16386.
[65] H. Beinert, M.C. Kennedy, C.D. Stout, Aconitase as iron–sulfur protein, enzyme, and iron regulatory protein, Chem. Rev. 96 (1996) 2335–2373.
[66] P.R. Gardner, I. Fridovich, Superoxide sensitivity of the *Escherichia coli* aconitase, J. Biol. Chem. 266 (1991) 19328–19333.
[67] W.E. Walden, From bacteria to mitochondria: aconitase yields surprises, Proc. Natl. Acad. Sci. U. S. A. 99 (2002) 4138–4140.
[68] S. Varghese, Y. Tang, J.A. Imlay, Contrasting sensitivities of *Escherichia coli* aconitases A and B to oxidation and iron depletion, J. Bacteriol. 185 (2003) 221–230.
[69] N.M. Brown, M.C. Kennedy, W.E. Antholine, R.S. Eisenstein, W.E. Walden, Detection of a [3Fe–4S] cluster intermediate of cytosolic aconitase in yeast expressing iron regulatory protein 1. Insights into the mechanism of Fe–-S cluster cycling. J. Biol. Chem. 277 (2002) 7246–7254.
[70] J.C. Drapier, J.B. Hibbs, Murine cytotoxic activated macrophages inhibit aconitase in tumor cells. Inhibition involves the iron–sulfur prosthetic group and is reversible. J. Clin. Invest. 78 (1986) 790–797.
[71] C. Bouton, J.C. Drapier, Iron regulatory proteins as NO signal transducers, Sci. STKE 2003 (2003) e17.
[72] N.K. Gray, K. Pantopoulos, T. Dandekar, B. Ackrell, M.W. Hentze, Translational regulation of mammalian and *Drosophila* citric acid cycle enzymes via iron-responsive elements, Proc. Natl. Acad. Sci. U. S. A. 93 (1996) 4925–4930.
[73] J. Wang, C. Fillebeen, G. Chen, B. Andriopoulos, K. Pantopoulos, Sodium nitroprusside promotes IRP2 degradation via an increase in intracellular iron and in the absence of S nitrosylation at C178, Mol. Cell. Biol. 26 (2006) 1948–1954.
[74] A. Stys, B. Galy, R.R. Starzynski, E. Smuda, J.C. Drapier, P. Lipinski, C. Bouton, Iron regulatory protein 1 outcompetes iron regulatory protein 2 in regulating cellular iron homeostasis in response to nitric oxide, J. Biol. Chem. 286 (2011) 22846–22854.
[75] M.C. Ghosh, W.H. Tong, D. Zhang, H. Ollivierre-Wilson, A. Singh, M.C. Krishna, J.B. Mitchell, T.A. Rouault, Tempol-mediated activation of latent iron regulatory protein activity prevents symptoms of neurodegenerative disease in IRP2 knockout mice, Proc. Natl. Acad. Sci. U. S. A. 105 (2008) 12028–12033.
[76] J. Wang, G. Chen, C. Filebeen, K. Pantopoulos, Insights on regulation and function of the iron regulatory protein 1 (IRP1), Hemoglobin 32 (2008) 109–115.
[77] S. Mueller, Iron regulatory protein 1 as a sensor of reactive oxygen species, Biofactors 24 (2005) 171–181.
[78] A. Daba, A.E. Koromilas, K. Pantopoulos, Alternative ferritin mRNA translation via internal initiation, RNA 3 (2012) 547–556.
[79] N.M. Brown, S.A. Anderson, D.W. Steffen, T.B. Carpenter, M.C. Kennedy, W.E. Walden, R.S. Eisenstein, Novel role of phosphorylation in Fe–S cluster stability revealed by phosphomimetic mutations at Ser-138 of iron regulatory protein 1, Proc. Natl. Acad. Sci. U. S. A. 95 (1998) 15235–15240.
[80] K.M. Deck, A. Vasanthakumar, S.A. Anderson, J.B. Goforth, M.C. Kennedy, W.E. Antholine, R.S. Eisenstein, Evidence that phosphorylation of iron regulatory protein 1 at Serine 138 destabilizes the [4Fe–4S] cluster in cytosolic aconitase by enhancing 4Fe–3Fe cycling, J. Biol. Chem. 284 (2009) 12701–12709.
[81] K. Pantopoulos, M.W. Hentze, Activation of iron regulatory protein-1 by oxidative stress *in vitro*, Proc. Natl. Acad. Sci. U. S. A. 95 (1998) 10559–10563.
[82] L.S. Goessling, D.P. Mascotti, M. Bhattacharyya-Pakrasi, H. Gang, R.E. Thach, Irreversible steps in the ferritin synthesis induction pathway, J. Biol. Chem. 269 (1994) 4343–4348.
[83] D.J. Haile, T.A. Rouault, J.B. Harford, M.C. Kennedy, G.A. Blondin, H. Beinert, R.D. Klausner, Cellular regulation of the iron-responsive element binding protein: disassembly of the cubane iron–sulfur cluster results in high-affinity RNA binding, Proc. Natl. Acad. Sci. U. S. A. 89 (1992) 11735–11739.
[84] O.S. Chen, K.L. Schalinske, R.S. Eisenstein, Dietary iron intake modulates the activity of iron regulatory proteins (IRPs) and the abundance of ferritin and mitochondrial aconitase in rat liver, J. Nutr. 127 (1997) 238–248.
[85] E.G. Meyron-Holz, M.C. Ghosh, K. Iwai, T. LaVaute, X. Brazzolotto, U.V. Berger, W. Land, H. Olivarerre-Wilson, A. Grinberg, P. Love, T.A. Rouault, Genetic ablations of iron regulatory protein 1 and 2 reveal why iron regulatory protein 2 dominates iron homeostasis, EMBO J. 23 (2004) 386–395.
[86] M. Neonaki, D.C. Graham, K.N. White, A. Bomford, Down-regulation of liver iron-regulatory protein 1 in haemochromatosis, Biochem. Soc. Trans. 30 (2001) 726–728.
[87] C. Fillebeen, D. Chahine, A. Caltagirone, P. Segal, K. Pantopoulos, A phosphomimetic mutation at Ser-138 renders iron regulatory protein 1 sensitive to iron-dependent degradation, Mol. Cell. Biol. 23 (2003) 6973–6981.
[88] J. Wang, C. Fillebeen, G. Chen, A. Biederbick, R. Lill, K. Pantopoulos, Iron-dependent degradation of apo-IRP1 by the ubiquitin–proteasome pathway, Mol. Cell. Biol. 27 (2007) 2423–2430.

[89] A.A. Salahudeen, J.W. Thompson, J.C. Ruiz, H.W. Ma, L.N. Kinch, Q. Li, N.V. Grishin, R.K. Bruick, An E3 ligase possessing an iron responsive hemerythrin domain is a regulator of iron homeostasis, Science 326 (2009) 718–721.
[90] A.A. Vashisht, K.B. Zumbrennen, X. Huang, D.N. Powers, A. Durazo, D. Sun, N. Bhaskaran, A. Persson, M. Uhlen, O. Sangfelt, C. Spruck, E.A. Leibold, J.A. Wohlschlegel, Control of iron homeostasis by an iron-regulated ubiquitin ligase, Science 326 (2009) 718–721.
[91] T. Moroishi, M. Nishiyama, Y. Takeda, K. Iwai, K.I. Nakayama, The FBXL5-IRP2 axis is integral to control of iron metabolism *in vivo*, Cell Metab. 14 (2011) 339–351.
[92] F. Mochel, M.A. Knight, W.H. Tong, D. Hernandez, K. Ayyad, T. Taivassalo, P.M. Andersen, A. Singleton, T.A. Rouault, K.H. Fischbeck, R.G. Haller, Splice mutation in the iron–sulfur cluster scaffold protein ISCU causes myopathy with exercise intolerance, Am. J. Hum. Genet. 82 (2008) 652–660.
[93] R.S. Eisenstein, P.T. Tuazon, K.L. Schalinske, S.A. Anderson, J.A. Traugh, Iron responsive element binding protein: phosphorylation by protein kinase C, J. Biol. Chem. 268 (1993) 27363–27370.
[94] M.R. Davis, K.M. Shawron, E. Rendina, S.K. Peterson, E.A. Lucas, B.J. Smith, S.L. Clarke, Hypoxia inducible factor-2 alpha is translationally repressed in response to dietary iron deficiency in Sprague–Dawley rats, J. Nutr. 141 (2011) 1590–1596.
[95] M. Zimmer, J. Lamb, B.L. Ebert, M. Lynch, C. Neil, E. Schmidt, T.R. Golub, O. Iliopoulos, The connectivity map links iron regulatory protein-1-mediated inhibition of hypoxia-inducible factor-2a translation to the anti-inflammatory 15-deoxy-delta12,14-prostaglandin J2, Cancer Res. 70 (2010) 3071–3079.
[96] W.G. Kaelin Jr., P.J. Ratcliffe, Oxygen sensing by metazoans: the central role of the HIF hydroxylase pathway, Mol. Cell 30 (2008) 393–402.
[97] A.J. Majmundar, W.J. Wong, M.C. Simon, Hypoxia-inducible factors and the response to hypoxic stress, Mol. Cell 40 (2010) 294–309.
[98] Y.M. Shah, T. Matsubara, S. Ito, S.H. Yim, F.J. Gonzalez, Intestinal hypoxia-inducible transcription factors are essential for iron absorption following iron deficiency, Cell Metab. 9 (2009) 152–164.
[99] M. Mastrogiannaki, P. Matak, B. Keith, M.C. Simon, S. Vaulont, C. Peyssonnaux, HIF-2alpha, but not HIF-1alpha, promotes iron absorption in mice, J. Clin. Invest. 119 (2009) 1159–1166.
[100] E.R. Anderson, X. Xue, Y.M. Shah, Intestinal hypoxia-inducible factor-2alpha (HIF-2alpha) is critical for efficient erythropoiesis, J. Biol. Chem. 286 (2011) 19533–19540.
[101] M. Taylor, A. Qu, E.R. Anderson, T. Matsubara, A. Martin, F.J. Gonzalez, Y.M. Shah, Hypoxia-inducible factor-2alpha mediates the adaptive increase of intestinal ferroportin during iron deficiency in mice, Gastroenterology 140 (2011) 2044–2055.
[102] M. Schranzhofer, M. Schifrer, J.A. Cabrera, S. Kopp, P. Chiba, H. Beug, E.W. Mullner, Remodeling the regulation of iron metabolism during erythroid differentiation to ensure efficient heme biosynthesis, Blood 107 (2006) 4159–4167.
[103] Y. Ke, E.C. Theil, An mRNA loop/bulge in the ferritin iron-responsive element forms *in vivo* and was detected by radical probing with Cu-1,10-phenanthroline and iron regulatory protein footprinting, J. Biol. Chem. 277 (2002) 2373–2376.
[104] S.S. Cooperman, E.G. Meyron-Holtz, H. Olivierre-Wilson, M.C. Ghosh, J.P. McConnell, T.A. Rouault, Microcytic anemia, erythropoietic protoporphyria, and neurodegeneration in mice with targeted deletion of iron-regulatory protein 2, Blood 106 (2005) 1084–1091.
[105] S.R. Smith, S. Cooperman, T. Lavaute, N. Tresser, M. Ghosh, E. Meyron-Holtz, W. Land, H. Ollivierre, B. Jortner, R. Switzer III, A. Messing, T.A. Rouault, Severity of neurodegeneration correlates with compromise of iron metabolism in mice with iron regulatory protein deficiencies, Ann. N. Y. Acad. Sci. 1012 (2004) 65–83.
[106] H.-Y. Kim, T. LaVaute, K. Iwai, R.D. Klausner, T.A. Rouault, Identification of a conserved and functional iron-responsive element in the 5′-untranslated region of mammalian mitochondrial aconitase, J. Biol. Chem. 271 (1996) 24226–24230.
[107] K.L. Schalinske, O.S. Chen, R.S. Eisenstein, Iron differentially stimulates translation of mitochondrial aconitase and ferritin mRNAs in mammalian cells, J. Biol. Chem. 273 (1998) 3740–3746.
[108] J.B. Goforth, S.A. Anderson, C.P. Nizzi, R.S. Eisenstein, Multiple determinants within iron-responsive elements dictate iron regulatory protein binding and regulatory hierarchy, RNA 16 (2010) 154–169.
[109] M.A. Khan, W.E. Walden, D.J. Goss, E.C. Theil, Direct Fe2 + sensing by iron-responsive messenger RNA:repressor complexes weakens binding, J. Biol. Chem. 284 (2009) 30122–30128.
[110] B. Galy, D. Ferring-Appel, S. Kaden, H.J. Grone, M.W. Hentze, Iron regulatory proteins are essential for intestinal function and control key iron absorption molecules in the duodenum, Cell Metab. 7 (2008) 79–85.
[111] P. Surdej, L. Richman, L.C. Kuhn, Differential translational regulation of IRE-containing mRNAs in *Drosophila melanogaster* by endogenous IRP and a constitutive human IRP1 mutant, Insect Biochem. Mol. Biol. 38 (2008) 891–894.
[112] K.P. Burdon, S. Sharma, C.S. Chen, D.P. Dimasi, D.A. Mackey, J.E. Craig, A novel deletion in the FTL gene causes hereditary hyperferritinemia cataract syndrome (HHCS) by alteration of the transcription start site, Hum. Mutat. 28 (2007) 742.
[113] C.R. Allerson, M. Cazzola, T.A. Rouault, Clinical severity and thermodynamic effects of iron-responsive element mutations in hereditary hyperferritinemia–cataract syndrome, J. Biol. Chem. 274 (1999) 26439–26447.
[114] W.E. Walden, A. Selezneva, K. Volz, Accommodating variety in iron-responsive elements: crystal structure of transferrin receptor 1 B IRE bound to iron regulatory protein 1, FEBS Lett. 586 (2012) 32–35.
[115] D.L. Zhang, R.M. Hughes, H. Ollivierre-Wilson, M.C. Ghosh, T.A. Rouault, A ferroportin transcript that lacks an iron-responsive element enables duodenal and erythroid precursor cells to evade translational repression, Cell Metab. 9 (2009) 461–473.
[116] E.A. Leibold, H.N. Munro, Characterization and evolution of the expressed rat ferritin light subunit gene and its pseudogene family: conservation of sequences with non-coding regions of ferritin genes, J. Biol. Chem. 262 (1987) 7335–7341.
[117] N. Aziz, H.N. Munro, Iron regulates ferritin mRNA through a segment of its 5′ untranslated region, Proc. Natl. Acad. Sci. U. S. A. 84 (1987) 8478–8482.
[118] M.W. Hentze, S.W. Caughman, T.A. Rouault, J.G. Barriocanal, A. Dancis, J.B. Harford, R.D. Klausner, Identification of the iron-responsive element for the translational regulation of human ferritin mRNA, Science 238 (1987) 1570–1573.
[119] E.A. Leibold, H.N. Munro, Cytoplasmic protein binds *in vitro* to a highly conserved sequence in the 5′ untranslated region of ferritin heavy- and light-subunit mRNAs, Proc. Natl. Acad. Sci. U. S. A. 85 (1988) 2171–2175.
[120] J.L. Casey, M.W. Hentze, D.M. Koeller, S.W. Caughman, T.A. Rouault, R.D. Klausner, J.B. Harford, Iron-responsive elements: regulatory RNA sequences that control mRNA levels and translation, Science 240 (1988) 924–928.
[121] A.I. Selezneva, G. Cavigiolio, E.C. Theil, W.E. Walden, K. Volz, Crystallization and preliminary X-ray diffraction analysis of iron regulatory protein 1 in complex with ferritin IRE RNA, Acta Crystallogr. Sect. F Struct. Biol. Cryst. Commun. 62 (2006) 249–252.
[122] C.M. Harrell, A.R. McKenzie, M.M. Patino, W.E. Walden, E.C. Theil, Ferritin mRNA: interactions of iron regulatory element with translational regulator protein P-90 and the effect on base-paired flanking regions, Proc. Natl. Acad. Sci. U. S. A. 88 (1991) 4166–4170.
[123] A.J. Bettany, R.S. Eisenstein, H.N. Munro, Mutagenesis of the iron-regulatory element further defines a role for RNA secondary structure in the regulation of ferritin and transferrin receptor expression, J. Biol. Chem. 267 (1992) 16531–16537.
[124] Z. Gdaniec, H. Sierputowska-Gracz, E.C. Theil, Iron regulatory element and internal loop/bulge structure for ferritin mRNA studied by cobalt(III) hexamine binding, molecular modeling, and NMR spectroscopy, Biochemistry 37 (1998) 1505–1512.
[125] B.R. Henderson, E. Menotti, C. Bonnard, L.C. Kuhn, Optimal sequence and structure of iron-responsive elements, J. Biol. Chem. 269 (1994) 17481–17489.
[126] B.R. Henderson, E. Menotti, L.C. Kuhn, Iron regulatory proteins 1 and 2 bind distinct sets of RNA target sequences, J. Biol. Chem. 271 (1996) 4900–4908.
[127] L.G. Liang, K.B. Hall, A model of the iron responsive element RNA hairpin loop structure determined from NMR and thermodynamic data, Biochemistry 35 (1996) 13586–13596.
[128] K. Volz, The functional duality of iron regulatory protein 1, Curr. Opin. Struct. Biol. 18 (2008) 106–111.
[129] S.G. Stevens, P.P. Gardner, C. Brown, Two covariance models for iron-responsive elements, RNA Biol. 319 (2011) 1047–1052.
[130] W.E. Walden, A.I. Selezneva, J. Dupuy, A. Volbeda, J.C. Fontecilla-Camps, E.C. Theil, K. Volz, Structure of dual function iron regulatory protein 1 complexed with ferritin IRE-RNA, Science 314 (2006) 1903–1908.
[131] D.J. Dix, P.-N. Lin, A.R. McKenzie, W.E. Walden, E.C. Theil, The influence of the base-paired flanking region on structure and function of the ferritin mRNA iron regulatory element, J. Mol. Biol. 231 (1993) 230–240.
[132] J. Dupuy, A. Volbeda, P. Carpentier, C. Darnault, J.M. Moulis, J.C. Fontecilla-Camps, Crystal structure of human iron regulatory protein 1 as cytosolic aconitase, Structure 14 (2006) 129–139.
[133] Y. Ke, J. Wu, E.A. Leibold, W.E. Walden, E.C. Theil, Loops and bulge/loops in iron-responsive element isoforms influence iron regulatory protein binding. Fine-tuning of mRNA regulation? J. Biol. Chem. 273 (1998) 23637–23640.
[134] P. Piccinelli, T. Samuelsson, Evolution of the iron-responsive element, RNA 13 (2007) 952–966.
[135] Y. Ke, H. Sierzputowska-Gracz, Z. Gdaniec, E.C. Theil, Internal loop/bulge and hairpin loop of the iron-responsive element of ferritin mRNA contribute to maximal iron regulatory protein 2 binding and translational regulation in the iso-iron-responsive element/iso-iron regulatory protein family, Biochemistry 39 (2000) 6235–6242.
[136] H. Gunshin, C.R. Allerson, M. Polycarpou-Schwarz, A. Rofts, J.T. Rogers, F. Kishi, M.W. Hentze, T.A. Rouault, N.C. Andrews, M.A. Hediger, Iron-dependent regulation of the divalent metal ion transporter, FEBS Lett. 509 (2001) 309–316.
[137] J. Butt, H.-Y. Kim, J.P. Basilion, S. Cohen, K. Iwai, C.C. Philpott, S. Altschul, R.D. Klausner, T.A. Rouault, Differences in the RNA binding sites of iron regulatory proteins and potential target diversity, Proc. Natl. Acad. Sci. U. S. A. 93 (1996) 4345–4349.
[138] H.A. Meehan, G.J. Connell, The hairpin loop but not the bulged C of the iron responsive element is essential for high affinity binding to the iron regulatory protein-1, J. Biol. Chem. 276 (2001) 14791–14796.
[139] H.H. Cho, C.M. Cahill, C.R. Vanderburg, C.R. Scherzer, B. Wang, X. Huang, J.T. Rogers, Selective translational control of the Alzheimer amyloid precursor protein transcript by iron regulatory protein-1, J. Biol. Chem. 285 (2010) 31217–31232.
[140] C.O. dos Santos, L.C. Dore, E. Valentine, S.G. Shelat, R.C. Hardison, M. Ghosh, W. Wang, R.S. Eisenstein, F.F. Costa, M.J. Weiss, An iron responsive element-like stem-loop regulates alpha-hemoglobin-stabilizing protein mRNA, J. Biol. Chem. 283 (2008) 26956–26964.
[141] B. Guo, Y. Yu, E.A. Leibold, Iron regulates cytoplasmic levels of a novel iron-responsive element-binding protein without aconitase activity, J. Biol. Chem. 269 (1994) 24252–24260.
[142] F. Samaniego, J. Chin, K. Iwai, T.A. Rouault, R.D. Klausner, Molecular characterization of a second iron-responsive element binding protein, iron regulatory protein 2, J. Biol. Chem. 49 (1994) 30904–30910.
[143] B. Guo, J.D. Phillips, Y. Yu, E.A. Leibold, Iron regulates the intracellular degradation of iron regulatory protein 2 by the proteasome, J. Biol. Chem. 270 (1995) 21645–21651.

[144] K. Iwai, R.D. Klausner, T.A. Rouault, Requirements for iron-regulated degradation of the RNA binding protein, iron regulatory protein 2, EMBO J. 14 (1995) 5350–5357.
[145] D.K. Kang, J. Jeong, S.K. Drake, N.B. Wehr, T.A. Rouault, R.L. Levine, Iron regulatory protein 2 as iron sensor. Iron-dependent oxidative modification of cysteine, J. Biol. Chem. 278 (2003) 14857–14864.
[146] J. Jeong, T.A. Rouault, R.L. Levine, Identification of a heme-sensing domain in iron regulatory protein 2, J. Biol. Chem. 279 (2004) 45450–45454.
[147] K. Yamanaka, H. Ishikawa, Y. Megumi, F. Tokunaga, M. Kanie, T.A. Rouault, I. Morishima, N. Minato, K. Ishimori, K. Iwai, Identification of the ubiquitin-protein ligase that recognizes oxidized IRP2, Nat. Cell Biol. 5 (2003) 336–340.
[148] H. Ishikawa, M. Kato, H. Hori, K. Ishimori, T. Kirisako, F. Tokunaga, K. Iwai, Involvement of heme regulatory motif in heme-mediated ubiquitination and degradation of IRP2, Mol. Cell 19 (2005) 171–181.
[149] E. Bourdon, D.K. Kang, M.C. Ghosh, S.K. Drake, J. Wey, R.L. Levine, T.A. Rouault, The role of endogenous heme synthesis and degradation domain cysteines in cellular iron-dependent degradation of IRP2, Blood Cells Mol. Dis. 31 (2003) 247–255.
[150] E.S. Hanson, M.L. Rawlins, E.A. Leibold, Oxygen and iron regulation of iron regulatory protein 2, J. Biol. Chem. 278 (2003) 40337–40342.
[151] J. Wang, G. Chen, M. Muckenthaler, B. Galy, M.W. Hentze, K. Pantopoulos, Iron-mediated degradation of IRP2, an unexpected pathway involving a 2-oxoglutarate-dependent oxygenase activity, Mol. Cell. Biol. 24 (2004) 954–965.
[152] K.B. Zumbrennen, E.S. Hanson, E.A. Leibold, HOIL-1 is not required for iron-mediated IRP2 degradation in HEK293 cells, Biochim. Biophys. Acta 1783 (2008) 246–252.
[153] T. Cardozo, M. Pagano, The SCF ubiquitin ligase: insights into a molecular machine, Nat. Rev. Mol. Cell Biol. 5 (2004) 739–751.
[154] M.D. Petroski, R.J. Deshaies, Function and regulation of cullin-RING ubiquitin ligases, Nat. Rev. Mol. Cell Biol. 6 (2005) 9–20.
[155] X. Bailly, S. Vanin, C. Chabasse, K. Mizuguchi, S.N. Vinogradov, A phylogenomic profile of hemerythrins, the nonheme diiron binding respiratory proteins, BMC Evol. Biol. 8 (2008) 244.
[156] W.C. Kao, V.C. Wang, Y.C. Huang, S.S. Yu, T.C. Chang, S.I. Chan, Isolation, purification and characterization of hemerythrin from *Methylococcus capsulatus* (Bath), J. Inorg. Biochem. 102 (2008) 1607–1614.
[157] C.E. Isaza, R. Silaghi-Dumitrescu, R.B. Iyer, D.M. Kurtz Jr., M.K. Chan, Structural basis for O2 sensing by the hemerythrin-like domain of a bacterial chemotaxis protein: substrate tunnel and fluxional N terminus, Biochemistry 45 (2006) 9023–9031.
[158] J.W. Thompson, A.A. Salahudeen, S. Chollangi, J.C. Ruiz, C.A. Brautigam, T.M. Makris, J.D. Lipscomb, D.R. Tomchick, R.K. Bruick, Structural and molecular characterization of the iron-sensing hemerythrin-like domain within F-box and leucine-rich repeat protein 5 (FBXL5), J. Biol. Chem. 287 (2012) 7357–7365.
[159] J. Wang, G. Chen, J. Lee, K. Pantopoulos, Iron-dependent degradation of IRP2 requires its C-terminal region and IRP structural integrity, BMC Mol. Biol. 9 (2008) 15.
[160] E.G. Meyron-Holtz, M.C. Ghosh, T.A. Rouault, Mammalian tissue oxygen levels modulate iron-regulatory protein activities *in vivo*, Science 306 (2004) 2087–2090.
[161] A. Hausmann, J. Lee, K. Pantopoulos, Redox control of iron regulatory protein 2 stability, FEBS Lett. 585 (2011) 687–692.
[162] G. Cairo, A. Pietrangelo, Nitric-oxide mediated activation of iron-regulatory protein controls hepatic iron metabolism during acute inflammation, Eur. J. Biochem. 232 (1995) 358.
[163] L. Tacchini, S. Recalcati, A. Bernelli-Zazzera, G. Cairo, Induction of ferritin synthesis in ischemic-reperfused rat liver: analysis of the molecular mechanisms, Gastroenterology 113 (1997) 946–953.
[164] K.B. Zumbrennen, M.L. Wallander, S.J. Romney, E.A. Leibold, Cysteine oxidation regulates the RNA-binding activity of Iron Regulatory Protein 2, Mol. Cell. Biol. 29 (2009) 2219–2229.
[165] A. Ozer, R.K. Bruick, Non-heme dioxygenases: cellular sensors and regulators jelly rolled into one? Nat. Chem. Biol. 3 (2007) 144–153.
[166] S. Kim, S.S. Wing, P. Ponka, S-nitrosylation of IRP2 regulates its stability via the ubiquitin–proteasome pathway, Mol. Cell. Biol. 24 (2004) 330–337.
[167] A.H. Chang, J. Jeong, R.L. Levine, Iron regulatory protein 2 turnover through a nonproteasomal pathway, J. Biol. Chem. 286 (2011) 23698–23707.
[168] C. Dycke, P. Charbonnier, K. Pantopoulos, J.M. Moulis, A role for lysosomes in the turnover of human iron regulatory protein 2, Int. J. Biochem. Cell Biol. 40 (2008) 2826–2832.
[169] E.H. Morgan, Inhibition of reticulocyte iron uptake by NH_4Cl and CH_3NH_2, Biochim. Biophys. Acta 642 (1981) 119–134.
[170] S.V. Torti, F.M. Torti, Ironing out cancer, Cancer Res. 71 (2011) 1511–1514.
[171] A. Cozzi, B. Corsi, S. Levi, P. Santambrogio, A. Albertini, P. Arosio, Overexpression of wild type and mutated human ferritin H-chain in HeLa cells: *in vivo* role of ferritin ferroxidase activity, J. Biol. Chem. 275 (2000) 25122–25129.
[172] O. Kakhlon, Y. Gruenbaum, Z.I. Cabantchik, Repression of ferritin expression increases the labile iron pool, oxidative stress, and short-term growth of human erythroleukemia cells, Blood 97 (2001) 2863–2871.
[173] A. Cozzi, B. Corsi, S. Levi, P. Santambrogio, G. Biasiotto, P. Arosio, Analysis of the biologic functions of H- and L-ferritins in HeLa cells by transfection with siRNAs and cDNAs: evidence for a proliferative role of L-ferritin, Blood 103 (2004) 2377–2383.
[174] A. Baldi, D. Lombardi, P. Russo, E. Palescandolo, A. De Luca, D. Santini, F. Baldi, L. Rossiello, M.L. Dell'Anna, A. Mastrofrancesco, V. Maresca, E. Flori, P.G. Natali, M. Picardo, M.G. Paggi, Ferritin contributes to melanoma progression by modulating cell growth and sensitivity to oxidative stress, Clin. Cancer Res. 11 (2005) 3175–3183.
[175] Z.K. Pinnix, L.D. Miller, W. Wang, R. D'Agostino Jr., T. Kute, M.C. Willingham, H. Hatcher, L. Tesfay, G. Sui, X. Di, S.V. Torti, F.M. Torti, Ferroportin and iron regulation in breast cancer progression and prognosis, Sci. Transl. Med. 2 (2010) 43ra56.
[176] C. Maffettone, G. Chen, I. Drozdov, C. Ouzounis, K. Pantopoulos, Tumorigenic properties of iron regulatory protein 2 (IRP2) mediated by its specific 73-amino acids insert, PLoS One 5 (2010) e10163.
[177] G. Chen, C. Fillebeen, J. Wang, K. Pantopoulos, Overexpression of iron regulatory protein 1 suppresses growth of tumor xenografts, Carcinogenesis 28 (2007) 785–791.
[178] M.L. Wallander, K.B. Zumbrennen, E.S. Rodansky, S.J. Romney, E.A. Leibold, Iron-independent phosphorylation of iron regulatory protein 2 regulates ferritin during the cell cycle, J. Biol. Chem. 283 (2008) 23589–23598.
[179] E.G. Meyron-Holtz, M.C. Ghosh, K. Iwai, T. LaVaute, X. Brazzolotto, U.V. Berger, W. Land, H. Ollivierre-Wilson, A. Grinberg, P. Love, T.A. Rouault, Genetic ablations of iron regulatory proteins 1 and 2 reveal why iron regulatory protein 2 dominates iron homeostasis, EMBO J. 23 (2004) 386–395.
[180] S.R. Smith, M.C. Ghosh, H. Ollivierre-Wilson, W. Hang Tong, T.A. Rouault, Complete loss of iron regulatory proteins 1 and 2 prevents viability of murine zygotes beyond the blastocyst stage of embryonic development, Blood Cells Mol. Dis. 36 (2006) 283–287.
[181] T. LaVaute, S. Smith, S. Cooperman, K. Iwai, W. Land, E. Meyron-Holtz, S.K. Drake, G. Miller, M. Abu-Asab, M. Tsokos, R.r. Switzer, A. Grinberg, P. Love, N. Tresser, T.A. Rouault, Targeted deletion of the gene encoding iron regulatory protein-2 causes misregulation of iron metabolism and neurodegenerative disease in mice, Nat. Genet. 27 (2001) 209–214.
[182] B. Galy, D. Ferring, M.W. Hentze, Generation of conditional alleles of the murine iron regulatory protein (Irp)-1 and -2 genes, Genesis 43 (2005) 181–188.
[183] B. Galy, D. Ferring, B. Minana, O. Bell, H.G. Janser, M. Muckenthaler, K. Schumann, M.W. Hentze, Altered body iron distribution and microcytosis in mice deficient in iron regulatory protein 2 (IRP2), Blood 106 (2005) 2580–2589.
[184] D. Ferring-Appel, M.W. Hentze, B. Galy, Cell-autonomous and systemic context-dependent functions of iron regulatory protein 2 in mammalian iron metabolism, Blood 113 (2009) 679–687.
[185] S.Y. Jeong, D.R. Crooks, H. Wilson-Ollivierre, M.C. Ghosh, R. Sougrat, J. Lee, S. Cooperman, J.B. Mitchell, C. Beaumont, T.A. Rouault, Iron insufficiency compromises motor neurons and their mitochondrial function in Irp2-null mice, PLoS One 6 (2011) e25404.
[186] C. Ferreira, P. Santambrogio, M.E. Martin, V. Andrieu, G. Feldmann, D. Henin, C. Beaumont, H ferritin knockout mice: a model of hyperferritinemia in the absence of iron overload, Blood 98 (2001) 525–532.
[187] B. Galy, S.M. Holter, T. Klopstock, D. Ferring, L. Becker, S. Kaden, W. Wurst, H.J. Grone, M.W. Hentze, Iron homeostasis in the brain: complete iron regulatory protein 2 deficiency without symptomatic neurodegeneration in the mouse, Nat. Genet. 38 (2006) 967–969 (discussion 969–970).
[188] I. De Domenico, M.B. Vaughn, P.N. Paradkar, E. Lo, D.M. Ward, J. Kaplan, Decoupling ferritin synthesis from free cytosolic iron results in ferritin secretion, Cell Metab. 13 (2011) 57–67.
[189] L. Vanoaica, D. Darshan, L. Richman, K. Schumann, L.C. Kuhn, Intestinal ferritin H is required for an accurate control of iron absorption, Cell Metab. 12 (2010) 273–282.
[190] B. Galy, D. Ferring-Appel, S.W. Sauer, S. Kaden, S. Lyoumi, H. Puy, S. Kolker, H.J. Grone, M.W. Hentze, Iron regulatory proteins secure mitochondrial iron sufficiency and function, Cell Metab. 12 (2010) 194–201.
[191] N.E. Sunny, E.J. Parks, J.D. Browning, S.C. Burgess, Excessive hepatic mitochondrial TCA cycle and gluconeogenesis in humans with nonalcoholic fatty liver disease, Cell Metab. 14 (2011) 804–810.
[192] P.R. Dallman, J.R. Goodman, Enlargement of mitochondrial compartment in iron and copper deficiency, Blood 35 (1970) 496–505.
[193] K.J. Hintze, E.C. Theil, DNA and mRNA elements with complementary responses to hemin, antioxidant inducers, and iron control ferritin-L expression, Proc. Natl. Acad. Sci. U. S. A. 102 (2005) 15048–15052.
[194] C. Beaumont, P. Leneuve, I. Devaux, J.Y. Scoazec, M. Berthier, M.N. Loiseau, B. Grandchamp, D. Bonneau, Mutation in the iron responsive element of the L ferritin mRNA in a family with dominant hyperferritinaemia and cataract, Nat. Genet. 11 (1995) 444–446.
[195] D. Girelli, R. Corrocher, L. Bisceglia, O. Olivieri, L. De Franceschi, L. Zelante, P. Gasparini, Molecular basis for the recently described hereditary hyperferritinemia–cataract syndrome: a mutation in the iron-responsive element of ferritin L-subunit gene (the "Verona mutation"), Blood 86 (1995) 4050–4053.
[196] M. Cazzola, B. Foglieni, G. Bergamaschi, S. Levi, M. Lazzarino, P. Arosio, A novel deletion of the L-ferritin iron-responsive element responsible for severe hereditary hyperferritinaemia–cataract syndrome, Br. J. Haematol. 116 (2002) 667–670.
[197] J. Kato, K. Fujikawa, M. Kanda, N. Fukuda, K. Sasaki, T. Takayama, M. Kobune, K. Takada, R. Takimoto, H. Hamada, T. Ikeda, Y. Niitsu, A mutation, in the iron-responsive element of H ferritin mRNA, causing autosomal dominant iron overload, Am. J. Hum. Genet. 69 (2001) 191–197.
[198] A.R. Curtis, C. Fey, C.M. Morris, L.A. Bindoff, P.G. Ince, P.F. Chinnery, A. Coulthard, M.J. Jackson, A.P. Jackson, D.P. McHale, D. Hay, W.A. Barker, A.F. Markham, D. Bates, A. Curtis, J. Burn, Mutation in the gene encoding ferritin light polypeptide causes dominant adult-onset basal ganglia disease, Nat. Genet. 28 (2001) 350–354.
[199] S. Luscieti, P. Santambrogio, B. Langlois d'Estaintot, T. Granier, A. Cozzi, M. Poli, B. Gallois, D. Finazzi, A. Cattaneo, S. Levi, P. Arosio, Mutant ferritin L-chains that

cause neurodegeneration act in a dominant-negative manner to reduce ferritin iron incorporation, J. Biol. Chem. 285 (2010) 11948–11957.
[200] B.B. Muhoberac, M.A. Baraibar, R. Vidal, Iron loading-induced aggregation and reduction of iron incorporation in heteropolymeric ferritin containing a mutant light chain that causes neurodegeneration, Biochim. Biophys. Acta 1812 (2011) 544–548.
[201] R. Vidal, L. Miravalle, X. Gao, A.G. Barbeito, M.A. Baraibar, S.K. Hekmatyar, M. Widel, N. Bansal, M.B. Delisle, B. Ghetti, Expression of a mutant form of the ferritin light chain gene induces neurodegeneration and iron overload in transgenic mice, J. Neurosci. 28 (2008) 60–67.
[202] C. Kannengiesser, A.M. Jouanolle, G. Hetet, A. Mosser, F. Muzeau, D. Henry, E. Bardou-Jacquet, M. Mornet, P. Brissot, Y. Deugnier, B. Grandchamp, C. Beaumont, A new missense mutation in the L ferritin coding sequence associated with elevated levels of glycosylated ferritin in serum and absence of iron overload, Haematologica 94 (2009) 335–339.
[203] T.C. Cox, S.S. Bottomley, J.S. Wiley, M.J. Bawden, C.S. Matthews, B.K. May, X-linked pyridoxine-responsive sideroblastic anemia due to a Thr388-to-Ser substitution in erythroid 5-aminolevulinate synthase, N. Engl. J. Med. 330 (1994) 675–679.
[204] P.D. Cotter, M. Baumann, D.F. Bishop, Enzymatic defect in "X-linked" sideroblastic anemia: molecular evidence for erythroid delta-aminolevulinate synthase deficiency, Proc. Natl. Acad. Sci. U. S. A. 89 (1992) 4028–4032.
[205] S.D. Whatley, S. Ducamp, L. Gouya, B. Grandchamp, C. Beaumont, M.N. Badminton, G.H. Elder, S.A. Holme, A.V. Anstey, M. Parker, A.V. Corrigall, P.N. Meissner, R.J. Hift, J.T. Marsden, Y. Ma, G. Mieli-Vergani, J.C. Deybach, H. Puy, C-terminal deletions in the ALAS2 gene lead to gain of function and cause X-linked dominant protoporphyria without anemia or iron overload, Am. J. Hum. Genet. 83 (2008) 408–414.
[206] I. De Domenico, D.M. Ward, G. Musci, J. Kaplan, Iron overload due to mutations in ferroportin, Haematologica 91 (2006) 92–95.
[207] A. Fernandes, G.C. Preza, Y. Phung, I. De Domenico, J. Kaplan, T. Ganz, E. Nemeth, The molecular basis of hepcidin-resistant hereditary hemochromatosis, Blood 114 (2009) 437–443.
[208] N.T. Shahidi, D.G. Nathan, L.K. Diamond, Iron deficiency anemia associated with an error of iron metabolism in two siblings, J. Clin. Invest. 43 (1964) 510–521.
[209] M.P. Mims, Y. Guan, D. Pospisilova, M. Priwitzerova, K. Indrak, P. Ponka, V. Divoky, J.T. Prchal, Identification of a human mutation of DMT1 in a patient with microcytic anemia and iron overload, Blood 105 (2005) 1337–1342.
[210] A. Iolascon, M. d'Apolito, V. Servedio, F. Cimmino, A. Piga, C. Camaschella, Microcytic anemia and hepatic iron overload in a child with compound heterozygous mutations in DMT1 (SCL11A2), Blood 107 (2006) 349–354.
[211] K.D. Coon, A.M. Siegel, S.J. Yee, T.L. Dunckley, C. Mueller, R.M. Nagra, W.W. Tourtellotte, E.M. Reiman, A. Papassotiropoulos, F.F. Petersen, D.A. Stephan, W.M. Kirsch, Preliminary demonstration of an allelic association of the IREB2 gene with Alzheimer's disease, J. Alzheimers Dis. 9 (2006) 225–233.
[212] M.A. Smith, K. Wehr, P.L. Harris, S.L. Siedlak, J.R. Connor, G. Perry, Abnormal localization of iron regulatory protein in Alzheimer's disease, Brain Res. 788 (1998) 232–236.
[213] J.A. Duce, A. Tsatsanis, M.A. Cater, S.A. James, E. Robb, K. Wikhe, S.L. Leong, K. Perez, T. Johanssen, M.A. Greenough, H.H. Cho, D. Galatis, R.D. Moir, C.L. Masters, C. McLean, R.E. Tanzi, R. Cappai, K.J. Barnham, G.D. Ciccotosto, J.T. Rogers, A.I. Bush, Iron-export ferroxidase activity of beta-amyloid precursor protein is inhibited by zinc in Alzheimer's disease, Cell 142 (2010) 857–867.
[214] P. Lei, S. Ayton, D.I. Finkelstein, L. Spoerri, G.D. Ciccotosto, D.K. Wright, B.X. Wong, P.A. Adlard, R.A. Cherny, L.Q. Lam, B.R. Roberts, I. Volitakis, G.F. Egan, C.A. McLean, R. Cappai, J.A. Duce, A.I. Bush, Tau deficiency induces parkinsonism with dementia by impairing APP-mediated iron export, Nat. Med. 18 (2012) 291–295.
[215] D.L. DeMeo, T. Mariani, S. Bhattacharya, S. Srisuma, C. Lange, A. Litonjua, R. Bueno, S.G. Pillai, D.A. Lomas, D. Sparrow, S.D. Shapiro, G.J. Criner, H.P. Kim, Z. Chen, A.M. Choi, J. Reilly, E.K. Silverman, Integration of genomic and genetic approaches implicates IREB2 as a COPD susceptibility gene, Am. J. Hum. Genet. 85 (2009) 493–502.
[216] S.L. Chappell, L. Daly, J. Lotya, A. Alsaegh, T. Guetta-Baranes, J. Roca, R. Rabinovich, K. Morgan, A.B. Millar, S.C. Donnelly, V. Keatings, W. MacNee, J. Stolk, P.S. Hiemstra, M. Miniati, S. Monti, C.M. O'Connor, N. Kalsheker, The role of IREB2 and transforming growth factor beta-1 genetic variants in COPD: a replication case–control study, BMC Med. Genet. 12 (2011) 24.

CHAPTER 5

IRON REGULATORY PROTEIN 2 IS REQUIRED FOR INSULIN PROCESSING AND B CELL FUNCTION

Abstract

Iron regulatory protein 2 (Irp2) is a key regulator of cellular iron metabolism in vertebrates. Irp2 controls the posttranscriptional expression of the iron uptake protein transferrin receptor 1 (TfR1) and the iron storage protein ferritin. Previous studies have shown that mice with a targeted deletion of the *Irp2* gene develop microcytic anemia, erythropoietic protoporphyria and neurobehavioral impairments. Here, we show that *Irp2*$^{-/-}$ mice develop fasting hyperglycemia, glucose intolerance and impaired glucose-stimulated insulin secretion from pancreatic β cells, all of which have been implicated in the pathogenesis of diabetes mellitus. Impaired glucose-stimulated insulin secretion in Irp2 deficient β cells is not due to reduced β cell mass or reduced insulin expression, but rather due to the accumulation of proinsulin in β cells and reduced mature insulin content caused by defective processing of proinsulin to mature insulin. Iron homeostasis is dysregulated in Irp2 deficient β cells as evidenced by decreased TfR1 expression and iron content, and increased ferritin expression and iron sequestration causing cellular iron deficiency. This is associated with reduced activity or levels of mitochondrial and cytosolic Fe-S proteins, suggesting that iron-sulfur (Fe-S) cluster biosynthesis is impaired in Irp2 deficient β cells. Increasing cellular iron in Irp2 deficient β cells restored proinsulin and insulin content to normal levels, and improved glucose-stimulated insulin secretion. These studies reveal a previously unidentified link between insulin processing and cellular iron homeostasis, and show that Irp2 is required for normal β cell function and whole body glucose homeostasis.

Introduction

Type 2 diabetes (T2D) develops when insulin target tissues become resistant to insulin, and pancreatic β cells are unable to fully compensate for reduced insulin sensitivity (Ashcroft and Rorsman, 2012; Kahn et al., 2009; Muoio and Newgard, 2008). Important factors contributing to reduced insulin secretion in T2D is the gradual decline of β cell function and the eventual loss of β cell mass. The mechanisms leading to β cell dysfunction are not fully understood, but defects in glucose sensing, mitochondrial function and endoplasmic reticulum (ER) stress are involved (Ashcroft and Rorsman, 2012; Scheuner and Kaufman, 2008; Kahn et al., 2009; Muoio and Newgard, 2008). Evidence has accumulated revealing a role for proinsulin misfolding in the ER and ensuing ER stress as early events in the pathogenesis of T2D (Sun et al., 2015; Weiss, 2013). Consistent with these findings, elevated circulating proinsulin is associated with the development of T2D in humans (Pradhan et al., 2003; Zethelius et al., 2003).

Evidence has revealed a role for iron in the pathogenesis T2D. Excess body iron stores, as measured by serum ferritin, are associated with an increased risk of T2D in patients with the genetic iron-overload disease hemochromatosis and in healthy individuals (Rajpathak et al., 2009; Simcox and McClain, 2013). The molecular mechanisms through which excess iron contributes to development of T2D are not completely understood, but likely involves insulin resistance as well as iron-induced oxidative β cell death (Cooksey et al., 2004; Hansen et al., 2012; Ristow et al., 2003; Simcox and McClain, 2013). Less is known about the consequence of iron deficiency in β cell function. Iron is required for the mitochondrial synthesis of Fe-S clusters and heme that are cofactors for electron transport complexes (ETCs), the TCA enzyme aconitase

and for the maturation of extramitochondrial Fe-S proteins involved in DNA metabolism, ER function and nucleotide metabolism (Maio and Rouault, 2015; Netz et al., 2014). Consequently, cellular iron deficiency can lead to mitochondrial dysfunction and cell death (Lill et al., 2012; Silva and Faustino, 2015). The importance of optimal Fe-S cluster biosynthesis is underscored by studies showing that mutations in Fe-S cluster biogenesis genes in humans cause neurological and metabolic diseases (Rouault, 2015; Stehling et al., 2014).

Cellular iron content must therefore be maintained within a narrow range to avoid the adverse consequences of iron depletion or excess. Maintaining cellular iron content within this physiologic range requires precise mechanisms for regulating its uptake and storage. In vertebrates, cellular iron homeostasis is controlled posttranscriptionally by iron-regulatory protein 2 (Irp2) (Anderson et al., 2012; Hentze et al., 2010; Rouault, 2006). Irp2 is a cytosolic protein that binds to RNA stem-loops known as iron-responsive elements (IREs) in the mRNAs of proteins involved in iron uptake (transferrin receptor 1 (TfR1, Tfrc)) and sequestration (ferritin), and regulates the stability or translation of these mRNAs. In iron-deficient cells, Irp2 binds to an IRE in the 5' untranslated region (UTR) of ferritin mRNAs to inhibit translation and to the IREs in the 3' UTR of the TfR1 mRNA to prevent its degradation. In iron-sufficient cells, Irp2 is targeted for proteasomal degradation (Salahudeen and Bruick, 2009; Vashisht et al., 2009), increasing ferritin translation and iron sequestration, and promoting *TfR1* mRNA degradation and reducing iron uptake. Irp2 regulation of ferritin and TfR1 precisely coordinates iron uptake and sequestration in response to fluctuations in cellular iron concentration, ensuring that cells acquire sufficient iron for their needs without causing toxicity. *Irp2*$^{-/-}$ mice develop

microcytic anemia and erythropoietic protoporphyria and exhibit neurological and behavioral impairments. Studies have shown that iron deficiency in neurons of *Irp2*$^{-/-}$ mice impairs the activity of several Fe-S containing ETCs and other Fe-S proteins causing mitochondrial dysfunction and neuron degeneration (Jeong et al., 2011). Taken together, these studies emphasize the importance of Irp2 in maintenance of optimal cellular iron homeostasis to avoid mitochondrial dysfunction and cell death (Cooperman et al., 2005; Galy et al., 2005b; Jeong et al., 2011; LaVaute et al., 2001; Zumbrennen-Bullough et al., 2014).

Here, we demonstrate that Irp2 is required for β cell function, and more specifically for the processing and secretion of insulin. A role for Irp2 in β cell function was demonstrated in *Irp2*$^{-/-}$ primary islets and recapitulated using the rodent insulinoma cell line INS-1 832/13 depleted of Irp2. Irp2 deficiency leads to increased proinsulin content and reduced insulin content and secretion. Cellular iron content is reduced due to decreased TfR1 expression, and increased iron sequestration in ferritin, leading to functional iron deficiency and impaired mitochondrial function. Our data suggest that defective proinsulin processing arises in part from mitochondrial dysfunction due to impaired biosynthesis of Fe-S clusters. Together, our results identify a mechanism that links iron homeostasis to the processing and secretion of insulin.

Materials and methods

The generation of mice with global deficiency of Irp2 has been previously described (Zumbrennen-Bullough et al., 2014). Briefly, *Irp2*$^{-/-}$ mice were generated by inserting a self-excision cassette containing neomycin (*Neo*^{r}) linked to cre-recombinase

(*Cre*) into exon 3 of the mouse *Irp2*$^{-/-}$ gene as previously described (Zumbrennen-Bullough et al., 2014.) This cassette (pACN) contains the Cre gene (driven by the testes-specific angiotensin-converting enzyme (tACE promoter) linked to *Neo*^{r} (driven by the polymerase II promoter) and is flanked by loxP sites allowing for excision of *Neo*^{r}as it passes through the male germ line. *Irp2*$^{-/-}$ mice were generated on a C57BL/6J and 129/Sv background and backcrossed with C57BL/6J for five generations. *Irp2*$^{-/-}$ and WT littermates were obtained from intercrosses from *Irp2*$^{+/-}$ parents. Male mice at 2- to 18-months of age were used for this study. Mice were kept in accordance with the recommendations in the Guide for the Care and Use of Laboratory Animals of the National Institutes of Health. The protocol was approved by the Institutional Animal Care and Use Committee (IACUC) of the University of Utah (Protocol Number: 13-02012). All mice were housed in a pathogen free environment with water and fed mouse breeder diet containing 270 mg Fe/kg (Teklad 8626) provided ad libitum. Mice were euthanized according to AVMA Guidelines for the Euthanasia of Animals**.** At the German Mouse Clinic (GMC; Neuherberg, Germany), mice were maintained in IVC cages with free access to water and standard mouse chow containing 183 mg Fe/kg (Altromin no.1324). All experiments and housing of the animals in the GMC were performed according to the German Law on the Protection of Animals (regulation 209.1/211-2531-70/07 by the Government of Upper Bavaria (Regierung von Oberbayern).

The rat insulinoma β INS1 832/13 β-cell line was kindly provided by Dr. Chris Newgard (Duke University). Cells were cultured in RPMI-1640 medium supplemented with 10% fetal calf serum, 10 mM HEPES, 2 mM L-glutamine, 1 mM sodium pyruvate, 0.05 β-mercaptoethanol (β-ME) and 5.0 ug/mL puromycin, grown at 37 ^{o}C with 5% CO_2

as described (Hohmeier et al., 2000). INS1 832/13 cells were stably transduced with empty vector (pLentiLox3.7puro) or an Irp2 shRNA (pLentiLox3.7puro::IRP2-4) (Zimmer et al., 2008) kindly provided by Dr. Othon Iliopoulos (Massachusetts General Hospital Cancer Center). Cells were treated with 50 ug/ml ferric ammonium citrate (FAC) or desferrioxamine DFO (50 um) for 24 - 48 h and lysates prepared for western blot analysis.

For glucose tolerance tests, animals were fasted for 16-17 h and baseline blood glucose was determined from tail-vein blood (Ascencia Elite XL Glucometer, Bayer Corp.). Conscious animals were then challenged with an intraperitoneal (ip) injection of glucose (2g/kg body weight, Sigma-Aldrich) and blood glucose levels were determined at 15-, 30-, 60-, 90-, and 120-min postinjection. For insulin tolerance tests, random-fed conscious animals were injected with human recombinant insulin (0.75U/kg body weight, Novalin R, Novo Nordisk). Tail-vein blood samples were taken before and 15-, 30-, 60-, 90-, 120-, and 150-min postinjection.

For plasma insulin analysis, 100 µl of tail-vein blood were collected from overnight fasted mice for baseline insulin measurements, and 30 min post-i.p. glucose injection (2g/kg body weight). Plasma insulin was measured using the Sensitive Rat Insulin RIA Kit (Linco Research, Inc.). For pancreatic insulin and proinsulin content, freshly harvested pancreata were incubated overnight in acid-ethanol mixture (1.5% HCl in 70% EtOH) at -20 °C. Tissue was homogenized and incubated overnight at -20 °C. Samples were centrifuged at 3000 x g for 15 min at 4 °C. Supernatant was neutralized with equal volume of 1 M Tris-HCl pH 7.5 and centrifuged at 15,000 x g for 10 min at 4 °C. Insulin was quantified using a Mouse Insulin ELISA (ALPCO) and proinsulin was

quantified using a Rat/Mouse Proinsulin ELISA (Mercodia) and normalized to total protein determined by Coomassie Plus Protein Assay Reagent (Thermo).

Mice were anesthetized using Avertin (0.015 ml/g body weight) and sacrificed by cervical dislocation. The pancreas was perfused through the common bile duct with 6 mL of Hanks balanced salt solution (HBSS, Invitrogen) containing 0.1 mg/mL DNase I (Roche), 25 mM HEPES and 0.3 mg/ml Liberase RI Purified Enzyme Blend (Roche). Pancreata were extracted and incubated in a 37 °C water bath for ~12 min in HBSS/Liberase RI solution. Pancreatic tissue was disrupted by vigorous shaking for 10 s and washed twice with HBSS containing 0.1 mg/mL DNase I and 10% heat inactive fetal bovine serum (FBS, Invitrogen). Islets were handpicked twice from exocrine tissue. For GSIS assays, 10 islets were size-matched and handpicked to a 96-well plate and incubated in Krebs-Ringer bicarbonate HEPES buffer (10 mM HEPES pH 7.35, 140 mM NaCl, 3.6 mM KCl, 0.5 mM NaH_2PO_4, 0.5 mM $MgSO_4$, 1.5 mM $CaCl_2$, 2 mM $NaHCO_3$, 10 mM HEPES, 0.1% bovine serum albumin (BSA), 2.6 mM glucose) for 1 h at 37°C. Islets were then treated with 16.7 mM glucose for an additional 1 h at 37 °C. Islets were sonicated in 1 ml HBSS at settling 4 with 10 x 1 s bursts (Brinkmann Sonic Dismembrator, Fisher Scientific).

For glucose-stimulated insulin and proinsulin secretion assays in EV and shIrp2 expressing INS1 832/13 cells, approximately 0.05 x 10^6 cells were plated onto a 24-well plate an grown to 100 % confluency. The standard culture medium containing 11 mM glucose was changed to medium containing 5 mM glucose 18 h before performing secretion assays. Cell were washed and preincubated for 2 h in HBSS (20 mM HEPES, pH 7.2 with 114 mM NaCl, 4.7 mM KCl, 1.2 mM KH_2PO_4, 1.16 mM $MgSO_4$, 2.5 mM

$CaCl_2$, 25.5 mM $NaHCO_3$, and 0.2% BSA. Insulin secretion was measured by static incubation in 0.8 mL of HBSS containing 3 mM or 15 mM glucose for a 2-h period. Insulin (ALPCO) and proinsulin (Mercodia) were assayed by ELISAs and normalized to total lysate protein using Coomassie Plus Protein Assay Reagent (Thermo).

Metal content was determined by digesting pancreas (20-30 mg) or isolated islets (100-200 islets) in 40% metal-free nitric acid at 95°C. Samples were diluted in water and analyzed by PerkinElmer Optima 3100XL inductively-coupled plasma optical emission spectrometer. Metal concentrations were corrected for dilution and normalized to total mg or number of islets.

Isolated islets (150-200) were lysed in Triton Lysis Buffer (10 mM Tris-HCl pH 7.4, 150 mM NaCl, 10 mM EDTA, 1% Triton X-100, 1 mM DTT and Cocktail Protease Inhibitor (Roche)) using a micro-dounce. Lysates were cleared by centrifugation and protein concentration was determined using Coomassie Plus Protein Assay Reagent. Islet lysates were boiled in lithium dodecyl sulfate (LDS) sample buffer (Invitrogen) containing 2.5% β-mercaptoethanol (β-ME) boiled in lithium dodecyl sulfate sample uPAGE 4-12% Bis-Tris gels (Invitrogen) with MES SDS-running buffer. INS1 832/13 cells expressing EV or shIrp2 were treated with FAC or DFO for 24 h and lysed in Triton Lysis Buffer. Cell lysates (30 ug protein) were analysis by 4-12% Bis-Tris gels as described above. Proteins were transferred to a Hybond-ECL nitrocellulose membrane (Amersham) and probed with the following antibodies: chicken anti-Irp1 polyclonal antibody (PAb) (Guo et al., 1994); rabbit anti-Irp2 PAb antibody (Yu et al., 1992); rabbit antiferritin-H PAb (H-53 Santa Cruz Biotechnology); mouse anti-TfR1 monoclonal antibody (MAb) (Zymed clone H68.4), rabbit anti-ferritin PAb (UT106) (Schneider and

Leibold, 2003; Zumbrennen-Bullough et al., 2014), rabbit antiCisd1 PAb (Proteintech 16006-1-AP) and beta-actin MAb (AC-15, Ambion). Horseradish peroxidase-conjugated secondary antibodies were bound and proteins were visualized using Western Lighting Chemiluminescence Reagent Plus (PerkinElmer Life Sciences). Membranes were stripped for 10 min at 65 °C in stripping buffer (62.5 mM Tris-HCl, pH 6.8, 100 mM β-ME and 2% SDS).

Pancreata were fixed with 4% buffered formalin immediately after dissection and embedded in paraffin. Pancreas sections (5 um) were rehydrated with xylene followed by decreasing concentrations of ethanol and antigen retrieval was performed using Dako Target Retrieval Solution at 90 ^{o}C for 30 min followed by cooling at room temperature for 20 min. For islet morphometric analysis, sections were taken at 120 um intervals for insulin staining using guinea pig antiinsulin PAb (Dako, 1:200) for 16 h followed by incubation with donkey antiguinea pig secondary antibody (Jackson ImmunoReseach, 1:500) for 1 h and visualization by 3'3'-diaminobenzidine (DAB). Images (4x) spanning the entire pancreas were acquired using Nikon Widefield CCD/Spinning Disk microscopes that were automatically stitched together to generate a compound image. Image J software was used to quantify islet area and the fraction of insulin-stained tissue area in four sections per pancreas for 2.5-, 7.5- and 18-month old mice (n = 3 - 6 mice per genotype). Five cell clusters were considered to be an islet. β cell mass was calculated by multiplying the fraction of insulin-stained tissue area by pancreas weight.

For immunofluorescence studies, pancreas sections were incubated in TBST blocking solution (Tris-buffered saline containing 0.1 % Tween) for 1 h at room temperature and then incubated with the following antibodies in TBST overnight at 4 ^{o}C:

rabbit antirat ferritin PAb (UT106 1:100) (Schneider and Leibold, 2003; Zumbrennen-Bullough et al., 2014), mouse antiTfR1 MAb (Zymed clone H68.4, 1:200), mouse antiinsulin MAb (Millipore clone E11D7, 1:100), rabbit antiGlut2 PAb (Millipore 07-1402, 1:200) and mouse anti-proinsulin Mab (Developmental Studies Hybridoma Bank, GS--9A8, 1:100). Sections were washed in PBS and then incubated with Alexa Fluor™ 488 or Alexa Fluor™ 567 antirabbit or antimouse IgG secondary antibodies in TBST for 1 h at room temperature. Images were acquired using an Olympus FV1000 confocal microscope at the same time using identical camera settings.

Total RNA was extracted from islets isolated from 39-49 week old WT and *Irp2*$^{-/-}$ mice using TRIzol reagent (Invitrogen). cDNA synthesis was performed with total RNA (0.5 ug - 1 ug) using SuperScript III First-Strand synthesis SuperMix for qRT-PCR (Invitrogen). qRT-PCR was performed on an ABI Prism 7900HT Sequence Detection System using TaqMan master mix and TaqMan Gene Expression Assays. The $\Delta\Delta CT$ method was used to determine mRNA-fold change. All experiments were performed using 5-6 mice per genotype and fold changes were normalized to *actb* levels.

Complex I and IV activities were measured in EV and shIrp2 expressing INS1 832/13 cells using Complex I and IV Enzyme Activity Dipstick Assay Kits (Mitosciences) following the manufacturer's protocol. Aconitase activity was assessed in mitochondrial and cytosolic extracts using an Aconitase Enzyme Activity Microplate Assay Kit assay (Abcam). Enriched mitochondrial and cytosolic fractions were prepared using Triton Lysis Buffer and 0.01% digitonin (Schneider and Leibold, 2003). ATP content measurements were performed on cell lysates from INS1 832/13 cells expressing EV and shIrp2. Cells were preincubated at 37 ^{o}C for 60 min in HBSS (secretion buffer)

containing 2.5 mM glucose and then incubated in either 5.0 mM glucose or 20 mM glucose for an additional hour. ATP content was measured in triplicate samples using the ATP Determination Kit (Molecular Probes).

Data are expressed as average mean ± standard errors of the means (SEM). For two-group comparison, a two-tailed Student's-t test was used. For multiple group comparisons, two-way analysis of variance (ANOVA) was used followed by Tukey's multiple comparison test. For all hypotheses the significance level was $p < 0.05$. Prism 6.0 (Graphpad) was used for statistical analysis.

Results

Mice with global deletion of *Irp2*$^{-/-}$ were generated by inserting a self-excision cassette containing neomycin (*Neo*^{r}) linked to cre-recombinase (*Cre*) into exon 3 of the mouse *Irp2*$^{-/-}$ gene as previously described (Zumbrennen-Bullough et al., 2012). Previous studies showed that *Irp2*$^{-/-}$ mice displayed dysregulation of ferritin and TfR1 in tissues and altered body iron distribution and developed mild microcytic anemia and neurodegenerative disease (Cooperman et al., 2005; Galy et al., 2005a; Galy et al., 2006; LaVaute et al., 2001; Zumbrennen-Bullough et al. 2014). In the GMC primary screen, plasma glucose concentrations were elevated in both random-fed and fasted 12-month old male *Irp2*$^{-/-}$ mice compared to WT (random-fed: *Irp2*$^{-/-}$, 211.2 ± 13.6 mg/dl versus WT, 150 ± 13 mg/dl glucose, n = 9-10, $p < 0.01$; fasted: *Irp2*$^{-/-}$, 118 ± 7.1 mg/dl versus WT, 95.0 ± 5.3 mg/dl; n = 7-10, $p < 0.05$). Glucose concentration showed a tendency to be elevated in random-fed 3-month old male *Irp2*$^{-/-}$ mice, and significantly elevated in female *Irp2*$^{-/-}$ mice. The observed changes in glucose homeostasis in 3-month old mice

were not attributable to alterations in lipid homeostasis as plasma total cholesterol, triglycerides, nonesterified fatty acids, and electrolytes were similar in *Irp2*$^{-/-}$ and WT mice. The determination of body composition by dual-energy X-ray absorptiometry (DEXA) showed a decreased lean mass in *Irp2*$^{-/-}$ mice and suggested an increased body fat content. No further differences in energy metabolism especially regarding food intake and energy expenditure were detected.

Next, to assess whole body glucose metabolism, intraperitoneal glucose tolerance tests (ipGTTs) were performed on overnight fasted 5-month old *Irp2*$^{-/-}$ and WT male mice. After glucose injection, *Irp2*$^{-/-}$ mice exhibit an increased peak glucose concentration and reduced glucose clearance compared to WT mice (Figure 5.1). Increased Area Under Curve (AUC) values indicate that *Irp2*$^{-/-}$ mice had developed glucose intolerance already at an age of 2-months without worsening over time in mice at 12- and 18-months of age (Figure 5.1B). *Irp2*$^{-/-}$ female mice (10- and 20-weeks of age) display significant, but less pronounced glucose intolerance (Figure S5.1) compared to males, and therefore, subsequent studies were performed solely in male mice. At all ages, *Irp2*$^{-/-}$ mice had significantly higher elevated fasting glucose levels compared to WT mice (Figure 5.1C).

To determine whether impaired glucose clearance in *Irp2*$^{-/-}$ mice is due to insulin resistance, insulin tolerance tests were performed in 5- and 18-month old *Irp2*$^{-/-}$ and WT mice. Comparable glucose disposal rates suggest glucose intolerance in *Irp2*$^{-/-}$ mice was not a consequence of insulin resistance (Figure 5.2A). We next performed euglycemic-hyperinsulinemic clamps in order to analyze whole-body and organ-specific insulin action in more detail. When exogenous insulin is administered to *Irp2*$^{-/-}$ mice, they

display increased insulin sensitivity evident by higher glucose infusion rates (GIR) compared to age and body composition-matched WT mice (Figure 5.2B and 5.C). Comparable whole body glucose turnover rates (Rd, Figure 5.2D) in both genotypes suggest improved insulin sensitivity in *Irp2*$^{-/-}$ mice is not caused by peripheral alterations in insulin action, but rather a more pronounced suppression of hepatic glucose production by insulin (Figure 5.2E). There were also no genotypic changes in whole body glycolysis rates (Figure 5.2F). Taken together these data suggested that glucose intolerance in *Irp2*$^{-/-}$ mice is primarily related to impaired β cell function.

In the fasted state (0 min), basal insulin levels tended to be lower in 5- and 18-month old *Irp2*$^{-/-}$ mice compared to WT. Intraperitoneal glucose injection in 5-month old *Irp2*$^{-/-}$ mice is followed by a comparable relative increase in plasma insulin concentrations from baseline levels compared to WT mice, but in contrast was weaker in 18-month old animals suggesting an age-dependent effect.

To measure pancreatic β cell sensitivity in response to elevations in plasma glucose hyperglycemic clamps were carried out in overnight fasted 7-month old *Irp2*$^{-/-}$ and WT mice. *Irp2*$^{-/-}$ mice showed fasting hyperglycemia (*Irp2*$^{-/-}$, 7.17 ± 0.39 *versus* WT, 6.06 ± 0.23 mmol glucose/L; $p = 0.02$; Figure 5.3A) and reduced basal plasma insulin concentrations (*Irp2*$^{-/-}$, 75.37 ± 15.80 *versus* WT, 281.12 ± 119 pmol insulin/L; $p < 0.05$; Figure 5.3B). Insulin secretion in response to hyperglycemia (~18 mM) is blunted in *Irp2*$^{-/-}$ (Figure 5.3A and 5.B). Calculation of the AUC during the first phase (0-15 min of the clamp) and steady state phase (60-105 min of the clamp) of the clamp showed that insulin secretion was reduced by 62% ($p < 0.05$) and 67% ($p < 0.05$), respectively, in *Irp2*$^{-/-}$ mice compared to WT mice (Figure 5.3B and 5.C). These results indicated that

glucose intolerance in *Irp2*$^{-/-}$ mice is due to impaired insulin secretion from β cells.

To determine the basis of abnormal insulin secretion in *Irp2*$^{-/-}$ mice, pancreatic insulin content was quantified in WT and *Irp2*$^{-/-}$ mice. Total pancreatic insulin was reduced by 22% in 2.5-month old *Irp2*$^{-/-}$ mice, and further reduced by 50% and 41% in 7.5- and 18-month old *Irp2*$^{-/-}$ mice, respectively, compared to age-matched WT mice (Figure 5.4A). By contrast, pancreatic proinsulin content and the proinsulin-to-insulin ratio increased in all *Irp2*$^{-/-}$ mice compared to WT mice (Figure 5.4B and C). Reduced insulin content in *Irp2*$^{-/-}$ mice was not due to reduced insulin transcription as the transcript levels of the two insulin genes, *Ins1* and *Ins2,* were not changed in *Irp2*$^{-/-}$ islets (Figure 5.4D). Morphometric quantification of insulin-stained paraffin-embedded pancreatic sections showed that islet area and β-cell mass were unaffected in 2.5- and 7.5-month old *Irp2*$^{-/-}$ mice; however, islet area and β-cell mass tended to be reduced in 18-month old *Irp2*$^{-/-}$ mice (Figure 5.4E and F). Insulin and glucagon immunostaining of *Irp2*$^{-/-}$ islets revealed normal morphology with insulin positive β cells uniformly distributed within the islet core and glucagon positive alpha cells on the periphery (Figure S2A). Glucagon expression was unaffected in *Irp2*$^{-/-}$ islets (Figure S5.2). As proinsulin is cleaved and processed by prohormone convertase 1/3 (PC1/3, Psk1), the expression of PC1/3 was evaluated in *Irp2*$^{-/-}$ islets. No change in PC1/3 expression was observed, suggesting that the defective insulin processing was not due to reduced PC1/3 expression (Figure S5.3). No change in expression or subcellular localization of the glucose transporter Glut2 was observed in *Irp2*$^{-/-}$ islets, indicating that defective insulin processing was not caused by a general defect in ER protein maturation in *Irp2*$^{-/-}$ β cells. Together, these results suggested that processing of proinsulin to mature insulin is

impaired in *Irp2*$^{-/-}$ β cells.

We next assessed glucose-stimulated insulin secretion (GSIS) in islets isolated from WT and *Irp2*$^{-/-}$ mice. *Irp2*$^{-/-}$ islets displayed reduced insulin content, increased proinsulin content and an increased proinsulin-to-insulin ratio compared to WT islets (Figure 5.4G-I). The secretory responses of WT and *Irp2*$^{-/-}$ islets under basal (2.5 mM) glucose and high (16.7 mM) glucose were assessed in a 1-h static assay. Insulin secretion was blunted in *Irp2*$^{-/-}$ islets under high glucose compared to WT islets, and tended to be lower under basal glucose (Figure 5.4J). When the amount of insulin secretion was calculated as a percentage of total islet insulin content, no significant difference in GSIS was observed between WT and *Irp2*$^{-/-}$ islet (Figure 5.4K). Together, these data demonstrated that reduced insulin secretion in *Irp2*$^{-/-}$ islets is caused at least in part by reduced insulin content.

Irp2 deficiency in mice is associated with destabilization of *TfR1* mRNA and derepression of ferritin synthesis that causes abnormal iron content in tissues such as brain, liver, intestine, and red cells (Cooperman et al., 2005; Galy et al., 2005b; LaVaute et al., 2001; Zumbrennen-Bullough et al., 2014). We thus assessed the consequence of Irp2 deficiency on iron content, and ferritin and TfR1 expression in WT and *Irp2*$^{-/-}$ islets. Total iron content was reduced by 47% in *Irp2*$^{-/-}$ islets compared to WT islets, while the content of Cu, Mn, and Zn was unaffected. Western blot analysis showed increased ferritin and reduced TfR1 expression in *Irp2*$^{-/-}$ islets compared to WT islets, while Irp1 levels were unaffected (Figure 5.5A). Consistent with reduced TfR1 protein levels, *TfR1* mRNA levels were also downregulated in *Irp2*$^{-/-}$ islets (Figure 5.5B). *Ftl1* mRNA levels were unchanged in *Irp2*$^{-/-}$ islets, although *Fth1* mRNA levels were unexpectedly

decreased, suggesting a transcriptional response to low iron levels (Figure 5.5B). We also assessed divalent metal transporter 1 (*Dmt1)* mRNA levels as it contains a 3'-IRE and its increased expression in mouse β cells causes iron overload (Hansen et al., 2012). *Dmt1* mRNA levels were unchanged in *Irp2*$^{-/-}$ islets, suggesting that reduced iron content in *Irp2*$^{-/-}$ islets was not due to Dmt1-dependent iron uptake (Figure 5.5B).

Consistent with western blot analysis, immunofluorescence studies revealed prominent costaining of ferritin with insulin in *Irp2*$^{-/-}$ β cells and reduced TfR1 staining compared to WT β cells (Figure 5.5C and 5.5D). These results showed that loss of Irp2 leads to reduced TfR1 expression and iron uptake, and increased ferritin expression and iron sequestration, which in turn, leads to functional cellular iron deficiency.

The role of Irp2 in insulin production and secretion was further studied in the rat insulinoma cell line INS1 832/13 depleted of Irp2 by stable expression of a shIrp2 RNA. Western blot analysis confirmed reduced Irp2 expression, concomitant increased ferritin and a modest reduction in TfR1 levels compared to cells expressing empty vector (EV) (Figure 5.6A). Treatment of cells with the iron chelator desferrioxamine (DFO) stabilized Irp2 and reduced ferritin levels, while ferric ammonium citrate (FAC) reduced Irp2 levels and increased ferritin levels in both EV and shIrp2 cells (Figure 5.6A), as previously reported for other cell types (Salahudeen and Bruick, 2009; Vashisht et al., 2009). Irp2 RNA-binding activity, as assessed by RNA electrophoretic mobility shift assays (RNA-EMSA), was reduced in shIrp2 cells, whereas Irp1 RNA-binding activity increased consistent with reduced iron in these cells (Figure 5.6B-C). In agreement with *Irp2*$^{-/-}$ islets studies, shIrp2-INS1 cells displayed reduced insulin content, increased proinsulin content and impaired GSIS compared to EV cells (Figure 5.6D-F). In

addition, glucose-stimulated proinsulin secretion increased by ~ 2-fold in shIrp2-INS1 cells compared to EV cells (Figure 5.6G). These results showed that shIrp2-INS1 cells recapitulate the abnormal proinsulin phenotype observed in *Irp2*$^{-/-}$ islets and that the proinsulin processing defect is likely in part cell-autonomous.

We next questioned whether iron supplementation normalizes proinsulin and insulin content, and insulin and proinsulin secretion in shIrp2-INS1 cells. FAC increased insulin and proinsulin content, and glucose-stimulated insulin and proinsulin secretion in shIrp2-INS1 cells to levels observed in EV cells (Figure 5.6D-G). When the amount of secreted insulin was normalized to insulin content, the increase in secretion seemed to result mostly, but not completely, from reduced insulin content. Collectively, our data showed that iron is required for normal insulin production and secretion from β cells.

Iron is required for the mitochondrial synthesis of Fe-S clusters that are cofactors for the electron transport complexes I, II, and III and for the TCA enzyme aconitase within mitochondria, as well as for the maturation of nuclear and cytoplasmic Fe-S proteins (Netz et al., 2014). Previous studies have shown that complex I, II, and III activities are reduced in neurons of *Irp2*$^{-/-}$ mice (Jeong et al., 2011) and is associated with mitochondrial dysfunction. We therefore assessed Fe-S biosynthesis in shIrp2-INS1 cells by measuring complex I activity (contains eight Fe-S clusters), complex IV activity (lacks Fe-S clusters but contains heme), and mitochondrial and cytosolic aconitases (each contain one Fe-S cluster). Complex I activity was reduced by 33% in shIrp2-INS1 cells compared to EV cells, while complex IV activity was unchanged (Figure 5.7A and B). FAC supplementation restored complex I activity in shIrp2-INS1 cells to levels in EV cells (Figure 5.7A). Mitochondrial and cytosolic aconitase activities were also reduced in

shIrp2-INS1 cells (Figure 5.7C). The reduction in cytosolic aconitase activity is consistent with increased Irp1 RNA-binding activity in shIrp2-INS1 cells (Figure 5.7C and Figure 5.6B). We also assessed the abundance of the extramitochondrial Fe-S proteins Cisd1 (MitoNEET) and Cisd2 (Naf-1, Miner1) in EV and shIrp2-INS1 cells treated with FAC or DFO (Figure 5.7D). Cisd1 is a mitochondrial outer membrane protein that is destabilized in HeLa cells after treatment with iron chelators (Ferecatu et al., 2014), while Cisd2 is predominately localized to the ER membrane with the Fe-S cluster facing the cytoplasm (Wiley et al., 2013). Cisd1 and Cisd2 levels were reduced in shIrp2-INS1 cells, and were further reduced in shIrp2-INS1 cells treated with DFO. Cisd1 and Cisd2 levels were restored in shIrp2-INS1 cells to EV levels (Figure 5.7D). These results suggested that iron deficiency due to loss of Irp2 impairs Fe-S biosynthesis as evidenced by reduced activity or levels of mitochondrial and extramitochondrial Fe-S proteins.

Reduced activity of mitochondrial respiratory complexes and the TCA enzymes can lead to energy deficiency and increase reactive oxygen species (ROS) production (REF). To determine whether changes in Fe-S protein activity or levels are associated with changes in energy production, ATP content was assessed in EV and shIr2p-INS1 cells. Cellular ATP content was reduced by 50% in shIrp2-INS1 cells compared to EV cells (Figure 5.7E). Basal ROS levels as measured by the cell-permeable indicator carboxy-H_2DCFDA fluorescence were similar in EV and shIrp2-INS1 cells, but were elevated in shIrp2-INS1 cells after exposure to H_2O_2 (Figure 5.7F), indicating that shIrp2-INS1 cells display an increased sensitivity to oxidative stress.

Discussion

Our lab has shown that *Irp2*$^{-/-}$ mice develop fasting hyperglycemia and glucose intolerance in addition to perturbations in iron homeostasis that results in microcytic anemia and protoporphyria, which are consistent with other models of IRP2 deficiency. The link between iron homeostasis and diabetes mellitus is well established. Individuals with the iron overload disorder hemochromatosis are prime examples of this association (Fleming and Ponka, 2012). Increased bodily iron stores and elevated serum ferritin in these individuals are risk factors for the development of T2D. The mechanisms that account for T2D risk in cases of excess iron are not fully understood, but likely involve peripheral insulin resistance and β-cell damage from increased oxygen radicals. In contrast, little is known about glucose metabolism and iron deficiency. The prevalence of iron deficiency in obesity is considerably high compared to individuals with a normal body mass index, and obesity is the number one risk factor for T2D (Jehn et al., 2004).

Irp2$^{-/-}$ mice exhibit reduced GSIS as a consequence of pancreatic insulin deficiency. Low insulin levels are associated with elevated proinsulin, which suggests a defect within the biogenesis of insulin. Studies that perturb processing enzymes, ER homeostasis, and Zn^{2+} transport (required for insulin hexamer formation in golgi vesicles) have resulted in reduced mature insulin and accumulation of proinsulin. The mechanisms in these studies are somewhat obvious due to known functions of mutated genes, however our case is not as straightforward. There is no apparent reduction in prohormone convertase levels or ultrastructural defects of the ER.

IRP2 knockdown in INS-1 β-cells recapitulates the insulin defects seen in *Irp2*$^{-/-}$ mice, in addition to reduced Complex 1 activity and ATP content. Our data showing

reduced activity or levels of Fe-S cluster containing proteins; Complex I, CISD1, CISD2, and IRP1 support a model of defective Fe-S cluster biogenesis or transfer of Fe-S clusters into apo-proteins. Given that iron supplementation can rescue the insulin defect in shIRP2 INS-1 β-cells, we conclude that cellular iron deficiency due to loss of IRP2 results in a reduction of Fe-S clusters.

This poses an important question. What role do Fe-S clusters play in diabetes, and how would reduced Fe-S cluster biogenesis affect insulin processing? Insight into these questions comes from studies of the Fe-S cluster assembly protein Frataxin. Mutations in frataxin cause the neurodegenerative disorder Friedrich's Ataxia (FA) that is marked by abnormal gait, scoliosis, heart disease, and diabetes. Mice with β-cell specific deletion of Frataxin are glucose intolerant and develop diabetes (Ristow et al., 2003). This was a consequence of increased ROS and loss of β-cell mass due to apoptosis. In our model however, we did not observe any loss of β-cell mass and no substantial elevation in ROS even though there appears to be increased sensitivity to oxidative stress.

Another Fe-S cluster containing protein has been associated with diabetes. Cdk5 regulatory associated protein 1-like 1 (CDKAL1) is one of the most reproducible genes linked to diabetes across ethnic populations, and encodes a mammalian methylthiotransferase (Dehwah et al., 2010). CDKAL1 is responsible for the addition of 2-methylthio-N^6-threonylcarbamoyladenosine (ms^2t^6A) to $tRNA^{Lys}$ (UUU) that is required for proper translation of AAA and AAG codons. Mice with β-cell specific deletion of CDKAL1 have reduced insulin secretion and become glucose intolerant (Wei et al., 2011). This study showed that β-cells in these mice fail to correctly translate

proinsulin that results in inability to recognize the C-peptide and A-chain cleavage site. We are currently testing this hypothesis in our *Irp2*$^{-/-}$ mice.

References

Anderson, C.P., Shen, M., Eisenstein, R.S., and Leibold, E.A. (2012). Mammalian iron metabolism and its control by iron regulatory proteins. Biochim. Biophys. Acta. *1823*, 1468-1483.

Anderson, S.A., Nizzi, C.P., Chang, Y.I., Deck, K.M., Schmidt, P.J., Galy, B., Damnernsawad, A., Broman, A.T., Kendziorski, C., Hentze, M.W., et al. (2013). The IRP1-HIF-2alpha axis coordinates iron and oxygen sensing with erythropoiesis and iron absorption. Cell Metab. *17*, 282-290.

Ashcroft, F.M., and Rorsman, P. (2012). Diabetes mellitus and the beta cell: the last ten years. Cell *148*, 1160-1171.

Cooksey, R.C., Jouihan, H.A., Ajioka, R.S., Hazel, M.W., Jones, D.L., Kushner, J.P., and McClain, D.A. (2004). Oxidative stress, beta-cell apoptosis, and decreased insulin secretory capacity in mouse models of hemochromatosis. Endocrinology *145*, 5305-5312.

Cooperman, S.S., Meyron-Holtz, E.G., Olivierre-Wilson, H., Ghosh, M.C., McConnell, J.P., and Rouault, T.A. (2005). Microcytic anemia, erythropoietic protoporphyria, and neurodegeneration in mice with targeted deletion of iron-regulatory protein 2. Blood *106*, 1084-1091.

Ferecatu, I., Goncalves, S., Golinelli-Cohen, M.P., Clemancey, M., Martelli, A., Riquier, S., Guittet, E., Latour, J.M., Puccio, H., Drapier, J.C., et al. (2014). The diabetes drug target MitoNEET governs a novel trafficking pathway to rebuild an Fe-S cluster into cytosolic aconitase/iron regulatory protein 1. J. Biol. Chem. *289*, 28070-28086.

Fernandez-Real, J.M., Lopez-Bermejo, A., and Ricart, W. (2002). Cross-talk between iron metabolism and diabetes. Diabetes *51*, 2348-2354.

Fernandez-Real, J.M., and Manco, M. (2014). Effects of iron overload on chronic metabolic diseases. Lancet Diabetes Endocrinol. *2*, 513-526.

Fernandez-Real, J.M., Penarroja, G., Castro, A., Garcia-Bragado, F., Hernandez-Aguado, I., and Ricart, W. (2002b). Blood letting in high-ferritin type 2 diabetes: effects on insulin sensitivity and beta-cell function. Diabetes *51*, 1000-1004.

Furuta, M., Yano, H., Zhou, A., Rouille, Y., Holst, J.J., Carroll, R., Ravazzola, M., Orci, L., Furuta, H., and Steiner, D.F. (1997). Defective prohormone processing and altered pancreatic islet morphology in mice lacking active SPC2. Proc. Natl. Acad. Sci. U.S.A. *94*, 6646-6651.

Gabrielsen, J.S., Gao, Y., Simcox, J.A., Huang, J., Thorup, D., Jones, D., Cooksey, R.C., Gabrielsen, D., Adams, T.D., Hunt, S.C., et al. (2012). Adipocyte iron regulates adiponectin and insulin sensitivity. J. Clin. Invest. *122*, 3529-3540.

Galy, B., Ferring-Appel, D., Kaden, S., Grone, H.J., and Hentze, M.W. (2008). Iron regulatory proteins are essential for intestinal function and control key iron absorption molecules in the duodenum. Cell Metab. *7*, 79-85.

Galy, B., Ferring-Appel, D., Sauer, S.W., Kaden, S., Lyoumi, S., Puy, H., Kolker, S., Grone, H.J., and Hentze, M.W. (2010). Iron regulatory proteins secure mitochondrial iron sufficiency and function. Cell Metab. *12*, 194-201.

Galy, B., Ferring, D., and Hentze, M.W. (2005a). Generation of conditional alleles of the murine iron regulatory protein (Irp)-1 and -2 genes. Genesis *43*, 181-188.

Galy, B., Ferring, D., Minana, B., Bell, O., Janser, H.G., Muckenthaler, M., Schumann, K., and Hentze, M.W. (2005b). Altered body iron distribution and microcytosis in mice deficient in iron regulatory protein 2 (IRP2). Blood *106*, 2580-2589.

Galy, B., Holter, S.M., Klopstock, T., Ferring, D., Becker, L., Kaden, S., Wurst, W., Grone, H.J., and Hentze, M.W. (2006). Iron homeostasis in the brain: complete iron regulatory protein 2 deficiency without symptomatic neurodegeneration in the mouse. Nat. Genet. *38*, 967-969; discussion 969-970.

Gao, Y., Li, Z., Gabrielsen, J.S., Simcox, J.A., Lee, S.H., Jones, D., Cooksey, B., Stoddard, G., Cefalu, W.T., and McClain, D.A. (2015). Adipocyte iron regulates leptin and food intake. J. Clin. Invest. *125*, 3681-3691.

Ghosh, M.C., Zhang, D.L., Jeong, S.Y., Kovtunovych, G., Ollivierre-Wilson, H., Noguchi, A., Tu, T., Senecal, T., Robinson, G., Crooks, D.R., et al. (2013). Deletion of iron regulatory protein 1 causes polycythemia and pulmonary hypertension in mice through translational derepression of HIF2alpha. Cell Metab. *17*, 271-281.

Guo, B., Yu, Y., and Leibold, E.A. (1994). Iron regulates cytoplasmic levels of a novel iron-responsive element-binding protein without aconitase activity. J. Biol. Chem. *269*, 24252-24260.

Hansen, J.B., Tonnesen, M.F., Madsen, A.N., Hagedorn, P.H., Friberg, J., Grunnet, L.G., Heller, R.S., Nielsen, A.O., Storling, J., Baeyens, L., et al. (2012). Divalent metal transporter 1 regulates iron-mediated ROS and pancreatic beta cell fate in response to cytokines. Cell Metab. *16*, 449-461.

Hentze, M.W., Muckenthaler, M.U., Galy, B., and Camaschella, C. (2010). Two to tango: regulation of Mammalian iron metabolism. Cell *142*, 24-38.

Hohmeier, H.E., Mulder, H., Chen, G., Henkel-Rieger, R., Prentki, M., and Newgard, C.B. (2000). Isolation of INS-1-derived cell lines with robust ATP-sensitive K+ channel-dependent and -independent glucose-stimulated insulin secretion. Diabetes *49*, 424-430.

Jeong, S.Y., Crooks, D.R., Wilson-Ollivierre, H., Ghosh, M.C., Sougrat, R., Lee, J.,

Cooperman, S., Mitchell, J.B., Beaumont, C., and Rouault, T.A. (2011). Iron insufficiency compromises motor neurons and their mitochondrial function in Irp2-null mice. PLoS One *6*, e25404.

Jung, I.R., Choi, S.E., Jung, J.G., Lee, S.A., Han, S.J., Kim, H.J., Kim, D.J., Lee, K.W., and Kang, Y. (2015). Involvement of iron depletion in palmitate-induced lipotoxicity of beta cells. Mol. Cell. Endocrinol. *407*, 74-84.

Kahn, S.E., Hull, R.L., and Utzschneider, K.M. (2006). Mechanisms linking obesity to insulin resistance and type 2 diabetes. Nature *444*, 840-846.

Kahn, S.E., Montgomery, B., Howell, W., Ligueros-Saylan, M., Hsu, C.H., Devineni, D., McLeod, J.F., Horowitz, A., and Foley, J.E. (2001). Importance of early phase insulin secretion to intravenous glucose tolerance in subjects with type 2 diabetes mellitus. J. Clin. Endocrinol. Metab. *86*, 5824-5829.

Kahn, S.E., Zraika, S., Utzschneider, K.M., and Hull, R.L. (2009). The beta cell lesion in type 2 diabetes: there has to be a primary functional abnormality. Diabetologia *52*, 1003-1012.

Khoo, C., Yang, J., Rajpal, G., Wang, Y., Liu, J., Arvan, P., and Stoffers, D.A. (2011). Endoplasmic reticulum oxidoreductin-1-like beta (ERO1lbeta) regulates susceptibility to endoplasmic reticulum stress and is induced by insulin flux in beta-cells. Endocrinology *152*, 2599-2608.

LaVaute, T., Smith, S., Cooperman, S., Iwai, K., Land, W., Meyron-Holtz, E., Drake, S.K., Miller, G., Abu-Asab, M., Tsokos, M., et al. (2001). Targeted deletion of the gene encoding iron regulatory protein-2 causes misregulation of iron metabolism and neurodegenerative disease in mice. Nat. Genet. *27*, 209-214.

Liew, C.W., Assmann, A., Templin, A.T., Raum, J.C., Lipson, K.L., Rajan, S., Qiang, G., Hu, J., Kawamori, D., Lindberg, I., et al. (2014). Insulin regulates carboxypeptidase E by modulating translation initiation scaffolding protein eIF4G1 in pancreatic beta cells. Proc. Natl. Acad. Sci. U S A *111*, E2319-2328.

Lill, R., Hoffmann, B., Molik, S., Pierik, A.J., Rietzschel, N., Stehling, O., Uzarska, M.A., Webert, H., Wilbrecht, C., and Muhlenhoff, U. (2012). The role of mitochondria in cellular iron-sulfur protein biogenesis and iron metabolism. Biochim. Biophys. Acta. *1823*, 1491-1508.

Liu, M., Hodish, I., Haataja, L., Lara-Lemus, R., Rajpal, G., Wright, J., and Arvan, P. (2010). Proinsulin misfolding and diabetes: mutant INS gene-induced diabetes of youth. Trends Endocrinol. Metab. *21*, 652-659.

Lopez, A., Cacoub, P., Macdougall, I.C., and Peyrin-Biroulet, L. (2015). Iron deficiency anaemia. Lancet.

Maio, N., and Rouault, T.A. (2015). Iron-sulfur cluster biogenesis in mammalian cells: New insights into the molecular mechanisms of cluster delivery. Biochim. Biophys. Acta. *1853*, 1493-1512.

Muoio, D.M., and Newgard, C.B. (2008). Mechanisms of disease: molecular and metabolic mechanisms of insulin resistance and beta-cell failure in type 2 diabetes. Nat. Rev. Mol. Cell. Biol. *9*, 193-205.

Neschen, S., Morino, K., Dong, J., Wang-Fischer, Y., Cline, G.W., Romanelli, A.J., Rossbacher, J.C., Moore, I.K., Regittnig, W., Munoz, D.S., et al. (2007). n-3 Fatty acids preserve insulin sensitivity in vivo in a peroxisome proliferator-activated receptor-alpha-dependent manner. Diabetes *56*, 1034-1041.

Neschen, S., Morino, K., Hammond, L.E., Zhang, D., Liu, Z.X., Romanelli, A.J., Cline, G.W., Pongratz, R.L., Zhang, X.M., Choi, C.S., et al. (2005). Prevention of hepatic steatosis and hepatic insulin resistance in mitochondrial acyl-CoA:glycerol-sn-3-phosphate acyltransferase 1 knockout mice. Cell Metab. *2*, 55-65.

Netz, D.J., Mascarenhas, J., Stehling, O., Pierik, A.J., and Lill, R. (2014). Maturation of cytosolic and nuclear iron-sulfur proteins. Trends Cell Biol. *24*, 303-312.

Oslowski, C.M., and Urano, F. (2011). The binary switch that controls the life and death decisions of ER stressed beta cells. Curr. Opin. Cell Biol. *23*, 207-215.

Poitout, V., Amyot, J., Semache, M., Zarrouki, B., Hagman, D., and Fontes, G. (2010). Glucolipotoxicity of the pancreatic beta cell. Biochim. Biophys. Acta. *1801*, 289-298.

Pradhan, A.D., Manson, J.E., Meigs, J.B., Rifai, N., Buring, J.E., Liu, S., and Ridker, P.M. (2003). Insulin, proinsulin, proinsulin:insulin ratio, and the risk of developing type 2 diabetes mellitus in women. Am. J. Med. *114*, 438-444.

Rajpathak, S.N., Crandall, J.P., Wylie-Rosett, J., Kabat, G.C., Rohan, T.E., and Hu, F.B. (2009). The role of iron in type 2 diabetes in humans. Biochim. Biophys. Acta. *1790*, 671-681.

Rhodes, C.J. (2005). Type 2 diabetes-a matter of beta-cell life and death? Science *307*, 380-384.

Ristow, M., Mulder, H., Pomplun, D., Schulz, T.J., Muller-Schmehl, K., Krause, A., Fex, M., Puccio, H., Muller, J., Isken, F., et al. (2003). Frataxin deficiency in pancreatic islets causes diabetes due to loss of beta cell mass. J. Clin. Invest. *112*, 527-534.

Rouault, T.A. (2006). The role of iron regulatory proteins in mammalian iron homeostasis and disease. Nat. Chem. Biol. *2*, 406-414.

Rouault, T.A. (2013). Iron metabolism in the CNS: implications for neurodegenerative

diseases. Nat. Rev. Neurosci.

Rouault, T.A. (2015). Mammalian iron-sulphur proteins: novel insights into biogenesis and function. Nat. Rev. Mol. Cell. Biol. *16*, 45-55.

Salahudeen, A.A., and Bruick, R.K. (2009). Maintaining Mammalian iron and oxygen homeostasis: sensors, regulation, and cross-talk. Ann. N.Y. Acad. Sci. *1177*, 30-38.

Scheuner, D., and Kaufman, R.J. (2008). The unfolded protein response: a pathway that links insulin demand with beta-cell failure and diabetes. Endocr. Rev. *29*, 317-333.

Schneider, B.D., and Leibold, E.A. (2003). Effects of iron regulatory protein regulation on iron homeostasis during hypoxia. Blood *102*, 3404-3411.

Silva, B., and Faustino, P. (2015). An overview of molecular basis of iron metabolism regulation and the associated pathologies. Biochim. Biophys. Acta. *1852*, 1347-1359.

Simcox, J.A., and McClain, D.A. (2013). Iron and diabetes risk. Cell Metab. *17*, 329-341.

Stehling, O., Wilbrecht, C., and Lill, R. (2014). Mitochondrial iron-sulfur protein biogenesis and human disease. Biochimie *100*, 61-77.

Sun, J., Cui, J., He, Q., Chen, Z., Arvan, P., and Liu, M. (2015). Proinsulin misfolding and endoplasmic reticulum stress during the development and progression of diabetes. Mol. Aspects Med. *42*, 105-118.

Uchizono, Y., Alarcon, C., Wicksteed, B.L., Marsh, B.J., and Rhodes, C.J. (2007). The balance between proinsulin biosynthesis and insulin secretion: where can imbalance lead? Diabetes Obes. Metab. *9*, 56-66.

Vashisht, A.A., Zumbrennen, K.B., Huang,. X., Powers, D.N., Durazo, A., Sun, D., Bhaskaran, N., Persson, A., Uhlen, M., Sangfelt, O., et al. (2009). Control of iron homeostasis by an iron-regulated ubiquitin ligase. Science *326*, 718-721.

Weiss, M.A. (2013). Diabetes mellitus due to the toxic misfolding of proinsulin variants. FEBS Lett. *587*, 1942-1950.

Wiley, S.E., Andreyev, A.Y., Divakaruni, A.S., Karisch, R., Perkins, G., Wall, E.A., van der Geer, P., Chen, Y.F., Tsai, T.F., Simon, M.I., et al. (2013). Wolfram Syndrome protein, Miner1, regulates sulphydryl redox status, the unfolded protein response, and Ca2+ homeostasis. EMBO Mol. Med. *5*, 904-918.

Wilkinson, N., and Pantopoulos, K. (2013). IRP1 regulates erythropoiesis and systemic iron homeostasis by controlling HIF2alpha mRNA translation. Blood *122*, 1658-1668.

Yu, Y., Radisky, E., and Leibold, E.A. (1992). The iron-responsive element binding

protein. Purification, cloning, and regulation in rat liver. J. Biol. Chem. *267*, 19005-19010.

Zethelius, B., Byberg, L., Hales, C.N., Lithell, H., and Berne, C. (2003). Proinsulin and acute insulin response independently predict Type 2 diabetes mellitus in men--report from 27 years of follow-up study. Diabetologia *46*, 20-26.

Zhu, X., Zhou, A., Dey, A., Norrbom, C., Carroll, R., Zhang, C., Laurent, V., Lindberg, I., Ugleholdt, R., Holst, J.J., et al. (2002). Disruption of PC1/3 expression in mice causes dwarfism and multiple neuroendocrine peptide processing defects. Proc Natl. Acad. Sci. U.S.A. *99*, 10293-10298.

Zimmer, M., Ebert, B.L., Neil, C., Brenner, K., Papaioannou, I., Melas, A., Tolliday, N., Lamb, J., Pantopoulos, K., Golub, T., et al. (2008). Small-molecule inhibitors of HIF-2a translation link its 5'UTR iron-responsive element to oxygen sensing. Mol. Cell *32*, 838-848.

Zumbrennen-Bullough, K.B., Becker, L., Garrett, L., Holter, S.M., Calzada-Wack, J., Mossbrugger, I., Quintanilla-Fend, L., Racz, I., Rathkolb, B., Klopstock, T., et al. (2014). Abnormal brain iron metabolism in irp2 deficient mice is associated with mild neurological and behavioral impairments. PLoS One *9*, e98072.

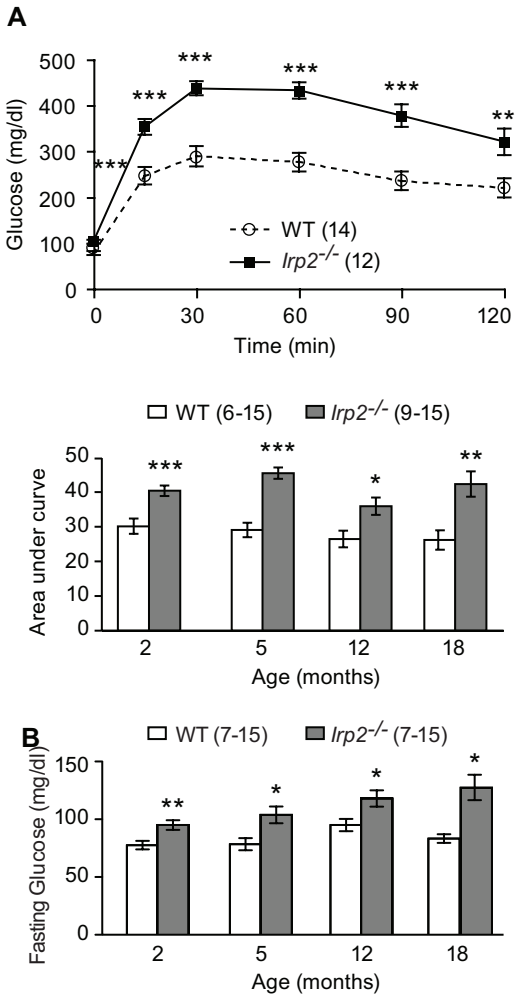

Figure 5.1. Fasting hyperglycemia and glucose intolerance in *Irp2*$^{-/-}$ mice
(A) Glucose tolerance test for 5-month old male WT and *Irp2*$^{-/-}$ mice. Glucose area under the curve (AUC) calculated from ipGTTs performed in WT and *Irp2*$^{-/-}$ mice at ages 2-, 5-, 12- and 18-months. (B) Plasma glucose concentrations of fasted *Irp2*$^{-/-}$ and WT mice. Data are expressed as means ± SEM and were compared by two-tailed Student's t-test. *$p < 0.05$, **$p < 0.01$, ***$p < 0.001$ relative to WT mice. Number of mice is indicated in parentheses.

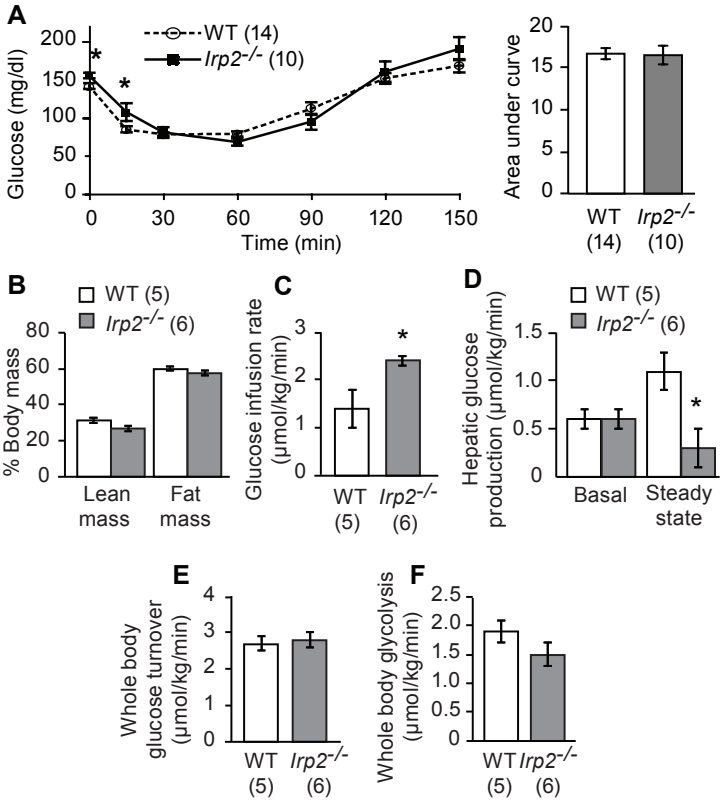

Figure 5.2. Glucose intolerance in *Irp2*$^{-/-}$ mice is not due to impaired peripheral and hepatic insulin action . (A) Insulin tolerance tests were performed in random-fed 5-month old male WT and *Irp2*$^{-/-}$ mice. Glucose AUC calculated from ITT is shown. (B) Percent body mass, (C) glucose infusion rate, peripheral glucose utilization rate , (D) insulin-mediated suppression of hepatic glucose production, (E) whole body glucose turnover and (F) whole body glycolysis from euglycemic-hyperinsulinemic clamp experiments conducted in fasted 7-month old male WT and *Irp2*$^{-/-}$ mice. Data are expressed as means ± SEM and were compared by two-tailed Student's t-test. *$p < 0.05$ relative to WT mice. Number of mice is indicated in parentheses.

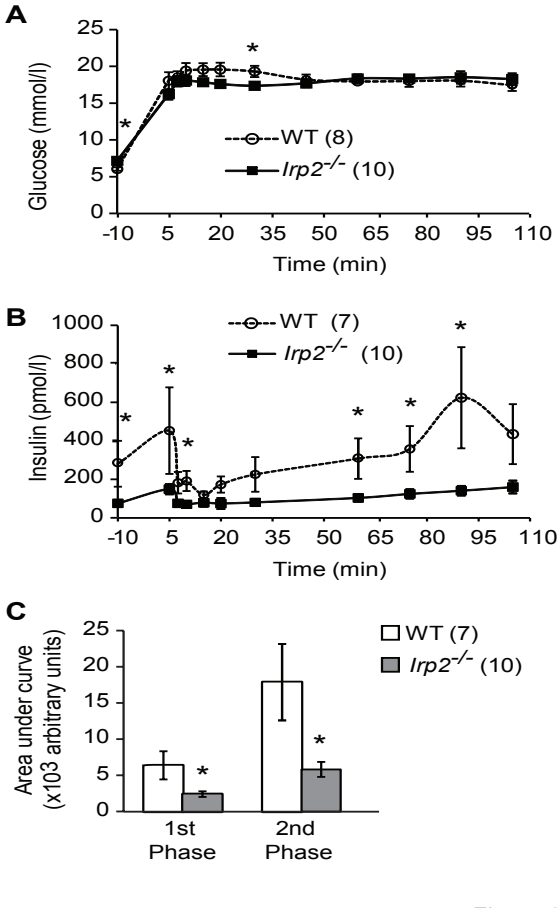

Figure 5.3. Impaired glucose-induced insulin secretion in *Irp2*$^{-/-}$ mice *in vivo.* Hyperglycemic clamps were performed in 7-month old, fasted male WT and *Irp2*$^{-/-}$ mice. *(A)* Glucose and *(B)* insulin levels were measured at the indicated times. *(C)* Insulin AUC corresponding to the first phase (5 min and 7.5 min) and second phase (60-110 min) of insulin secretion are shown. Data are expressed as means ± SEM and were compared by two-tailed Student's t-test. *$p < 0.05$ relative to WT mice. Number of mice is indicated in parentheses.

Figure 5.4. Accumulation of pancreatic proinsulin is associated with reduced insulin content and secretion in *Irp2*$^{-/-}$ islets, (A) Pancreatic insulin and (B) proinsulin content and (C) proinsulin-to-insulin ratio (P/I) in 2.5-, 6.5- and 18-month old WT and *Irp2*$^{-/-}$ mice. (D) qRT-PCR analysis shows no difference in Ins1 and Ins2 expression in islets from 10-month old WT and *Irp2*$^{-/-}$ mice. Values were normalized to β-actin mRNA and are expressed as fold change relative to WT. (E) Quantification of islet area and (F) β cell mass in insulin-stained paraffin-embedded pancreatic sections from 2.5-, 7.5- and 18-month old WT and *Irp2*$^{-/-}$ mice. Mass was calculated by multiplying the fraction of insulin-positive β cell area by pancreatic wet weight. Total insulin content (G), proinsulin content (H) and (I) proinsulin-to-insulin ratio quantified in islets from 7.5-month old WT and *Irp2*$^{-/-}$ mice. (J) Static incubation of islets from WT and *Irp2*$^{-/-}$ mice under basal (2.5 mM) glucose followed by stimulation with high (16.7 mM) glucose for 1 h and normalized to total islet protein. (K) Insulin secretion in (J) was normalized to total islet insulin content. Insulin and proinsulin content were assayed using ELISAs and normalized to total pancreatic or total islet protein. Data are means ± SEM and were compared by two-tailed Student's t-test; *$p < 0.05$, **$p < 0.01$ and ***$p < 0.001$. Number of mice is indicated in parentheses.

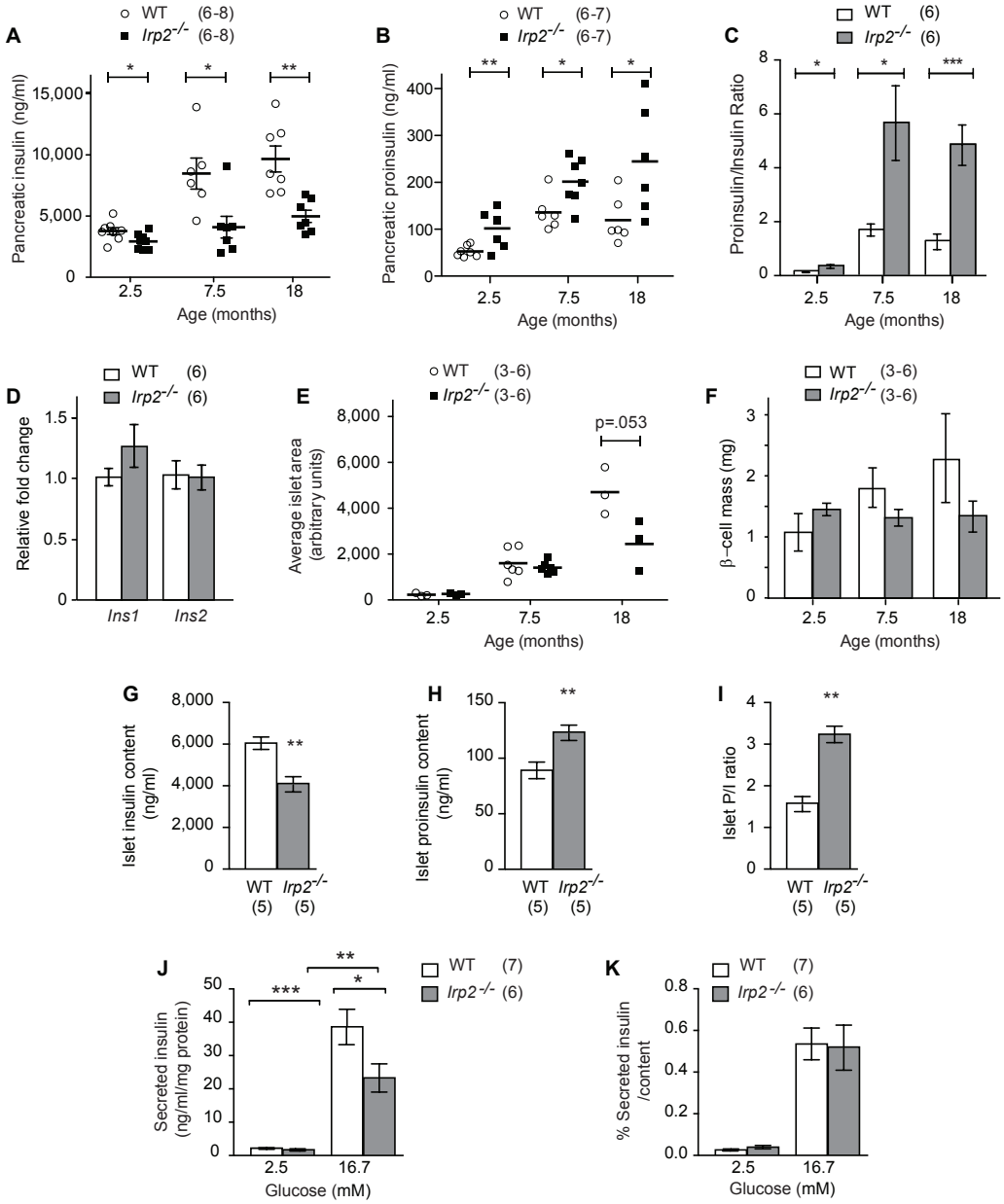
A
WT (6-8)
Irp2-/- (6-8)
Pancreatic insulin (ng/ml)
15,000
10,000
5,000
0
2.5
7.5
18
Age (months)
B
WT (6-7)
Irp2-/- (6-7)
Pancreatic proinsulin (ng/ml)
400
300
200
100
0
Age (months)
C
WT (6)
Irp2-/- (6)
Proinsulin/Insulin Ratio
8
6
4
2
0
Age (months)
D
WT (6)
Irp2-/- (6)
Relative fold change
1.5
1.0
0.5
0
Ins1
Ins2
E
WT (3-6)
Irp2-/- (3-6)
p=.053
Average islet area (arbitrary units)
8,000
6,000
4,000
2,000
0
Age (months)
F
WT (3-6)
Irp2-/- (3-6)
β-cell mass (mg)
3
2
1
0
Age (months)
G
Islet insulin content (ng/ml)
8,000
6,000
4,000
2,000
0
WT (5)
Irp2-/- (5)
H
Islet proinsulin content (ng/ml)
150
100
50
0
WT (5)
Irp2-/- (5)
I
Islet P/I ratio
4
3
2
1
0
WT (5)
Irp2-/- (5)
J
WT (7)
Irp2-/- (6)
Secreted insulin (ng/ml/mg protein)
50
40
30
20
10
0
2.5
16.7
Glucose (mM)
K
WT (7)
Irp2-/- (6)
% Secreted insulin /content
0.8
0.6
0.4
0.2
0.0
2.5
16.7
Glucose (mM)

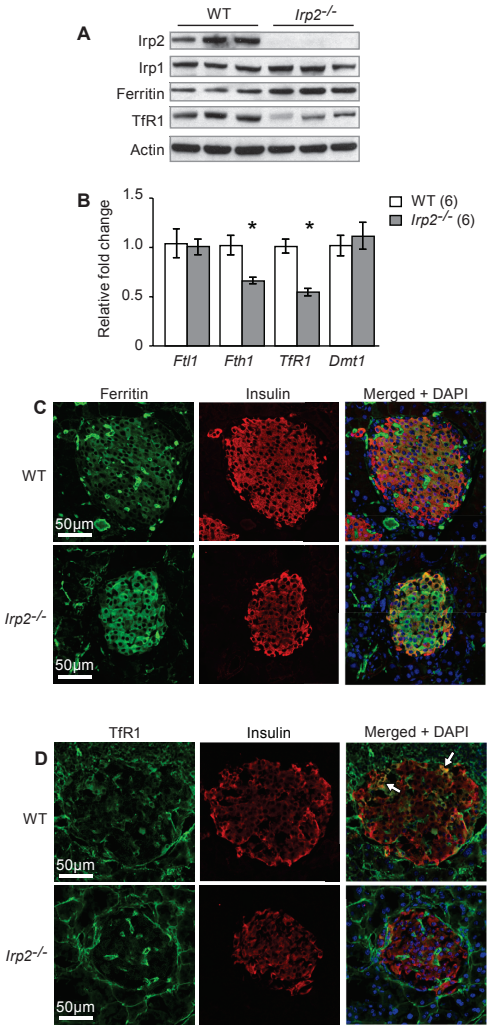

Figure 5.5. Dysregulated iron metabolism in *Irp2*$^{-/-}$ islets. (A) Western blot analysis shows IRP2, IRP1, ferritin and TFR1 levels in islets isolated from 8-month old WT and Irp2-/- mice (n = 3 mice per genotype). β-actin is a loading control. (B) qRT-PCR of *Ftl1*, *Fth1*, *Tfr1* and *Dmt1* in WT and *Irp2*$^{-/-}$ islets. The Dmt1 TaqMan assay detects both -IRE and +IRE Dmt1 mRNA variants. Values were normalized to β-actin mRNA and expressed as relative fold change to WT (n = 6 mice per genotype). Data are expressed as mean ± SEM and were compared using two-tailed Student's t-test. *$p < 0.05$, ***$p < 0.001$. (C and D) Paraffin-embedded pancreatic sections from 8-month old WT and Irp2$^{-/-}$ mice were immunostained with antibodies to ferritin (green) or TfR1 (green) and costained with insulin antibodies (red). The insulin antibody detects both insulin and proinsulin. Nuclei are stained with DAPI (blue). Arrows in D show β cells costained with TfR1 and insulin.

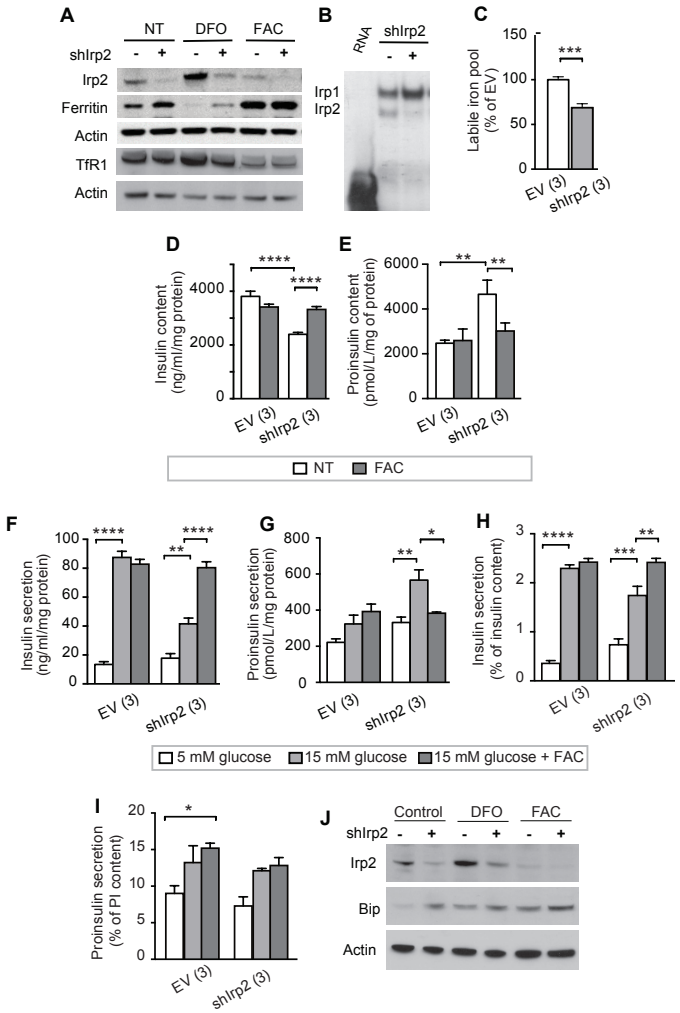

Figure 5.6. Iron improves insulin content and secretion in Irp2 deficient INS1 β-cells. (A) Western blot analysis of IRP2, ferritin and TFR1 levels in INS1 832/13 insulinoma cells expressing a shIrp2 or empty vector (-). Cells were grown with or without DFO (50 uM) or FAC (50 ug/ml) for 18 h. β-actin is a loading control. (B) EV- and shIrp2-INS1 cell lysates were analyzed by RNA-EMSA using a 32P-labeled ferritin-IRE. Irp1- and Irp2-RNA complexes are indicated. (C) Cellular labile iron pool in EV- and shIrp2-INS1 cells measured by the calcein method. (D) Total insulin content and (E) proinsulin content in EV and shIrp2-INS1 cells grown with or without FAC. F) Glucose-stimulated insulin and (G) proinsulin secretion in EV- and shIrp2-INS1 cells grown with our without FAC. Insulin and proinsulin were assayed in cells under low (5 mM) glucose and after stimulation with high (15 mM) glucose for 1 h and were normalized to total cellular protein. (H) Insulin and (I) proinsulin secretion in F and G normalized to total insulin content or proinsulin content. The assays in (C-I) were performed in triplicate from three independent experiments. Data are expressed as means ± SEM and were compared by two-tailed Student's t-test or two-way ANOVA. *p< 0.05; **p < 0.01; ***p < 0.001; ****p < 0.0001.

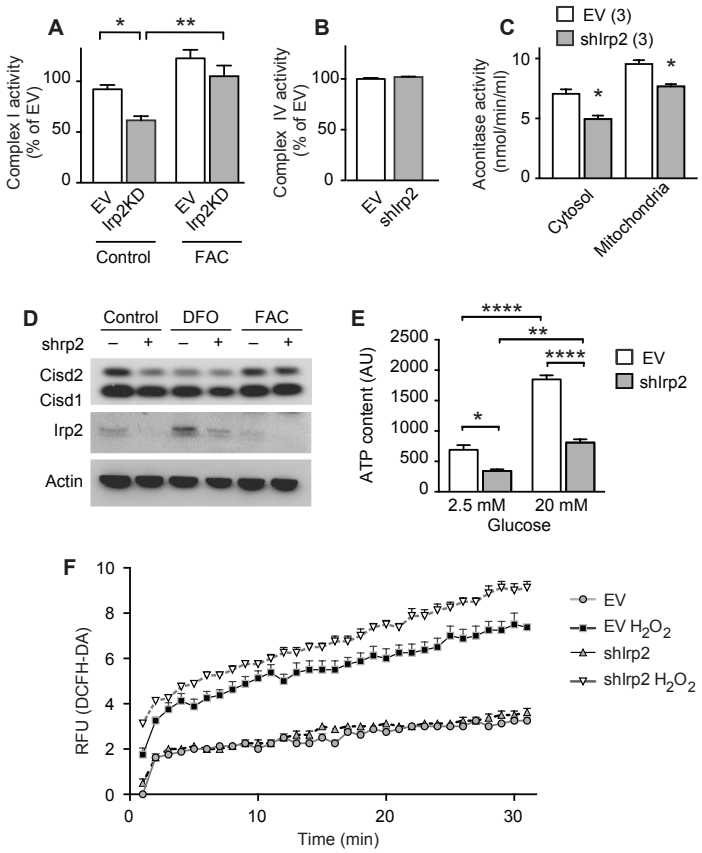

Figure 5.7. Cellular iron deficiency reduces the activity or abundance of Fe-S proteins in Irp2 deficient INS1 β-cells. (A) Complex I activity in lysates from EV and shIrp2-INS1 cells in the presence of FAC (50 ug/ml) for 18 h normalized to total lysate protein. (B) Complex IV activity in EV- and shIrp2-INS1 cell lysates normalized to total protein content. (C) Cytosolic and m-aconitase activity in EV and shIrp2-INS1 cells normalized to total lysate protein. Western blot analysis shows enrichment of c-aconitase (Irp1) and m-aconitase in cytosolic and mitochondrial fractions, respectively. (D) Western blot analysis of the Fe-S proteins CISD1 and CISD2 in EV- and shIrp2-INS1 cell lysates grown in DFO (50 uM) or FAC (50 ug/ml) for 18 h. Irp2 and β-actin are shown. (E) ATP content was measured in lysates of EV and shIrp2-INS1 cells grown in the presence of FAC for 18 h and normalized to total protein. (F) Accumulation of basal ROS levels over 30 min as measured by the cell-permeable indicator carboxy-H_2DCFDA fluorescence.

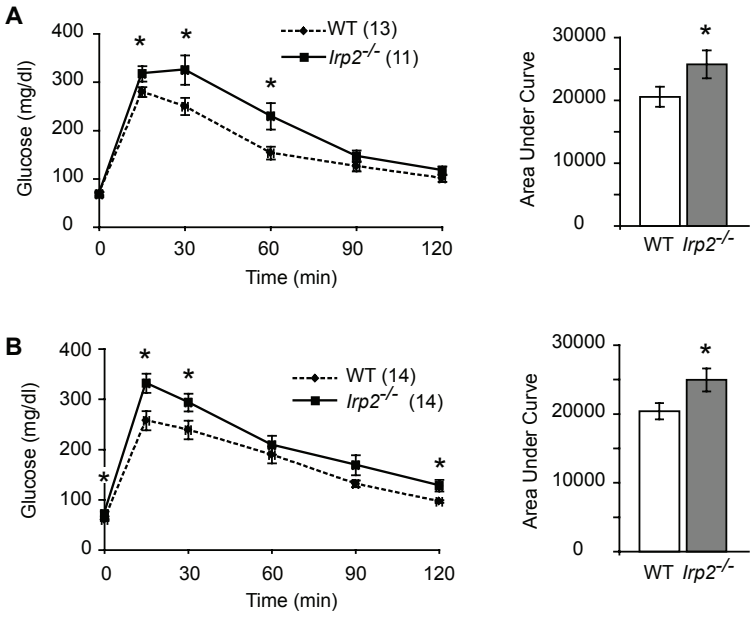

Figure S5.1. Glucose intolerance in female WT and *Irp2*$^{-/-}$ mice. Glucose tolerance tests were performed on female (A) 10-week-old and (B) 20-week-old WT and *Irp2*$^{-/-}$ mice. Glucose AUC for the data are shown. Data are expressed as mean ± SEM and compared by Student's t-test. *$p < 0.05$ relative to WT mice. Number of animals is shown in parentheses.

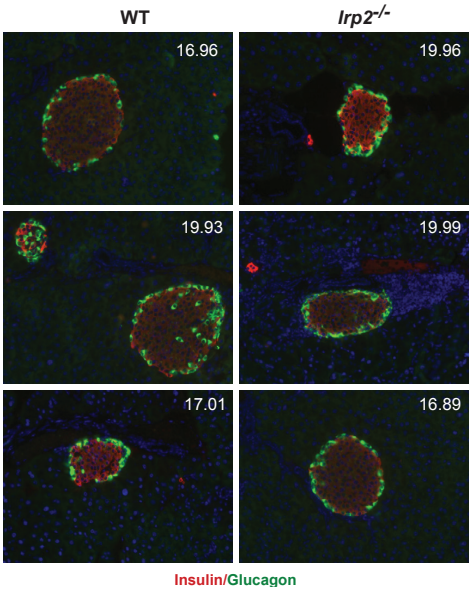

Figure S5.2. Islet morphology and glucagon expression is normal in *Irp2*$^{-/-}$ mice. Paraffin-embedded pancreatic sections from 12-month-old WT and Irp2$^{-/-}$ mice (n = 3 mice per genotype) were costained with antibodies to insulin (red) and glucagon (green). Nuclear DNA was detected by DAPI stain (blue).

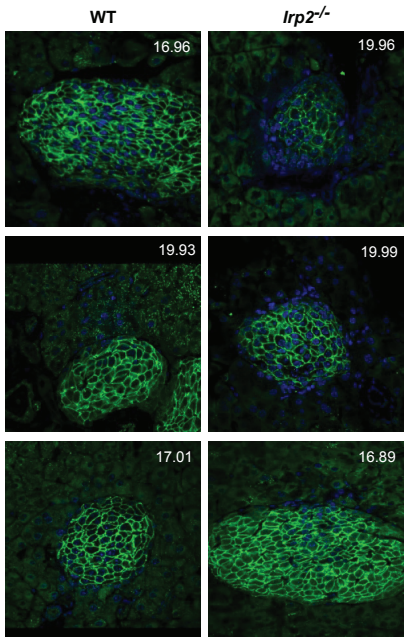

Figure S5.3. Glut2 expression and localization in *Irp2*$^{-/-}$ islets. Immunostaining of paraffin-embedded pancreatic sections from 7.5-month old WT and *Irp2*$^{-/-}$ mice (n = 3 mice per genotype) using Glut2 antibodies (green) revealed no difference in Glut2 expression or subcellular localization in *Irp2*$^{-/-}$ mice. This suggests that processing of a membrane localized protein that is process in the secretory compartment is normal in Irp2$^{-/-}$ islets. Nuclear DNA was detected by DAPI stain (blue).

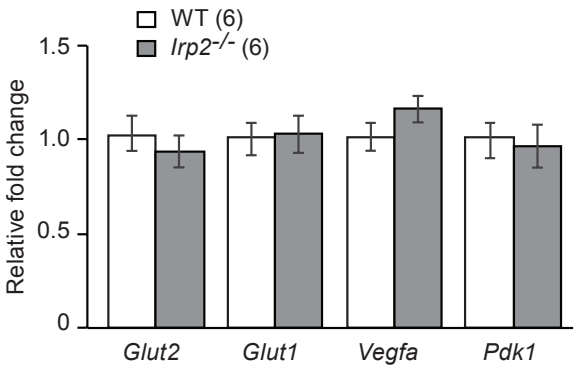

Figure S5.4. Gene expression analysis of HIF-1 targets in *Irp2*$^{-/-}$ islets. qRT-PCR analysis of HIF-1 transcriptional targets from 7.5-month old WT and *Irp2*$^{-/-}$ mice (n = 3 mice per genotype) using Taqman Gene Expression probes for the indicated targets. Data revealed no change in HIF-1 targets.

CHAPTER 6

CONCLUSION

The dual nature of iron has far reaching implications in both healthy and pathological states. In this regard, organisms have evolved elaborate mechanisms to maintain iron levels within a physiological window that is optimal for life. Importantly, these mechanisms are highly conserved throughout Metazoa, underscoring the importance of regulating iron homeostasis. Defective iron regulation can have drastic health consequences ranging from iron deficient anemia to severe organ failure from the iron overload disease hemochromatosis. In this dissertation, we used two distinct models to study mechanisms of iron homeostasis to better understand the role of iron and its regulation in key biological processes.

In the nematode *C. elegans*, we discovered a novel pathway that integrates nuclear receptor and insulin signaling to regulate intestinal iron uptake that is important for the innate immune response. Using a suppressor screen that rescued growth in low iron conditions we identified NHR-14 to be a potent inhibitor of iron import through the iron importer SMF-3. The mechanism by which this occurs relies on the nuclear localization of the newly identified transcription factor PQM-1. Specifically, we found that NHR-14 prevents nuclear localization of PQM-1 resulting in its cytoplasmic retention. Mutant worms lacking NHR-14 have significantly more PQM-1 localized to the nucleus, thus causing drastic changes in gene expression. Importantly, *smf-3* expression is highly induced in these mutants in a manner that is partially dependent on PQM-1. Future studies will need to address the molecular mechanisms behind the regulation of PQM-1 by NHR-14. Specifically how NHR-14 inhibits nuclear localization of PQM-1. Protein-protein interactions, posttranslational modifications, and indirect transcriptional regulation are all reasonable hypotheses.

In addition to increased iron uptake, these mutants have a primed innate immune response that enhances resistance to the pathogens *Pseudomonas aeruginosa* and *Salmonella enterica*. This response consists of the upregulation of numerous genes involved in the *C. elegans* immune response. Among this repertoire, we consider *smf-3* regulation a critical component of innate immunity by regulating iron availablitly. This is a significant finding in the context of nutritional immunity and the molecular arms race between host and pathogen to aquire or sequesters iron. Given that NHR-14 is rapidly degraded in response to bacterial infection suggests a novel pathway used to sense and respond to pathogens. It is an interesting possibility that NHR-14 senses pathogen associated molecular patterns through its ligand-binding domain to initiate a cascade of events that ends with a robust transcriptional immune response.

We also identified NHR-14 to be a homolog of the mammalian HNF4α, a transcription factor that is critical for development and many metabolic processes. Similar to what we observed in *C. elegans*, mice lacking HNF4α specifically in intestinal cells had a significant increase in the expression of the mammalian iron importer DMT-1. Considering the importance of HNF4α in the development and function of the intestine, combined with its associated risk in chronic inflammatory diseases, it is interesting to speculate potential therapeutic interventions that focus on iron management. Signifcant evidence has also emerged highlighting the importance of the gut microbiome for proper intestinal function. Recent data have shown that oral iron administration to combat anemia in infants adversely affects the gut microbiome, leading to enhanced pathogen colonization and intestinal inflammation. Whether HNF4α plays a role in regulating iron bioavailabilty for the gut microbiome remains to be determined.

This dissertation also examines the role of IRP2 in pancreatic β-cell function and its impact on whole body glucose metabolism. We observed that mice lacking IRP2 have impaired glucose homeostasis that is highlighted by fasting hyperglycemia and hypoinsulinemia reminiscent of type 1 diabetes. Cellular iron homeostasis in β-cells of these mice is defective rendering them functionally iron deficient. Notably, iron uptake by TfR1 is significantly reduced while iron storage by ferritin is elevated. We found that hypoinsulinemia is associated with an accumulation of proinsulin, suggesting a defect in the insulin biosynthesis pathway. Given that we could rescue this defect in a clonal β-cell model by increasing iron levels provides strong evidence that insulin processing is iron-dependent.

Insulin production and secretion are the primary functions of pancreatic β-cells, and these processes rely heavily upon healthy mitochondria and ER function. We found that IRP2 deficient β-cells have defective mitochondria characterized by a reduction in Complex 1 activity and total ATP levels. Similarly we found these cells to have increased ER stress that is associated with sensitivity to reactive oxygen species. It has recently become appreciated that ER function is tightly linked to Fe-S cluster biosynthesis in the mitochondria, such that many key ER associated proteins utilize these cofactors. Here we speculate that iron deficiency in β-cells due to loss of IRP2 results in impaired Fe-S cluster biogenesis, negatively affecting Fe-S cluster containing proteins of the ER. This disruption is likely contributes to the observed defects in insulin processing. These findings are significant in the context of global health, where billions of individuals suffer from iron deficiency. Further investigation into the link between iron

deficiency and diabetes is warranted, with the potential for significant contributions to how we treat and manage diabetes.